Development of Novel Flavin - Catalysed Transformations

Murray, Alexander

Award date:
2015

Awarding institution:
University of Bath

DEVELOPMENT OF NOVEL FLAVIN – CATALYSED TRANSFORMATIONS

Alexander Thomas Murray

A thesis submitted for the degree of Doctor of Philosophy

University of Bath

Department of Chemistry

April 2015

Abstract

Flavin catalysis has been developed as an environmentally benign route to novel redox chemistry, and the utility of these catalytic systems as simple models of flavoenzyme mechanism has been discussed. A system for oxidising aldehydes to carboxylic acids under flavin catalysis using a Bayer-Villiger type mechanism has been developed, which shows similarities to the enzyme *bacterial luciferase*. An oxidation of primary amines, using alloxan as co-catalyst and a sulfide as reducing agent, was developed. This was found to work efficiently using air as terminal oxidant, and by extensive mechanistic studies involving EPR spectroscopy, kinetics and UV/visible spectroscopy we propose a radical mechanism. The similarities in some kinetic properties of our system to *monoamine oxidase* (B isozyme) led us to re-evaluate some previously published pK_a dependence data. The catalytic activity of alloxan itself was evaluated, in conjunction with a Cu(I) co-catalyst, and was found to be effective in oxidation of amines, including oxidative cross-coupling, as well as for diimide-like reductions of alkenes and alkynes with hydrazine. Finally, flavin-indole charge transfer chemistry was found to promote selective C3-deuteration of indoles. The CT complex was isolated and found to form a flavin-indole covalent bond under certain conditions. Additionally, we found that *in situ* DCl generation was a viable method for indole deuteration with very short reaction time and high selectivity compared to previous methods.

Contents

Acknowledgements

Firstly, I must thank Dr. Dave Carbery for giving me the opportunity to carry out the work within the group. The advice, support, infectious enthusiasm and countless coffees ‘to just work through this mechanism one more time’ were exactly what doing a PhD is all about!

Secondly, my industrial supervisor, Dr. Matt John at GSK. I must thank Matt for my three months over at GSK in Stevenage, as well as the frequent trips to Bath/London/wherever for a quick project update and a beer (or in the case of the impromptu Great British Beer Festival trip, just a beer)

I would also like to thank the Carbery group, firstly Matt, Nath and Steve for welcoming me and teaching me the ropes upon my first arrival, then Christina, Cristina (aka Spanish), Fab, Chris and Matt, in succession a generally great bunch of people to work with. Additional sharers of lab space I’d like to thank also are Liam and Giles, a.k.a the Panti.

Particular people I’d like to thank are, in no particular order, Spanish, for general enthusiasm if not for Spanish radio, Christina, for sharing a wide variety of cat pictures throughout the last 2+ years, Fab, for generally keeping the lab running smoothly and being the perpetually organised and together lab worker that I am totally not, as well as doing a lot of the hard work on kinetics for the flavin amine project, and Chris, for much interesting scientific discussion, many beers and generally becoming one of my best friends (and in particular one infamous night in Manchester!)

I must also thank various people who have contributed to this work, firstly I have worked with a series of extremely talented undergraduates. Special mentions go out to Pascal, who I never met but did great initial optimisation work on the flavin/aldehyde project, Myles, for all the hard work on the initial substrate scope and some kinetics on the flavin/amine work (and for coming out for beers with me instead of his sister’s farewell party!), Rose, for excellent work on kinetics of Cu amine oxidation and alkene reduction, and Jon, for initial work on the indole chemistry.

I am also indebted to various people for work with different techniques. Firstly, Floriana, Dan, and in particular Alistair and Amga at Manchester for really going above and beyond with gathering all the EPR data that is so crucial to the work presented. I owe you, guys. Secondly, Chris and Aron, for computational work. This is probably a good time to thank Aron's group a.k.a. 'Walsh and the Boys', and in particular Dr. K. Tobias Butler, for many interesting discussions and Friday night beers.

Further help I've had comes from Lauren Hatcher for crystallography work, John 'The Magnet' Lowe for NMR assistance, particularly with DOSY spectroscopy, Anneke Lubben for MS manual injections as well as letting me have a play on the new machine, and Chris Pudney over in biochemistry for insight into flavin UV/vis chemistry as well as stopped flow work.

And thanks to Clint and Alfred.

Abbreviations

Ac	acetyl
AIBN	azobisisobutyronitrile
Ar	aryl
A.U.	arbitrary units
Bn	benzyl
br.	broad
cat.	catalyst
COSY	correlation spectroscopy (^{1}H- ^{1}H)
CT	charge transfer
CuAO	copper-containing amine oxidase
δ	chemical shift relative to Me_4Si in parts per million
d	doublet
DCM	dichloromethane
DDQ	2,3-Dicyano-5,6-dichloroparabenzoquinone
DFT	density functional theory
DMA	dimethylacetamide
DMF	dimethylformamide
DMSO	dimethyl sulfoxide
DOSY	diffusion ordered spectroscopy
DMS	dimethyl sulfide

e^-	electron
ee	enantiomeric excess
ENDOR	electron nuclear double resonance
EPR	electron paramagnetic resonance
eq	molar equivalents
ES	electrospray
ESEEM	electron spin echo envelope modulation
Et	ethyl
FAD	flavin adenine dinucleotide
FMN	flavin mononucleotide
GC	gas chromatography
h	hours
hep.	heptet
HFIP	1,1,1-3,3,3-hexafluoroisopropanol
HPLC	high performance liquid chromatography
HSQC	heteronuclear single quantum coherence
HYSCORE	hyperfine sublevel correlation
IBX	2-iodoxybenzoic acid
IPA	isopropanol
^{i}Pr	isopropyl
IR	infrared
ISC	inter-system crossing
KIE	kinetic isotope effect

k_{obs}	observed rate constant
LED	light emitting diode
m-	*meta*
M	mol L^{-1}
MAO	monoamine oxidase
*m*CPBA	*meta*-chloroperbenzoic acid
Me	methyl
MeSal	3-methylsalicylate
min.	minutes
M.S.	molecular sieves
MS	mass spectrometry
MW	microwave
NAD	nicotinamide adenine dinucleotide
NHC	*N*-heterocyclic carbine
^{n}Hep	*n*-heptyl
NMO	*N*-methylpiperidine oxide
NMR	nuclear magnetic resonance
NOE	Nuclear Overhauser effect
^{n}Pr	*n*-propyl
o-	*ortho*
Oxone®	potassium peroxymonosulfate
p-	*para*
p	pentet

Petrol	40:60 petroleum ether
Ph	phenyl
phen	1,10-phenanthroline
q	quartet
RF	radio frequency
r.t.	room temperature
s	singlet
SCE	standard calomel electrode
SET	single electron transfer
sex.	sextet
SHE	standard hydrogen electrode
SPS	solvent purification system
SSRI	selective serotonin reuptake inhibitor
t	triplet
^{t}Bu	*tert*-butyl
TEMPO	(2,2,6,6)-Tetramethylpiperidin-1-yl-oxyl
TFA	trifluoroacetic acid
TFE	2,2,2,-trifluoroethanol
THF	tetrahydrofuran
TLC	thin layer chromatography
TMS	trimethylsilyl
UV	ultraviolet

1. Introduction

1.1 The Flavin Moiety in Nature

Riboflavin (Vitamin B2) is a ubiquitous enzyme cofactor found in all biological systems, with up to 3% of genes in an average organism coding for a protein requiring a flavin as cofactor.[1] Flavoproteins are responsible for a wide variety of oxidation and reduction reactions (they are *oxidoreductases*),[2] In humans, a deficiency causes the disorder *ariboflavinosis*, also known as 'pellagra sine pellagra'.[3] Additionally, some organisms are described as having 'flavin intensive lifestyles' and these include pathogens such as the bacteria *Mycobacterium Tuberculosis*.[2]

Riboflavin **1** is a nitrogen-rich heterocycle based on the tricyclic isoalloxazine system (Figure 1), which consists of a pteridine ring oxidised on one side to the corresponding imide, connected to an additional benzene ring.[4]

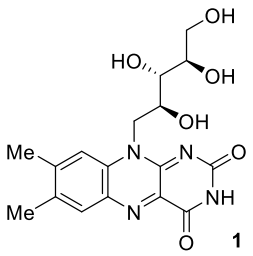

Figure 1. Structure of riboflavin

Riboflavin; the basic flavin unit found in nature, is synthesised from ribytylaminopyridinedione **2** *via* a two-step process. Firstly, lumazine **3** is synthesised, followed by Diels-Alder dimerization, then formation of riboflavin **1** by elimination of an equivalent of **2**.[5,6]

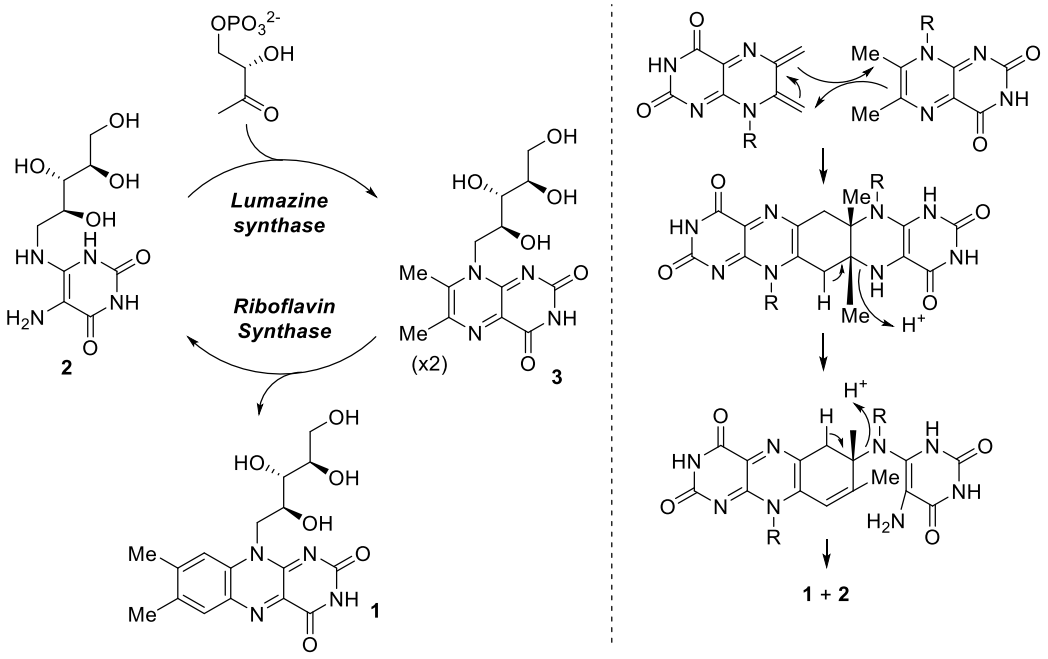

Scheme 1. Simplified catalytic cycle for biological riboflavin synthesis, and key steps in riboflavin synthase

Flavins are common cofactors in enzyme catalysis; flavin cofactors often occur as flavin adenine dinucleotide (FAD) **4** and flavin mononucleotide (FMN) **5** (Figure 2).[7]

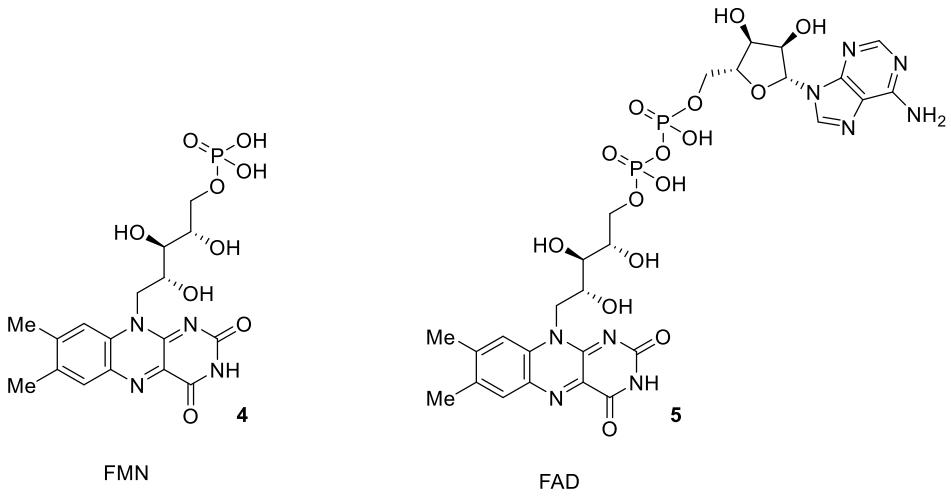

Figure 2. Structures of flavin adenine dinucleotide and flavin mononucleotide

Flavins can exist in three forms; the most stable oxidised form, an intermediate radical semiquinone form and a fully reduced form. (Figure 3).[8]

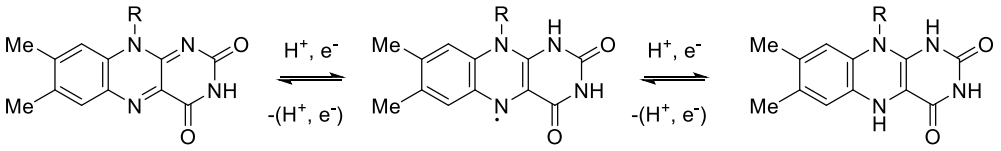

Figure 3. The oxidised, reduced and semiquinone forms of a flavin

The redox activity of the reduced form is illustrated by one major use in nature of the FAD cofactor: transfer of electrons required for the dehydrogenation of succinate to fumarate, a key step in the citric acid cycle (Scheme 2).[7]. Dihydroflavin **6** spontaneously reoxidises and so the enzyme can turn over.

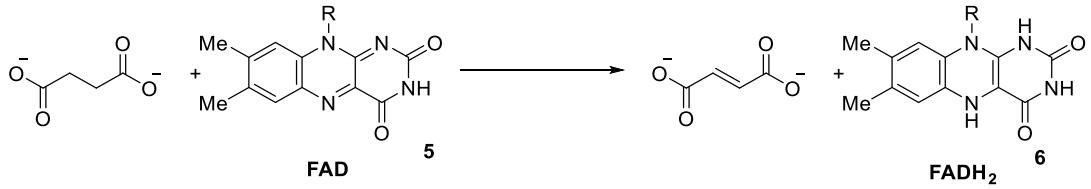

Scheme 2. Flavin-mediated dehydrogenation of succinate as part of the citric acid cycle

1.2 Flavin containing monooxygenases (FMOs)

Flavin-containing enzymes (flavoenzymes) are involved in various oxidation reactions *in vivo*, including the aforementioned electron transfer/dehydrogenation and oxygen transfer. In the latter case, liver flavoenzymes such as FAD-containing monooxygenase catalyse a wide variety of degradations of small molecules in organisms, including metabolism of xenobiotics. These transformations include oxidations of aldehydes, amines, sulfides and even oxidation of aromatic rings.[9,10,11,12]

The active species in these flavin-catalysed reactions is the highly reactive hydroperoxide **7** which originates from addition of molecular oxygen into the reduced (flavin-H_2) form. (Scheme 2).[13]

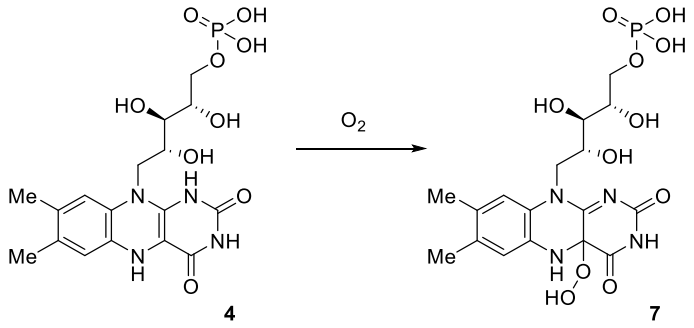

Scheme 3. O_2 addition to FMN-H_2

This results in a general catalytic cycle as shown, with the reduced form coming from an external cofactor such as NADH and undergoing O_2-mediated oxidation followed by nucleophilic attack by the substrate and regeneration of oxidised catalyst.

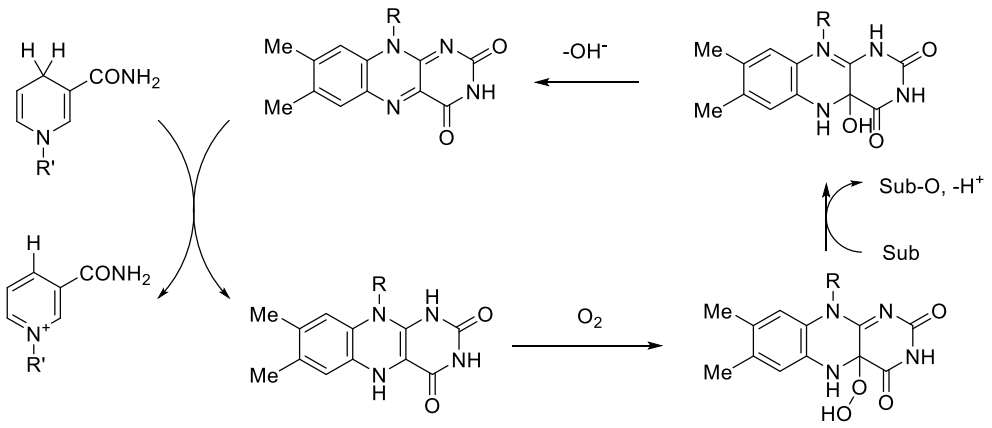

Scheme 4. Generalised catalytic cycle for flavin monooxygenases with NADH as terminal hydride donor

FMO enzymes tend to have a 'prosthetic' i.e. non-covalently bound flavin cofactor, and their mechanisms are relatively similar and well understood. They have two-electron redox character and not showing much involvement of the semiquinone. An exception is as a transient intermediate in O_2-mediated oxidation, where a superoxide and flavin make a radical pair. This is initially through the anionic reduced flavin, followed by electron transfer, relatively slow inter-system crossing and recombination (Scheme 5).[14]

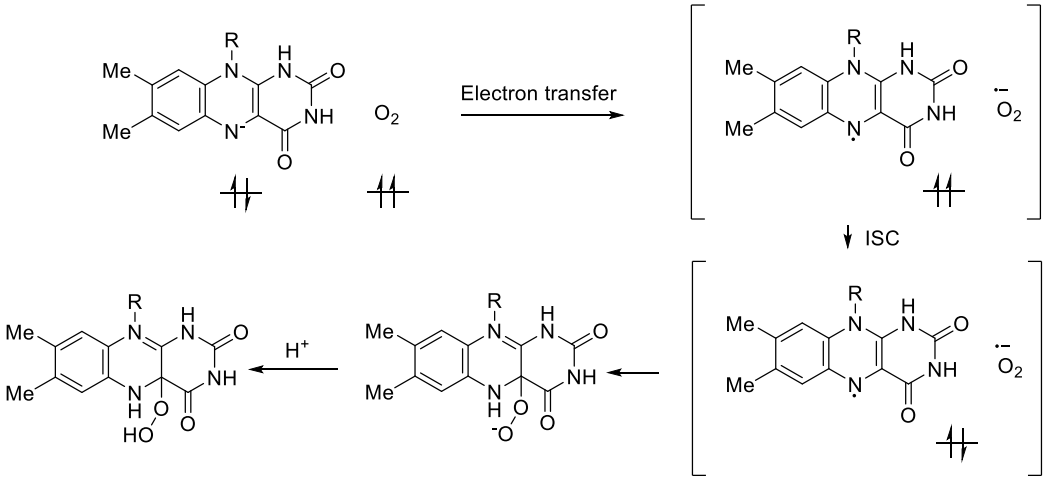

Scheme 5. Relevant electron transfers in O_2-mediated reoxidation of flavins

One particular feature of the reactivity of flavins in bacteria is *bioluminescence.* This is the chemiluminescence exhibited by an organism while an enzymatic reaction is occurring. An example is the bacterial luciferase enzyme which luminesces on reaction with long-chain aliphatic aldehydes. The aldehyde is oxidised to the carboxylic acid during this process. The light emission is thought to be from the hydrated flavin **8** (described as an 'excited state') decaying with expulsion of water to the starting flavin mononucleotide (Scheme 6).[15] This enzyme, and similar examples such as Bayer-Villiger monooxygenase, are mechanistically interesting because the usual mechanism is in effect reversed, with attack of a *nucleophilic* hydroperoxide on the electrophilic carbonyl followed by B-V type breakdown of a tetrahedral intermediate; mirroring the dual nucleophilic and electrophilic oxidative nature of common peracids such as *m*CPBA.

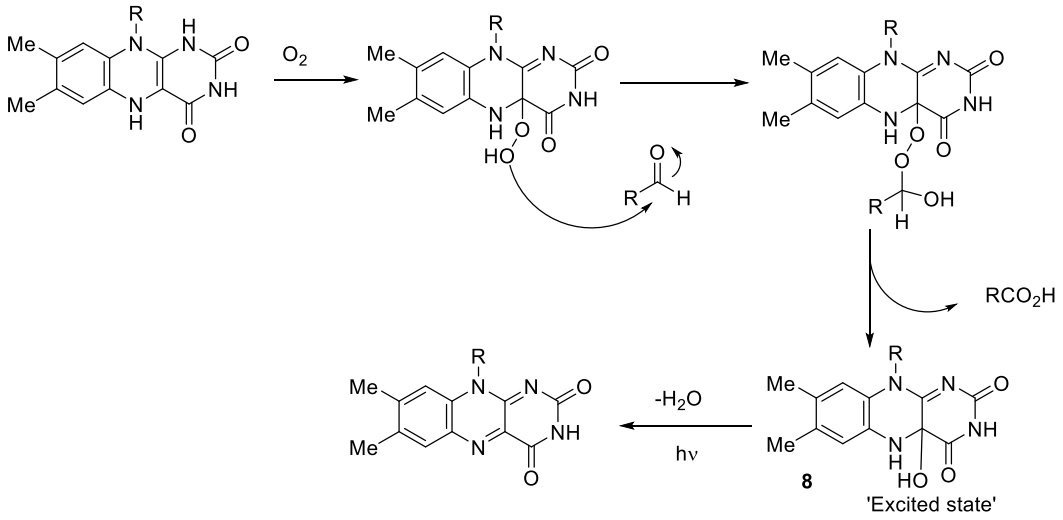

Scheme 6. Mechanism of bacterial luciferase exhibiting chemiluminescence

1.3 Flavin containing oxidases

In the mechanism of flavin-containing monooxygenases, the reductive half-reaction is achieved by reaction of oxidised flavin with an endogenous reductive cofactor, usually NADH. In the case of oxidase enzymes, however, this step is achieved by reaction of flavin with the substrate directly (Scheme 7). This is followed by O_2-mediated reoxidation, again, but this time with the hydroperoxide being an unwanted byproduct which is extruded and rapidly externally disproportionated by catalase.[1]

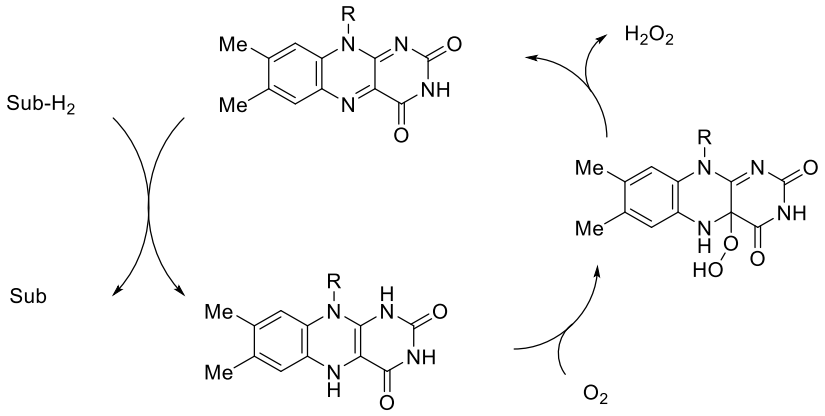

Scheme 7. General course of a flavin oxidase-catalysed reaction

Additionally, and in contrast to FMOs, these enzymes generally possess a covalent linkage to the flavin, and often the semiquinone is thought to be more relevant to the reactivity of the enzyme.[1]

Examples of these flavin oxidases include glucose oxidase, D-amino acid oxidase (Old Yellow Enzyme), xanthine oxidase, and monoamine oxidase, with the latter being perhaps the most well studied and yet challenging to model mechanistically.[16]

1.3.1 Monoamine oxidase

Monoamine oxidase (MAO) was discovered in 1928 and initially named 'tyramine oxidase' after tyramine, the decarboxylation product of tyrosine, which is a good substrate for the enzyme.[17] The enzyme is a flavin-dependent oxidase responsible for the oxidation of amine to the corresponding aldehyde with reduction of O_2 to H_2O_2, *via* a transient imine.

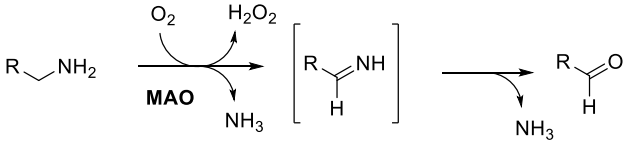

Scheme 8. Oxidative deamination of a monoamine by MAO enzyme

It was later discovered that MAO can be subdivided into two isozymes, MAO-A and MAO-B. Sharing a 70% structural similiarity,[18] and with similar active sites, these two enzymes are responsible for the breakdown of a wide range of biologically active amines. MAO-A acts primarily on substrates which are electron rich at a β-aromatic ring, such as tryptamine and epinephrine, and MAO-B on benzylamine and phenethylamine, with tyramine and dopamine being approximately equal, as determined by steady state k_{cat} values.[19]

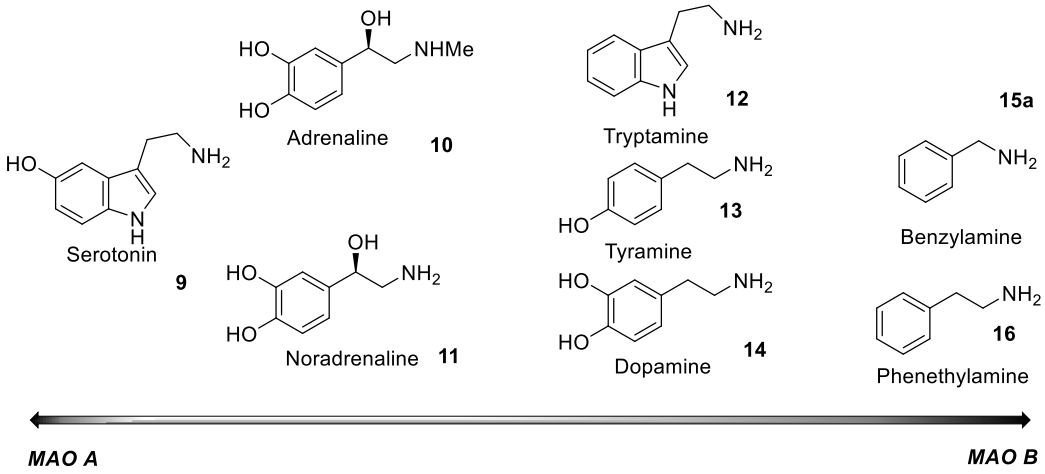

Figure 4. Qualitative schematic showing relative rate of oxidation of monoamines by MAO-A and MAO-B

Low levels of MAO, specifically MAO-A have been implicated with increased behavioural aggression, known as the 'warrior gene'. The 3R allele is associated with 'aggressive responses to provocation', in both mouse models and humans.[20] This has been extensively discussed in the popular media as a partial explanation for violent or criminal behaviour, with a convicted murderer in the USA avoiding the death penalty partially by having this low activity form.[21]

The hydrazide **17**, iproniazid, was originally developed as an anti-tuberculosis drug but then found to be an inhibitor of MAO, leading to antidepressant effects. Indeed, this was the first drug specifically marketed for depression. Since then, a plethora of MAO inhibitors have been developed, some of which are shown in Figure 5 (**17-20**).[22-24]

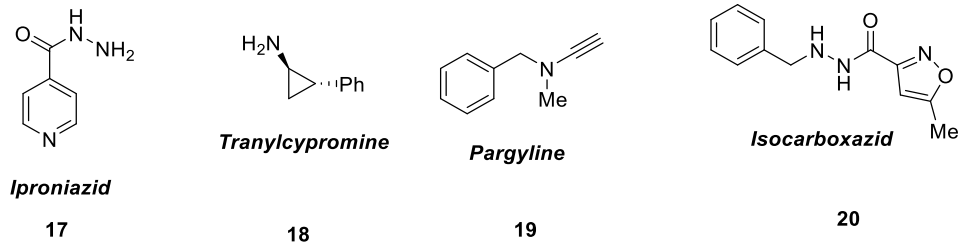

Figure 5. Selected examples of MAO inhibitors

However, these drugs are notorious for their contraindications such as drug interactions with any amine-containing or serotonin-raising drug (such as SSRIs). Additionally, ingestion of high levels of tyramine such as are found in some cheeses can lead to a hypertensive crisis if a patient is on classic non-selective MAO therapy.[25]

Additionally, more selective and reversible MAO inhibitor have been developed. Moclobemide (**21**) and rasagiline (**22**) are examples of MAO-A and MAO-B selective reversible inhibitors respectively.[26] MAO-A inhibitors tend to be selective antidepressants due to increases serotonin levels, whereas MAO-B inhibition has antiparkinsonian properties due to the increase in dopamine levels. MAO-B inhibitors are an invaluable adjuvant to the standard regimen of L-DOPA for the treatment of Parkinson's disease.[27]

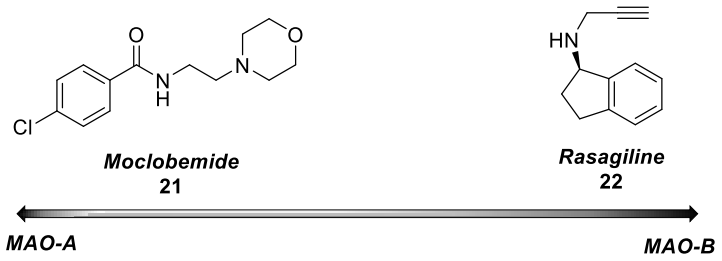

Figure 6. Schematic of examples of selective MAO inhibitors

Additionally, there has been increasing interest in the use of MAO inhibitors as neuroprotective agents; MAO inhibitors have been proposed as prophylactics for age-related dieseases such as Parkinson's disease and Alzheimer's disease *via* an anti-apoptosis mechanism, as well as protecting against potential environmental neurotoxins that are metabolised by MAO into their destructive form.[28,29]

Another recent use of MAO inhibitors has been in epigenetic modulation, by acting on the flavin-dependent lysine-specific demethylase 1 (LSD1) enzyme.[30] Epigenetics refers to any genetic change that is *not* related to a change in the DNA sequence.[31] In this case, the highly basic histones which make up chromatin in DNA spools can be modified by methylation/demethylation and the enzyme controlling the latter process, LSD1, is inhibited by MAO inhibitors.

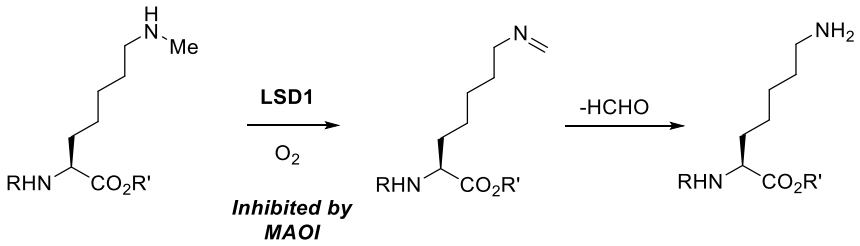

Scheme 9. Mechanism of action of LSD1 and its inhibition

1.3.2 Mechanistic properties of MAO

For such a critical enzyme, there is still no consensus mechanism for either the A or B monoamine oxidase isozymes, which nevertheless are still generally considered to be the same. Given both A and B share a strong deuterium kinetic isotope effect on the α-hydrogen, it can be inferred that *C-H* bond breaking is rate limiting in both cases. Therefore, it seems that this can occur by removal of a proton, a hydrogen atom or a hydride, and indeed all three of these mechanisms have been proposed at various points over the last thirty years.

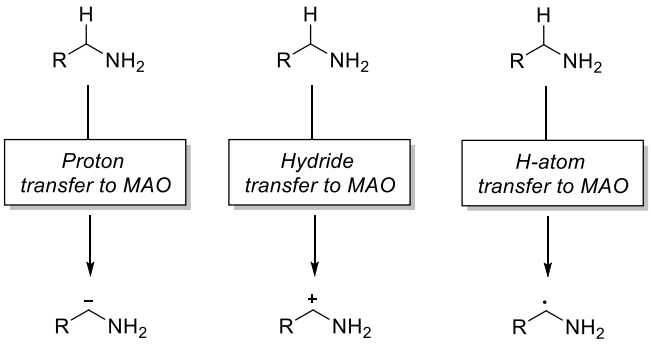

Scheme 10. Possible modes of hydrogen removal from amine α-carbon by MAO

Removal of a proton has been perhaps the most discussed possibility for the *C-H* cleavage step of the catalytic activity of MAO. The increase in acidity at the α-hydrogen required for this step has been proposed either as a covalent binding of amine to flavin[32] or a single electron transfer to form an aminium radical cation.[33]

Figure 7. Intermediates for proton removal proposed by Edmondson (left) and Silverman (right)

Problems with these approaches are, in the first instance, that secondary and particularly tertiary amines are good substrates for monoamine oxidase, which would not be expected, particularly in the latter case, for a covalent flavin adduct. An infamous example is that of the tertiary amine neutotoxin MPTP, which was 'discovered' after a chemistry graduate in the 1970s attempted to illicitly manufacture the synthetic opioid desmethylprodine (**24**), but during the final esterification step from **23** the molecule also underwent elimination leading to a mixture of products **24** and **25** (Scheme 11). The student developed rapid, early-onset Parkinson's disease.[34]

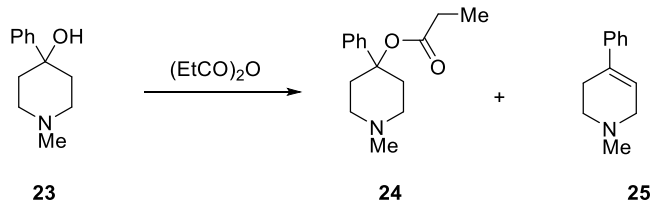

23 **24** **25**

Scheme 11. Synthesis of desmethylprodine **24** and elimination product MPTP **25**

The reason for this effect was later found to be the successive oxidations of the alkene to the pyridinium cation MPP^+ (**27**) in glial cells (Scheme 12), which is the active toxin responsible for redox uncoupling and free radical build up.[35]

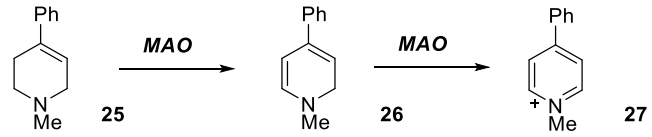

25 **26** **27**

Scheme 12. MAO oxidation of MPTP **25** to MPP^+ **27**

Silverman's mechanism does not apparently suffer from these discussed problems. A single electron transfer to form a radical cation followed by proton removal should be possible even for a tertiary amine. Furthermore, Silverman observed the rapid ring opening of cyclopropyl, cyclobutyl and cubanyl amines **28-30** in the presence of MAO (Scheme 13).[36-38]

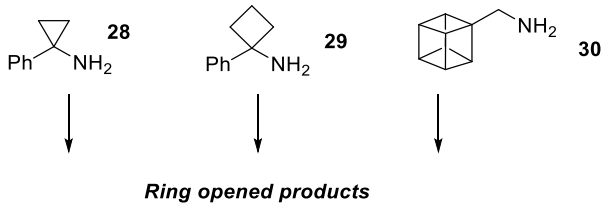

Scheme 13. MAO-catalysed ring opening of strained amines

However, one problem with this mechanistic pathway is that, for example, the peak oxidation potential for a primary amine is +1.5 V whereas flavoenzymes are in the region of -0.49 - +0.19 V. Nevertheless, for an irreversible process this is not necessarily insurmountable.[33]

In addition, it is notable that no discrete intermediates build up to observable populations during this rate-limiting *C-H* cleavage step. This is true of the covalent flavin adduct but also of the radical cation mechanism proposed by Silverman, with no EPR evidence for either a flavin anionic semiquinone or radical cations, nor stopped-flow evidence for the suggesting any radical species present is either short-lived or spin-paired.[39-41]

Another mechanism discussed is abstraction of hydride by flavin from the amine (Scheme 14). There is certainly strong evidence for such a mechanism for other flavoenzyme oxidases such as D-amino acid oxidase. However, this would not be consistent with the ^{15}N kinetic isotope effects observed by Edmondson which suggest asynchronicity between *C-H* bond breaking and $sp^3 \rightarrow sp^2$ nitrogen rehybridisation.[42]

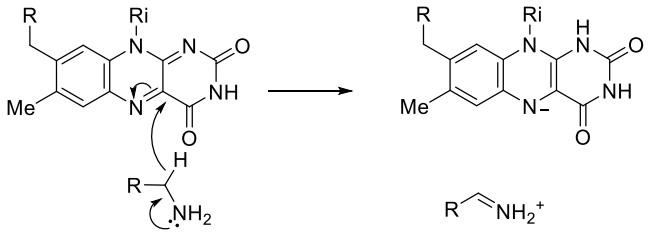

Scheme 14 Hydride transfer mechanism showing synchronous nitrogen rehybridisation

Finally, a hydrogen atom transfer from amine to flavin has also been discussed, but this was discounted on the grounds that there was not a sufficiently reactive H-abstracting species in the enzyme active site to overcome the inherent bond dissociation energy of the α-hydrogen *C-H* bond.[43] Additonally, a truly stepwise version of this mechanism suffers from the same issues as the former two; the lack of observable intermediates during catalysis.

Ramsay has demonstrated that the oxidative and reductive half-reactions of the flavoenzyme are in fact dependent on the presence of substrate in the active site; with reoxidation of an amine *ternary complex* proceeding significantly faster than of the free flavoenzyme.[19] There was, however, no correlation observed between rate enhancement in the reductive and oxidative half reactions. The fact that the oxidative half reaction was faster in the presence of product shows that a ternary complex mechanism operates. However, in the specific case of β-phenethylamine **16** with *both* MAO-A and MAO-B the reductive half-reaction was much faster, but as the steady-state rate was roughly equivalent the rate determining step was thus the slow oxidation of the free enzyme; in a so-called 'ping-pong' mechanism. Unlike most MAO substrates, β-phenethylamine **16** did *not* display a ^{2}H kinetic isotope effect; i.e. *C-H* bond breaking appears not to be rate-limiting in this case.[40,44]

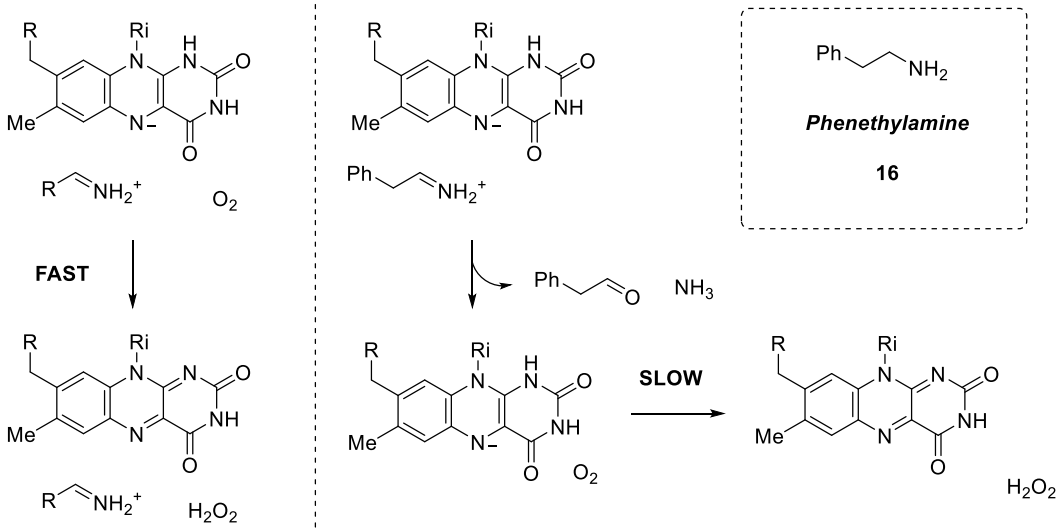

Scheme 15. The oxidative half reaction in MAO is different for **16** than most other common substrates

It has been assumed that MAO-A and MAO-B share the same mechanistic *C-H* bond breaking step, due to their structural similarities. However, Edmondson recently reported that in a series of substituted benzylamines the Hammett correlation was opposite in sign for MAO-A and MAO-B, with A having ρ= +0.8 and B having ρ = -0.9 (at pH 9.0).[45] This means that the A type oxidising electron deficient benzylamines faster than electron rich and the opposite being the case for MAO-B. Edmondson suggests that this implies a proton removal for MAO-A, and a hydride transfer type mechanism in the case of MAO-B.[46]

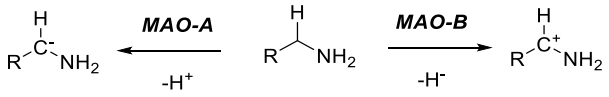

Scheme 16. Possible differing mechanisms for MAO isozymes as discussed by Edmondson

1.3.3 MAO A structure

Human monoamine oxidase A has been crystallised in the presence of either clorgyline or harmine, both MAO inhibitors. The length of the protein is 513 amino acid residues, the protein crystallises as a monomer. The flavin cofactor is covalently linked, as is common for flavin-containing *oxidases*, *via* a cysteinyl linkage on the C8a carbon, and then to the amino acid chain by an unusual *cis*-amide linkage. Key residues which are highly conserved and surround the cofactor are a lysine, tryptophan, and tyrosine directly parallel.[47] A representation of the active site is shown (Figure 8).[48]

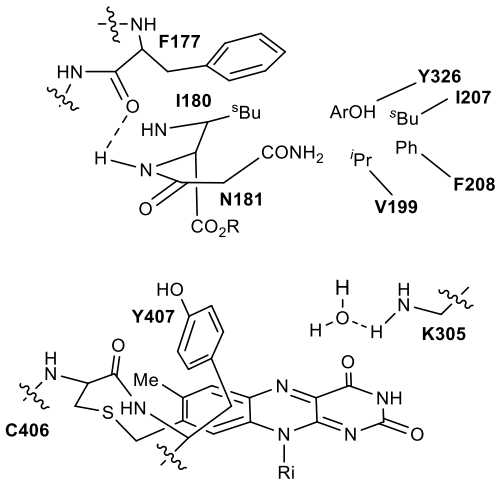

Figure 8. Active site of MAO-A

One notable point about the active site residues is that they form a hydrophobic ‘aromatic cage’ around the ‘entry point’ to the flavin-containing enzyme cavity. Differences in the size, shape and polarity of the cage is thought to relate to the differing substrate profiles of the A and B isozymes.[49]

1.3.4 MAO B structure

MAO-B has been found to have 70% structural similarity relative to human MAO-A. The shape of its secondary structure is also broadly similar.

Monoamine oxidase B has been crystallised in the presence of the non-inhibitor, but sluggish, substrate 4-nitrobenzylamine **31**. This is unsurprising bearing in mind Edmondson's measured Hammett ρ value of -0.9. The linkage and most of the surrounding key amino acid residues are similar, with the cysteinyl link, cis-amide and tyrosine residue all still present. Key differences are in the 'aromatic cage' region, where a leucine (**L171**, Figure 9) replaces an isoleucine (**I180**, Figure 8), a cysteine (**C172**, Figure 9) replaces an asparginine (**N181**, Figure 8), and an isoleucine (**I198**, Figure 9) replaces a phenylalanine (**F208**, Figure 8). In this case we can also see the 'cage' region by the bound substrate (entry point circled, Figure 9 - **II**). However, it should be bourne in mind that as a sluggish substrate to the point of competitive inhibition and possessing strong H-bond acceptors, **31** may not be the best representation of a typical MAO-B substrate.

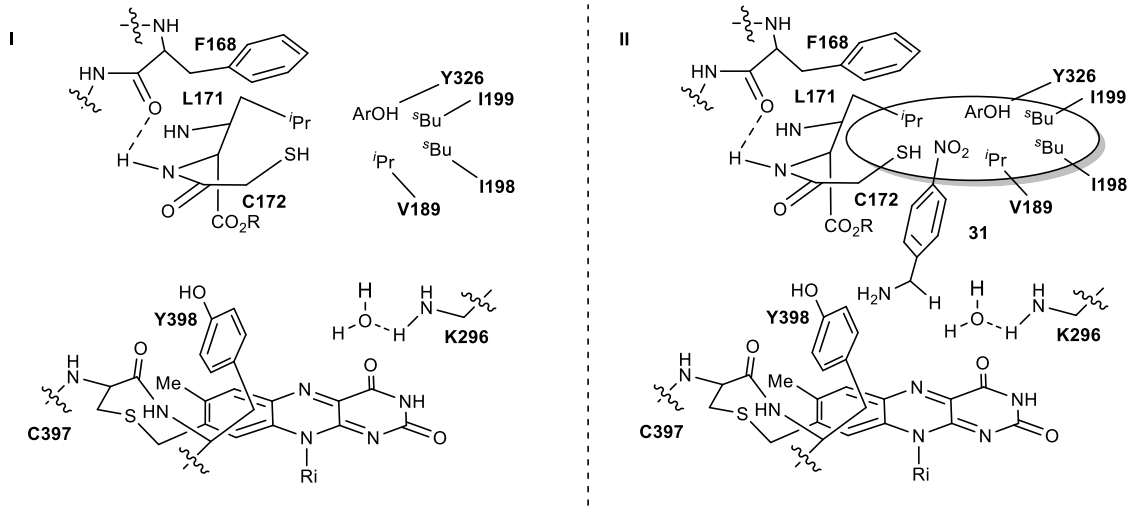

Figure 9. The active site region of MAO-B (**I**) and MAO-B with inhibitor **31** (**II**), highlighting the aromatic cage

This means that the cavity of MAO-B is more hydrophobic than B, and additionally smaller in size. This could be one reason why smaller but more non-polar molecules such as benzylamines are MAO-B substrates, but does not seem sufficient to explain such dramatic selectivity differences.

In both cases, the flavin active site is often discussed as bent, which is more commonly associated with reduced flavins. A recent discussion has highlighted the possibility that X-rays themselves could be the culprit for an oxidised flavin appearing non-linear.

X-rays ionisation of H_2O has the potential to generate a free electron capable of reducing the flavin, and in the case of the flavoenzyme NrdI this was shown to be the case by hybrid-DFT calculations and alternate measurements using Raman spectroscopy, and its interactions with X-ray irradiation.[50]

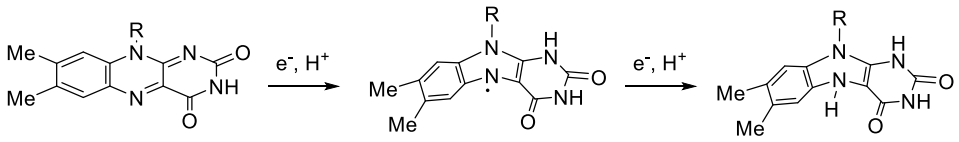

Scheme 17. Interconversion of flavin between redox states by the action of X-ray water ionisation, with consequent bending

1.4 Flavin monooxygenase biomimicry

Naturally occurring flavins such as FMN and FAD have aroused extensive interest in their potential for catalysis in the context of organic synthesis. However, it has been found that in the absence of a protein environment, the hydroperoxides are too unstable to be synthetically useful, instead tending to spontaneously undergo the reverse reaction, eliminating H_2O_2.[51]

The first flavin mimic with a stable hydroperoxide form both for the study of the proposed mechanism of flavin-catalysed reactions and for the use of flavins in synthesis was the flavinium perchlorate **32,** as synthesised by Bruice and Kemal (Scheme 18).[51]

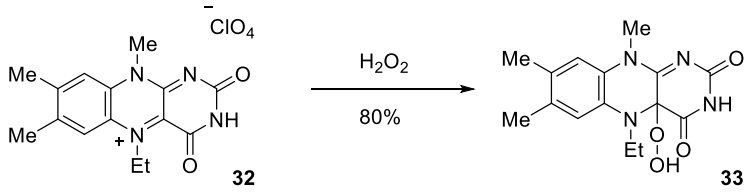

Scheme 18. First synthesis of a flavin hydroperoxide outside of an enzyme

Model flavin hydroperoxide **33** was synthesised and demonstrated to have oxidative activity much stronger than ^{t}BuOOH (factor of ~10^3-10^6) but somewhat weaker than *m*CPBA and other organic peracids (factor of ~10^3) with regard to its activity as an electrophilic oxidant towards sulfides, amines and iodide.

The electrophilic reactions of the hydroperoxide **33** discovered by Bruice are summarised below (Table 1).[52] Sulfides, tertiary amides and iodide ion are readily oxidised to the corresponding sulfoxide, amine *N*-oxide and triiodide respectively.

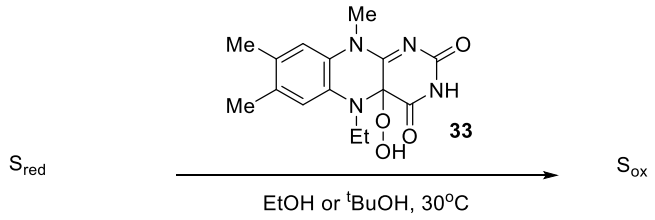

Table 1. Reactions of stoichiometric flavin hydroperoxide **33**

Entry	Reactant	Product	Rate constant / M^{-1} s^{-1}
1	**34a**	**34b**	0.12
2	**35a**	**35b**	0.12
3	I^- **36a**	I_3^- **36b**	6.0

Also observed was the degradation of this hydroperoxide in many cases, especially in chlorinated solvents, to the spirohydantion **37** (Scheme 6).

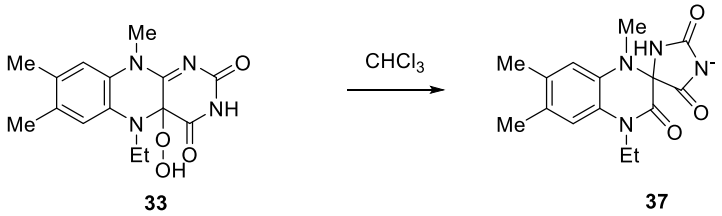

Scheme 19. Rearrangement of flavin hydroperoxide to spirohydantoin in chlorinated solvent

Intermediates of this type were also implicated in the reaction of **33** with alkenes, as a reagent for the formation of epoxides. In $CHCl_3$, some epoxide **40** is formed (Scheme 20) but it is suggested that it is not **33** but decomposition intermediate carbonyl oxide **38** (rapidly formed when **33** is exposed to chlorinated solvent) that performs some epoxidation. The terminal flavin degradation product is spirohydantion **37**.

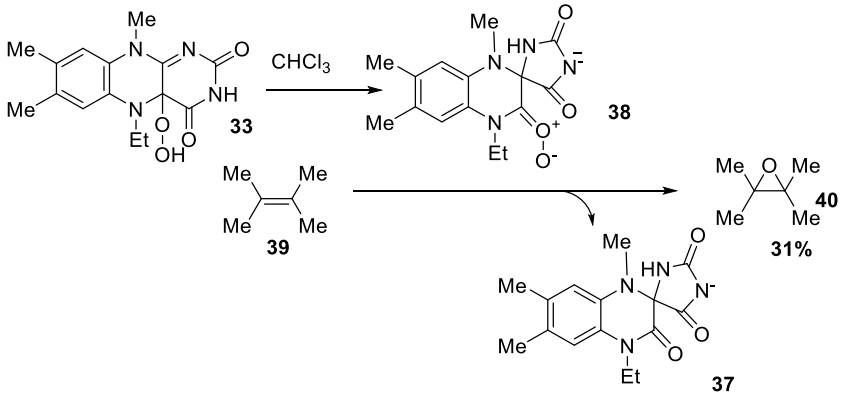

Scheme 20. Epoxidation mediated by spirohydantoin-carbonyl oxide

The hydroperoxide was shown to luminesce on mixture with aldehydes and therefore was the first synthetic analogue of bacterial luciferase. However, conversion of aldehyde to the corresponding carboxylic acids was low (Scheme 21).[51]

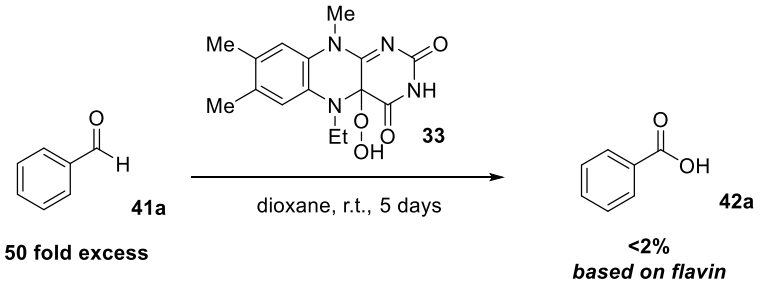

Scheme 21. Chemiluminescent oxidation of benzaldehyde

Oae et al. showed that while the natural flavin monooxygenases are selective for secondary and tertiary amines, flavin hydroperoxide **33** oxidised all types of amine, giving benzaldehyde oxime from benzylamine, hydroxylamines from secondary amines, nitrones from hydroxylamines and amine *N*-oxides from tertiary amines (Table 2).[53]

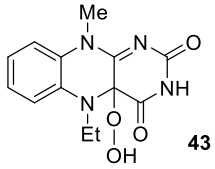

43

Dioxane, 30°C

Table 2. Oxidation of amines by flavin hydroperoxide

Entry	Reactant		Product		Yield/%
1	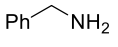	**15a**	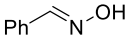	**44**	**90**
2	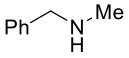	**45a**	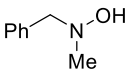	**45b**	**100**
3	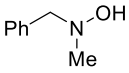	**46a**	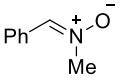	**46b**	**53**
4	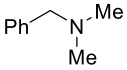	**47a**	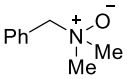	**47b**	**100**

In these cases the flavin hydroperoxides are generated from flavinium salt and H_2O_2, unlike in nature where a reduced flavin reacts with O_2. Therefore, there are two possible pathways for generation of flavin hydroperoxide in synthesis and so two possible catalytic cycles for flavin-catalysed monooxygenase mimcry; one using O_2 and a reducing agent, and one with terminal oxidant H_2O_2 (Scheme 22).

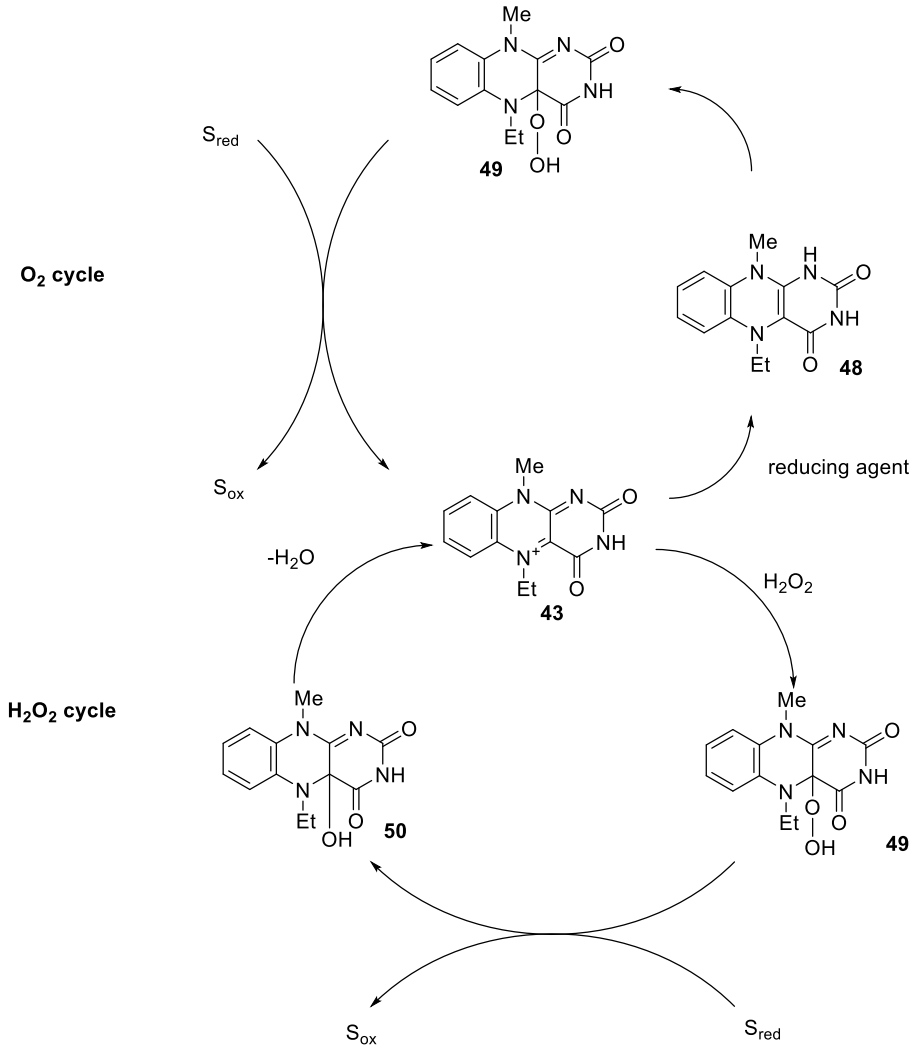

Scheme 22. Two example catalytic cycles for flavin-catalysed oxidation

The first catalytic use of flavins in this manner was reported in 1989 by Murahashi *et al.*, where they demonstrated catalytic oxidation of sulfides using flavinium perchlorate **51** and H_2O_2 (Scheme 23).[54] Secondary amines were also good substrates for the electrophilic oxidation, yielding nitrones in high yields presumably *via* double oxygen addition and elimination.

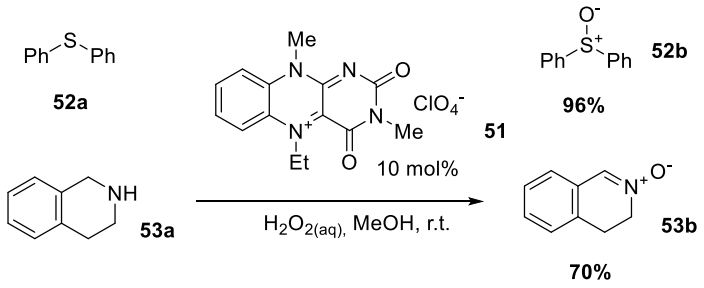

Scheme 23. First examples of flavin/H_2O_2 catalysed sulfide and amine oxidation

The same group later developed the reaction using O_2 as an oxidant and $N_2H_4.H_2O$ to reduce the flavin, giving similar results with the same substrates and a greatly reduced loading of organocatalyst (Scheme 24).[55] In this case trifluoroethanol was an effective solvent; one reason for this was proposed to be the supposed high solubility of dioxygen gas in this solvent.[56] Hydrazine monohydrate was used as a stoichiometric reductant to generate the reduced dihydroflavin which reacts with O_2 to form the flavin hydroperoxide. Only water and molecular nitrogen are by-products of the oxidation.

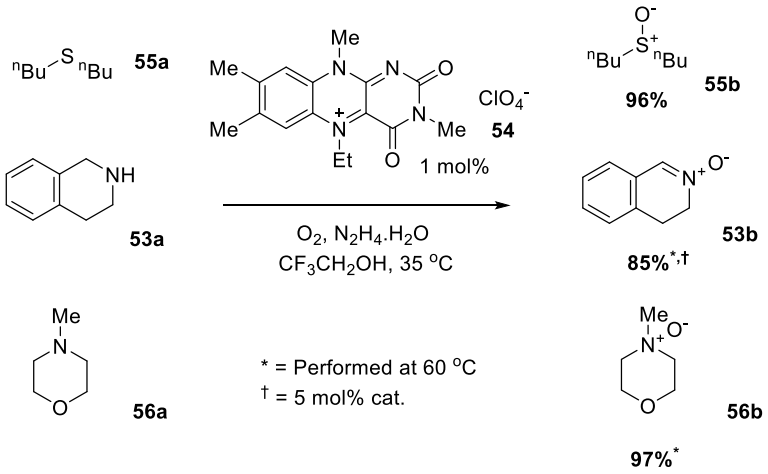

Scheme 24. Examples of aerobic sulfide and amine oxidations using hydrazine and molecular oxygen

Within the Carbery group, bridged flavinium chlorides **57**-**59** have been utilised as an organocatalyst for the synthesis of sulfoxides using H_2O_2 as terminal oxidant (Scheme 25).[57]

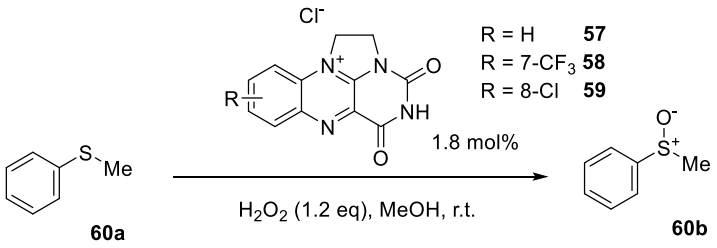

Scheme 25. Bridged flavinium-catalysed sulfoxidation

Electronic factors were seen to be important. aliphatic sulfides or aromatic sulfides with electron donating substituents (e.g. –OMe, -NH_2) were complete in less than 1 h whereas the 4-cyanothioanisole required elevated temperature to complete the reaction. This is consistent with an electrophilic mechanism for oxygen transfer. All three flavinium catalysts tested were effective catalysts, however the 8-Cl derivative **59** was the most effective in this instance. Additionally, methanol was chosen as a solvent because it offered optimum catalyst solubility and thus reproducibility.

The bridged valinol-derived flavinium salt **61** developed by Cibulka was also effective at sulfoxidation with H_2O_2 as terminal oxidant under similar conditions (Scheme 26).[58]

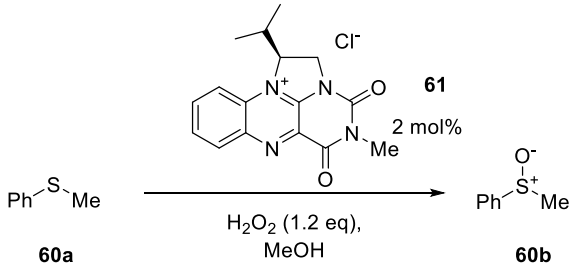

Scheme 26. Valinol-derived bridged flavinium catalysed sulfoxidation

As this flavin contained a stereogenic centre it was hoped to be useful for the synthesis of chiral sulfoxides, especially with evidence for two diastereomers of **62** formed in a 3:1 ratio in favour of *(R,S)*-**62**. However, the highest ee recorded was only 4%.

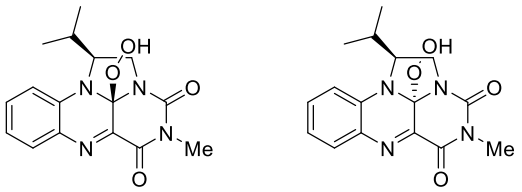

Scheme 27. Two diastereomers of addition product of **61** and H_2O_2

Amine oxidation was also attempted but it was found after conversion to the amine oxide of 18% the flavin was degraded to the bicyclic system **63** under these basic conditions (Scheme 27).

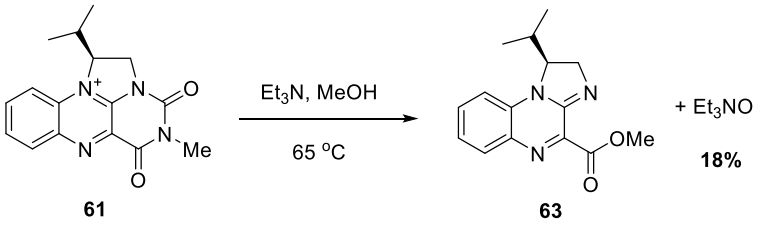

Scheme 28. Degradation product of attempted amine oxidation

More successful was the Bayer-Villiger oxidation of cyclobutanone **64a** to lactone **64b** which proceeded in quantitative yield (Scheme 28.). This is an example of nucleophilic flavin monooxygenase chemistry, presumably assisted by the degree of ring strain in the starting material relieved by Bayer-Villiger oxidation.

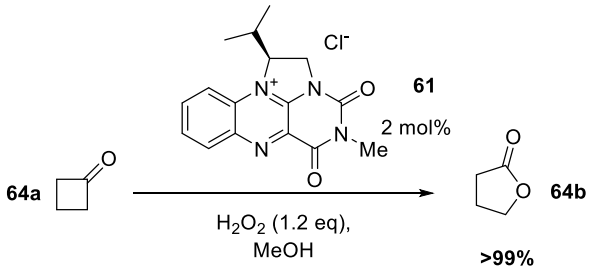

Scheme 29. Bayer-Villiger oxidation of cyclobutanone catalysed by valinol-derived flavinium chloride **61**

More recently, alternative reducing agents for aerobic flavin-catalysed sulfoxidation have been developed including an aqueous variant using ascorbic acid and flavinium perchlorate **54** by Imada and Naota,[59] and formic acid/Et_3N by Murahashi, using flavinium triflate **65** which was also suitable for the oxidation of thiols to disulfides.[60] Importantly the use of salts other than perchlorate makes these flavins more attractive for scaling up, due to the known explosion hazards of perchlorate salts.[61]

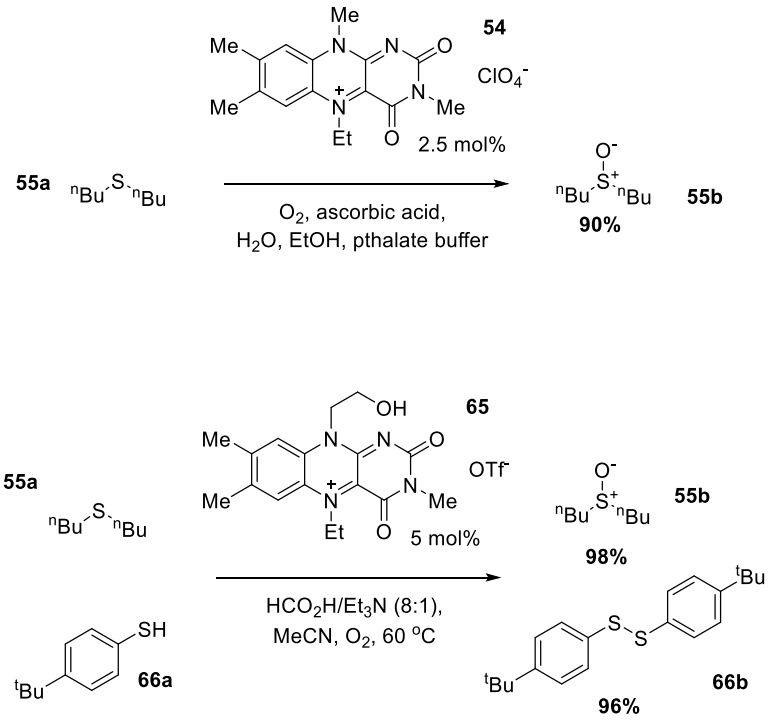

Scheme 30. Formation of sulfoxides using ascorbic acid as reductant, and sulfoxides and disulfides with **65** using HCO_2H/Et_3N respectively

Cibulka developed the aerobic oxidation of boronic acids to the corresponding alcohols using **54** and hydrazine, primarily of phenols from arylboronic acids but with some reactivity for alkyl boronic acids. For substrates incompatible with hydrazine, ascorbic acid could be used alternatively.[62]

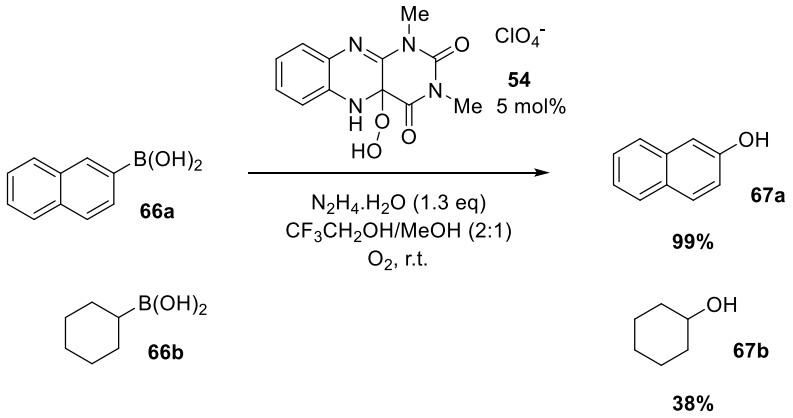

Scheme 31. Flavinium-catalysed aerobic boronic acid oxidation

1.4.1 Nucleophilic reactions of flavin hydroperoxides

As well as oxidation reactions in which the flavin hydroperoxide acts as an electrophile, nucleophilic reactions catalysed by flavins are known. The most well studied of these is the flavinium-catalysed Bayer-Villiger reaction. The Bayer-Villiger reaction is more commonly performed uncatalyzed using organic peracids such as *m*CPBA or peracetic acid, and converts a ketone to the corresponding ester (Scheme 32).

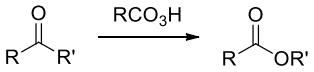

Scheme 32. A typical Bayer-Villiger Oxidation

Flavinium perchlorate **68** was shown by Mazzini to catalyse the Bayer-Villiger reaction of cyclobutanone **69** to lactone **70**, with H_2O_2 as terminal oxidant. The corresponding lactones were produced in good yields (Scheme 33). [63]

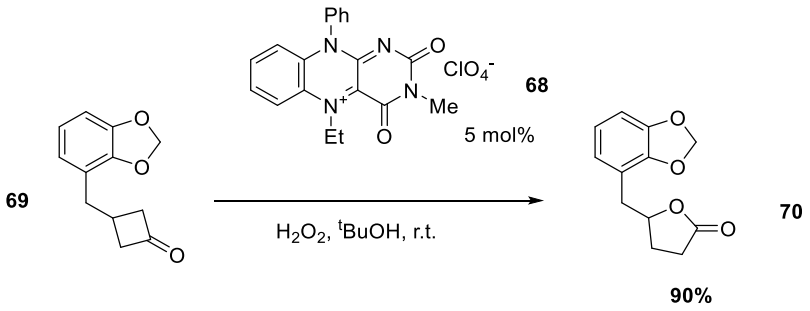

Scheme 33. flavinium-catalysed Bayer-Villiger oxidation of cyclobutanones

The proposed mechanism of this reaction is as follows, and invokes the presence of the *nucleophilic* flavin hydroperoxide **72** (Scheme 34).

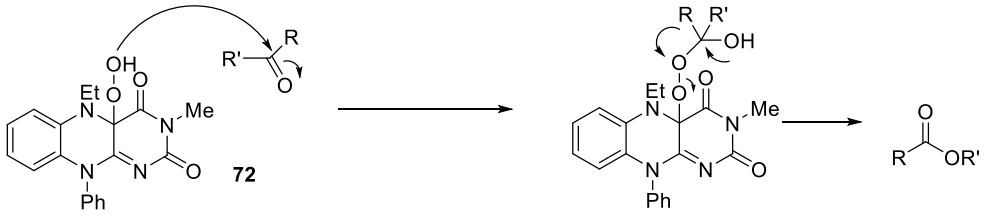

Scheme 34. Flavin-catalysed Bayer-Villiger oxidation: proposed mechanism

Murahashi and co-workers also prepared semi-synthetic flavinium perchlorate **73** (three steps from natural (-)-riboflavin) and used this to effect aerobic Bayer-Villiger oxidation of **74** to **75** with O_2 and metallic zinc as the flavin reductant (Scheme 35).[64]

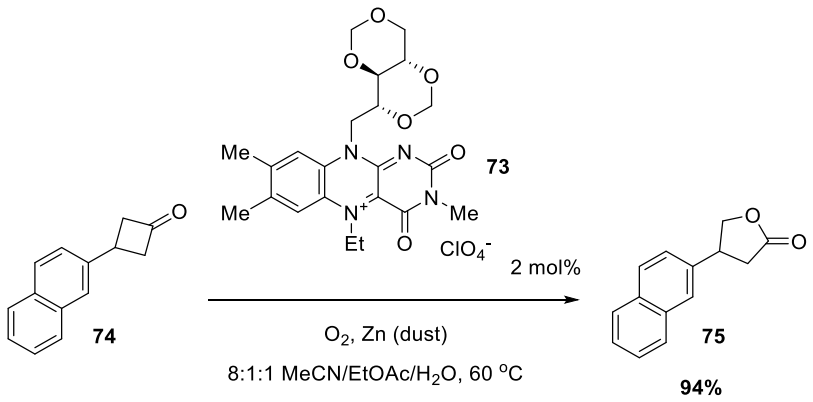

Scheme 35. Aerobic Bayer-Villiger oxidation using flavinium catalyst **73**

The authors observe a remarkable preference for nucleophilic over electrophilic oxidation under these conditions (Scheme 36), with almost exclusive Bayer-Villiger oxidation occurring in competition experiments, even when paired with very easily oxidised species such as **76a**.

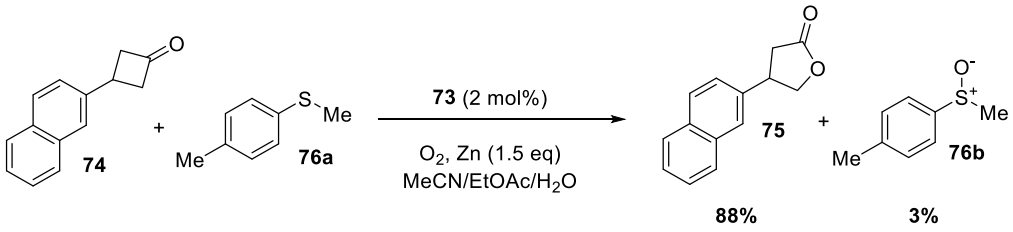

Scheme 36. Competition experiment to probe nucleophilic vs. electrophilic flavin hydroperoxide reactivity

Interestingly, the selectivity is reversed when **73** and H_2O_2 are used, or Zn/O_2 conditions used in a protic solvent such as CF_3CH_2OH. This is rationalised by the requirement for an *anionic* flavin peroxide of the form $FlOO^-$, which is strongly nucleophilic and unlikely to act as an electrophile in heteroatom oxidations such as sulfoxidation. Acidic solvent generates the hydroperoxide and so allows electrophilic oxidations.

Recently, the scope of this Baeyer-Villiger type reaction was extended by Foss and co-workers with their flavin-catalysed Dakin oxidation of electron-rich aldehydes such as **78** to catechols (**79**) with H_2O_2 using flavin hydroperoxide **77** (Scheme 37).[65]

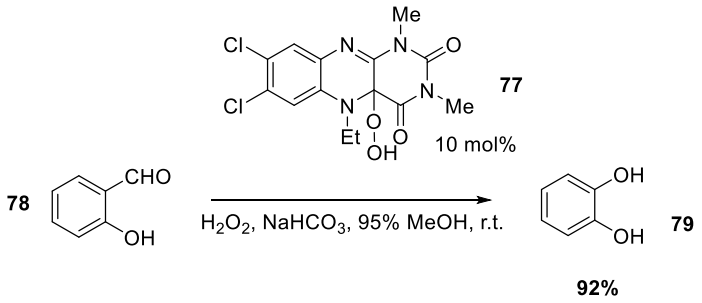

Scheme 37. Aerobic Dakin oxidation of aldehyde **78** to catechol **79**

The phenol comes from a Baeyer-Villiger type mechanism through intermediate **79'** followed by loss of formate (Scheme 38).

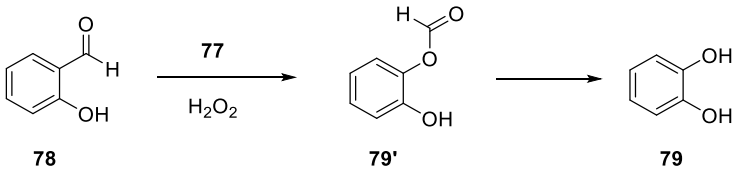

Scheme 38. Mechanism of flavin-catalysed Dakin oxidation

Although one example of a zinc-mediated reduction of the flavin and aerobic oxidation to the flavin hydroperoxide and subsequent aldehyde oxidation was demonstrated in this work, Foss later encountered problems with formation of zinc bisphenolates and thus turned to an alternative reducing agent, the Hantzch ester **81**.[66] Interestingly this is perhaps one of the more truly 'biomimetic' systems studied, as the Hantzch ester is somewhat similar to the NADH cofactor which usually performs flavin reduction in FMOs *in vivo*.[67]

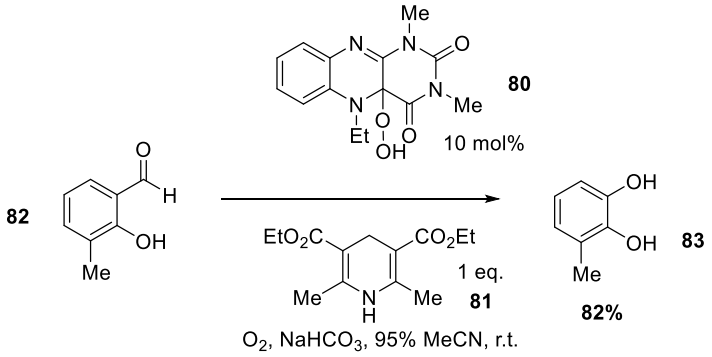

Scheme 39. Aerobic Dakin oxidation using NADH mimic **81**

There is a change in electronic properties of the flavin between these two manuscripts (7,8-dichloro flavin peroxide **77** to 7,8-dihydro flavin peroxide **80**). While the peroxyflavin intermediate is stabilised by electron withdrawing groups, the rate of O_2 reoxidation of reduced flavin is lowered by these.[68,69] Therefore, which H_2O_2-mediated Dakin oxidations can be performed with the most electron withdrawing of flavin substituents, when O_2 is used as terminal oxidant, a balance between these factors must be considered.

1.5 Flavin oxidase biomimicry

An early attempt to model a flavin oxidase enzyme in the ground state was by Mariano and co-workers, with the oxidative deamination of benzylamine **15a** to imine **85a** by both **54** and neutral 3-methyllumiflavin **84**, the latter promoted by Brønsted or Lewis acids at elevated temperature (Scheme 40).[70]

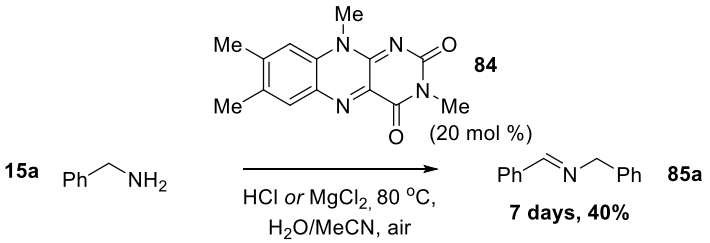

Scheme 40. MAO mimicry: oxidase chemistry using flavin **84**

The authors state that the reaction works in the dark (unlike a similar photocatalysed room temperature version within the same group).[71] They find the N5-ethyl perchlorate performs similarly, indicating that H^+/$MgCl^+$ performs a similar role to alkylation. Additionally, **86** can be formed at r.t. between **15a** and **54** (Figure 10); this forms aldimine and reduced flavin upon heating in the presence of more free amine. This is stated as evidence for Edmondson's nucelophilic model of MAO mechanism.[32]

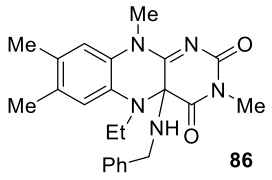

Figure 10. Proposed intermediate in amine dehydrogenation

To overcome problems of low ground state reactivity, other flavin have been developed for oxidase mimicry such as the ethylene-bridged flavinium chlorides **57**, **58** and **59** developed by Sayre (Figure 11).[68]

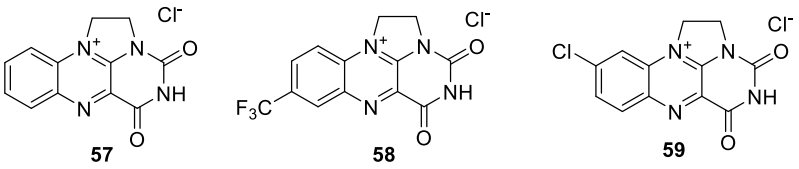

Figure 11. Bridged flavins **57**-**59** developed by Sayre

Sayre describes these species as '*bridged high-potential flavins'* due to their increased ground state reduction potential, and they were used for dehydrogenation of various species such phenylhydrazine, thiols and amines (Scheme 9), using stoichiometric flavin except in the case of the amine where 18% catalyst loading was used and some modest turnover achieved.

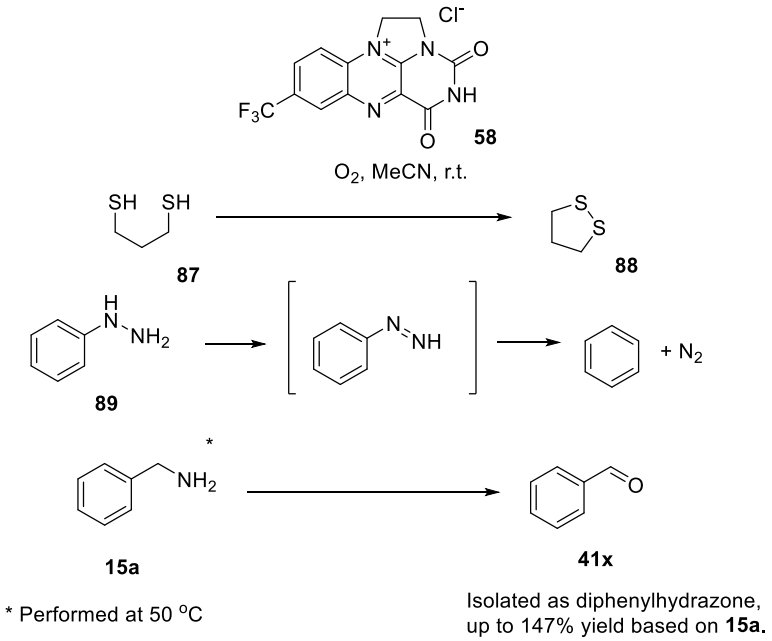

Scheme 41. Reactions mediated by bridged flavin **58**

Synthesis of ^{13}C-enriched analogues of **c** and subsequent *in situ* ^{13}C NMR spectroscopy of the reaction of benzylamine with **90** and **91** elucidated the mechanism of this reaction proceeding *via* a C10-amine adduct (Scheme 42).[72]

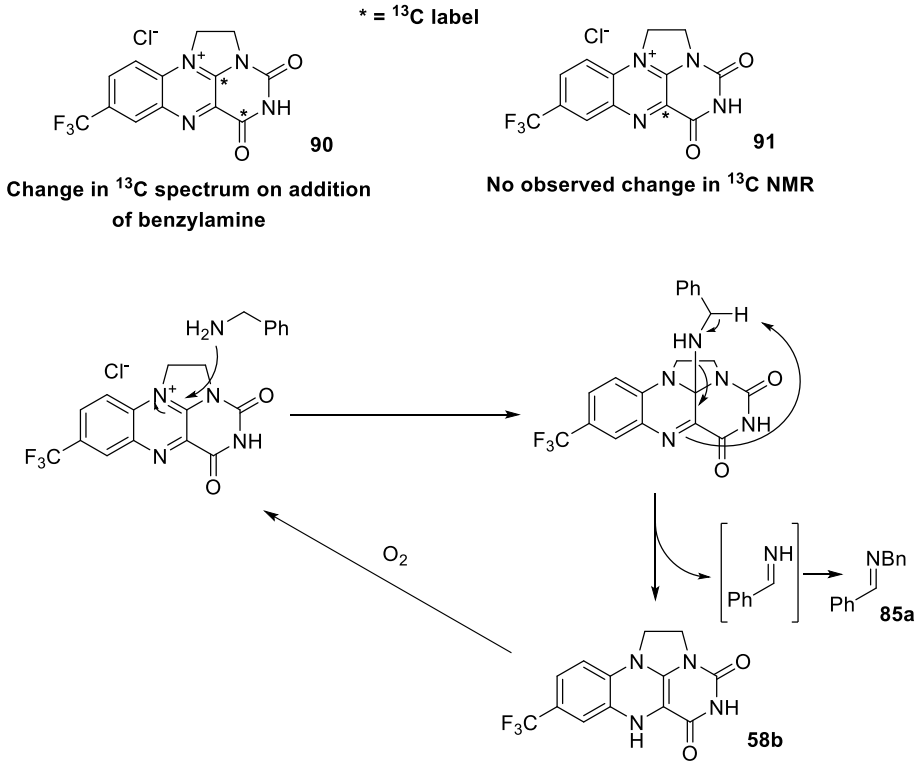

Scheme 42. Amine oxidation with catalyst **23**

Sayre suggests that the limitations of this reaction are the slow reoxidation of **58b** to the oxidised catalyst (as opposed to **57**, which is more rapidly oxidised but less electrophilic so slower to accept benzylamine), and the competing degradation to spirohydantoin **92** (Figure 12). Decomposition to the spirohydantoin was also noted as a possible limitation by Mariano.[70]

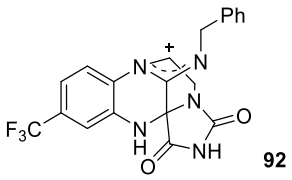

Figure 12. Spirohydantoin-amidine adduct side product of amine oxidation

Foss and co-workers achieved dehydrogenation chemistry based on their work with the Hantzch ethyl ester **81**, achieving oxidative aromatisation of dihydropyridines and benzothiazolines, forming pyridines and benzothiazoles respectively. This could also be performed in a one-pot fashion; condensing the required partially saturated heterocycle *in situ* and then performing the oxidation (Scheme 43).[73]

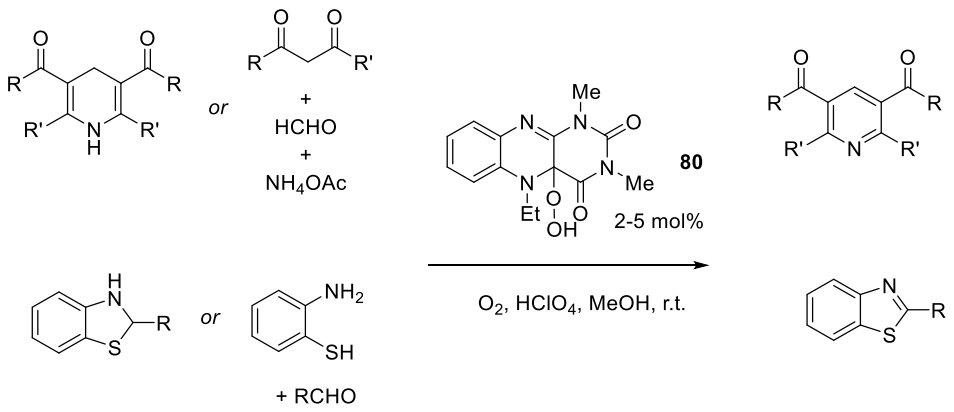

Scheme 43. Oxidative aromatisations of dihydropyridines and benzothiazolines catalysed by **80**

The perchloric acid is a key additive in this case; helping to 'shunt' loss of H_2O_2, removing it from the system and allowing turnover.

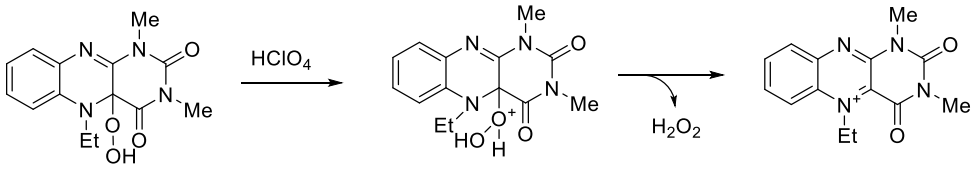

Scheme 44. $HClO_4$-promoted removal of H_2O_2 allows catalytic turnover

1.5.1 Photochemical flavin-catalysed oxidation

Another method of performing dehydrogenations of amines and alcohols using flavins is by irradiation in order to access excited states and increase the reactivity of the flavin.

Flavins can form an excited state by irradiation with visible light, usually a 440 nm LED.[74] This 'excited state flavin' is a much stronger oxidant than the flavin in its ground state and so can more readily oxidise a desired substrate, leaving the reduced flavin which is air oxidised. The overall reaction gives a two electron oxidation of the substrate and reduction of O_2 to H_2O_2.

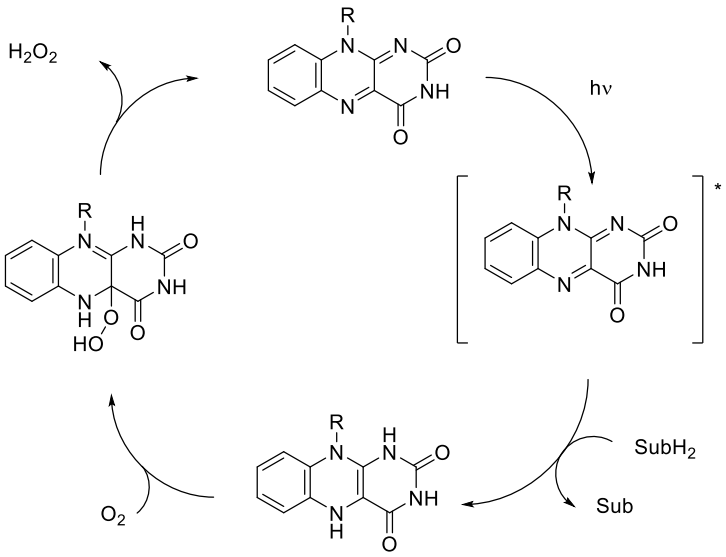

Scheme 45. General mechanistic pathway for photoassisted dehydrogenation chemistry catalysed by a flavin

Flavin-catalysed photooxidation of amines has been developed using tetraacetylriboflavin **93** and visible light to perform this transformation using air as terminal oxidant. Selective debenzylation of benzyl amines, such as amino acid derivative **94** was also accomplished.[75]

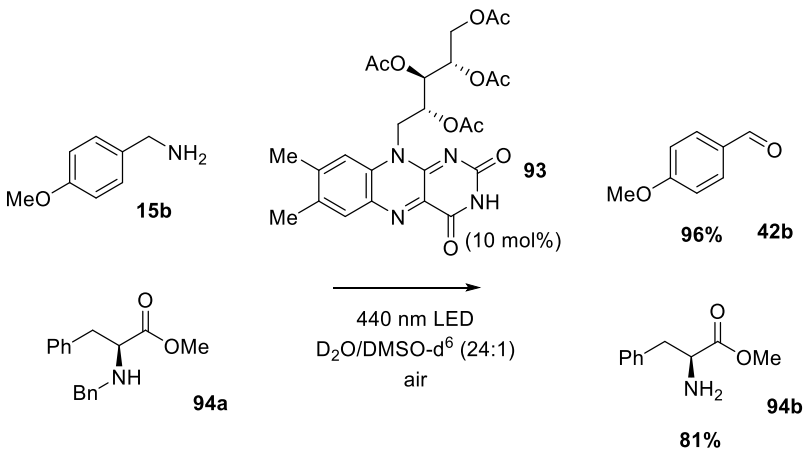

Scheme 46. Oxidative deamination of benzylamines and oxidative debenzylation of amines using photoexcited flavin **93**

The photooxidation of alcohols to aldehydes was also achieved *via* flavin photocatalysis. The presence of a thiourea moiety within the flavin greatly enhanced the activity of the catalyst. This was proposed to be due to a hydrogen bonding interaction, reversibly binding the substrate and making subsequent electron transfer events effectively intramolecular.

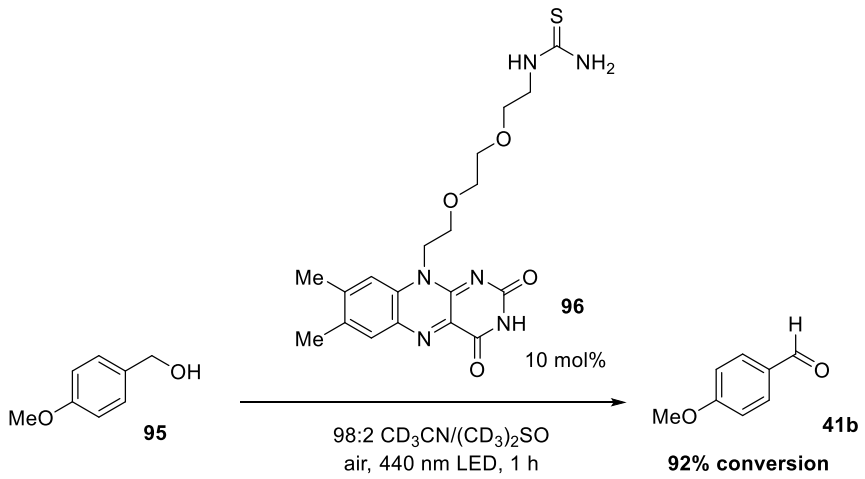

Scheme 47. Thiourea-substituted flavin alcohol oxidation

Expanding on this work, a range of benzylic alcohols were photooxidised using riboflavin tetraacetate immobilised on fluorinated silica gel, although only electron rich alcohols reacted very effectively.

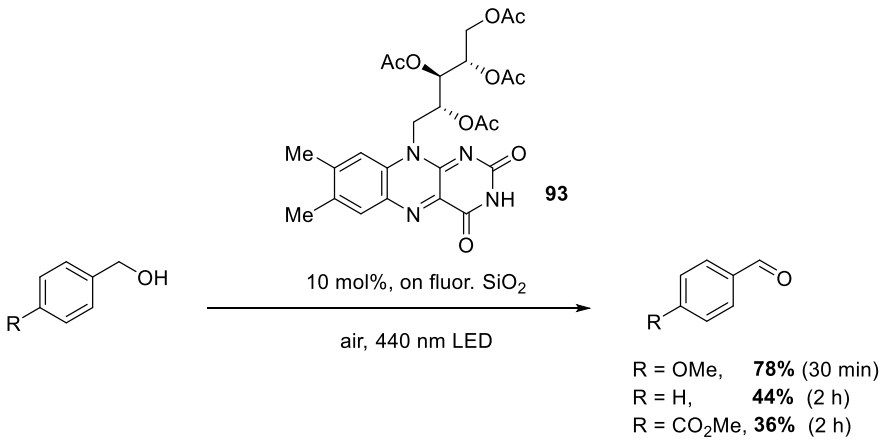

Scheme 48. Heterogeneous flavin-catalysed alcohol oxidation using a fluorous SiO_2 stationary phase

1.6 Tandem Flavin catalysis

Alkene dihydroxylation is a ubiquitous transformation in organic synthesis. The most popular reagent is OsO_4, which is a highly toxic and volatile metal oxide. Initially used stoichiometrically, the reaction was made catalytic in osmium reagent by use of *N*-methylmorpholine oxide (NMO) as terminal oxidant by the Upjohn company, and Sharpless later developed the Nobel-prize winning asymmetric version using quinine-derived ligands.[76,77]

As NMO can be produced from the corresponding amine by the action of flavin hydroperoxide, Bäckvall and co-workers used **97** and H_2O_2 as a terminal oxidant to develop a highly atom economical dihydroxylation both in the presence and absence of Sharpless chiral ligands (Scheme 18).[78] This is an improved procedure in terms of atom economy from the usual dihydroxylations which use either stoichiometric NMO or $K_3Fe(CN)_6$.

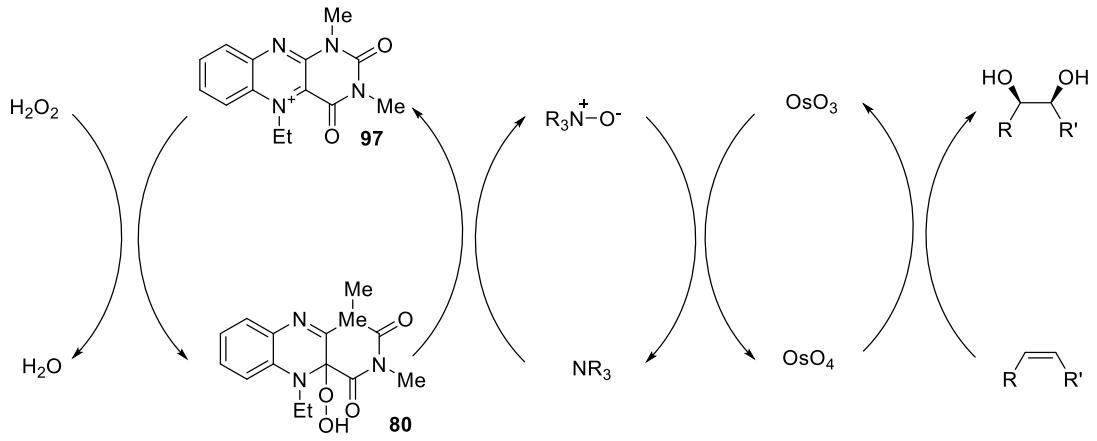

Scheme 49. Flavin-co-catalysed *syn*-dihydroxylation

Another example of a flavin-co-catalyzed reaction is the use of flavins with *N*-heterocyclic carbenes (NHCs) as co-catalysts for oxidation of aldehydes. The reaction is proposed to occur by firstly forming the aldehyde-NHC adduct (acyl anion equivalent) and subsequent oxidation of the formed carbanion by the oxidised flavin.[79] Formed products were either the acid, or when reaction was performed in alcoholic solvent or the presence of an alcohol, the ester. This reaction mimics the action of flavin pyruvate oxidase, which uses both thiamine; the natural thiazolium NHC-like cofactor, together with an additional flavin cofactor.[80]

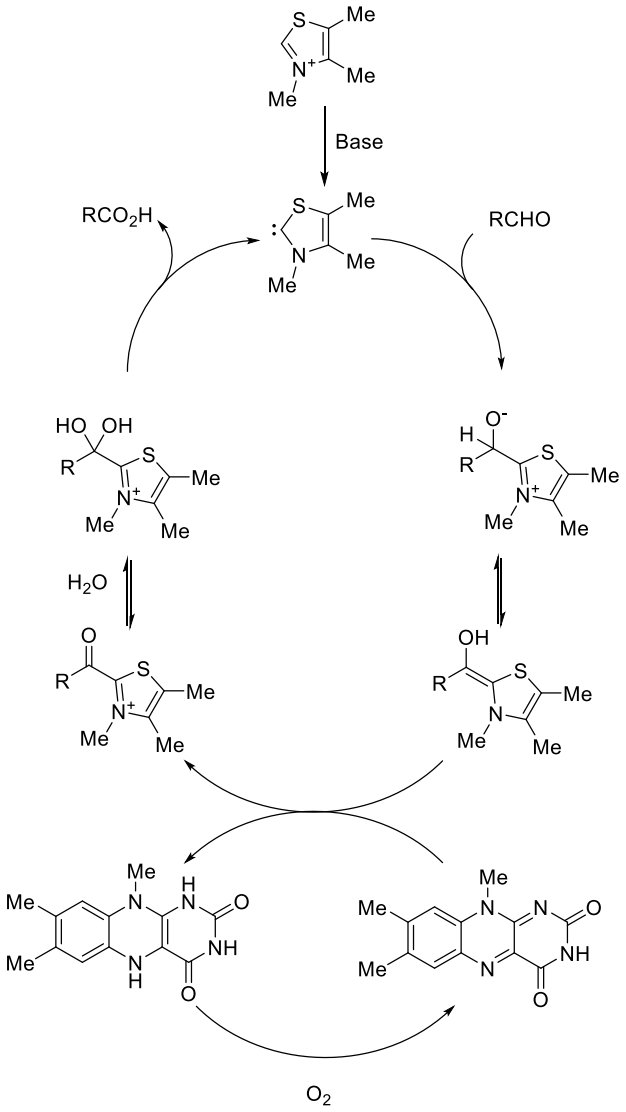

Scheme 50. Proposed mechanism for flavin/NHC catalysed aldehyde oxidation

An example of this was the oxidative esterification of benzaldehyde performed using flavin **84** and imidazolium iodide **98**.[81]

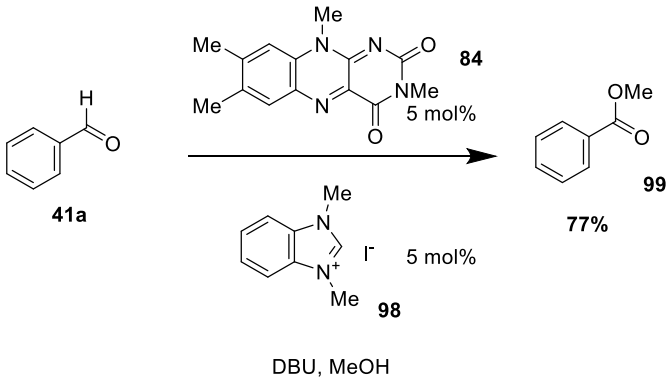

Scheme 51. Oxidative esterification of benzaldehyde using **84** and **99**

Additionally, the authors found that they could synthesise a single 'flavin-imidazolium' catalyst **100** which was active in the same reaction (yield of PhCHO = 42%).

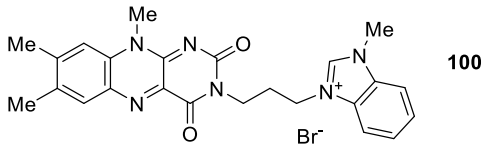

Figure 13. Flavin-NHC catalyst **100**

Diederich reported an electrochemical catalytic variant using an electrochemical method to induce flavin turnover. Aromatic aldehydes reacted well, but yields of aliphatics were poor, presumably due to competing formations of acetals and hemiacetals.[82]

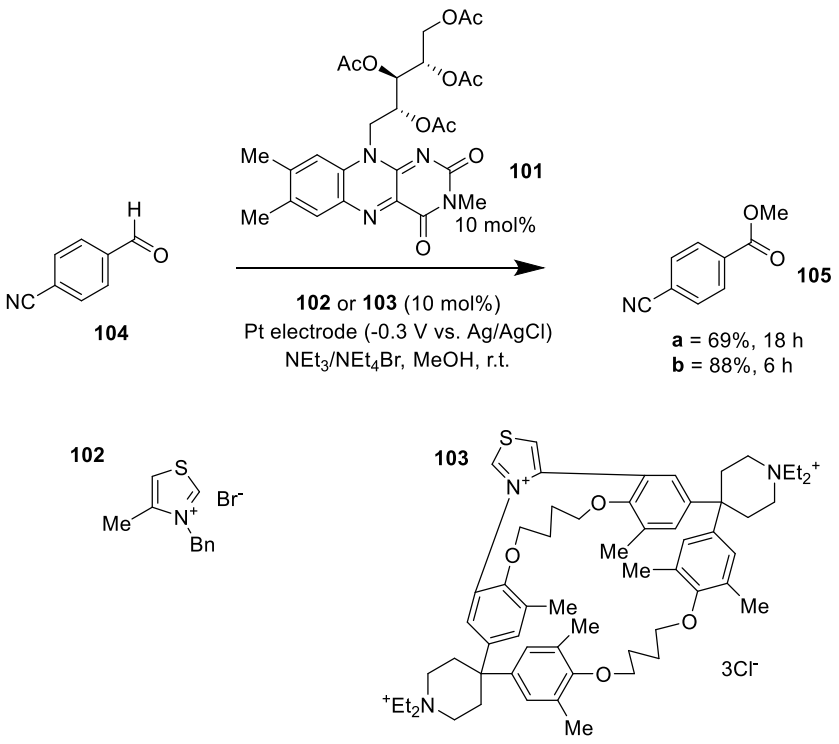

Scheme 52. Electrochemical tandem flavin/NHC catalytic oxidation using thiazolium **a** or macrocyclic thiazolium **103**

Notably, time taken to oxidise **104** was enhanced by the use of the cyclophane-like NHC macrocycle **103** in place of **102**, probably due to non-covalent complexation of the aryl aldehyde substrates. Alkyl aldehydes were poor substrates presumably due to hemiacetal formation; additionally the choice of small molecule or macrocyclic NHC had little effect in this case.

Building on this work, Iida and Nashima developed a variant using air as terminal oxidant and the chiral NHC **107** which was applied to the oxidative esterification and thioesterification of aldehydes with racemic secondary alcohols which underwent a concurrent kinetic resolution reaction.[83]

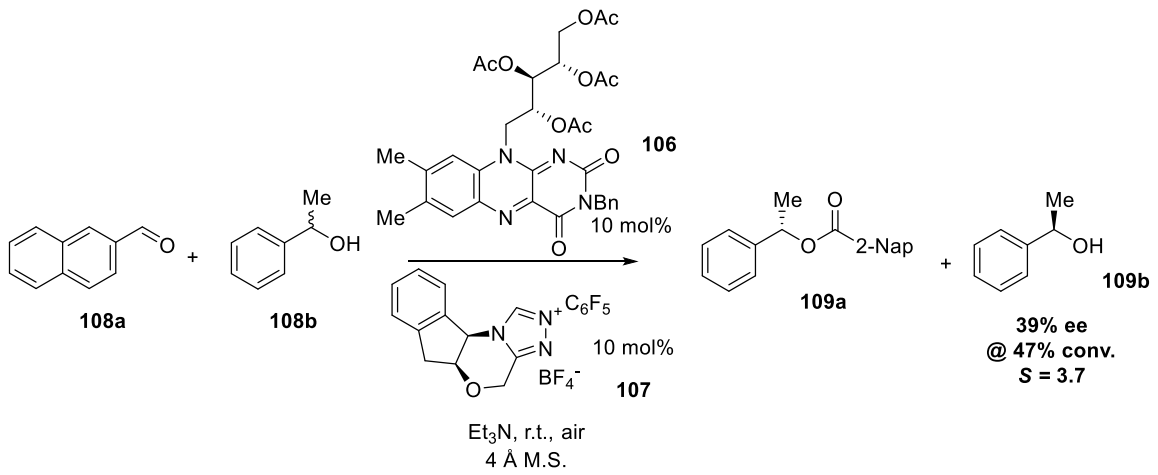

Scheme 53. Kinetic resolution of alcohols by tandem flavin/NHC oxidative esterification with aldehydes

Thioesterification and amidation were also possible but minimal enantioselectivity was observed in these cases. Another point of interest was the ability, utilising the NHC catalyst, to perform a tandem benzoin condensation/oxidative esterification reaction, with asymmetric benzoin reaction of benzaldehyde under nitrogen followed by exposure to air to form the product **111** (Scheme 54).

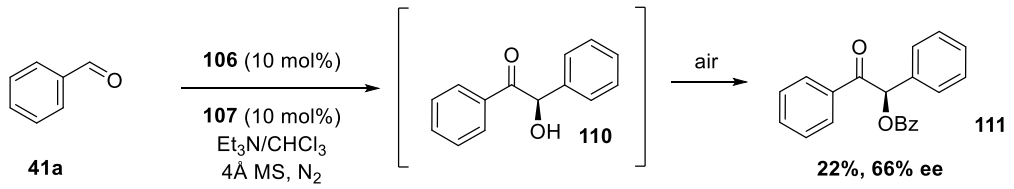

Scheme 54. Tandem asymmetric benzoin condensation/oxidative kinetic resolution

The benzoin reaction produces mainly *R*-benzoin, but the oxidative esterification is selective for the *S* product. For this reason, a moderate ee is observed for the ester **111** but a small (0.6%) amount of benzoin **110** is obtained with very high enantiopurity (98%).

1.7 Asymmetric flavin catalysis

The first example of asymmetry in flavin catalysis was the cyclophane-derived flavin **112**, found by Shinkai to oxidise sulfides to sulfoxides using H_2O_2 as terminal oxidant (Scheme 55). The cyclophane bridge is thought to block one face of the flavin so oxygen can be delivered only from one side. The maximum ee obtained with this system was 65%. The electrophilic character of oxidation can be seen by the very low reactivity of 4-cyanothioanisole.[84]

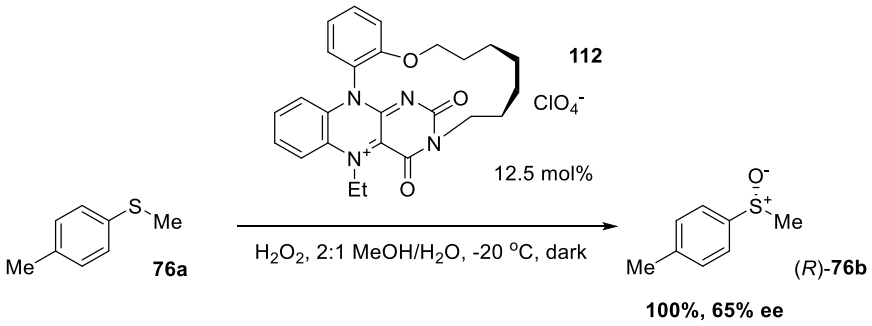

Scheme 55. Flavinium cyclophane used for asymmetric sulfoxidation

Additionally, asymmetric flavin oxidations were achieved by Cibulka and co-workers using the planar chiral catalyst **113** to oxidise sulfides to sulfoxides with ee of up to 54% (Scheme 56).[85]

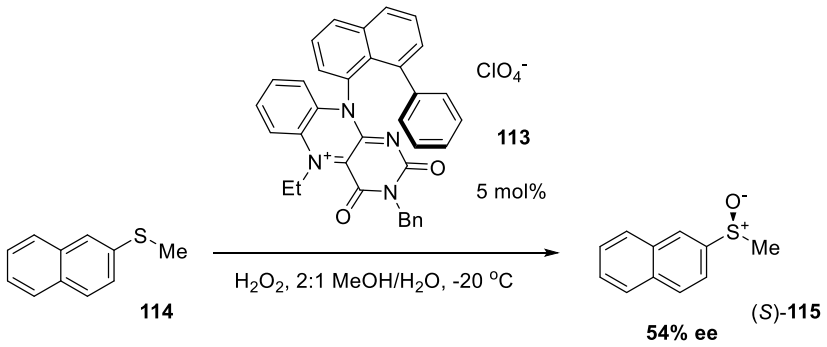

Scheme 56. Planar-chiral flavinium salt used for asymmetric sulfoxidation

Asymmetric sulfoxidation was also achieved by Yashima using a polymeric flavin catalyst **116** with hydrogen peroxide as oxidant in THF at low temperature.[86]

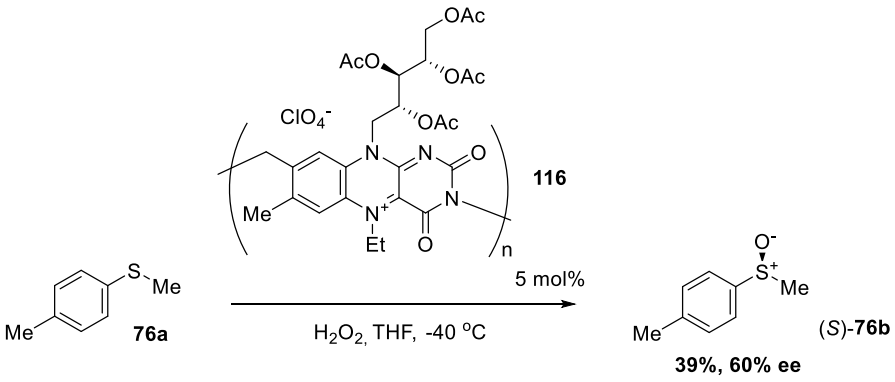

Scheme 57. Optically active riboflavin polymer used for asymmetric sulfoxidation

The polymeric flavin chain was proposed to be helically twisted pairs of stacked riboflavin sheets based on NOE observations and circular dichroism spectroscopy. The polymeric form had much higher enantioselectivity than the analogous flavinium monomer, showing the influence of supramolecular chirality on the reactivity.

This polymeric flavin could also be used for the vapochromic recognition of primary and secondary amines, with common low-molecular weight amine vapours such as isopropylamine and diethylamine causing a colour change from purple to yellow, which could be reversed by treatment with perchloric acid.

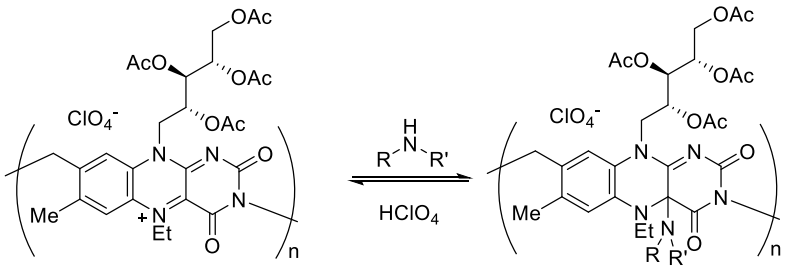

Scheme 58. Riboflavin polymer used for reversible amine sensing

Asymmetric oxidation was also achieved for nucleophilic flavin catalysis, using the chiral bisflavin **117** for Baeyer-Villiger oxidation with up to 74% ee (Scheme 59). Each flavin moiety in the C_2-symmetric bisflavin blocks the face of the other, thus engendering selectivity. [87]

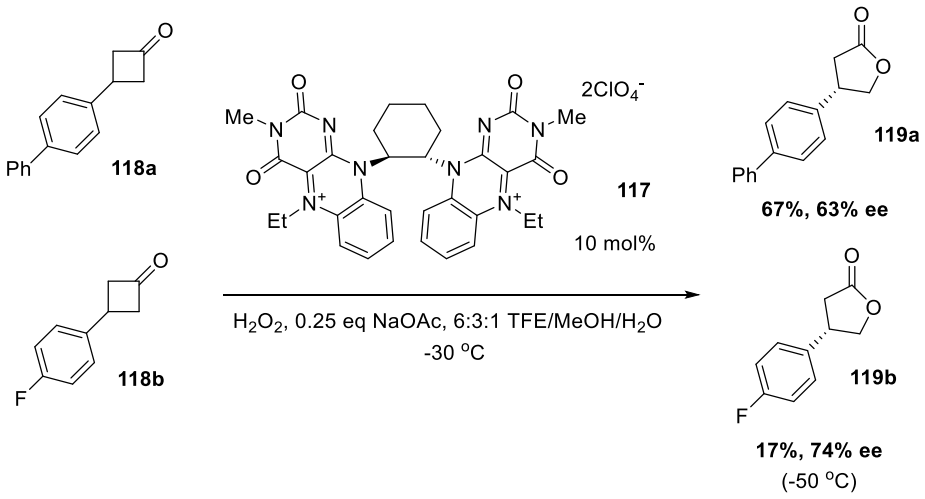

Scheme 59. Asymmetric Bayer-Villiger reaction using C_2-symmetric chiral bisflavin **117**

Trifluoroethanol enhances the rate, but unfortunately also the rate of the background reaction of H_2O_2-mediated processes,[88] so a mixed solvent system was used, with MeOH promoting higher enantioselectivities but leading to somewhat slower reactions.

1.8 Flavin-catalysed diimide hydrogenation

The selective reduction of alkenes is an ongoing challenge in synthetic chemistry, particularly by methods that do not rely on transition metals or hydrogen gas.[89] One example of such a metal-free hydrogenation is a diimide reduction, whereby the reactive diazene transfers hydrogen to an alkene, with the driving force being the production of nitrogen gas.[90]

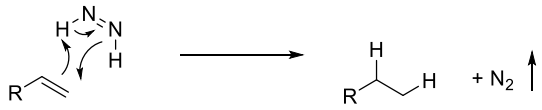

Scheme 60. Example of a diimide hydrogenation

Various methods for the generation of diimide have been developed, particularly by decomposition of an arylsulfonyl hydrazide.[91,92]

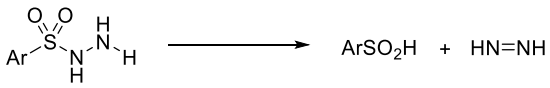

Scheme 61. Generation of diimide from arylsulfonyl hydrazide

However, an ideal entry to diimide hydrogenation would be to generate diimide from hydrazine itself by oxidation, a method offering much higher atom economy.

Imada developed the first flavin-catalysed hydrogenation using hydrazine and dioxygen to form the diimide (Scheme 62). This process is notable for being a rare example of a hydrogenation performed under an atmosphere of oxygen.[93]

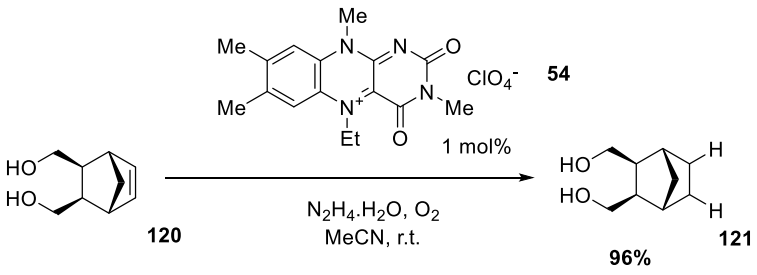

Scheme 62. Flavin-catalysed alkene hydrogenation by diimide generation

This process showed remarkable selectivity for hydrogenation over oxidation processes that occur under similar conditions using the allyl sulfide **122b**[55], forming propyl phenyl sulfide **123b** except when trifluoroethanol was used whereby the acidic reaction medium deactivates hydrazine and thus allows oxygenation to occur, forming **123b'**.

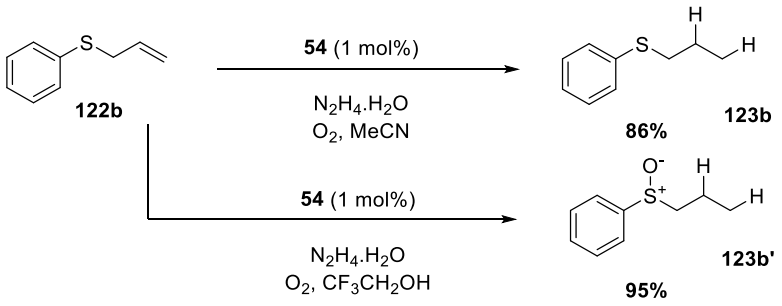

Scheme 63. Solvent selectivity for sulfoxidation/hydrogenation vs. hydrogenation only

Minaard developed an alternative flavin active in hydrogenation reactions, the reductively alkylated flavin **124** derived in only one step from riboflavin. This catalyst also effectively promoted a series of alkene reductions, also tolerating oxidisable functional groups and benzyl ethers such as **125**, the latter of which would be unstable to transition metal catalysed hydrogenation methods.

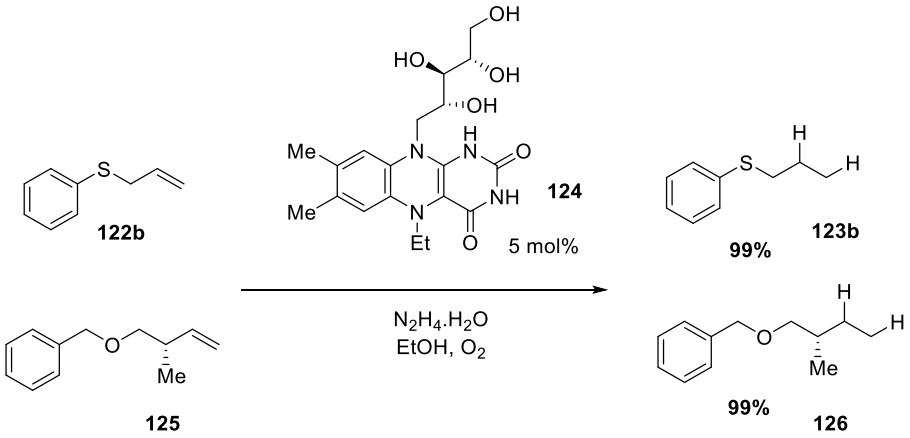

Scheme 64. Reduced riboflavin as a hydrogenation catalyst

Imada also evaluated a series of neutral flavins in their activity as hydrogenation catalysts. While none were as effective as the flavinium perchlorate **54**, the neutral flavins are considerably easier to synthesise, store and handle, making their use still attractive in this context (Scheme 65). Only neutral riboflavin **1** failed to react, due to its low solubility in organic solvents.[94]

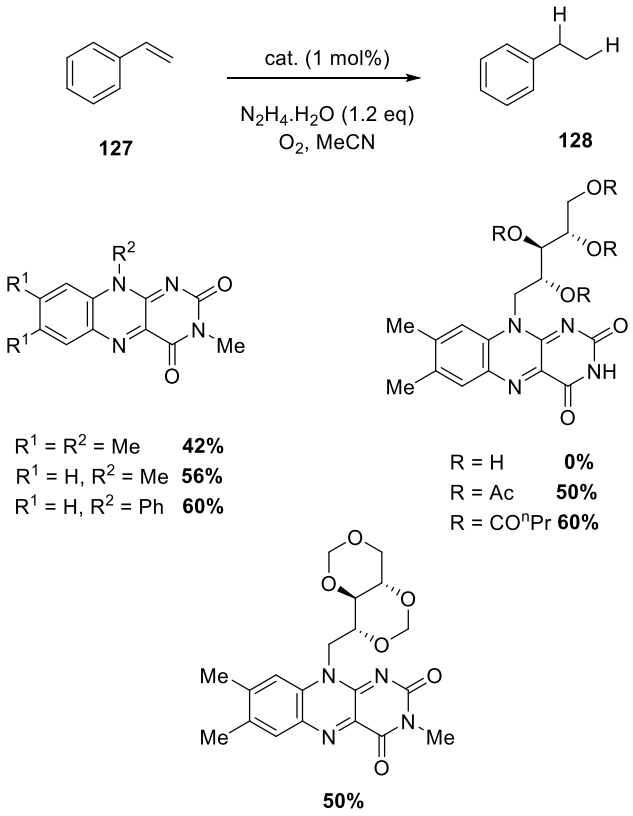

Scheme 65 Selection of neutral flavins active in reduction of styrene.

In this case, the greater stability of neutral flavins allowed catalyst recycling for up to three cycles of hydrogenation, *via* organic-organic (hexane/MeCN) liquid-liquid extraction, to remove the non-polar alkanes and reuse the flavin.

While the first examples of this reaction reduced generally neutrally polarised or electron deficient alkenes,[94,95] the bridged flavins were found capable of reducing electron-rich alkenes such as enamides **129a-b** (Scheme 66).[96]

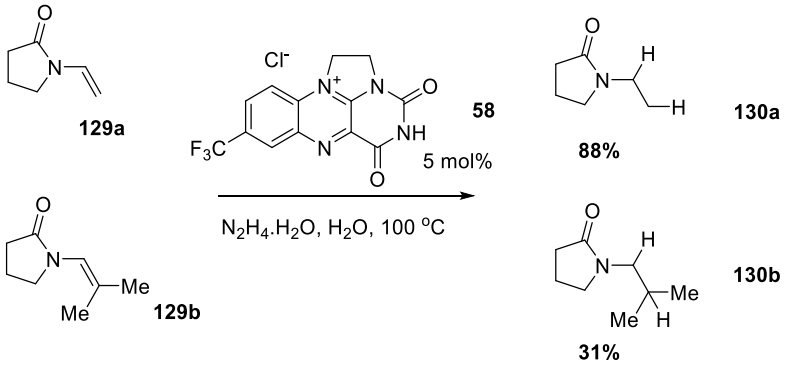

Scheme 66. Flavin-catalysed hydrogenation of electron rich alkenes

Interestingly, in this case, reaction occurred not at all, or only sluggishly, in solvents examined by Imada such as MeCN, whereas in water at reflux reaction was relatively facile. Substrate scope was good, with even trisubstituted alkenes reacting in moderate yield.

2 Flavin-catalysed aldehyde oxidation

2.1 Introduction

The use of flavinium catalysis has been previously explored in the group both in electrophilic reactions with sulfides, and with generation of diimide from hydrazine and subsequent reduction of electron-rich alkenes.[57,96]

It was intended to use flavinium catalysis in further oxidative transformations. One possibility was for the flavin hydroperoxides to generate hypervalent iodine species. These could then react with a substrate in a dual organocatalytic process.[97]

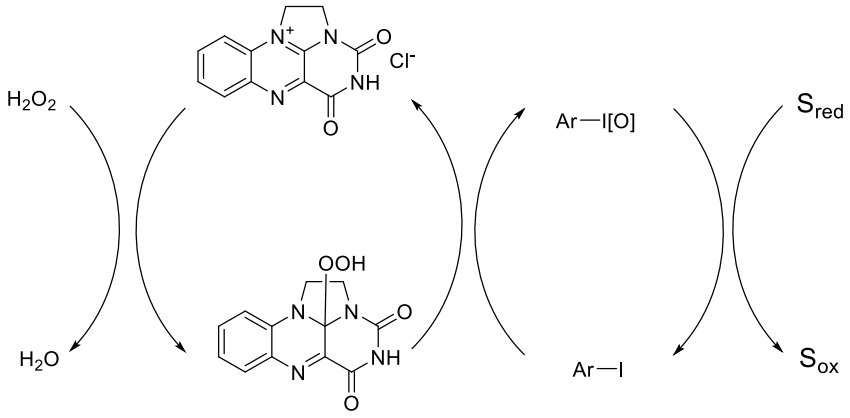

Scheme 67. Proposed tandem catalytic mechanism with flavin and hypervalent iodine reagent

There is precedent for reactions generating catalytic amounts of hypervalent organoiodines; either IBX or iodine(III) species, using Oxone® or *m*CPBA as a terminal oxidant.[98,99] Given the flavin hydroperoxides are known to have a much greater oxidation potential than H_2O_2 alone, we proposed this system would possess sufficient oxidising power to complete the described tandem catalytic cycle. Key advantages of the use of H_2O_2 as a terminal oxidant would be greter atom economy and elimination of waste, and the substoichiometric generation of an oxidant such as IBX would obviate its poor solubility profile.[100]

Furthermore, precedent for this transformation included Bruice's observation that flavin hydroperoxides are efficient oxidants for I^- to I(O).[52] We thus considered the possibility that this could be applicable to organoiodides.

Additionally, we considered the potential scope for further investigation of nucleophilic flavin catalysis. While flavin-catalysed Bayer-Villiger reaction is well known,[63] flavins are known in nature to selectively oxidise long chain aldehydes to the corresponding carboxylic acids, in a process thought to be mechanistically similar to the Baeyer-Villiger reaction.[15] While this has been demonstrated by Bruice on an analytical scale with low, substoichiometric efficiency, there have been no previous examples of this reaction in the context of an efficient synthetic transformation.[101,102]

2.2 Initial explorations and focus on aldehyde oxidation

Flavinium chlorides **57-59** were selected, as developed originally by Sayre and subsequently used in our group, as suitable oxidation catalysts.

Firstly, the flavinium chlorides **57** and **58** were synthesised by a four-step process that could be easily telescoped, starting from S_NAr substitution of electron deficient aryl chlorides and fluorides **131** and **132** with ethanolamine **133**. Transfer hydrogenation of formed nitroanilines **134** and **135** with ammonium formate and Pd/C (which must be in the Pd(0) state) gave dianilines **136** and **137**. Subsequent condensation with alloxan monohydrate **138a** followed by $SOCl_2$-mediated cyclisation to yield the flavin mimics **57** and **58** used in this series of studies.

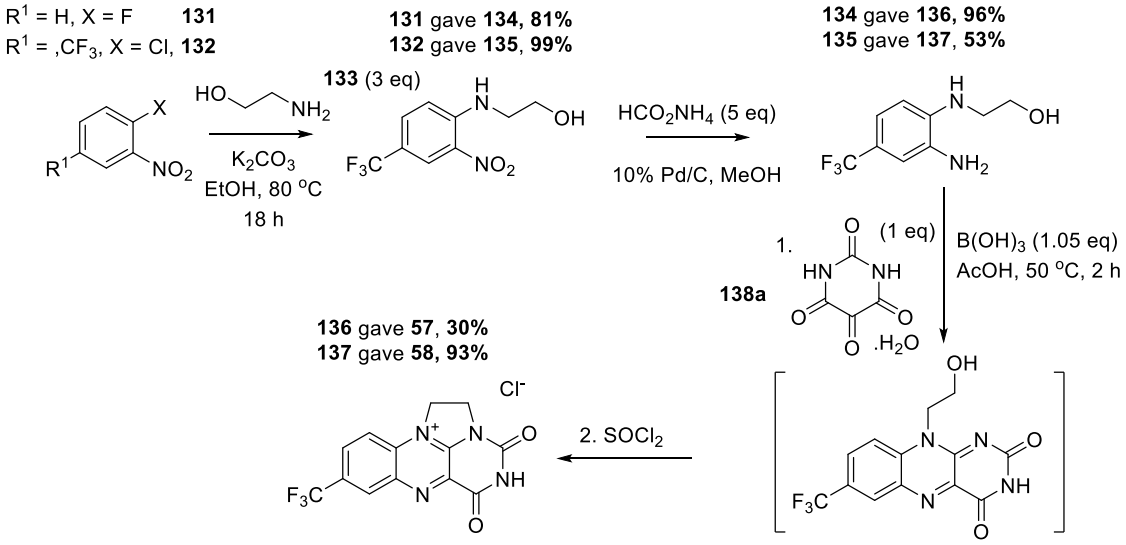

Scheme 68. Synthesis of flavinium chlorides **57** and **58**

A slightly different procedure is used for Cl-substituted flavinium chloride **59**, whereby the reduction step is mediated by Sn/HCl in order to avoid ring dechlorination of **140**/**141**.

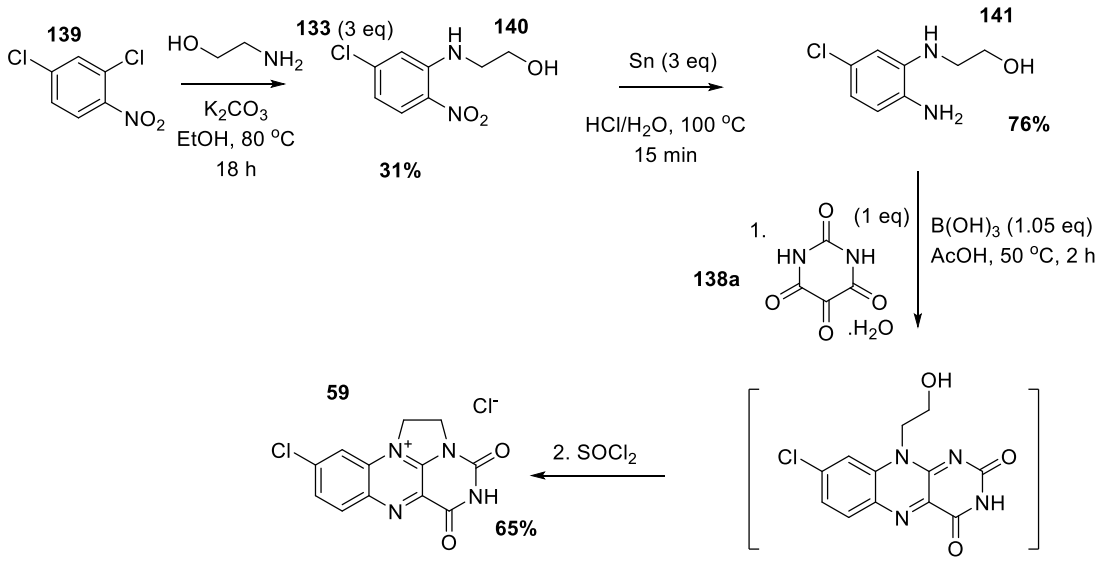

Scheme 69. Synthesis of **59**

Initial investigations focused on the the possibility of co-catalytic oxidations of primary alcohols to aldehydes or carboxylic acids with flavinium salt **23** and a potential precursor to 2-iodoxybenzoic acid (IBX), with H_2O_2 as terminal oxidant, but it was discovered that neither benzyl alcohol **142a** nor 4-nitrobenzyl alcohol **142b** were easily oxidised (Scheme 70).

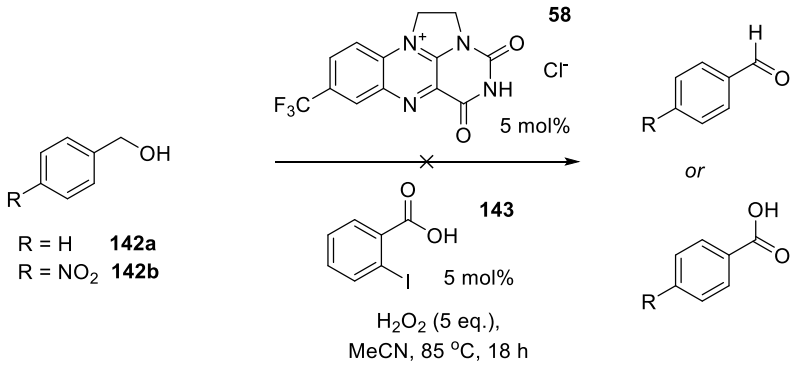

Scheme 70. Attempted co-catalytic IBX alcohol oxidation

However, it was found that 4-nitrobenzaldehyde (**41c**) was oxidised efficiently to 4-nitrobenzoic acid **42c** with the same conditions (Scheme 71).

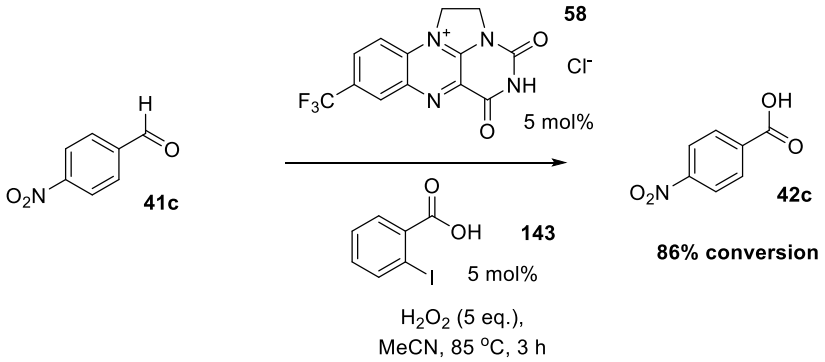

Scheme 71. Aldehyde oxidation with flavin and non-essential IBX precursor

The IBX precursor was not required for oxidation to occur, but flavin was essential to achieve good conversion. Therefore, it appeared that flavin hydroperoxide was the active species in this catalytic reaction. A different mechanism would be expected to occur in this case; while involvement of the iodine species would imply an electrophilic oxidant, flavin hydroperoxide would be expected to proceed *via* a nucleophilic B-V type mechanism.

4-nitrobenzaldehyde was oxidised to the corresponding carboxylic acid by the action of flavinium salts **57-59** and H_2O_2. The initially used trifluoromethyl derivative **58** was the most active. The optimisation of conditions is shown (Table 3).[103]

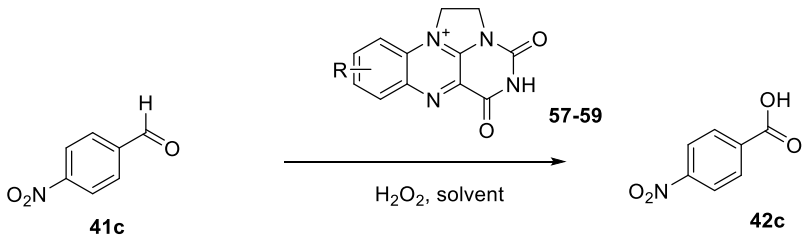

Table 3. Optimisation of flavin-catalysed aldehyde oxidation

Entry	Solvent	Catalyst	H_2O_2 (Equiv)	T (^oC)	t (h)	Conversion (%)
1	MeCN	**57** (5%)	1.25	85	1	49
2	MeCN	**59** (5%)	1.25	85	1	54
3	MeCN	**58** (5%)	1.25	85	1	60
4	MeCN	**58** (5%)	1.25	r.t.	3	1
5	MeCN	**58** (5%)	1.25	50	3	1
6	Dimethylcarbonate	**58** (5%)	1.25	85	3	27
7	Dimethoxyethane	**58** (5%)	1.25	85	3	56
8	H_2O	**58** (5%)	1.25	85	3	16
9	Toluene	**58** (5%)	1.25	85	3	5
10	THF	**58** (5%)	1.25	85	3	20
11	Et_2O	**58** (5%)	1.25	85	3	0
12	EtOAc	**58** (5%)	1.25	85	3	56
13	MeCN	**58** (5%)	1.25	85	3	66
14	MeCN	**58** (2.5%)	1.25	85	3	79
15	MeCN	**58** (1%)	1.25	85	3	76
16	MeCN	None	1.25	85	3	6
17	MeCN	**58** (2.5%)	1.5	85	3	96
18	MeCN	**58** (2.5%)	1.5	85	18	100
19	MeCN	**58** (2.5%)	0	85	18	0

Interestingly, a lower loading of catalyst seems to increase the rate of reaction; it is unclear exactly why this is the case, but one possibility is that aggregation behaviour of flavins occurs at higher concentrations.[104] Reaction was effective in acetonitrile but non-polar solvents yielded poor reactivity, possibly due to a lack of catalyst solubility and immiscibility of the aqueous H_2O_2 solution. The reaction was observed to be relatively sensitive to the loading of H_2O_2, with noticeable differences between even 1.25 and 1.5 equivalents of terminal oxidant.

A control reaction was also performed to see if oxidation occurred without H_2O_2; i.e. if the oxidation required H_2O_2 or if atmospheric O_2 was in fact the terminal oxidant; and it appears to be the former (entry 19). A further control (entry 16) showed a fairly slow oxidation of aldehyde in the absence of flavin catalyst, possibly *via* a Payne oxidation-type mechanism,[105] but the flavin hydroperoxide oxidised aldehydes much faster, as expected.

2.3 Oxidation of aromatic aldehydes

The substrate scope of this reaction was investigated, giving mostly high yielding oxidation to the corresponding carboxylic acids with aromatic aldehydes (Table 4).

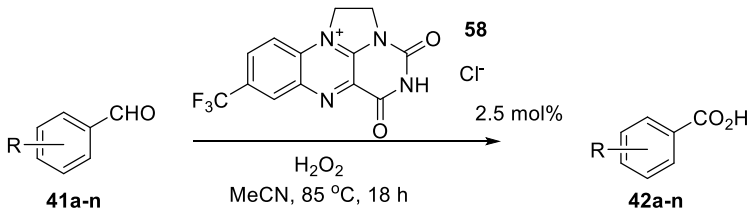

Table 4. Oxidation of aromatic aldehydes

Entry	R	eq. H_2O_2	Product	Yield/%	Phenol by-product/%*
1	4-NO_2	1.5	**42c**	89	
2	3-NO_2	1.5	**42d**	80	
3	2-NO_2	1.5	**42e**	90	
4	4-Cl	5	**42f**	94	
5	3-Cl	5	**42g**	94	
6	2-Cl	5	**42h**	91	
7	4-Me	5	**42i**	78	
8	3-Me	5	**42j**	90	
9	2-Me	5	**42k**	64	
10	4-OMe	5	**42b**	23	38 (**144a**)
11	3-OMe	5	**42l**	37	
12	2-OMe	5	**42m**	50	31 (**144b**)
13	H	5	**42a**	73	
14	picolinaldehyde	1.5	**42n**	90	

*= determined by ^{1}H NMR spectroscopy of crude reaction mixture

To a certain extent reaction appears related to the electrophilicity of the starting aldehyde, with nitro-substituted and the electron-withdrawing heterocycle picolinaldehyde giving the acids in high yield with a low loading of H_2O_2. After increasing the H_2O_2 loading, electron neutral aromatic aldehydes oxidise well but methoxy benzaldehydes give a lower yield and in the case of the strongly resonance-donating *para* and *ortho* substituted examples **41b** and **41m**, there is significant formation of a phenol by-product. The competing mechanism is the migration of the electron-rich aromatic group instead of hydride, followed by cleavage of the formyl ester to form the substituted phenol (Scheme 72). This is similar to the reaction observed by Foss in his flavin-catalysed Dakin oxidation.[65]

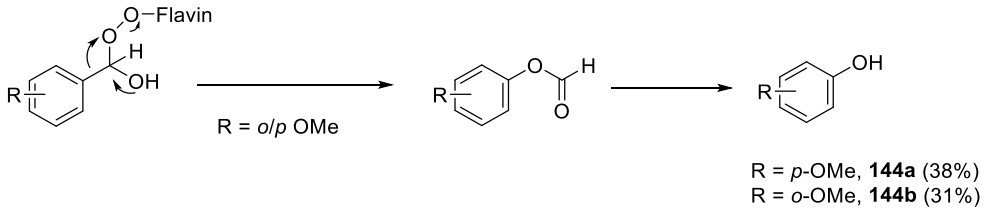

Scheme 72. Mechanism of Dakin oxidation pathway

This seems an adequate explanation for the reactivity trend; with the exception that the *meta* methoxy benzaldehyde **41k** (entry 11) is not electron donating and yet still reacts only in moderate yield.

2.4 Oxidation of aliphatic aldehydes

The oxidation was also attempted with aliphatic aldehydes and generally gave excellent yield of carboxylic acid with low loading of H_2O_2 (Table 5). The reaction tolerates alkenes and, as a neutral process, does not promote elimination (entry 5) as might other H_2O_2 systems using acidic additives.[106]

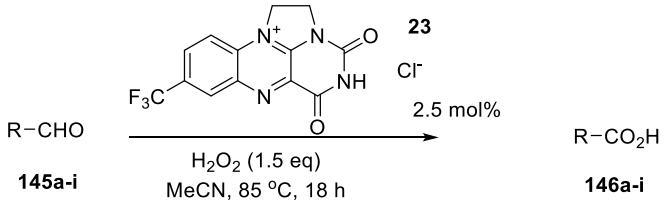

Table 5. Oxidation of aliphatic aldehydes

Entry	R	Product	Yield/%
1	cyclohexyl	**146a**	99
2	C_6H_{13}	**146b**	86
3	$C_{14}H_{29}$	**146c**	70
4	$^tBuCH_2$	**146d**	98
5	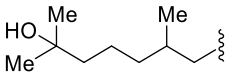	**146e**	85
6	^tBu	**146f**	60*
7	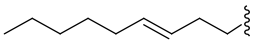	**146g**	64
8	$PhCH_2$	**146h**	55
9	$PhCH_2CH_2$	**146i**	43

* = 40% *t*-butanol observed in ^1H NMR spectrum

However, non-conjugated alkyl-aryl substrates gave only moderate yield. In these cases the starting material was consumed, but in the particular case of **145i** (entry 9) the aldehyde peroxyhemiacetal **147** was observed in the crude ^{1}H NMR spectrum (Scheme 74). This may be due to H_2O_2 alone being able to attack the aldehyde carbonyl in this case, but the tetrahedral intermediate not reacting further in the absence of flavin. Alternatively, there is a possibility that the intermediate is simply so stable regardless that the rate of breakdown is lower than that of flavin dissociation from the tetrahedral intermediate.

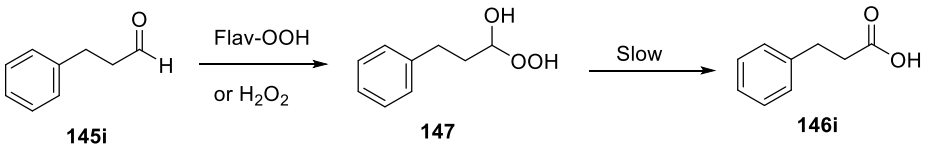

145i **147** **146i**

Scheme 73. Possible explanation of low yield in oxidation of **145i**

Also notable is the observation of *t*-butanol in the crude ^{1}H NMR spectrum of the oxidation of **145f** (entry 6). This is due to the high migratory aptitude of a tertiary alkyl group; comparable to that of a hydride, and thus Dakin oxidation is observed. No alcohol by-products were seen for any other alkyl substrate, including α-disubstituted aldehydes (entry 1).

2.5 Mechanism of the flavin-catalysed aldehyde oxidation

Our proposed mechanism for this reaction is addition of H_2O_2 to the flavinium salt **58** to hydroperoxide **148** followed by nucleophilic attack on the carbonyl to form a peroxyhemiacetal which gives the acid after hydride migration and dehydration of **149**, as shown (Scheme 74).

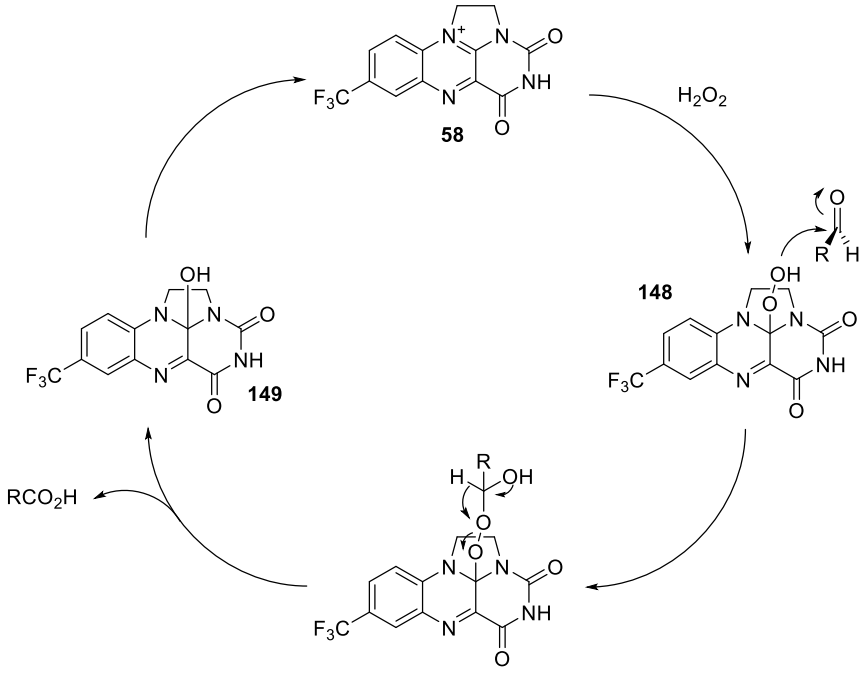

Scheme 74. Proposed mechanism of aldehyde oxidation by flavin hydroperoxide

Another possible mechanism would proceed *via* an aldehyde hydrate mechanism, as proposed in the oxidation of betaine aldehyde **150**, with the flavin acting as an electron acceptor in a hydride transfer (Scheme 75).[107,108]

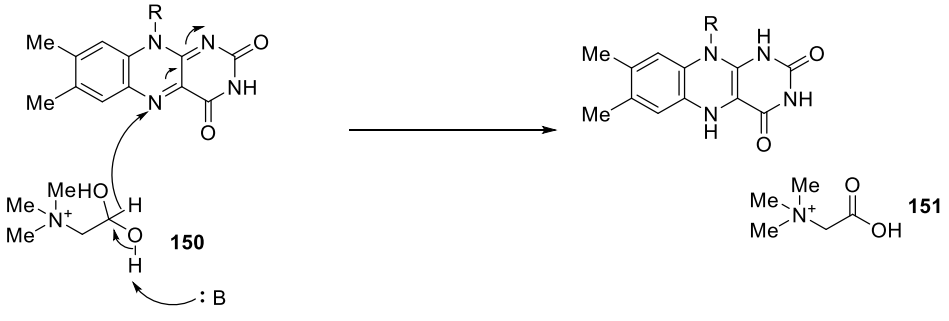

Scheme 75. Mechanism of oxidation of betaine aldehyde by choline oxidase

Although we did not extensively probe the kinetics of this reaction, evidence against would appear to be that for a hydride transfer we would expect electron rich substrates to react more effectively, as a transition state with carbocation-type character would be more stabilised for an electron donating group than an electron withdrawing group. Instead, it appeared that in most cases electrophilicity of the aldehyde was positively correlated with the efficiency of the reaction.

To investigate if the oxidation involves an aldehyde hydrate, an oxidation of chloral hydrate **152**, an aldehyde which exists with the equilibrium far towards the hydrated state, was attempted (Scheme 76).

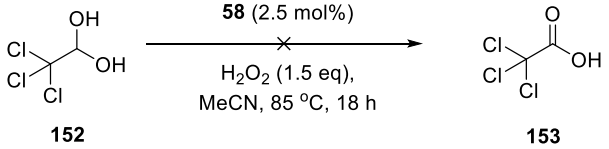

152 153

Scheme 76. Attempted oxidation of chloral hydrate

The lack of reactivity of this highly electrophilic aldehyde suggests that the mechanism is more likely to be the nucleophilic Baeyer-Villiger type mechanism, and not one similar to the structure of choline oxidase. Therefore, nucleophilic flavin hydroperoxide cannot add into the vacant π^* orbitals as occurs with an aldehyde carbonyl.

Additionally, the aforementioned investigations of choline oxidase found that 3,3-dimethylbutyraldehyde **145d** was a potent inhibitor of this enzyme. In our catalytic system, however, it was an excellent substate, oxidised in 98% yield (table 5, entry 4).

3 Flavin-catalysed amine oxidation

3.1 Oxidation of primary amines by flavin-catalysed dehydrogenation

Amines can be oxidised *in vivo* by both oxygen transfer and dehydrogenation. Tertiary amines can be oxidised by monooxygenation by FMO enzymes, with the genetic disease trimethylaminuria (caused by a build-up of Me_3N) apparent if this enzyme is not coded for.[109] However, in nature, primary amines are oxidised by oxidase enzymes, which can additionally oxidise secondary and tertiary amines. Nevertheless, there are few examples of flavin-catalysed amine dehydrogenation in a synthetic context, nor of their mechanistic relevance to enzymology.

Although the monooxidation of secondary and tertiary amines by synthetic flavin hydroperoxides has been extensively studied,[54,55] the reactions of primary amines under these conditions are less well known. Decomposition by ring-opening of flavin catalysts by amines in the presence of methanol has been reported,[58,72] as has the formation of oxime with stoichiometric flavin (monooxygenase chemistry).[53]

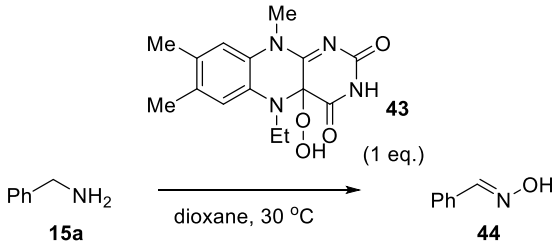

Scheme 77. Stoichiometric oxime production by flavin hydroperoxide **43**

Imine or aldehyde products have been formed (oxidase chemistry), but a maximum turnover number of around 2.[53,68] Additionally, these systems used harsh conditions such as Brønsted or Lewis acid additives, elevated temperatures and long reaction times (days), and as such could not be considered truly biomimetic or biorelevant.

We were nevertheless interested in accessing either monooxygenase or oxidase chemistry by altering the conditions. In a model system, how could we select for FMO chemistry over an oxidase such as MAO or D-amino acid oxidase, or *vice versa*?

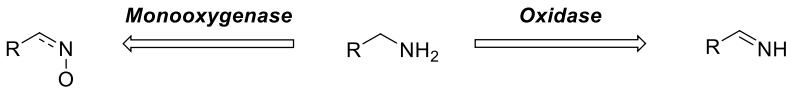

Scheme 78. Oxidase vs monooxygenase activity for primary amine

It was decided to attempt an oxidation of benzylamine to the corresponding oxime or secondary imine either using a H_2O_2/flavin catalytic system or with molecular oxygen and a reducing agent (Scheme 32). The former we expected would promote monooxygenase chemistry; the latter was more open to speculation as to the mechanistic pathway reaction would take.

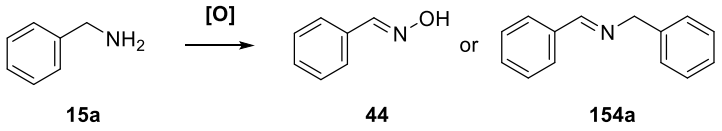

Scheme 79. Possible products of benzaldehyde oxidation

We found, in fact, that even using H_2O_2 it was the imine that was obtained, albeit in fairly low yield, and not especially reproducibly. However, we were unsure if this was due to trace oxygen entering the reaction mixture.

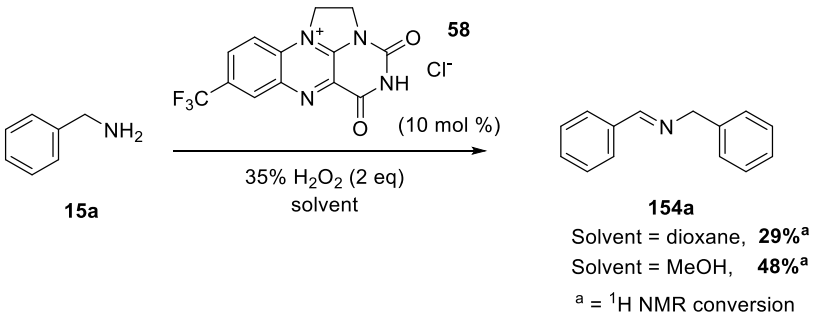

Scheme 80. Initial experiments using H_2O_2

Upon reactions with air, and using zinc as a reducing agent; in a modified version of the Murahashi protocol for aerobic Baeyer-Villiger oxidation,[64] the corresponding imine was formed albeit apparently with minimal catalyst turnover (Table 15). The procedure was performed with TFE as a solvent, as this homogenised the reaction and was precedented for flavin/O_2 chemistry involving amines.[55] Chloroform initially appeared to be a reasonable solvent for this reaction but was not reproducible due to limited flavin solubility, a factor previously encountered within the group working with flavins and chlorinated solvents.[57] We tried Sn and Ni as alternative metal additives with no more success. Despite hydrazine being the reductant of choice in previous examples of oxidations of secondary and tertiary amines, this was not an effective additive in this case.

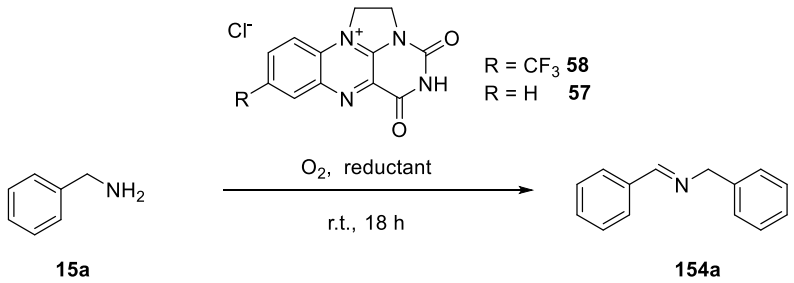

Table 6. Attempted oxidations of benzylamine

Entry	Catalyst	cat %	Reductant	Eq. red.	Solvent	Conv. /%
1	**58**	2.5	Zn	1.5	$CHCl_3$	15
2	**57**	2.5	Zn	1.5	$CHCl_3$	30
3	**57**	2.5	Sn	1.5	$CHCl_3$	<5
4	**57**	2.5	Ni	1.5	$CHCl_3$	<5
5	**57**	2.5	Zn	1.5	TFE	10
6	**57**	10	Zn	3	TFE	20
7	**57**	2.5	$N_2H_4.H_2O$	2	TFE	<5

One possible problem in this reaction was suspected to be degradation of the catalyst either to spirohydantoin type species or *via* base and alcohol imide ring opening as observed by both Sayre and Cibulka, to which there was not an obvious solution.[58,72] We proposed another possibility which would account for the near-stoichiometric production of imide, which was that as a four-electron oxidant, O_2 oxidises the reduced flavin formed by amine dehydrogenation all the way up to the hydroperoxide rather than the desired flavinium salt to restart the catalytic cycle. Although H_2O_2 can be removed by acid (e.g. $HClO_4$; in the so-called 'shunt process') this would not be feasible, as would protonate the basic nitrogen on the amine.[73]

Therefore, after unsuccessful attempts to substitute O_2 with an alternative oxidant such as DDQ or $CuCl_2$, under inert atmosphere, concurrent with a return to the use of the CF_3-substituted catalyst **58**, we decided to add a sulfide, known to react readily with flavin hydroperoxides. This was chosen in order to complete a catalytic cycle consistent with Edmondson's proposed polar mechanism for flavin oxidases, backed up by the previous evidence for this mechanism in model systems by Mariano and Sayre (Scheme 33).[57,70,72]

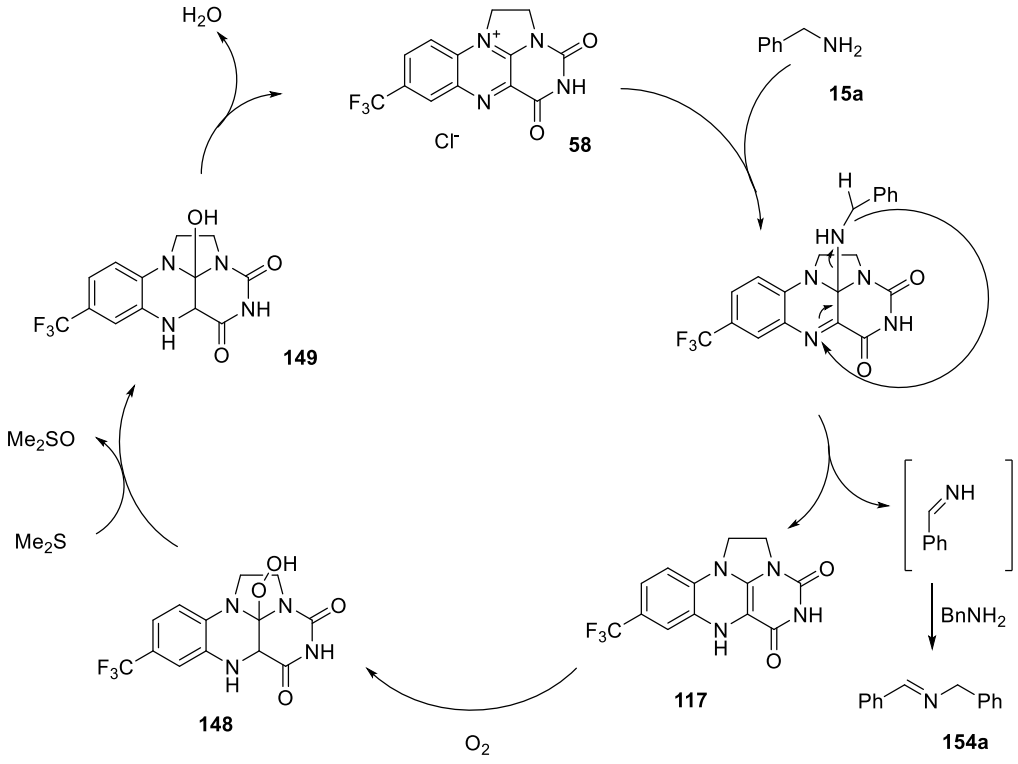

Scheme 81. Proposed mechanism for sulfide-assisted amine dehydrogenation

Both tetrahydrothiophene and dimethyl sulfide promoted the flavin-catalysed oxidation of benzylamine to **154a**, under O_2 atmosphere in a reasonably fast reaction, without the need for any external oxidants (Scheme 34).

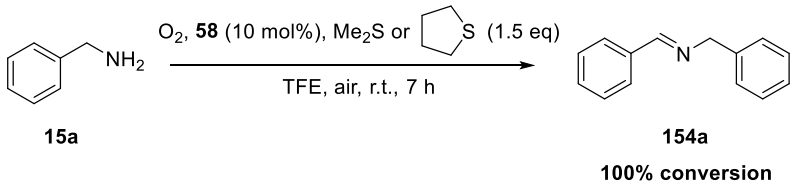

Scheme 82. Oxidation of benzylamine with flavin and sulfide

3.2 Optimisation of flavin-catalysed amine dehydrogenation

Optimisation studies were performed on the system, investigating catalyst loading, solvent selection and the effect of the partial pressure of terminal oxidant (Table 16).

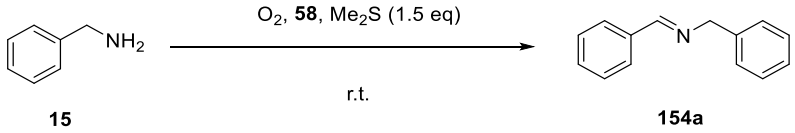

Table 7. Optimisation of flavin-catalysed amine dehydrogenation

Entry	Mol% catalyst	Solvent	O_2 source	Time /h	Conversion/%
1	10	TFE	O_2	7	100
2	10	TFE	O_2	4	64
3	5	TFE	O_2	7	50
4	2.5	TFE	O_2	7	24
5	10	TFE	air	3	56
6	10	$(CF_3)_2CHOH$	air	3	50
7	10	MeOH	air	3	22
8	10	MeCN	air	3	24
9	10	THF	air	3	1
10	10	CH_2Cl_2	air	3	1
11	10	PhMe	air	3	0
12	0	TFE	air	3	0
13	10	TFE	none	3	0
14	10	TFE	air	3	50[a]

[a] Reaction performed in the dark

Reaction was most efficient in fluorinated solvents such as TFE and hexafluoroisopropanol (HFIP, entry 6), with some but less effective reaction (near-stoichiometric) taking place in MeOH and MeCN. Minimal or no reaction was observed in non-polar solvents, possibly due to catalyst insolubility. Use of ambient air rather than O_2 did not greatly affect reaction efficiency, and the reaction was equally efficient in the dark, showing the flavin is not acting as a photosensitizer or photoinitiator.

3.2.1 Reproducibility issues and solution

The synthesis of flavin **58** as originally described by Sayre and used with minor modifications within our group is as shown (Scheme 83). The synthesis consists of an initial S_NAr substitution of **132** with ethanolamine, followed by hydrogenation of the nitro group to form **135** and a two-step procedure whereby the dianiline is condensed with alloxan **z** to give uncyclised flavin precursor **155** followed by $SOCl_2$-mediated cyclisation to finally give the flavin **58** which is purified by a final recrystallization from HCO_2H/Et_2O.[57,72]

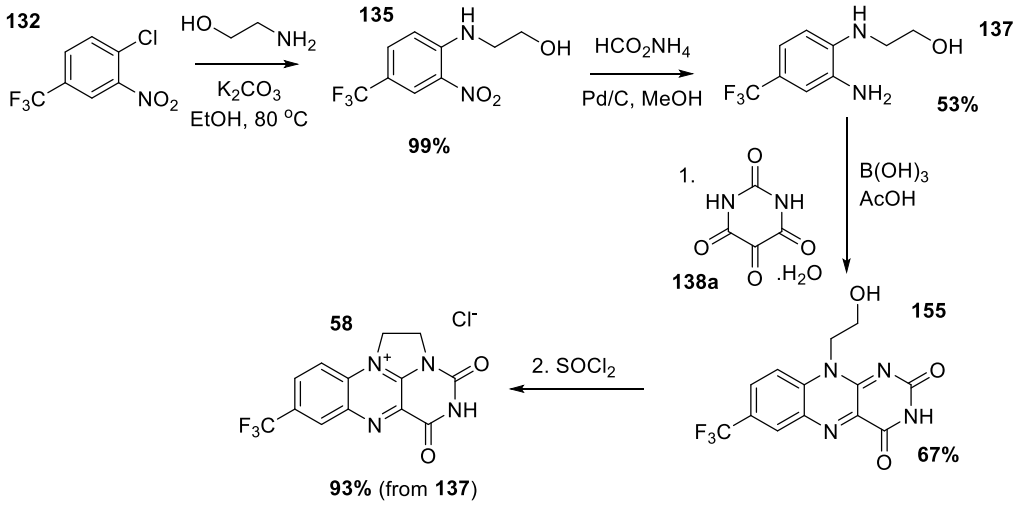

Scheme 83. Synthetic steps in the production of flavin **58**

When some batches of flavin **58** were synthesised, we were surprised to find no reaction or minimal reactivity upon subjection of benzylamine to our conditions with the new catalyst. The spectroscopic properties of the ineffective batches of **58** were not appreciably different in physical and spectroscopic properties (^{1}H NMR, ^{13}C NMR, IR, HRMS, UV/vis, m.p.) and also were effective at promoting other flavin-catalysed reactions developed within the group such as aldehyde oxidation and sulfoxidation.

We considered the possibility of an unknown contaminant being responsible for the loss of activity in these reactions, so revisited the synthetic procedure for the initial synthesis of **58**. Revisiting each synthetic step with careful purification, we discovered that in the reduction of nitro compound **135** to dianiline **137**, when the reaction was performed without intermediate purification, inactive catalyst tended to be ultimately generated. However, when subjected to flash chromatography a different product was observed. When *this* was taken through the synthetic sequence an active catalyst was obtained. The discrepancies between ^{1}H NMR spectra of the two compounds are shown below, with spectrum **A** referring to the initial aniline and **B** to our new product.

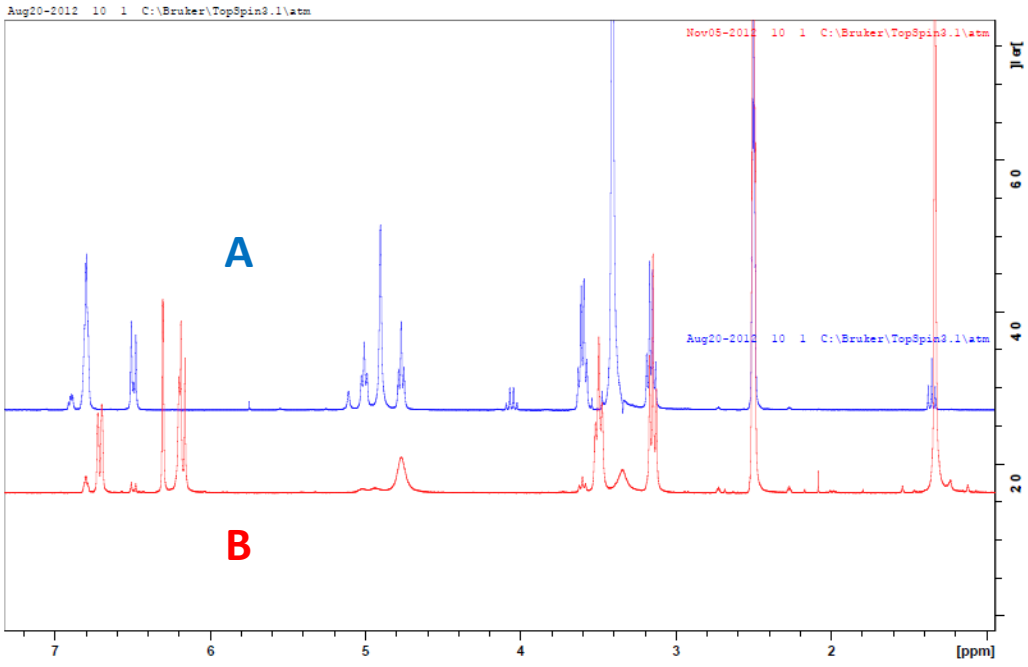

Figure 14. ^{1}H NMR spectra of **137** (**A**) and unknown product (**B**)

We determined that spectrum **B** was in fact that of the acetonide aminal **156** formed by rinsing the collection tubes with acetone.

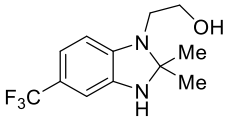

Figure 15. Aminal **156** formed by exposure of **137** to acetone

The compound could be conveniently and consistently prepared by stirring **137** in acetone. The aminal presumably is readily removed in the next step by the acidic conditions (heating in AcOH) so we considered that some sort of reversible protection of the sensitive, oxidisable dianiline might be related to minimising formation of deleterious impurities.

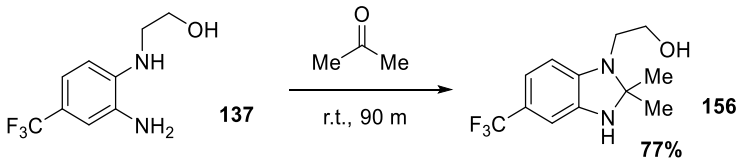

Scheme 84. Intentional synthesis of aminal **156**

However, we still found reproducibility in our system difficult to achieve. We then turned our attention to the possibility that rather than an impurity being an inhibitor of amine oxidation, perhaps it was an impurity that was the actual catalytic species. Such a hypothesis would fit with the observation that batches of catalyst that were previously reactive became less so after multiple recrystallisations, and that 'crude' batches of flavin could be the most effective. This was additionally backed up by the observation that our samples of **58** which were inactive in amine oxidation were in fact equally effective in sulfoxidation, aldehyde oxidation and diimide reduction chemistry.

Our intial hypothesis was that it might be the uncyclised flavin **155** which was responsible for the catalytic activity. Although these neutral isoalloxazines are usually only effective in dehydrogenation chemistry in the photoexcited state,[75] we nevertheless considered them as a potential active species. After isolation and purification of **155**, mixing this compound with previously 'inactive' flavin **58** did indeed promote reaction, although **155** alone was not an effective catalyst.

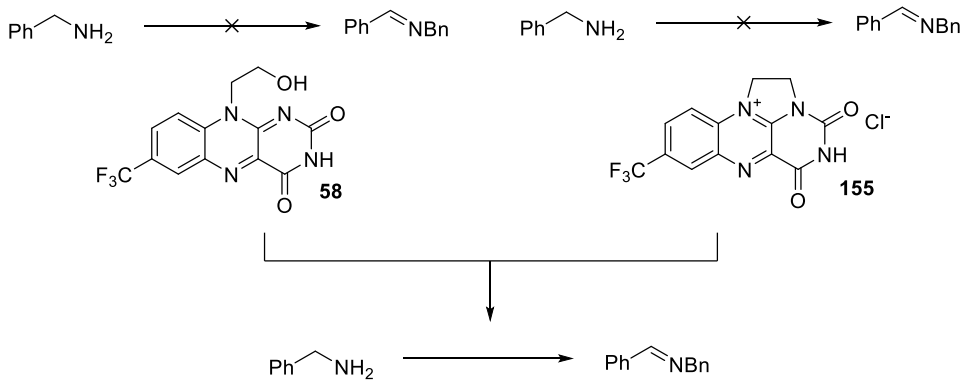

Scheme 85. Dual flavin catalysis apparently promoting amine oxidation

It appeared that the reaction was more effective with mostly **58**, but reactivity trends were not entirely clear (Table 8).

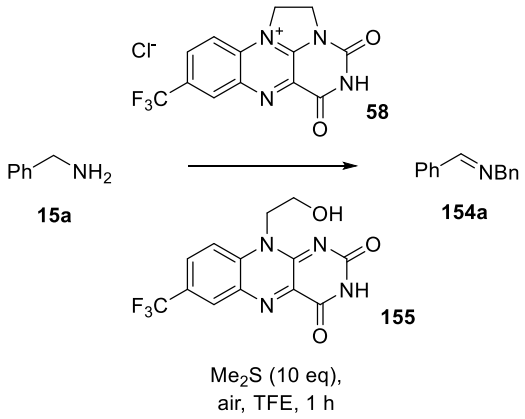

Table 8. Ratios of **58**/**155** – effect on catalysis

Entry	Mol % **58**	Mol % **155**	Conversion / %
1	3	1	80
2	2	2	30
3	1	3	42
4	4	0	<5
5	0	4	<5

We investigated an analogue of **155** to probe which features were essential to promote reactivity. The methoxy analogue **159** was synthesised using the same procedure.

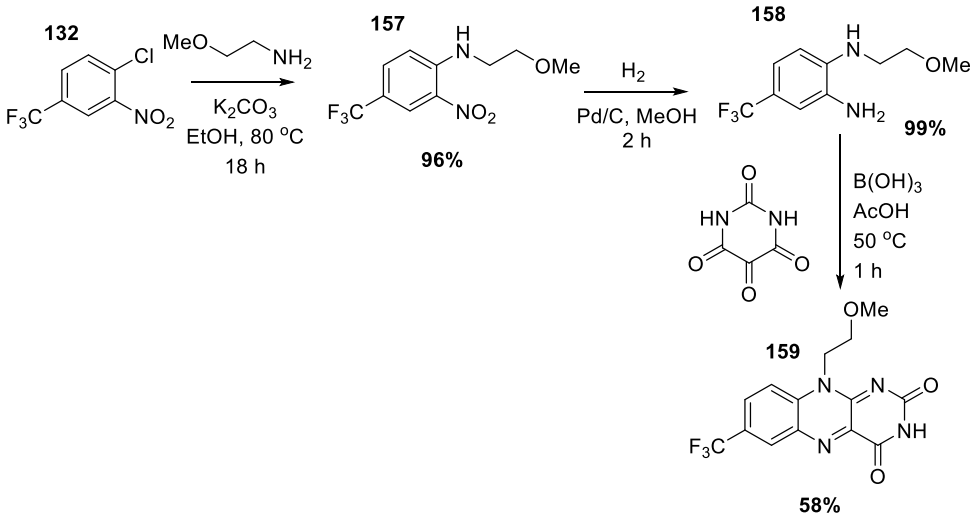

Scheme 86. Synthesis of methoxy analogue **159** of uncyclised flavin **155**

With this compound, the crude **159** promoted reaction effectively in conjunction with flavin **58** but when this product was purified by column chromatography it became inactive. This suggested that it may have been some other present compound, not the 'uncyclised' flavin, which was responsible for activity.

3.2.2 – Reproducibility issues – Alternative hypothesis

We considered the possibility that it was the *other* component of this condensation i.e. the alloxan **138a** which was the cocatalyst for amine oxidation. This was indeed the case; after initial consideration that it might be the boric acid acting as a co-catalyst we instead found alloxan **138a** to be an effective cooxidant; which nevertheless was ineffective without the additional presence of flavin **58**.

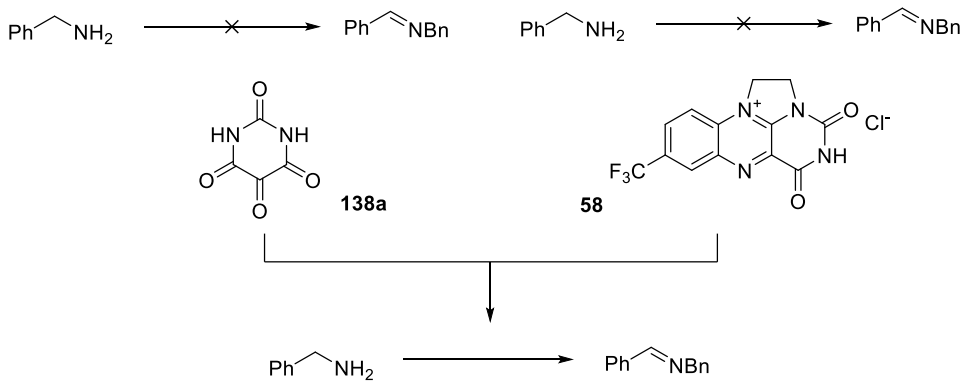

Scheme 87. Flavin/alloxan tandem catalysis

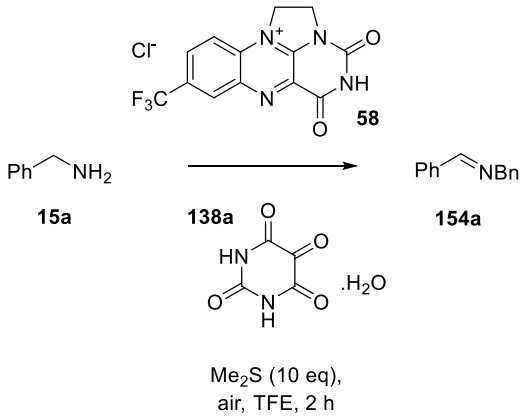

Table 9. Presence of **58**/**155** – effect on catalysis

Entry	Mol % **58**	Mol % **138a**	Conversion / %
1	10	1	>95
2	10	0	<5
3	0	1	<5

It transpired that the reason 'uncyclised' flavin **155** was apparently an active cocatalyst was that it had a very similar R_f to alloxan on silica gel (whereas the less polar methoxy analogue **159** was easily separable). Additionally, alloxan did not show up easily as an impurity in NMR or other spectra, or UV or common TLC staining techniques, particularly in small amounts. The working batch of catalyst we had been using contained 10% alloxan (so every entry in Table 8 contained, in fact, 9 mol% flavin **58** and 1 mol% alloxan **138a**). Additionally, this now explains why aminal protection to form **156** more frequently yielded active catalyst, with the slow removal of this group meaning the reaction was incomplete in the time period, thus leaving some alloxan to be carried through to the following step.

3.3 Alloxan

Alloxan is one of the oldest named organic chemicals, discovered in 1828 by Wöhler and Liebig, formed by the action of nitric acid on uric acid.[110]

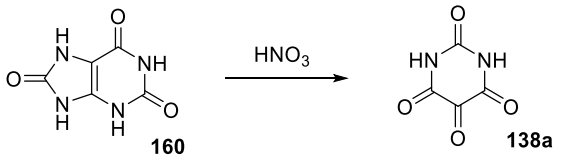

Scheme 88. Synthesis of alloxan by oxidation of uric acid

Its most common use since 1943 has been the artificial generation of Type I (insulin dependent) diabetes in rats.[111] This mechanism is believed to proceed by generation of *reactive oxygen species*. The alloxan enters the pancreas by its recognition as a glucose molecule, and is reduced by glutathione to dialuric acid. Upon autooxidation back to alloxan with O_2, there is concurrent formation of reactive oxygen species such as $O_2^{\bullet-}$ and $OH^{\bullet}$.[112]

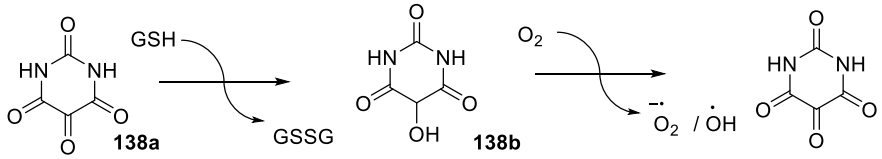

Scheme 89. Alloxan-mediated production of reactive oxygen species *in vivo*

Given this information, we began to consider the possibility of radical mechanisms for the oxidation of benzylic amines to imines, perhaps similar to Silverman's proposal for the MAO enzyme.[33] Equally importantly, we could use this information to develop a reproducible and more efficient oxidative process.

Firstly, however, we investigated whether other tricarbonyls were suitable for promoting this reaction. Ninhydrin was inactive, despite its known stoichiometric reactivity with amines given its common use as an amine selective stain for thin layer chromatography.

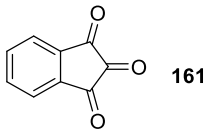

Figure 16. structure of ninhydrin **161**

We then decided to synthesise the corresponding N,N-dimethylalloxan **163** in order to investigate whether this structurally very similar compound was also active as a cofactor in this oxidation. This material was synthesised by oxidation of *N*,*N*-dimethylbarbituric acid with selenium dioxide, in a modified version of a published procedure, and isolated as an 1:2 mixture of tricarbonyl and hydrate.[113]

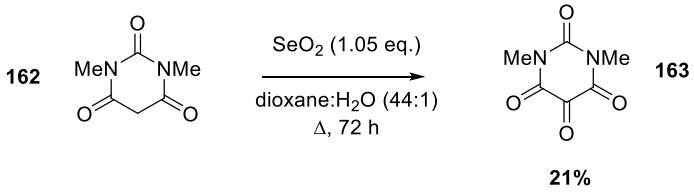

Scheme 90. Synthesis of *N*,*N*-dimethylalloxan **163**

However, use of **163** in place of alloxan was not successful, suggesting the varying tautomeric forms of the protonated reagent are important. A possible reason for this is the ability of the 'standard' alloxan to undergo keto-enol tautomerisation. Recent work has uncovered that enol tautomers are ca. 1 V more readily oxidisable than their keto type forms, and this has specifically been discussed in the context of alloxan.[114,115]

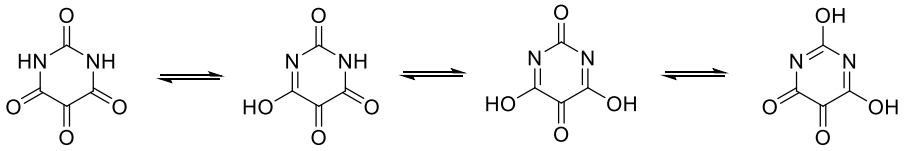

Figure 17. Possible alloxan tautomers

3.4 Flavin/alloxan catalytic amine oxidation

With a reproducible procedure in hand, we found we could drop the loadings of both catalysts to 2 mol% each respectively, especially with the sequential addition of catalysts, adding 1 + 1 mol % of **58** and **138a** and the same again after 2 h. This yielded a clean, aerobic amine oxidation which was usually complete in 5 h and required only a simple filtration on base-washed silica to give the product imine **s** as a pure compound.

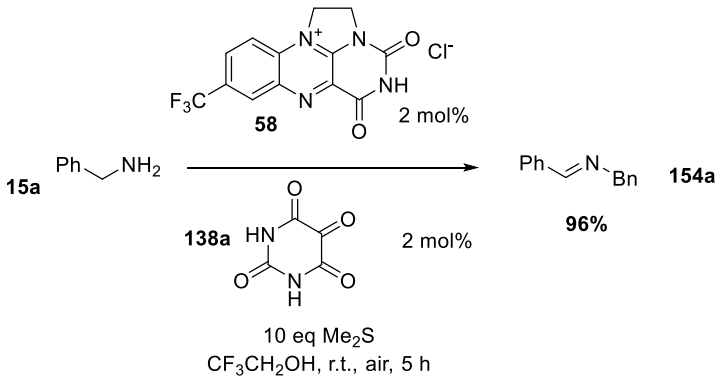

Scheme 91. A reproducible synthesis of imine **154a** by dual organocatalysis

We then proceeded to oxidise a range of benzylic amines to the corresponding imines, seen in Table 10.

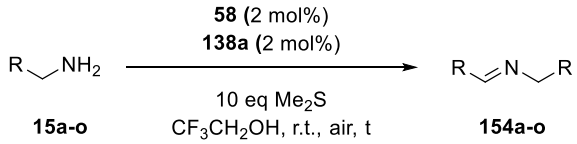

Table 10. Scope of flavin/alloxan-catalysed amine dehydrogenation

Entry	R	Product	Time /h	Yield/%
1	Ph	**154a**	5	96
2	4-Me-C_6H_4	**154c**	5	99
3	4-OMe-C_6H_4	**154b**	5	95
4	4-^{t}Bu-C_6H_4	**154d**	5	93
5	4-Cl-C_6H_4	**154e**	18	77
6	4-F-C_6H_4	**154f**	18	98
7[a]	4-CF_3-C_6H_4	**154g**	18	37
8	3-Me-C_6H_4	**154h**	5	91
9	3-OMe-C_6H_4	**154i**	5	72
10	2-Me-C_6H_4	**154j**	5	96
11	2-OMe-C_6H_4	**154k**	5	68
12	2-Cl-C_6H_4	**154l**	18	66
13	2-furyl	**154m**	18	70
14	2-thiophenyl	**154n**	5	87
15	1-napthyl	**154o**	5	72
16	1-heptyl	-	18	0

[a] 4% **58** and 4% **138a** used

The reaction was generally efficient for most benzylic amines, with the exception of the very electron deficient **154g** (entry 7), which was incomplete after an extended reaction time even when increasing the catalyst loading. The reaction tolerates 5-membered heterocyclic amines such as furfurylamine **15m** and 2-thiophenemethylamine **15n** (Table 10, entries 13, 14), which can be resistant to oxidation by transition metal mediated methods.[116,117] Electron rich substrates were particularly readily oxidised, although extending the reaction time tended to give aldehyde, which appeared to be *via* further oxidation rather than hydrolysis.

Aliphatic amines not only are not oxidised, but indeed inhibit the reaction. If a 1:1 mixture of benzylamine and hexylamine are subjected to the reaction conditions no oxidised products are observed at all.

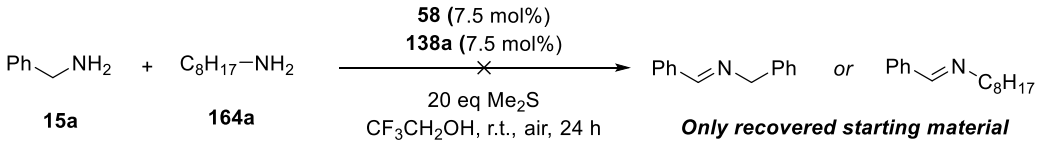

Scheme 92. Inhibitory effect of octylamine **164a**

This may be due to irreversible binding of aliphatic amine to one of the two catalyst electrophilic sites. Secondary and α-branched amines were poor substrates for this reaction; the latter possibly for steric reasons. Additionally, use of benzylamine.HCl salt as a substrate yielded no oxidised products; but addition of bases to the catalytic system (K_2CO_3 or Et_3N) also inhibited the reaction.

3.5 Amine oxidative cross-coupling

Several recent publications involving oxidations with quinone catalysts has shown that in some cases, it is possible to cross-couple amines to imines with an oxidation followed by an equilibrium, with continuous oxidation of released **15a** promoting highly selective formation of cross product **167** (Scheme 41).[116,118]

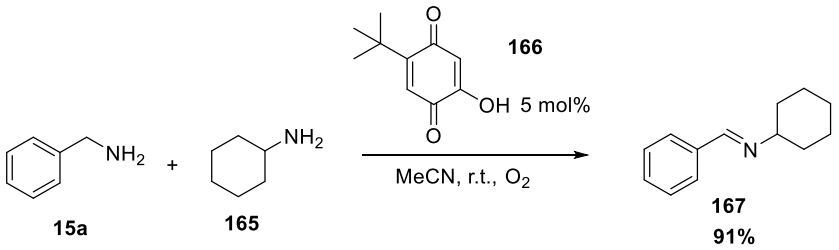

Scheme 93. Example of an aerobic amine oxidative cross-coupling[116]

Exploratory attempts at this type of reaction using benzylamine and aniline gave a mixture of products somewhat in favour of the homo-coupled imine. However, as discussed by Stahl, anilines can be quite difficult to oxidatively cross-couple due to the lower nucleophilicity of the aniline compared to an alkyl amine (which we could not use as it was an inhibitor in this case).

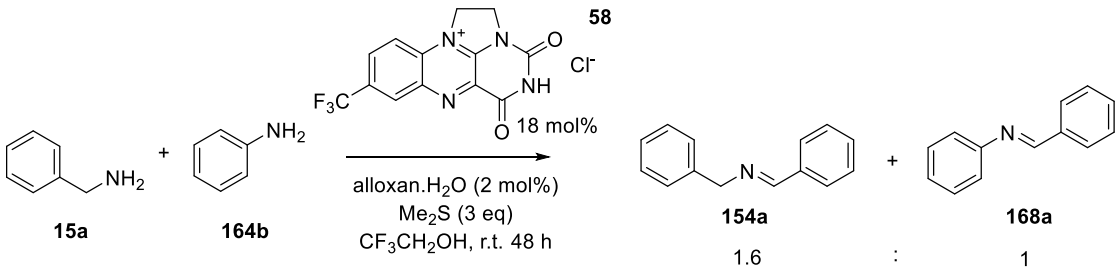

Scheme 94. Ratio of homocoupled product **154a** with cross-coupled **168a**

This initial example was using the ‘mixed’ catalyst containing only small amounts of alloxan as cocatalyst. When we equalised the proportions of catalysts and added the catalysts portionwise we found that the reaction was much more selective, even with a lower loading of flavin catalyst.

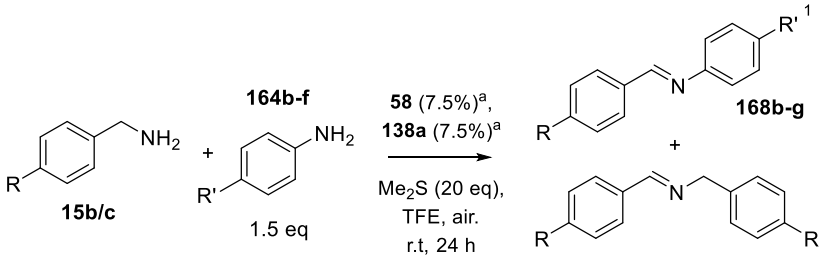

Table 11. Flavin/alloxan catalysed oxidative cross coupling

Entry	R	R'	Product	Yield/%	Selectivity[b]
1	Me	H	**168b**	73[c]	17:1[c]
2	Me	Me	**168c**	99	>25:1
3	Me	OMe	**168d**	73	19:1
4	Me	Cl	**168e**	82	1.6:1
5	Me	F	**168f**	98	4:1
6	OMe	H	**168g**	96	7:1

a) Added as three portions of 2.5%, the latter two after 3 h and 6 h. b) Determined by ^{1}H NMR analysis of reaction mixture c) Determined by measurement of ^{1}H NMR signals against an internal standard of 1,3,5-trimethoxybenzene, yield refers to cross-product only.

The dependence on adding catalysts portionwise is possibly related to deactivation of one or both of them. The aniline is much less nucleophilic than the benzylic amine, so at the start of the reaction there is a greater amount of homocoupled product formed. However, as the aniline is not oxidised under the reaction conditions due to lacking α-hydrogens, it follows that any small amount of hydrolysed product should immediately be oxidised and so condense with an aniline, so long as we maintain a high ratio of catalyst to released amine throughout the reaction time.

To confirm the identity of substates which were not separable from homocoupled product we independently synthesised the imines by condensation, and spectra were compared.

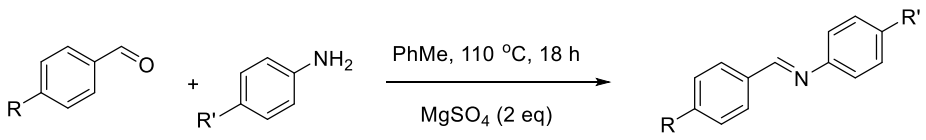

Table 12. Condensation of imines to cross-check data

Entry	R	R'	Yield/%
1	Me	H	98
2	Me	OMe	73
3	Me	Cl	97
4	Me	F	95
5	H	OMe	95

Although aliphatic amines were not available as 'easier' less oxidisable substrates for this reaction due to their aforementioned catalyst deactivation, we also attempted to cross-couple *para*-methylbenzylamine **15c** with α-methylbenzylamine **169**. Despite this transformation being facile under Stahl's conditions,[116] only homocoupled amine **154c** was observed.

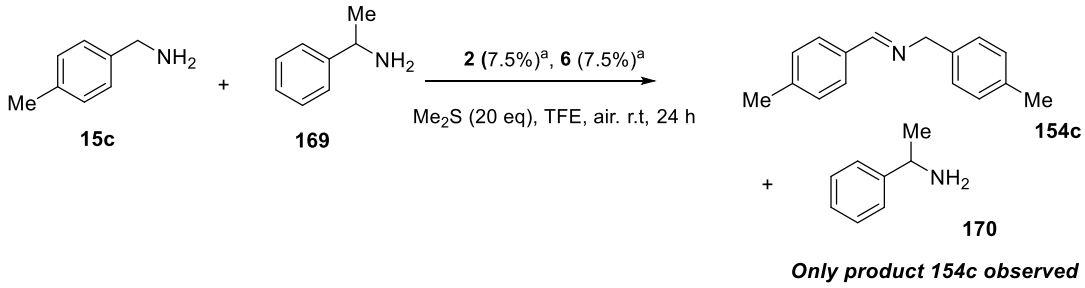

Scheme 95. Homocoupling of **15c** under the cross-coupling conditions

As **169** would be expected to have a similar level of nucleophilicity to **15c**, it is unclear exactly why this was the case. The mechanistic pathway of transamination may not be the same as in Scheme 93, especially given a potential radical pathway, whereby the stabilised nature of the α-methylbenzylamino radical might be a hindrance to reaction turnover.

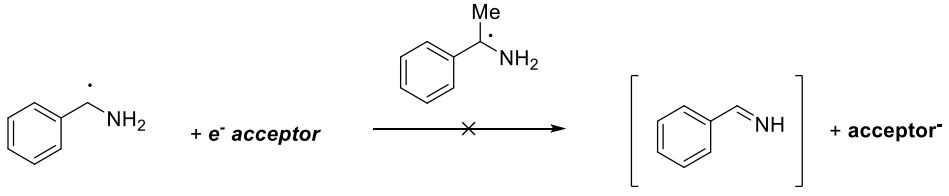

Scheme 96. Possible origin of lessened reactivity in presence of **169**

3.5.1 Oxidative cross coupling of electronically dissimilar benzylic amines

Bearing in mind the hypothesis that the product distribution of electronically dissimilar amines would be strongly influenced by the rate of oxidation of the amines, and that therefore electron rich benzylic amines should to be oxidised faster than electron deficient ones, we attempted an oxidative cross coupling of two dissimilar benzylic amines. This type of oxidative dynamic process has recently been described by Miljanić.[119]

An equimolar amount of an electron-rich and electron deficient benzylic amine were mixed, in order to probe the ratio of products formed in this reaction. We chose 4-methylbenzylamine **15c** and 4-(trifluoromethyl)benzylamine **15g** in order to probe this effect. Firstly, however, The two cross imine products **171a** and **171b** were synthesised as these were novel compounds and we needed standards to compare which imine was which, as we considered it unlikely the four products would be separable.

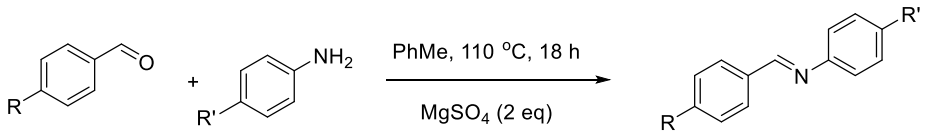

Table 13. Condensation route to novel imines

Entry	R	R'	Product	Yield/%
1	Me	CF_3	**171a**	94
2	CF_3	Me	**171b**	37

Upon mixing an equivalent amount of 4-methylbenzylamine **15b** and 4-(trifluoromethyl)benzylamine **15g** and adding catalyst in three portions of 2.5% as previously described in Table 12, we observed the major isomer **171a** as 55% of the total imine products.

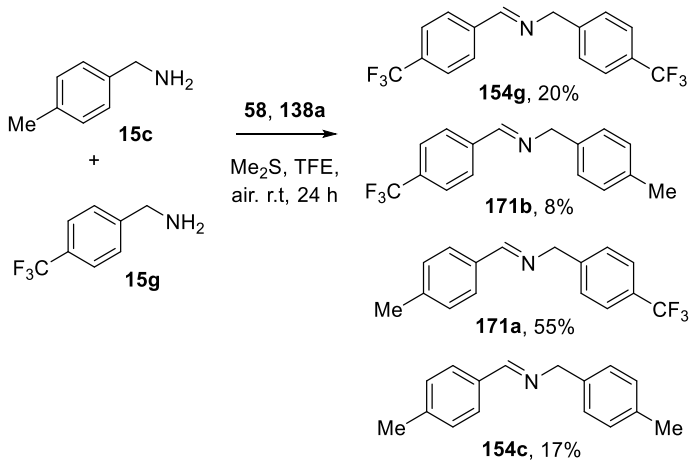

Scheme 97. Oxidative self-sorting of electronically dissimilar benzylamines **15c** and **15g**, and possible products **154g, 171b, 171a** and **154c**

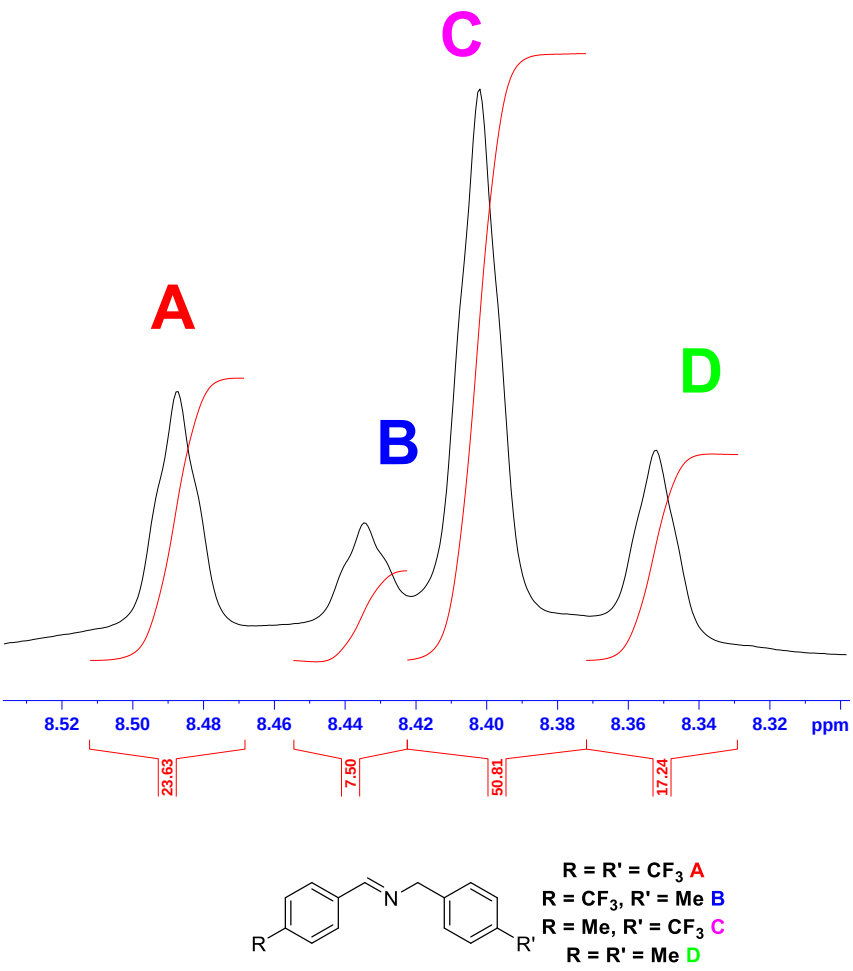

Figure 18. Imine region of ^{1}H NMR spectrum of reaction mixture

Given there are four possible imine products and both starting materials can be irreversibly oxidised by the reaction conditions, there is a natural limitation to the ratio of imines in favour of **171a**. This nevertheless serves as evidence along the lines of a competition experiment, for the bias towards electron-rich amines as substrates in the reaction, and is an example of a self-sorting process involving imines as discussed by Stoddart.[120] In principle, this could be extended to a greater and more diverse library of imines, though in this case, HPLC or GC would be a more appropriate analytical tool.

4 Flavin-catalysed amine oxidation: Mechanistic studies

4.1 Introduction - From NMR to EPR

Our initial intention was to investigate the kinetics of the imine forming reaction by *in situ* ^{1}H NMR spectroscopic monitoring. However, when this was attempted, the reaction mixture was impossible to lock upon addition of Me_2S. One explanation for the repeated inability to observe an NMR spectrum in TFE was that paramagnetic species might be present.

This would be an important observation given the previously discussed implication of radical intermediates in some flavin amine oxidases, and the well-studied radical chemistry of alloxan. Accordingly, an electron paramagnetic resonance study was initiated, in order to observe if radical intermediates were being generated.

4.2 Electron Paramagnetic Resonance Spectroscopy: Theory

Electron paramagnetic resonance spectroscopy (EPR spectroscopy), also known as electron spin resonance (ESR) spectroscopy, is a magnetism-based technique used in the observation of systems containing unpaired electrons (radicals) i.e. it requires spin quantum number $S \geq ½$. It is essentially the electron spin equivalent of NMR spectroscopy, and an EPR transition is the flipping of the electron between the two possible spin states. Unlike in NMR, the frequency is fixed and the magnetic field strength is varied. EPR frequencies are divided into bands, each using a different instrument. These are S-Band (4 GHz), X-Band (9 GHz, the most common EPR experiment), Q-Band (34 GHz) and W-Band (94 GHz), the latter of which being the only one which requires an NMR- like superconducting magnet.

The electromagnetic energy applied to flip between spin states is defined by the equation.

$$E = m_s g \beta_e H$$

Where E is the applied energy, i.e. electromagnetic radiation of a given frequency, m_s is the spin quantum number, g is the *g factor* (a dimensionless constant that relates observed magnetic moment to spin quantum number), β_e is the *Bohr Magneton* (= 9.2740×10^{-34} J T^{-1}) and H is the strength of the magnetic field applied in Gauss.

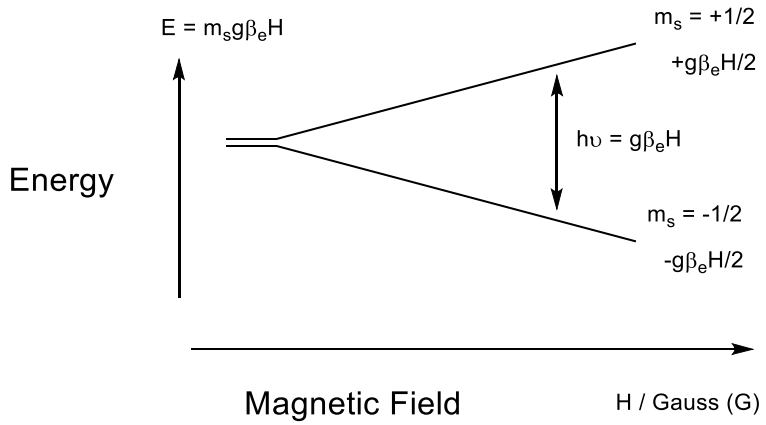

Figure 19. Field splitting in EPR spectroscopy

From the diagram we can see that the field strength can be varied such that the resonance condition is met and the frequency applied is the same energy as the splitting between the two spin states.[121]

The g factor is equal to 2.0023193043617(15) for a free electron (g_e).[122] In real materials, $g \neq g_e$, but for organic radicals the difference is not great, with hydrocarbon based radicals at $2.002 \leq g \leq 2.003$ and N- or O-based radicals at $2.003 \leq g \leq 2.006$ (transition metal ions can have significantly different g values).[123]

Other than the g factor, in the case of organic materials, the most important information that can be derived from an EPR spectrum is probably the *hyperfine coupling*, which is the interaction of electron and nuclear spin, and is analogous to nuclear-nuclear spin coupling in NMR spectra. This has a *hyperfine coupling constant* (A).[124]

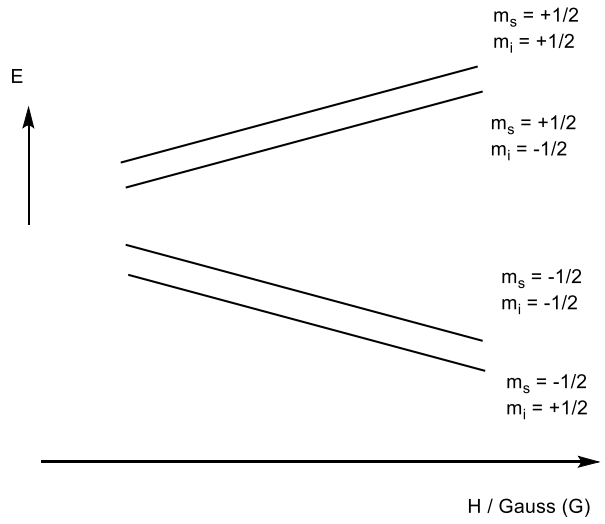

Figure 20. Hyperfine coupling constant levels

The hyperfine coupling can be used in order to determine which spin-active nuclei have significant spin density on them, i.e. to what extent a radical is delocalised and thus stabilised, and the immediate electronic environment of the electron. Importantly, in the case of flavins and other heterocycles, and unlike in NMR spectroscopy, quadrupolar broadening is not an issue due to the much greater sensitivity of EPR, so hyperfine coupling to ^{14}N can be readily observed.[121,123]

Hyperfine couplings and continuous wave (CW)-EPR spectra in general are usually assigned by numerical simulation of the proposed spectrum. Computational methods revealing a calculated spin density such as DFT and *ab initio* methods are also useful in this context.

4.2.1 Pulsed EPR techniques

While EPR is usually performed as a continuous wave (CW) technique, this is in contrast to NMR whereby a pulse sequence is usually followed by a Fourier transform operation, is used to obtain a spectrum. This can be more difficult with EPR as the microwave systems are less tunable than the RF radiation used in an NMR spectrometer.

When an electron is placed in a magnetic field, its magnetic moment will precess about the magnetic field in a manner analogous to a gyroscope about its axis. This precession is perturbed by applying a pulse of microwave radiation. The free induction decay (non-equilibrium magnetisation) is measured and a Fourier transform applied, just as in NMR spectroscopy.

In a rotating reference frame, such that spin precession is stationary, if first a 90^{o} and then an 180^{o} pulse is applied, the second pulse flips the slower spins from the first pulse 'behind' the faster. Upon these catching up and overtaking, a *spin echo* is observed.[124,125]

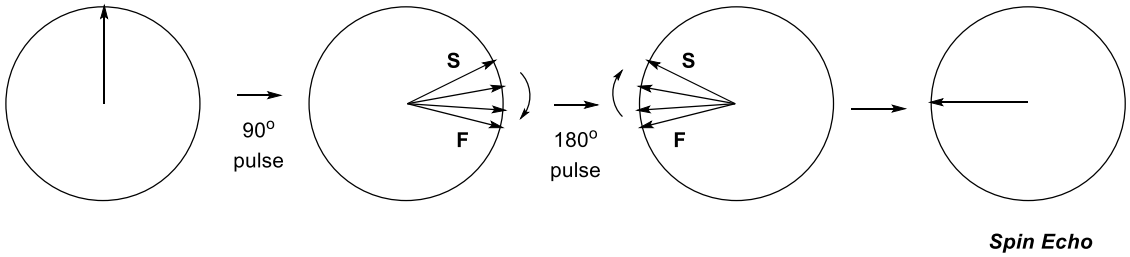

Figure 21. Rotating reference frame depiction of the generation of a spin echo

This is an example of a two-pulse (Hahn) spin echo; stimulated (greater than two pulses) spin echoes can also be generated.

One example of an EPR experiment that can be performed in either a continuous wave or pulsed fashion is electron nuclear double resonance (ENDOR) spectroscopy, which is based on the application of both a microwave and RF frequency, in what can be viewed as a hybrid 'NMR-EPR' experiment. An important aspect of ENDOR methods is that for an electron spin coupled to n nuclear spins, in the ENDOR there are 2n lines whereas in classic EPR spectroscopy the number of lines is 2^n.[124]

Important 2D NMR experiments additionally include ESEEM (electron spin echo envelope modulation). ESEEM involves the measurement of the exponential decay after the spin echo, and measuring the deviations from an ideal exponential decay that result from the weak interactions from nuclei with $I > 0$ hyperfine and quadrupolar interactions. This can be used to (for example) distinguish coupling from protons and from ^{14}N.[124,125]

An even more powerful tool is HYSCORE, standing for hyperfine sublevel correlation spectroscopy. HYSCORE is essentially an ESEEM experiment whereby the pulse times are varied in two dimensions, giving a 2D pulsed-EPR spectrum which superficially looks like a 2D NMR spectrum, such as a COSY or HSQC experiment. In this case it is used to deconvolute complex hyperfine interactions.[126]

4.3 EPR spectroscopy: results

The first EPR sample was prepared by adding Me_2S to a solution of flavin **58** in trifluoroethanol, as given this combination was incompatible with NMR methods, we suspected that the electron rich sulfide could be transferring a single electron to electron deficient flavin.

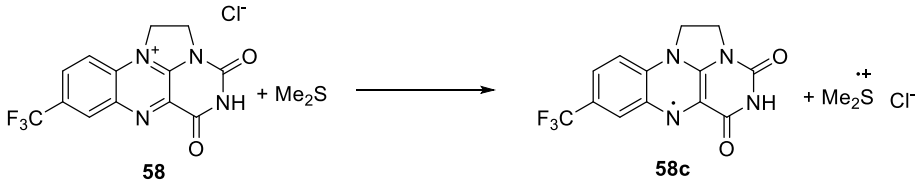

Scheme 98. Proposed single electron transfer between **58** and dimethylsulfide

The sample was run either under air or degassed and sealed with no differences in the EPR spectrum or lifetime. Firstly, a CW X-band experiment was run and displayed in Figure 22. A radical was detected, but there were discrepancies with the expected structure **58c**.

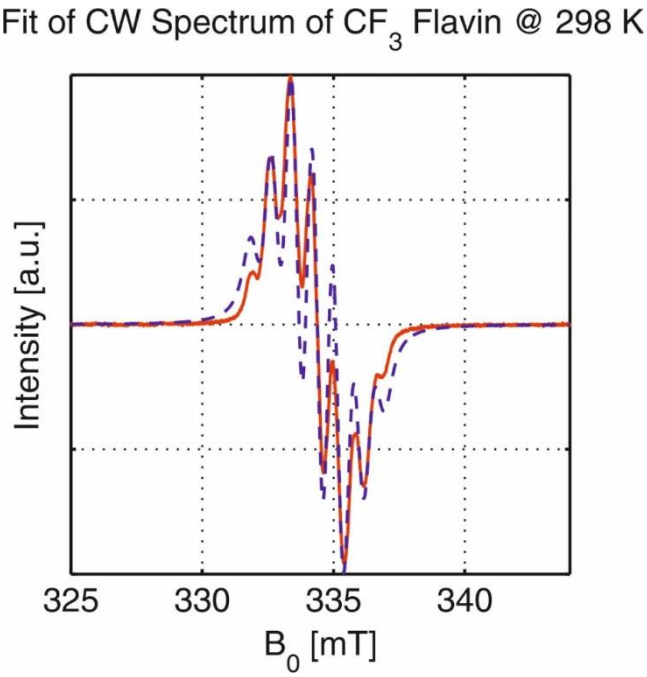

Figure 22. Experimental (red, solid) and calculated (blue, dotted) EPR spectra of **58** + Me_2S in trifluoroethanol

The continuous wave X-band EPR experiment allowed characterisation of the strongest hyperfine interactions and thus the areas of greatest spin density.[121] The *g* factor reflects the global electronic structure, while the hyperfine structure is determined by the local spin density distribution in the vicinity of the nuclei; in this case EPR-active ^{14}N, ^{1}H and ^{19}F around the flavin heterocyclic ring system.

As flavin and sulfide in TFE is a liquid solution at 298 K, and the radicals have a virtually non-restricted molecular degree of freedom, e.g. free tumbling or rapid reorientation, and so any anisotropy in the *g* factor and in the hyperfine splittings is observed as an average.

The isotropic coupling to three nearly equivalent ^{14}N nuclei gives rise to the hyperfine structure. The isotropic hyperfine coupling described accounts for ~ 22 MHz (0.8 mT) and so the unpaired electron has spin density distribution of ~20% in the 2*p* orbital of a ^{14}N atom.[127]

The protons lie in the plane of the $\boldsymbol{\pi}$ orbital occupied by the unpaired electron of the semiquinone flavin ring. Even the largest proton coupling of ~21 MHz (0.75 mT) only amounts to a fractional density distribution of ~1.5% in the *s* orbital of a hydrogen atom.[121]

In order to assign a structure for our semiquinone species, numerical simulations were performed and there was good agreement between the simulated and real spectrum, for a flavinium radical *cation* **58d**, as we see a large degree of coupling on N(5).

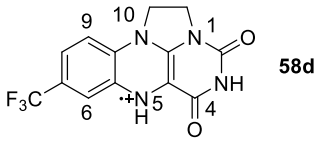

58d

Figure 23. Flavinium radical cation **58d** displaying relevant atom numberings

This was surprising because we had initially expected to observe a neutral semiquinone based on an expected single electron transfer from a cationic flavin. However, given the starting material is positively charged but analogous to a neutral flavin, it can be argued that **58d** radical cation is analogous to natural neutral semiquinones formed by a proton-coupled single electron trasnfer, whereas a neutral flavin in this case might be more like the radical *anion* found in nature from single electron transfer alone.

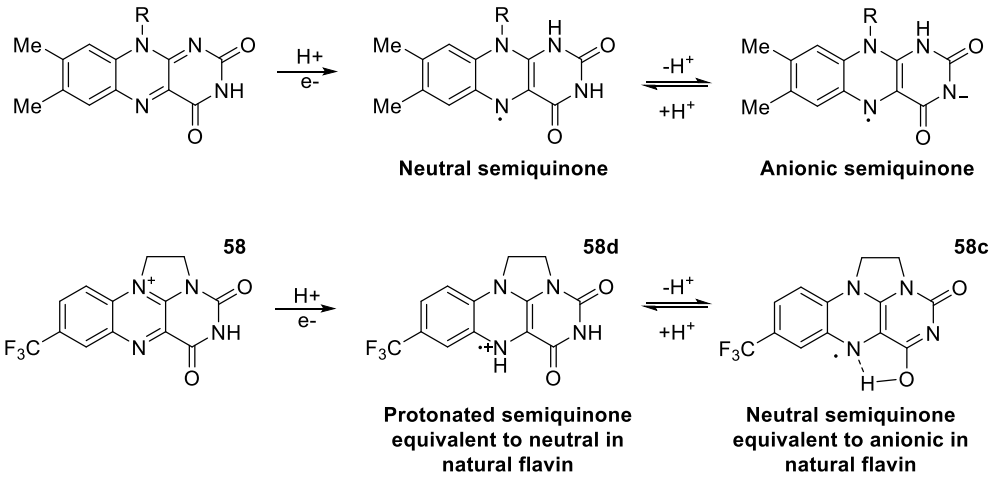

Scheme 99. Formation and protonation states of flavin semiquinones in nature and in this system

Further data was collected to observe the interacting ^{14}N nuclei. The four-pulse EPR experiment, hyperfine sublevel correlation spectroscopy (HYSCORE),[126] was used to obtain information about the surrounding magnetic nuclei around the unpaired electron spin.

This 2D ESEEM method has the ability to resolve weak hyperfine interactions (<5 MHz) of remote nuclei with the unpaired electron spin, which are masked or suppressed by EPR broadening in the hyperfine structure. The ESEEM signal appears only if the allowed and forbidden EPR transitions are simultaneously induced by microwave pulses.[128] In the case of the ^{14}N nucleus with the spin $I = 1$, the time-independent spin-Hamiltonian includes an additional nuclear quadrupole interaction term.[128]

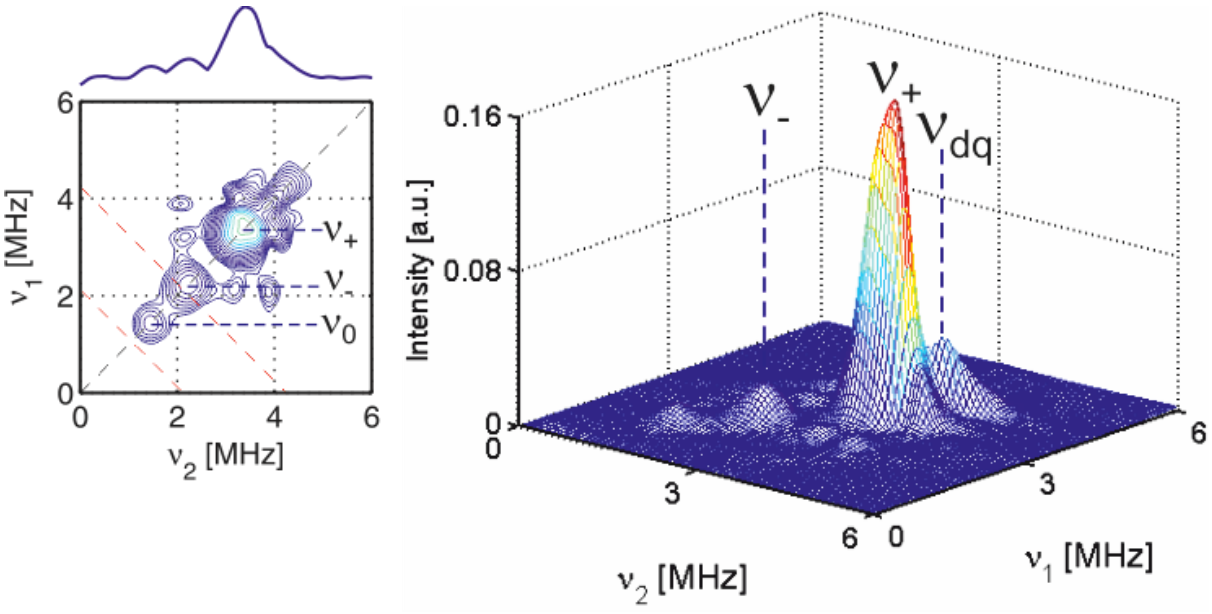

Figure 24. Contour presentation (**left**) of the X-band natural abundance ^{14}N HYSCORE spectrum of flavin semiquinone **2a'**

The X-band ^{14}N HYSCORE spectrum resolves the three contour-peaks from the three nuclear frequencies (Figure 24).[129] In orientation-disordered samples such as frozen solutions used in this work, not all transitions contribute equally to the spectrum due to their differing orientations.[130] In this case, the component n_+ dominates the other two n_0 and n_- components, unsurprisingly for a molecule that deviates far from an ideal spherical geometry.

Intensities of contour-peaks are significantly influenced by the selection of the time *t* between the first and second pulses. For this reason, several experiments at different time *t* were performed in order to detect all contour-peaks contributing to the HYSCORE spectrum. The nuclear quadrupole and hyperfine couplings are assigned to ^{14}N(5) and ^{14}N(10).

It became possible to determine the reduced magnitude of relatively large hyperfine couplings from other nitrogen atoms following the ^{2}H/^{1}H substitution of solvent, i.e. use of CF_3CD_2OD in place of CF_3CH_2OH. However, we did *not* see deuterium substitution of the N(5) proton upon the use of deuterated solvent.

It is possible, therefore, that the source of the proton is in fact the highly acidic dimethyl sulfide radical cation (pK_a = -1.8).[131] This transferred proton then appears not to exchange with deuterated solvent.

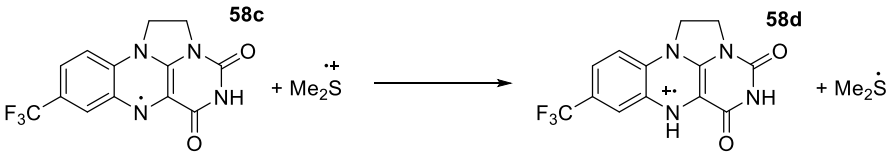

Scheme 100. Proton transfer between **58c** and $Me_2S^{+\bullet}$

One additional surprising feature of this spectrum was observation of coupling to fluorine. Our calculations of spin density (see **4.3.2**) showed no spin density at all on the carbons next to fluorine, as would be expected by a simple arrow pushing exercise. One possible explanation is hyperconjugation between the singly-occupied π orbital in the resonance form with the radical on C7 and the σ* C-F bond. Of additional note is that ^{1}H-^{19}F coupling in NMR spectroscopy is quite long range (up to 5 carbons away).[132]

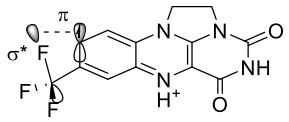

Figure 25. A hyperconjugation rationale for ^{19}F hyperfine coupling

4.3.1 Benzylamine derived radical

Upon addition of alloxan **138a** and benzylamine **15a**, a completely new EPR spectrum was observed which appears to correspond to the dibenzylaminyl radical, consistent with an H-abstraction mechanism. This radical demonstrated relative long-term stability (on the order of hours-days) and therefore is consistent with an oxygen-starved resting state, consistent with our observation that oxidation of the amine does not readily occur without stirring of the reaction vessel.

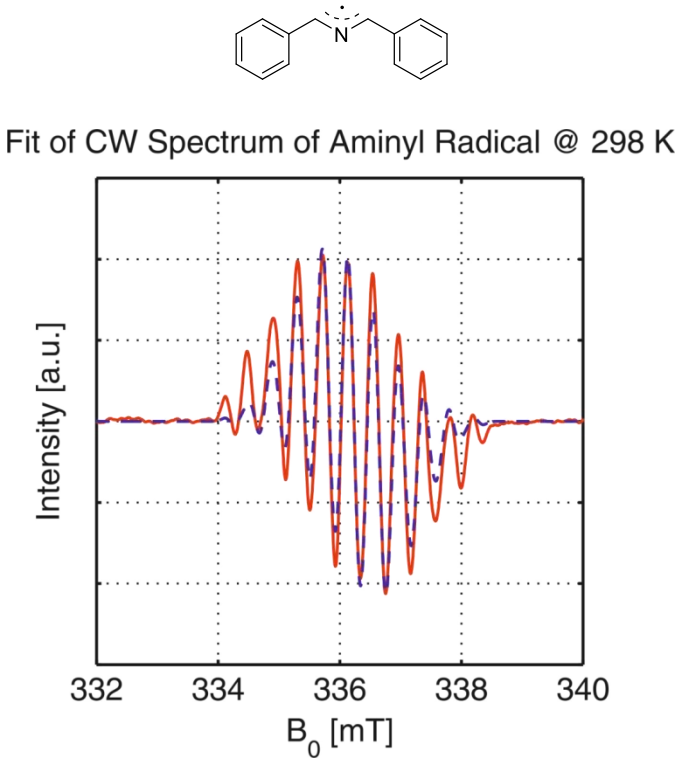

Figure 26. Amine based radical **172**, EPR spectrum (CW, X-Band, 298K) and numerical simulation (red solid and blue dotted lines respectively)

For this species, eight proton nuclei (I = 1/2) are nearly equally coupled. The radical first contains protons on its two rings that are grouped into the two nearly equivalent sets but with slightly different isotropic couplings of ~ 11 MHz and ~ 9 MHz, respectively. Again, the spin polarization mechanism is responsible for the resolved hyperfine splittings from these ring protons. The central nitrogen atom carries a significant spin density distribution and contributes to a slight asymmetry of the absorption derivative; as a result its neighbouring two protons also possess the same order of the isotropic coupling; ~ 13 MHz. Numerical simulations were again performed that suggested a symmetrical, dibenzyl imine based radical.

4.3.2 Simulated spin densities

The spin densities of the two radicals of interest were calculated using hybrid DFT and post-Hartree Fock methods in order to corroborate the EPR spectroscopy discussed. The spin density was indeed modelled to be localised primarily on the N(5) carbon

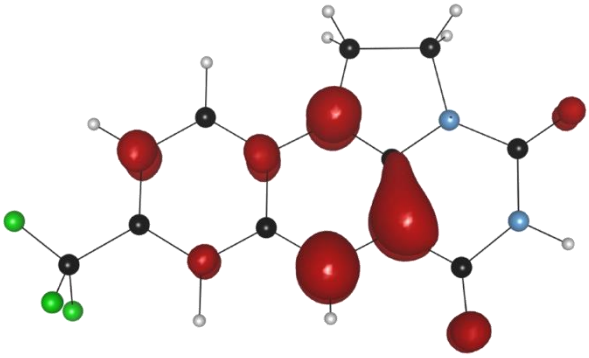

Figure 27. Calculated spin density of flavinium radical cation **58d**

. The lack of spin in the region of the trifluoromethyl group, as would be expected from a simple 'arrow pushing' exercise, fits with the proposed explanation of a hyperconjugation interaction with the adjacent aryl carbon π-systems.

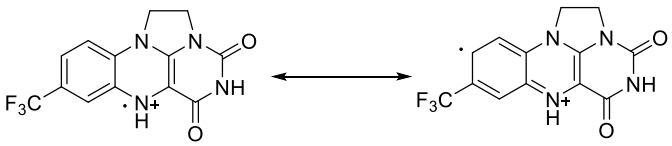

Scheme 101. Resonance forms of **58d**

Radical **172** also showed a highly symmetric spin density which correlated with that observed in the EPR; a highly delocalised and symmetric radical with potential for hyperfine coupling to the benzylic protons on both aryl rings.

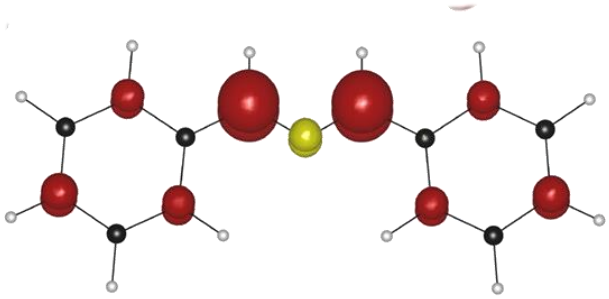

Figure 28. Calculated spin density of radical **172**

4.4 Kinetic monitoring of the flavin/alloxan catalysed amine oxidation

4.4.1 Rate laws

The rate of a chemical reaction is defined by its *rate equation*. A rate equation is of the form

$$r = k[A]^x[B]^y \ldots$$

Where r is the rate of reaction, k is a rate constant, and [A] and [B] are concentrations of reactants. *x* and y represent the *order* of reaction; the extent to which that concentration affects the rate law. An example is if $x = 0$, the rate of reaction is independent of [A], whereas if $x \neq 0$ then [A] is involved in the rate determining step. The overall order of the reaction is the sum of these powers.[133]

Depending on the reaction in question, rate equations can be determined either by the use of the initial rate, where linearity of a series of experimental data points is assumed over the initial period of the reaction, or by a mathematical treatment of the data set such that it is linear (the integrated rate equation).

The latter method also gives information about the order, as usually (though not always) a linear plot of [reactant] vs. time is zero order in the component being consumed/observed (i.e. the 'starting material' in a typical organic reaction). A linear plot of ln[reactant] vs. time is typically first order in [reactant], and finally 1/[reactant] vs. time being linear signifies second order kinetics in [reactant].

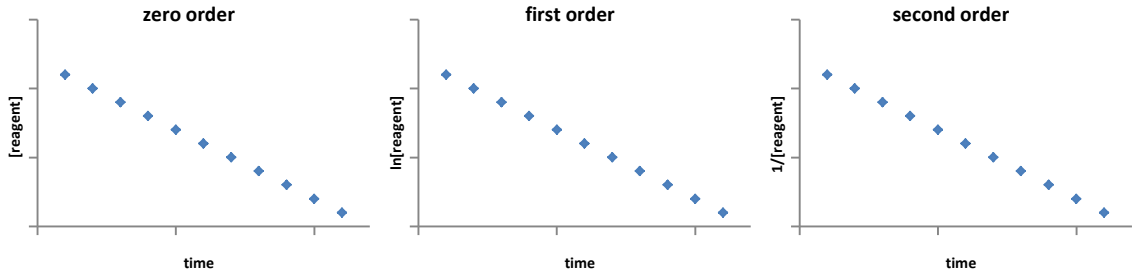

Figure 29. Representative examples of the three cases for a reagent

In more complex cases, fractional orders tend to relate to either a chain reaction process or an aggregation, whereby the species of interest is present as an oligomer but reacts as a monomer. Inverse order is a reaction inhibitor.[134]

A complementary method for the determination reaction orders is with a log/log plot, where time and rate are both read as logarithms, and the slope of the plot gives the order of reaction.[135]

4.4.2 Kinetic Monitoring: Method

Firstly, a suitable method of physical monitoring for determining the kinetics of the reaction was required. As the reaction mixture was paramagnetic in nature, we found it impossible to use *in situ* NMR kinetics methodology to follow the progress of the reaction. Additionally, although we attempted *in situ* IR spectroscopic monitoring (ReactIR®), a lack of IR peak resolution precluded its use.

Instead, normal phase HPLC, using a cyano-capped silica column, was selected in order to monitor the reaction, by way of aliquot sampling. We were unable to directly observe the amine in this fashion; but there were no side reactions as gauged by NMR spectroscopy (and isolation of product by mass generally corresponding to NMR internal standard yields or conversions). Therefore, cross-checking against ^{1}H NMR spectroscopy increased our confidence in the method in order to use it for kinetic analyses.

We used a solvent system of 95:5 or 90:10 hexane:IPA, with an additive of 0.1% ethylenediamine added to the IPA. We observed a sharp peak at 1.9 min for naphthalene and a fairly broad one at 8 – 11 min for imine **154a**, at a wavelength of 260 nm.

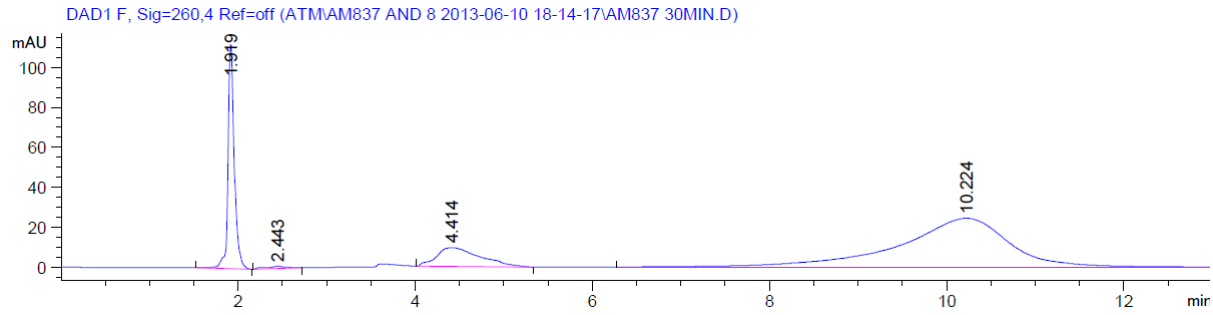

Figure 30. Example HPLC trace showing naphthalene (1.919 min) and imine (10.224 min)

Given imines are non-polar species this possibly represents some sort of interaction between the eluent and product, such as the formation of 'crossed' imines with ethylenediamine, which although ill-defined was a fortuitously effective way of separating two quite non-polar molecules on a normal phase analytical column.

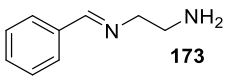

173

Figure 31. Possible structure of imine-ethylenediamine adduct observed in HPLC

By injection of solutions of known concentrations of naphthalene and imine **154a** we were able to obtain a response factor of 1.53, meaning we could calibrate our method to concentrations of product and thus, the remaining starting material. This was, as previously mentioned, benchmarked by an NMR cross-check.

In addition, we ran a kinetic experiment three times in order to confirm that the method was reproducible, the standard error is shown (Figure 32).

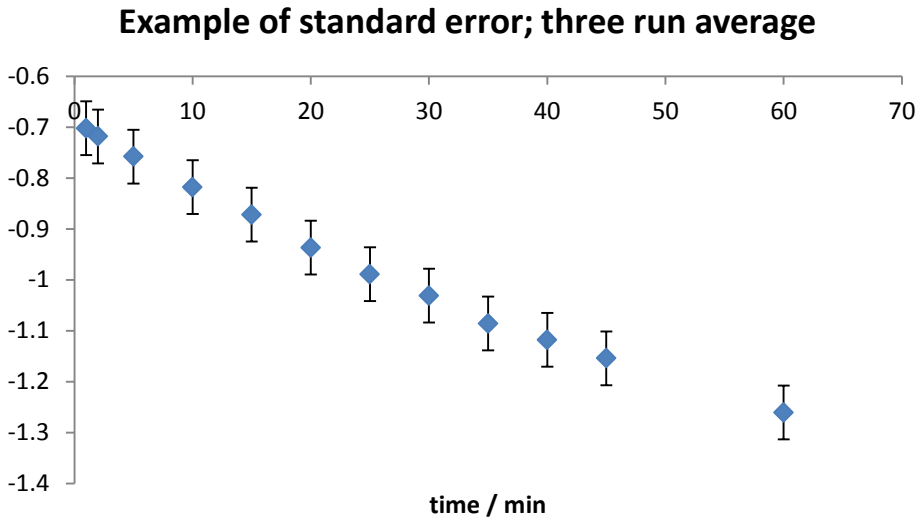

Figure 32. Example standard errors for amine oxidation kinetics

4.4.3 Rate dependence of amine

Firstly, we determined the order of reaction in benzylamine **15a** to be first order. The first suggestion that this was the case was that applying a logarithmic function to the plot of the progress of the reaction gave a linear fit.

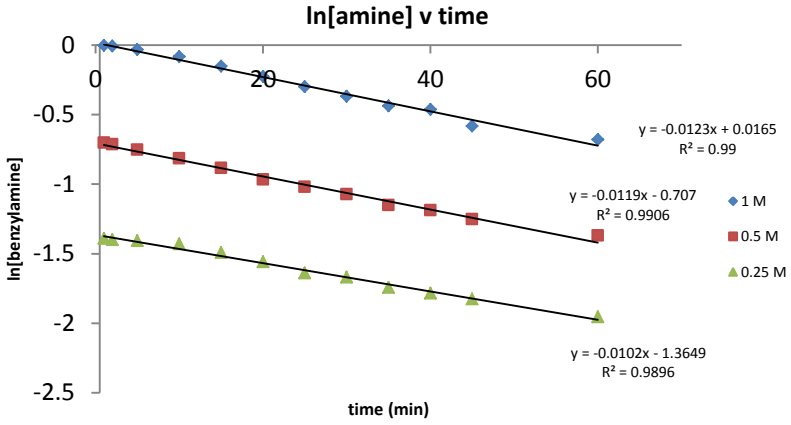

Figure 33. Varying concentrations of [amine]

Additionally, when entering the slopes of the lines into a log-log plot, we found a slope of 1 – the rate of reaction doubles with doubling the concentration; therefore the reaction is first order, consistent with and benzylamine being involved in the rate determining step.

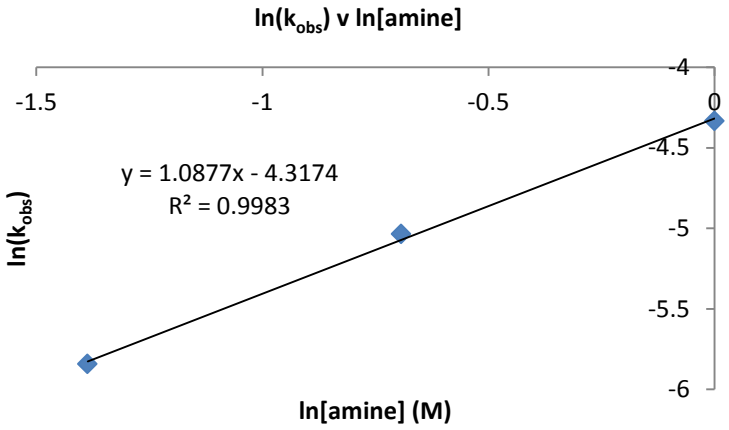

Figure 34. Log-log plot of k_{obs} and [amine]

4.4.4 Rate dependence of catalysts

The rate dependence on [Flavin] **58** was measured over a range of 25 → 400 μM, and was found to be fractional order, with a linear relation on a log-log plot of 0.25 (deviation from this value occurred at low concentration).

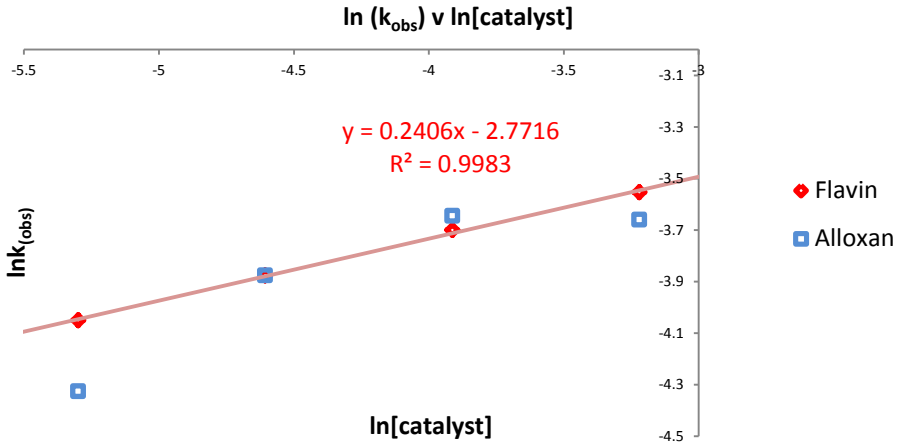

Figure 35. Effect of [flavin] and [alloxan] on rate

We considered two distinct possibilities for this observation: Firstly, the flavin was acting as a promoter in a classical radical initiated reaction such as observed with compounds such as AIBN.[136] Secondly, that aggregation effects were important in this case, i.e. the flavin is aggregated in solution but reacts as a monomer. This flavin aggregation, proceeding *via* hydrogen bonding between two imides rather than π-stacking, has been discussed in the context of flavin photocatalysis (although in this case further aggregation occurs *via* the aryl ring π-stacking).[104]

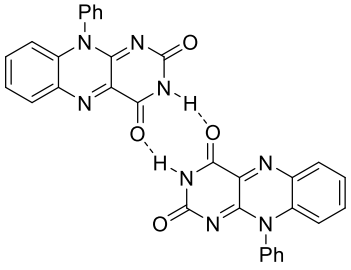

Figure 36. H-bonded flavin observed in solid state

Alloxan **158a** was also found to have non-integral order, with k_{obs} being measured at 25 – 400 µM giving also a non-linear log-log relationship and looking much more like saturation-type kinetics: increasing [alloxan] beyond about 100 µM did not appear to affect the rate.

This could be explained either by a solubility limit of alloxan in CF_3CH_2OH, which is perhaps unlikely as alloxan is relatively insoluble until reaction initiates anyway, or that there is a termination or inhibitory step or side reaction pathway which involves alloxan in some way.

A further possibility is that a change in rate determining step occurs between one which involves alloxan at low concentrations of alloxan but saturates at higher concentrations of alloxan, thus becoming rate insensitive.

4.4.5 Rate dependence of O_2

We found that it was harder to quantify the dependence of rate on air. An O_2 atmosphere promoted a somewhat faster reaction but using a 10% O_2 atmosphere did not significantly decrease the observed rate. Notably, omitting stirring gave minimal reaction, comparable to completely excluding air and running the reaction under an atmosphere of N_2.

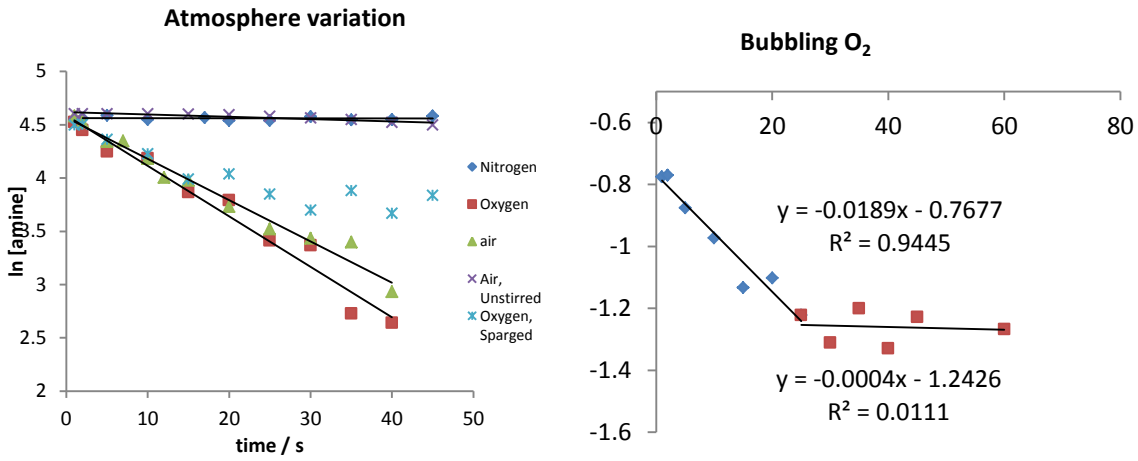

Figure 37. Effect of atmosphere on rate

A closer examination of the reaction in which O_2 was constantly bubbled into the reaction mixture shows that the reaction was initially relatively fast, but halted after 25 minutes. This could be evidence for a termination process that is O_2-dependent. A possibility is that O_2 acts as a competitive electron acceptor that, when present in high concentration, accepts electrons preferentially to another reactive species critical for catalytic turnover.

4.4.6 Rate dependence on Me_2S

We varied the concentration of Me_2S present in the reaction and monitored its effect on rate. It appears that there is minimal rate dependence on Me_2S, although some is required to be present for efficient reaction. This is in contrast to the observation that the reaction was promoted by increasing loading of Me_2S during our initial optimisation experiments; however we only ran the reactions for kinetic monitoring in most cases for 45 – 60 mins, correlating to a conversion of ~35 – 40%. Therefore, perhaps the reaction is prone to stalling without a greater concentration of Me_2S present.

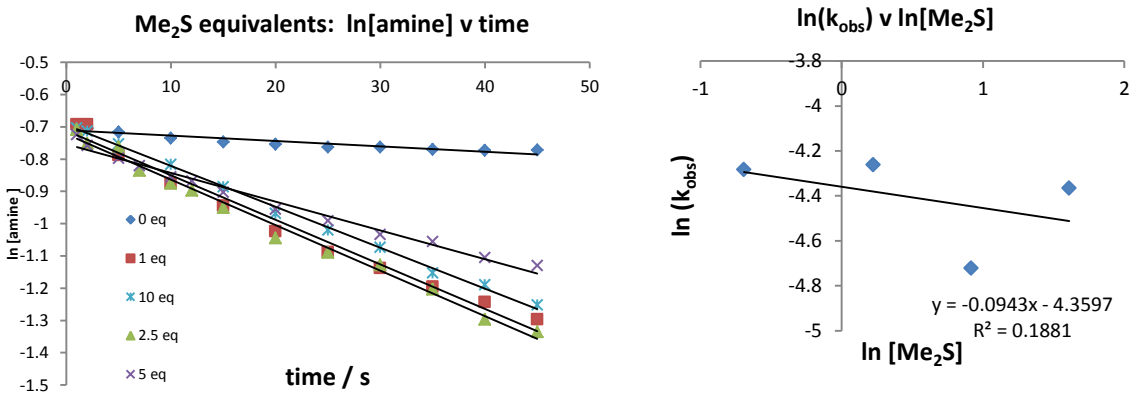

Figure 38. Varying amount of Me_2S, effect on rate

4.4.7 Rate dependence on flavin type

A comparison of CF_3 – substituted flavin **58** to des-CF_3 **57** was undertaken, because this flavin has a standard reduction potential much closer to that of natural flavin cofactors (+66 mV relative to SHE vs. +40 mV relative to SHE for MAO-B)[68,137]

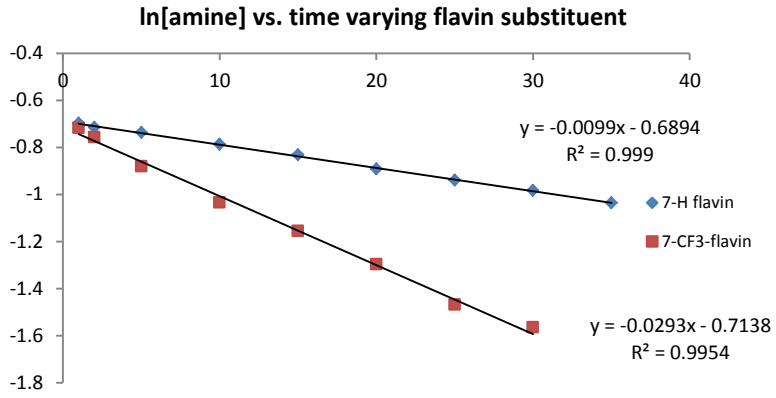

Figure 39. Varying substitution of flavin (**58** vs **57**)

4.4.8 Kinetic isotope effect

A kinetic isotope effect is the change in rate of a reaction upon isotophic substitution of an atom, and is defined by the equation

$$KIE = \frac{k_L}{k_H}$$

Where k_L is the light isotope and k_H the heavy isotope. This occurs because of the differing bond strengths of an bond between a heavier atom and protium/deuterium. Additionally, quantum tunnelling pathways are more accessible for bonds to H than bonds to D.[138] For most heavy atoms this change is small, although ^{13}C and ^{15}N kinetic isotope effects are routinely measured.[139,140] The difference is essentially related to the differing bond strengths, with the heavy isotope forming a stronger, more difficult to break bond. Quantum tunnelling effects may also become important.[133] In general, KIEs of measurable significance occur on substitution of D for H if H abstraction (either as a hydride, proton or hydrogen atom) is rate limiting. These KIEs can be quite large, with the reaction of deuterated product potentially 6 – 10 times faster.[133]

We decided to probe whether C-H bond breaking was rate determining in benzylamine oxidation by comparison of **15a** with its deuterated analogue. The corresponding α-deutero benzylamine **175** was synthesised by reduction of benzonitrile **174** with $LiAlD_4$.

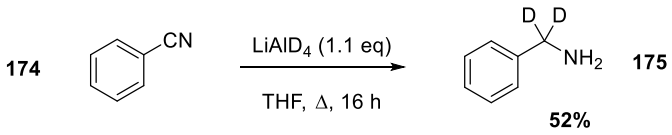

Scheme 102. Synthesis of α-deutero benzylamine **175** by reduction with $LiAlD_4$

When run as independent experiments, we found that the isotopically enriched benzylamine was slower reacting than the corresponding protic amine.

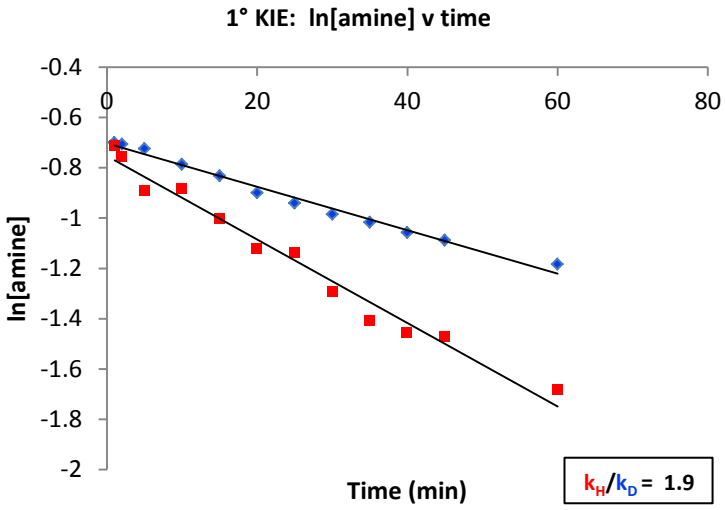

Figure 40. Primary kinetic isotope effect of $PhCH_2NH_2$ **15a** (red) vs. $PhCD_2NH_2$ **175** (blue)

The kinetic isotope effect was 1.9, strongly suggesting that C-H bond breaking is rate limiting in this reaction.

Upon observation of the product, no scrambling of H/D in the NMR spectrum was detected; with deuterium on both the imine and benzylic sp^3 positions. This indicates there is no exchange of deuterium for hydrogen with solvent or incidental moisture. This is consistent with the fact we noticed *no* deuterium in the EPR spectrum when the reaction was performed in CF_3CD_2OD.

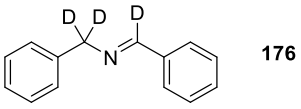

176

Figure 41. Product formed by oxidation of **175**

4.4.9 Kinetic dependence of *para*-substitution of benzylamines

The Hammett equation describes the relationship of the rate of a reaction to substituted benzene derivatives with the electronic nature of their substituents expressed in terms of the empirical parameter σ. The equation takes the form[141]

$$log\left(\frac{k}{k_0}\right) = \sigma\rho$$

In this equation, σ is the aforementioned Hammett parameter, ρ is the substituent independent reaction constant, and k and k_0 are the rates of the substituted system in question and its parent H-substituted ring respectively. We investigated the initial rates of 4-methoxybenzylamine, 4-methylbenzylamine, benzylamine, 4-fluorobenzylamine and 4-chlorobenzylamine. Given rate is determined by *C-H* bond breaking we expected to observe some degree of rate dependence upon varying ring electronics.

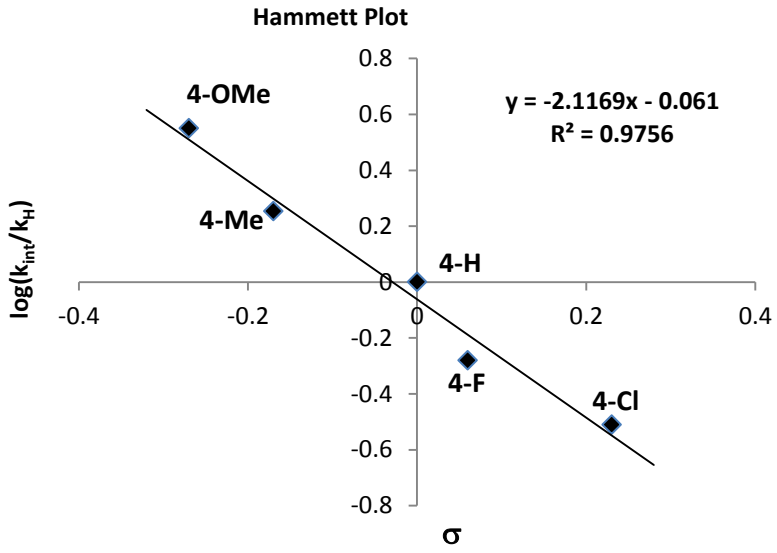

Figure 42. Hammett plot of rate vs. *para*-amine substitution

The negative slope indicates that the reaction is faster with electron rich substituents than with electron withdrawing groups positioned on the aromatic ring. This suggests that there is an intermediate which is electrophilic in character. This could be *via* abstraction of either a hydride or a hydrogen atom (for an electrophilic radical) but would be inconsistent with proton transfer.

4.4.10 Job plot

Job's method of continuous variation is a method originally developed in enzymatic chemistry in order to determine the stoichiometry of binding of substates.[142] The total molarity of two interacting components is kept constant but the mole fraction of each is varied. In this case, we attempted desired to investigate the relation of [flavin] and [alloxan] and so determine if stoichiometric binding between the two occurs. This study would also ascertain if there is a maximum reaction rate at a certain concentration of each component.

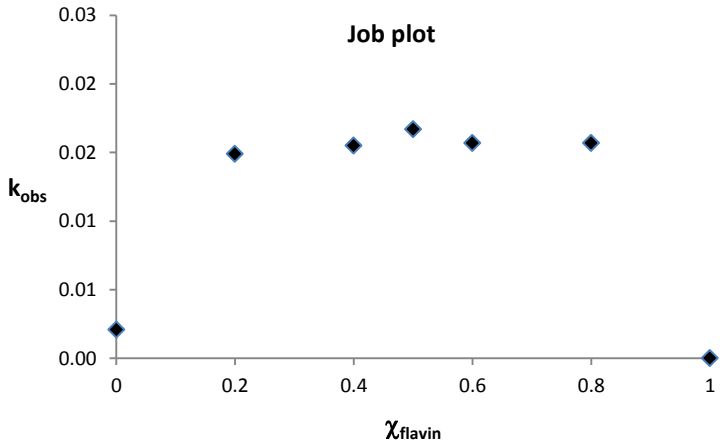

Figure 43. Job plot of mole fraction flavin

The observed reaction rate was insensitive in so far as each catalyst was present in the reaction. This implies that there is no stoichiometric binding between **58** and **138a**, and is consistent with the complex kinetics observed in the rate laws for the catalysts, without a rate dependence on the formation of one component.

4.4.11 Change in order

As the reaction progressed beyond 1 h, the quality of the fit for first order kinetics in [amine] diminished. Upon further investigation it appeared the latter part of the reaction was in fact *zero* order. This is unusual, because rate would normally be expected to be more dependent on [reagent] as this concentration decreases. Concentration of dissolved oxygen becoming rate-limiting could be an explanation for this.

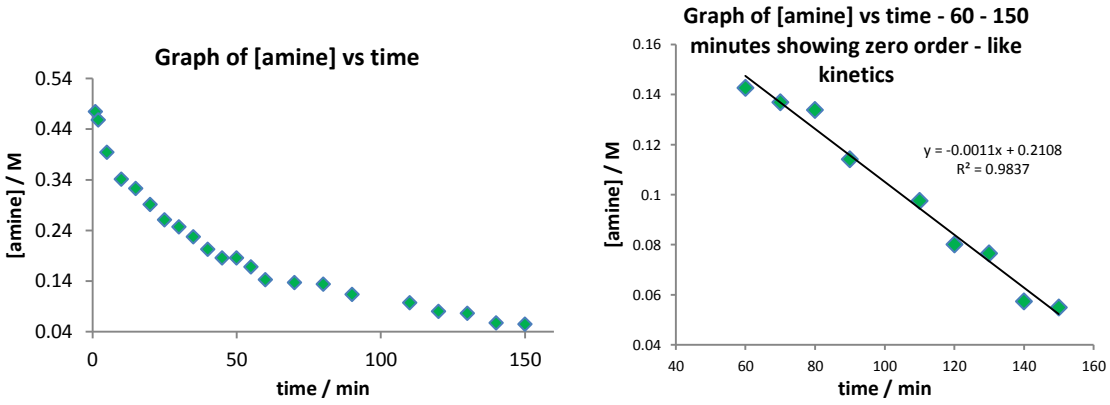

Figure 44. Zero order like kinetics in latter stages of amine oxidation

4.5 Probing flavin aggregation states by DOSY spectroscopy

Diffusion ordered nuclear magnetic resonance (DOSY) spectroscopy is a technique used to indirectly probe the molecular weights of compounds in a system, by separation of their diffusion coefficients. A larger molecule would be expected to diffuse more slowly through a given solvent, and so the size, whether related to a discrete molecule or aggregation state, be assessed. Signals with a higher diffusion coefficient relax faster in the series of NMR pulses observed than those with a low diffusion coefficient.[143]

Although apprehensive about NMR based experiments on our system due to the paramagnetic character of the reaction, we decided to measure the diffusion coefficient of the flavin in solution, as a starting point. The results of the experiment are shown below.

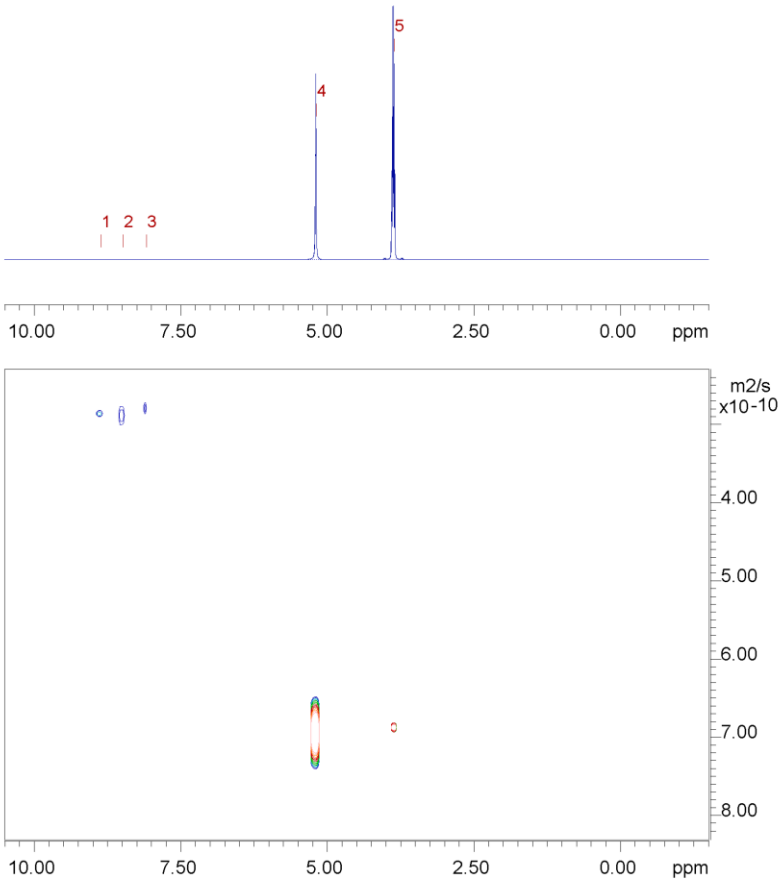

Figure 45. DOSY plot of flavin in TFE. Peaks 1, 2 and 3 represent the flavin aromatic peaks of interest, peak 4 and 5 are the solvent. The y axis of the 2D NMR plot is diffusion coefficient

Using the Manchester NMR methodology group's method of estimation of molecular weight from DOSY, we obtained from the diffusion coefficient of 2.78 x 10^{-10} – 2.90 x 10^{-10} m^2 s^{-1} depending on the chosen peak. These yielded estimated molecular weights of 777 – 852 Da, corresponding to an aggregation number of 2.5 – 2.8.[144,145]

In CD_3OD, our diffusion coefficient was 9 x 10^{-10} m^2 s^{-1}, corresponding to a molecular weight of ~280 Da, consistent with a monomer (309 Da), so it appears solvent polarity or dielectric constant plays a key role in these interactions.

While these values are approximates, this does suggest that in TFE, the flavin is either dimeric or trimeric. This is unlikely to be due to π-stacking due to the cationic character of the flavin, but could instead be an imide-bridged dimer as shown. A trimer is harder to rationalise by hydrogen bonding, but perhaps could occur due to further, hydrophobic interactions between flavin molecules (see crystallography section). Alternatively, there could be an associated solvent bound to a dimeric flavin.

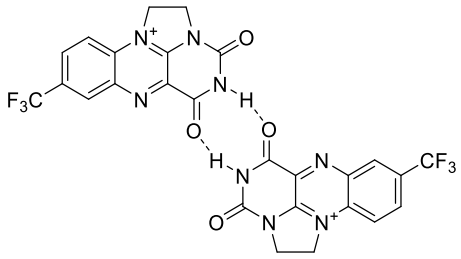

Figure 46. Flavin dimer through imide H-bonding

However, an important caveat to these results is that DOSY based estimates of molecular weight from diffusion coefficient have the limitation of assuming a spherical system. Flavins are near-planar, and dimeric structures of the type depicted in Figure 46 are further still from idealised spherical geometry. The method of estimation of molecular weight is based on the Stokes-Einstein equation[146]

$$D = \frac{k_B T}{6\pi\eta r}$$

Where k_B is the Boltzmann constant, T temperature, η viscosity and r the radius of an assumed particle from which molecular weight can be determined. However, greater deviations from linearity will have correspondingly greater errors in estimated MW.

When we added increasing amounts of Me_2S to the system, to a point still giving resolvable NMR spectra, we found that the diffusion coefficient actually increased, giving a decreased MW down to 700 Da This could be due to a flavin dimer with a dimethyl sulfide molecule bound in a charge transfer interaction: [2 **Fl**.DMS]$^{2+}$ has a molecular weight of 711 Da, fairly close to the estimated value.

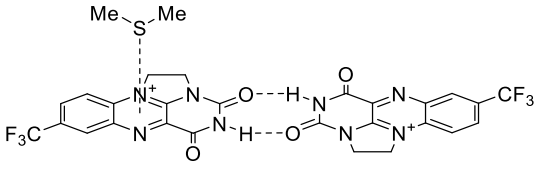

Figure 47. Dimeric flavin with CT bound dimethyl sulfide

4.6 Mass spectrometry

The mass spectra of these reaction mixtures were observed in an attempt to observe intermediates in the process of catalysis. Given *C-H* bond breaking appeared to be rate determining, we hoped to observe any intermediates formed; for example if amine was covalently bound to either flavin or alloxan prior to *C-H* bond breaking. Indeed, given there is some background and/or stoichiometric reactivity with alloxan alone, and additionally given Sayre's observing of the C_{10a} adduct of benzylamine to the flavin by isotopic enrichment and ^{13}C NMR spectroscopy there was precedent for buildup of intermediates for either compound.[72]

Instead, in addition to the expected species (cationic flavin, amine, imine) was a peak at m/z=298.080 This appears to be equivalent to the decomposition product observed by both Cibulka and Sayre when these types of alloxazine are reacted with base in methanol, the latter present in the ES/MS injection loop.[58,72]

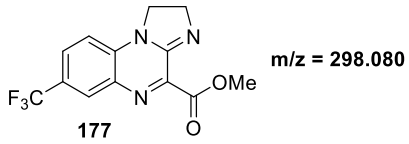

Figure 48. Suspected decomposition product as observed by ES/MS and characterised by Sayre

In this case, the imide has been cleaved and methanol has been incorporated in the system.

4.7 Crystal structure

Flavin **58** was crystallised from formic acid/diethyl ether. By slow vapour diffusion of the volatile ether antisolvent we were able to grow crystals suitable for single crystal X-Ray crystallography.

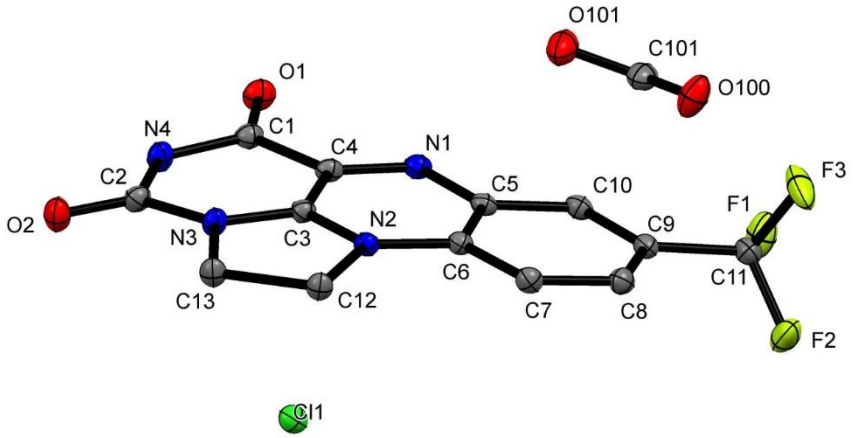

Figure 49. Crystal structure of flavin **58**, co-crystallised with HCO_2H

The flavin crystallised as a 1:1 solvate with formic acid, in the monoclinic $P2_1/n$ space group, and the flavin adopts a strained planar arrangement leading to slight curvature; however this is centred round the chloride counter-ion which has a cation-anion separation of 3.281 Å, almost analogous to previously discussed flavin CT complexes.

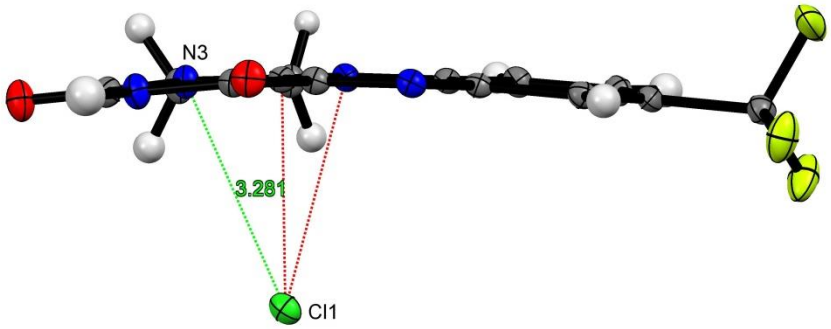

Figure 50. Cation – anion separation and slight curvature observed

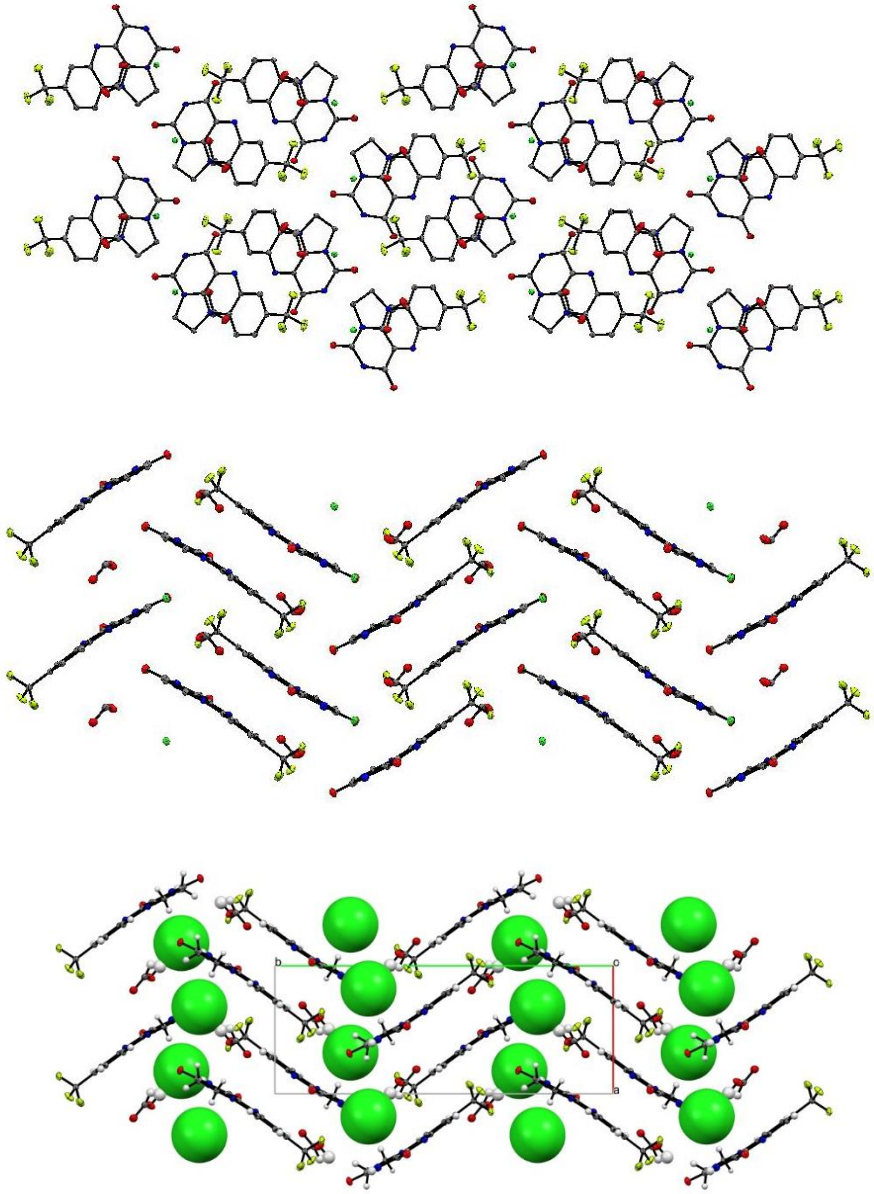

Figure 51. Crystal packing, two angles and space filling, the latter also showing the unit cell

The crystal packing is that of a ‘herringbone’ type motif, with chains of flavin cations along the α direction. As expected from their cationic nature, they do not π-stack, with instead a formic acid occupying the space between flavinium groups. As seen from the space-filling model, which indicates the actual size of the chloride ions, the chloride ions are in non-connected cavities rather than channels; indicating that it is unlikely ions could be transported throughout the flavin in the solid state.

There are two formal hydrogen bonds in the structure; one between the flavin and the chloride and between the chloride and the formic acid (Figure 52).

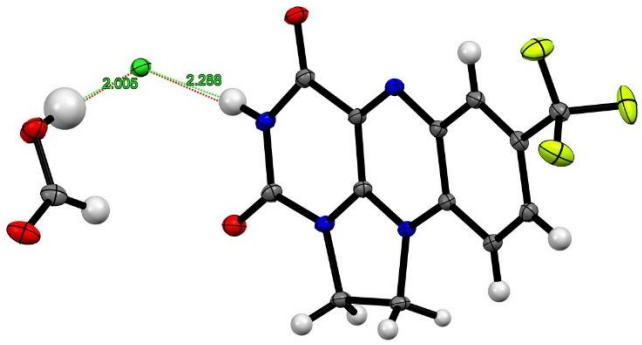

Figure 52. Inter-atomic distances between atoms in flavin crystal structure

Each CF_3 group is involved in three C-H---F and OH---F interactions. This may explain the surprisingly well-ordered CF_3 groups in this instance, which can often show high levels of rotational disorder, even at low temperatures.[147]

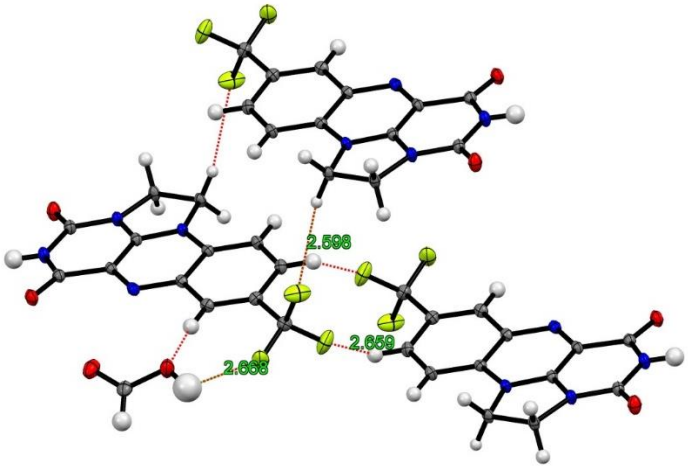

Figure 53. H-F interactions in solid state

Alternatively, although this refers to the semiquinone radical cation in solution, the EPR spectrum shows some hyperfine contribution from the CF_3 presumably *via* a long-range hyperconjugation type communication. This could be either a cause or a consequence of a conformational 'lock' on the CF_3 group. This effect could also be a contributor towards aggregation behaviour observed in CF_3CH_2OH, as discussed in the DOSY section (**4.6**).

4.8 UV/visible spectroscopy

One of the most prevalent methods for studying flavin cofactors, particularly free FAD or FMN groups, is UV/visible spectroscopy. Flavins have two distinct peaks at $\lambda_{max} \approx 360$ and ≈ 450 nm.[148]

In particular, the rates of reductive and oxidative half reactions are generally observed by 'stopped flow' spectroscopy whereby very rapid mixing and measurement at a specific wavelength is used to conduct accurate kinetic measurements on the millisecond timescale.[19,149-151]

The original report of flavinium chloride catalyst **58** showed peaks at 396 and 340 nm in water and at 388 and 340 nm in acetonitrile. Upon reduction with sodium dithionite ($Na_2S_2O_4$) or sodium borohydride respectively, these shifted to 362 and 312 nm in water and a single peak at 304 in MeCN.[68]

In our system it was first necessary to examine the oxidised flavin in the solvent of interest, trifluoroethanol, whereby we observed λ_{max} values of 400 and 354 nm.

Upon the addition of dimethyl sulfide under anaerobic conditions we observed a peak begin to appear at 329 nm. This is consistent with the previously reported flavin semiquinone spectra which consisted of 'shoulders' at a slightly lower wavelength from the main oxidised flavin peak.[152] Decresed intensity of absorbtion consistent with two-electron flavin reduction was not observed under these conditions.

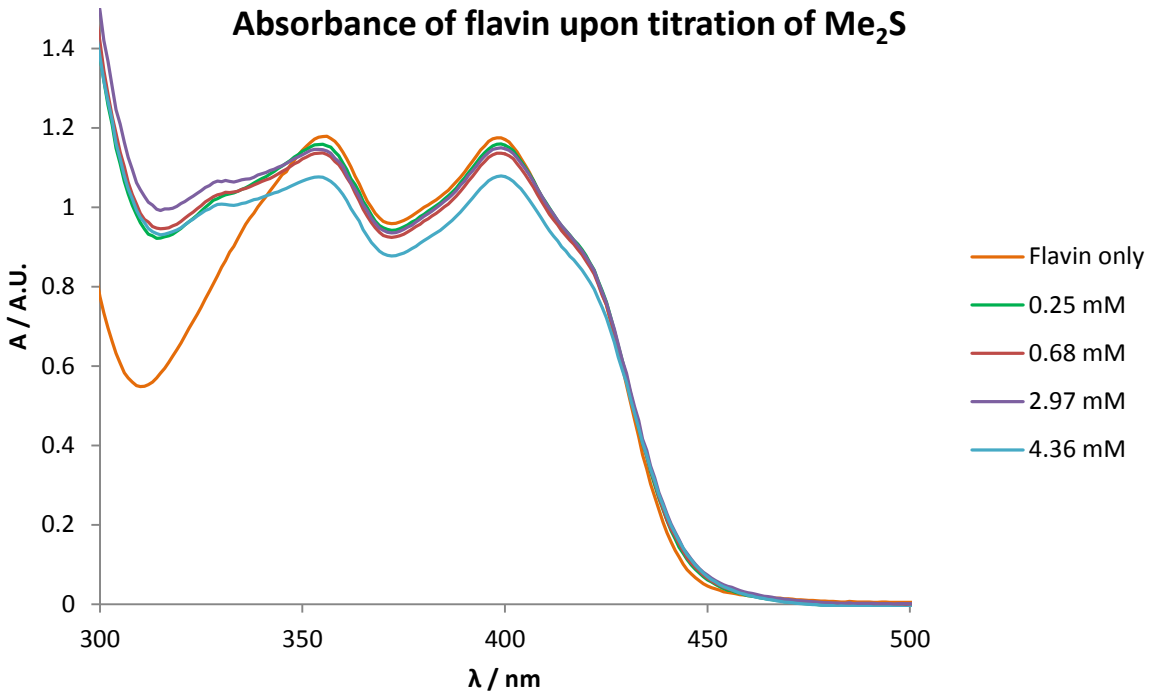

Figure 54. Possible formation of flavin semiquinone upon one-electron reduction of flavin with Me_2S, taken at r.t. with background Me_2S subtracted

Upon adding larger volumes of dimethyl sulfide we observed the formation of a strong charge-transfer (CT) band, with the concurrent re-increase in intensity, probably due to overlap of this charge-transfer event. Even at high concentrations, we found dimethyl sulfide not to act as a strong enough reductant to form a dihydroflavin, consistent with our hypothesis that single-electron flavin reduction occurs upon addition of dimethyl sulfide. This is perhaps not surprising, with dimethyl sulfide having a very high oxidation potential of +999 mV vs. SCE, even one-electron oxidation must either be only due to Me_2S being present in great excess or due toirreversibility of reaction.[153]

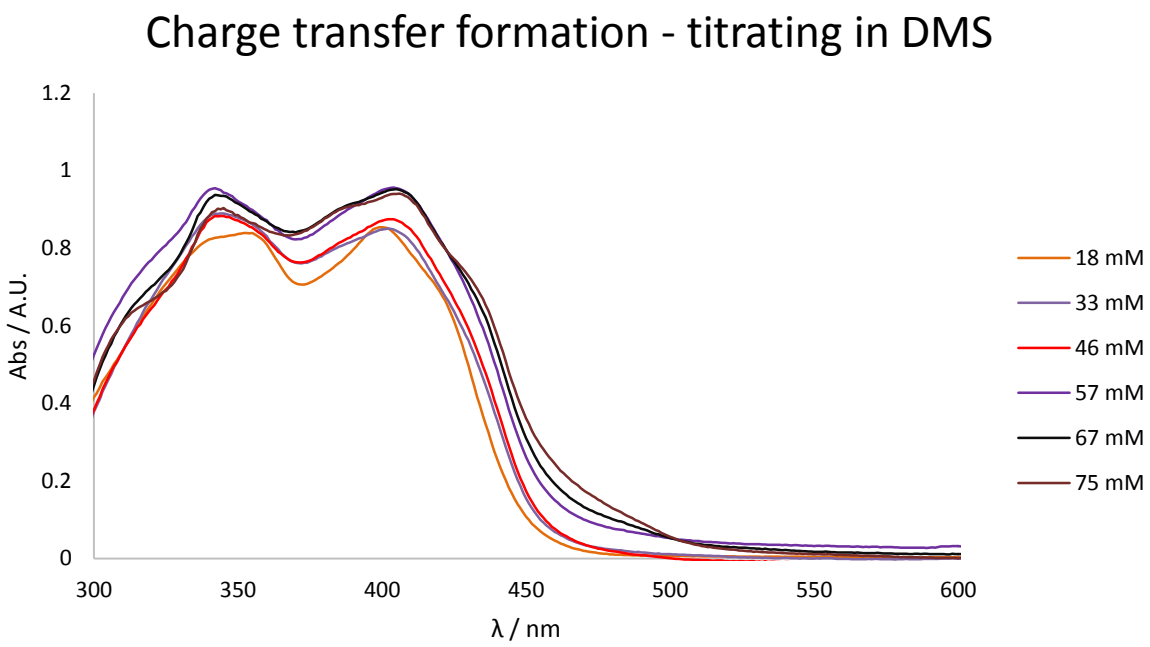

Figure 55. Formation of charge-transfer complex, taken at r.t. with background Me_2S subtracted

This is unusual in that we appear to see less semiquinone formation in the more concentrated DMS solutions, but instead, a charge-transfer type interaction. However, expected features in this artificial flavin system may not be fully consistent with the usually studied FAD and FMN molecules, so our proposed structural features are only estimations.

4.8.1 Stopped flow techniques

Stopped flow is a UV or fluorescence experiment involving rapid mixing of substrates in order to obtain insight into very fast chemical processes by following a change in spectral absorbance at a given wavelength. The 'dead time' of the instrument; the time of mixing before spectral changes can be observed, is that of milleseconds.

The first attempts we made in the use of stopped flow spectroscopy used relatively low concentrations of Me_2S as seen in Figure 56.

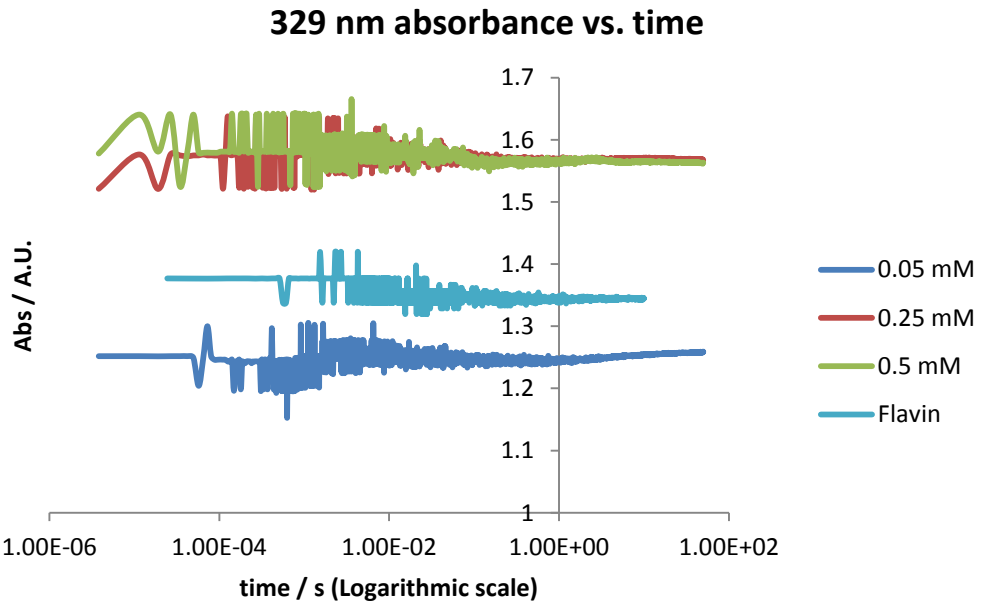

Figure 56. Monitoring of semiquinoid formation by stopped flow UV spectroscopy, taken at r.t. with background Me_2S absorbance subtracted

It can be seen that the transition is too fast to measure, with increases in absorbance occurring within the dead time of the instrument.

Concentration of Me_2S was then increased in order to observe rate of formation of the charge transfer interaction. For this experiment, temperature was also reduced in order to try and slow down the rate of CT formation.

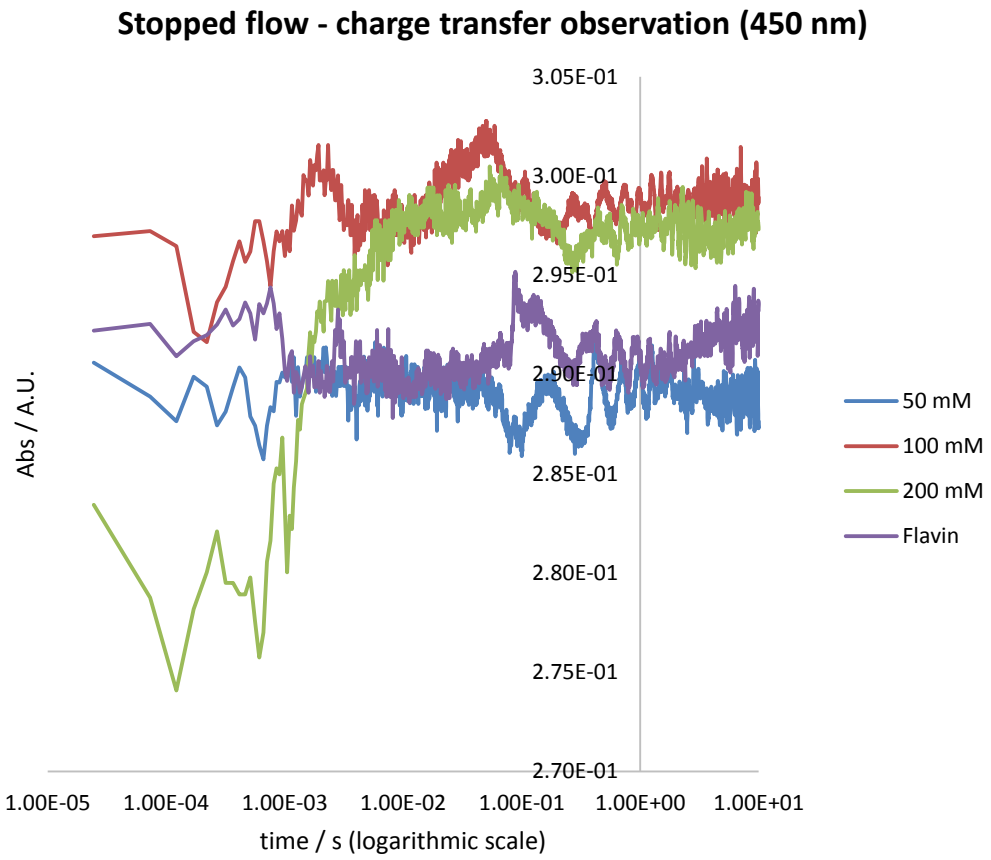

Figure 57. Monitoring of charge transfer formation by stopped flow UV spectroscopy, taken at 5 ˚C with background Me_2S absorbance subtracted

At 100-200 mM of DMS, we observed the formation of a CT complex. Interestingly, we appeared to see the increase of absorbance only at the *higher* concentration of 200 mM, with the initial decrease occurring starting from below the absorbance level of the flavin itself.

4.8.2 Monitoring of murexide formation

A deep purple colour was observed to form during this reaction, as it progressed. This gave a broad peak at λ = 520 nm, corresponding to the dye *murexide* (Scheme 103). Murexide is a purple dye first isolated by Wohler and Liebig from snake excrement.[154] Murexide, in our case, appears to be formed from one molecule of alloxan, one molecule of reduced alloxan (dialuric acid) and one molecule of ammonia. The ammonia is likely to be that liberated from the condensation of amine to form the secondary aldimine we obtain as the final product of our reaction. Indeed, prior to our discovery of alloxan as an active co-catalyst in our reaction, observing purple colouration was one qualitative way of judging whether the reaction was likely to be successful.[155]

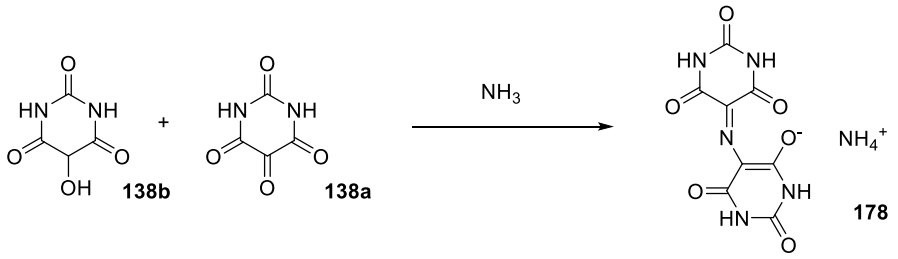

Scheme 103. Formation of murexide and its relation to alloxan redox activity, and product formation.

Upon dilution of an aliquot of reaction mixture into water, there was formation of a peak at 520 nm, which corresponds to that of murexide (lit = 521 nm).[156]

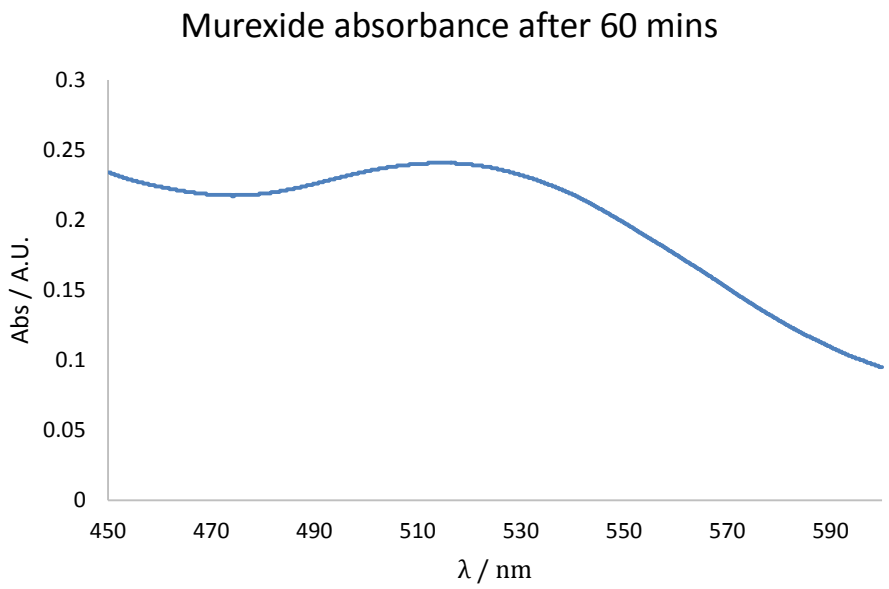

Figure 58. Formation of murexide in reaction mixture

Given that murexide formation would irreversibly deactivate alloxan as a catalyst, its formation was probed by means of UV/visible kinetic experiments. The relative mole fraction of flavin and alloxan was varied, as in a Job plot, and measured the initial rate of increase of murexide absorbance (at 520 nm).

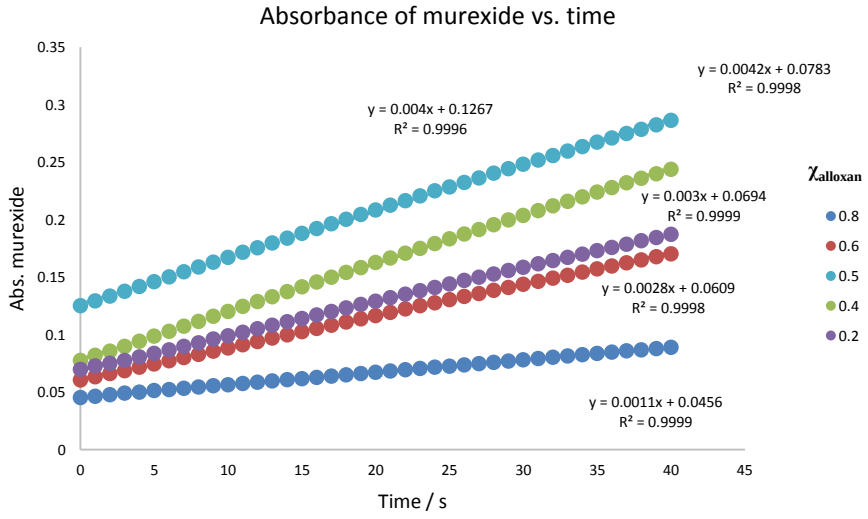

Figure 59. Initial absorbances of murexide at different $\chi_{alloxan}$

We found that there was a clear maximum of initial rate of murexide production at $\chi_{alloxan}$ = 0.4-0.5, with the lowest rate of all occurring at the *highest* concentration of alloxan, $\chi_{alloxan}$ =0.8.

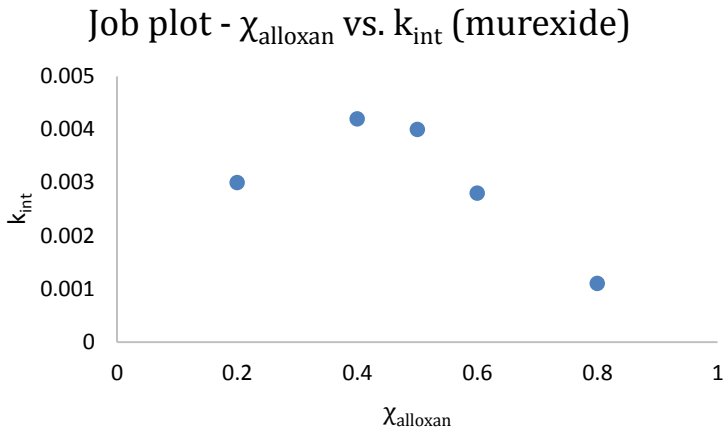

Figure 60. Job plot of k_{int} (murexide absorbance) against mole fraction of alloxan relative to flavin

This indicates that murexide formation is *independent* of alloxan concentration, but related to an interaction of flavin and alloxan. This Job plot is not a plateau like that of rate of amine oxidation, indicating that murexide production is not directly related to rate of amine formation. Given an apparent maximum of $\chi_{alloxan}$ = 0.5 indicating a 1:1 interaction of flavin and alloxan, our interpretation is that formation of **178** originates from an off-cycle over-reduction of **138a**, mediated by a reduced flavin species.

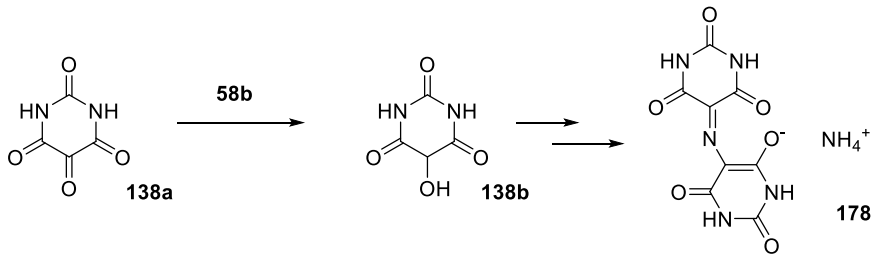

Scheme104. Possible over-reduction mediated by dihydroflavin **58b**

4.9 Overall proposed mechanism for the flavin-catalysed amine oxidation

Taking into account all the data presented in the previous chapter, we can suggest answers to our various questions about aspects of the mechanism of the reaction.

Based on the observation of a radical derived from benzylamine **15a** in the EPR spectrum leads to a proposal of a homolytic model amine C-H bond cleavage, and based on our kinetic isotope effect experiment we suggest that this is rate limiting.

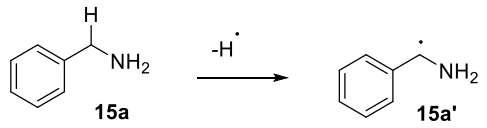

Scheme 105. Homolytic C-H cleavage

We must additionally take into account the Hammett correlation, which shows that this radical must be electrophilic in nature as would be expected due to the SOMO overlap with the electron rich *N*-lone pair. Although it is commonly believed that radical reactions tend to have negligible Hammett values, in fact many can be substantial,[157] including a recent example involving alcohol oxidation.[158]

Additionally, a key observation is the relatively linear change in rate with concentration of flavin of 0.25 on a log-log plot. While DOSY ^{1}H NMR spectroscopy did not reveal an aggregation factor as high as 4, it is nevertheless possible that a tetrameric flavin resting state exists upon addition of amine, which we cannot measure the NMR spectra for. In particular, the flavin rings are strongly polarised and in addition to imide-imide interactions these can be arranged in a herringbone type fashion as observed in the solid state.

This would suggest, if the monomer is the active state, that the flavin is also involved in the key, rate-determining C-H bond cleavage step. Given the evidence from EPR that the role of the sulfide is as a proton-coupled single electron reductant acting on the flavin, the remaining key question is the role of the alloxan in 'completing' the reaction.

A key to solving this problem was Scaiano's observation that the reaction of α-amino radicals with benzil is one of the fastest known interactions between a radical and a closed-shell organic molecule. Given the key, highly oxidisable 1,2-dicarbonyl we considered the possibility that alloxan fulfils a similar role in our system.[159] Therefore, it is proposed that alloxan acts accepts a second electron from the α-amino radical, and so forms a single electron reduced species that should posess sufficient lifetime to react with ambient oxygen.

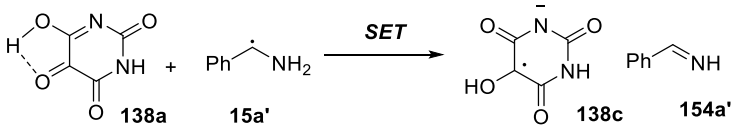

Scheme 106. Single electron transfer between α-amino radical and alloxan **138a** (amide tautomer shown)

Hydroperoxy radicals are powerful species for H-abstraction;[160] the process required to return a dihydroflavin to the semiquinoid state.

This correlates with the solvent of choice being trifluoroethanol, as it dissolves all components but has a relatively low dielectric constant (8.5[161]). Hydroperoxy radicals in water are generally deprotonated and exist as superoxide (O_2^-),[162] whereby they act as a reductant *not* an oxidant,[163] but the pK_a would be determined by water's high dielectric constant (80.1[138]). In *air*, (1.0006[164]) the radical is mostly protonated, forming hydroperoxy radical, which *is* an oxidant.[165]

An additional point is that superoxide dismutase, which decomposes these type of species, is an inhibitor of alloxan-induced pancreatic damage.[166]

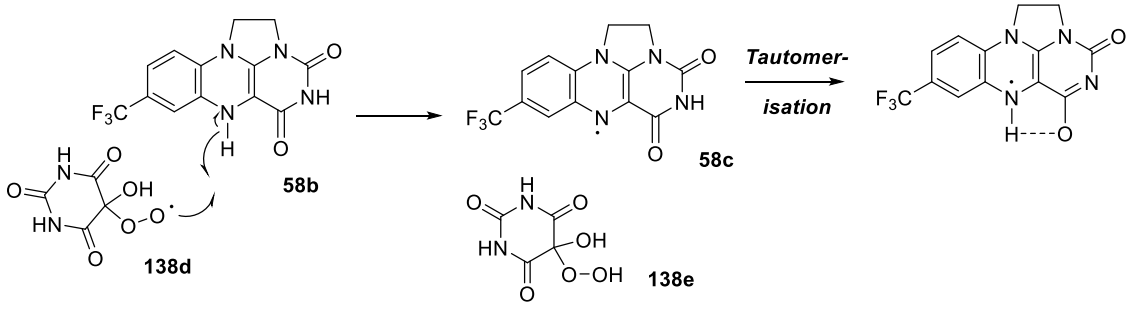

Scheme 107. H atom transfer between alloxan hydroperoxyl **138d** and dihydroflavin **58b**

Alloxan hydroperoxide **138e** would then be expected to be regenerated by Me_2S-mediated reduction, consistent with the observation that stoichiometric amounds of DMSO are produced for every amine oxidation event in our reaction.

Taking all these factors into consideration, a proposed 'global' catalytic cycle for this oxidation is shown below.

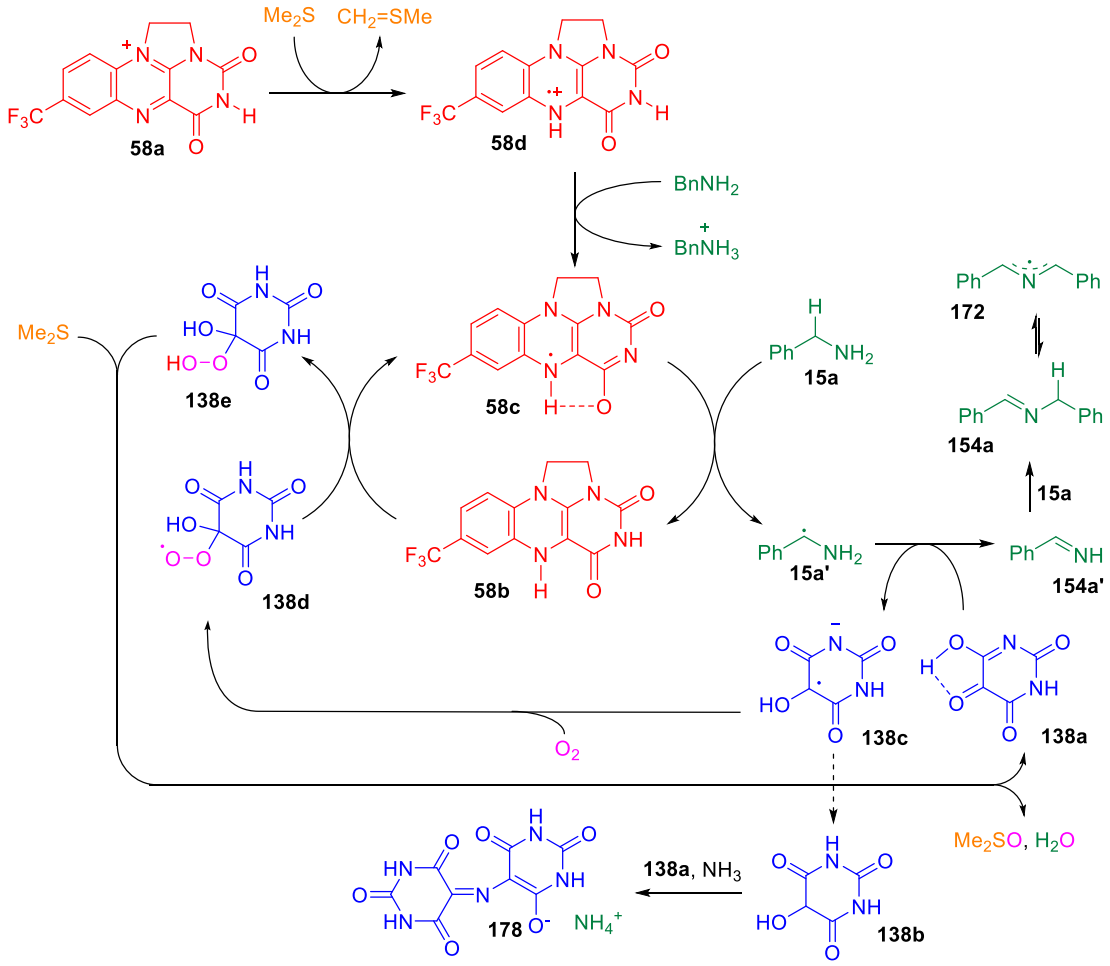

Scheme 108. Proposed mechanism

Further important aspects relevant to the proposed cycle are the observation of the formation of *murexide* **178**, Given the rate independence of the formation of **178** from amine oxidation, this is thought to be an off-cycle over-reduction pathway. Indeed, there is a report of ascorbic acid being used as an amine oxidant in this manner, but stoichiometrically due to formation of "brightly coloured Schiff bases" which are presumably analogous in structure.[167]

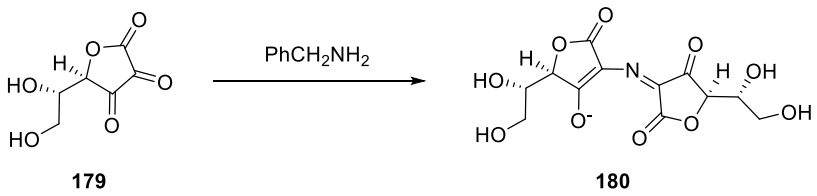

Scheme 109. Formation of Possible structure of analogous catalyst deactivation product from ascorbic acid mediated amine oxidation

The background reaction observed when no flavin, or sulfide, is present may be due to this type of quinoidal polar mechanism. It is notable both that the initial rate of the reaction is different, and that removing either flavin or sulfide has a similar effect on the background rate, as would be expected from a semiquinone-based 'active' mechanism but a background reactivity dependent on alloxan alone.

4.10 Relevance of mechanistic studies to MAO mechanism of action

Current proposals for the activity of the MAO enzyme are the single electron transfer mechanism proposed by Silverman and the dipolar mechanism proposed by Edmondson, both of which proceed through a C-H cleavage step of proton removal.

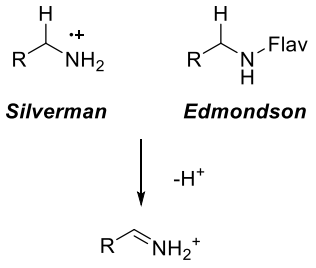

Scheme 110. Differing proton removal steps proposed by Silverman and Edmondson

The monoamine oxidase enzyme has many differences from our model system. Notably, the flavin system is neutral rather than cationic, with the consequent difference in standard reduction potential. Additionally, there is no obvious enzymatic feature that parallels the alloxan in our system, and it being enclosed in a hydrophobic cavity. However, in view of the rate-dependence on flavin, the similarities between measured Hammett and KIE values at pH 9.0 to those measured for monoamine oxidase *B*, and the fact we observe true, efficient catalytic turnover, led to an attempt to rationalise the enzyme's activity in light of our findings.

Firstly, we proposed a MAO-B mechanism that involves rate-limiting H-atom abstraction which is mediated by a flavin semiquinone radical, based on the key features of the mechanism we propose for our model system. An analogous second step would be fast electron transfer to a suitable acceptor followed by reoxidation of catalyst by O_2.

The *cis*-amine linked tyrosine residue Y398 points the phenol unit towards the oxidised flavin. Charge transfer, assisted by the hydrogen bonding water, effectively forms a *pseudo*-cationic flavin, with post-CT charge dispersion making the reverse electron transfer less favourable.[168] The tyrosyl radical acts as a second electron acceptor, potentially with parallels to alloxan in our model system.[169] Consistent with this is the observation that a non-linear relationship is discernible in the reductive half-reaction between MAO-B and $BnNH_2$ when conducted in a high-strength, static magnetic field, consistent with diradical character.[149]

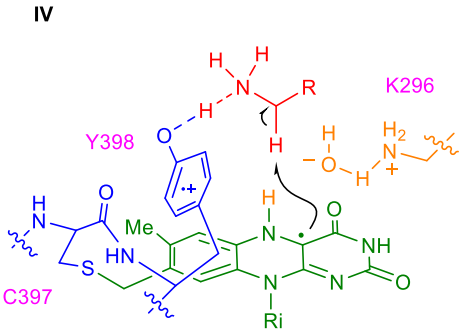

Figure 61. Proposed key step in MAO-B mechanism

In addition to our model system, we also revisited the work of Ramsay and the substrate-specific rate enhancements of MAO-A and B by various substrates.[19] Notably, there is a clear correlation between substrate pK_a and k_{cat} for both MAO A and B, with the B isozyme in particular displaying a linear relationship.

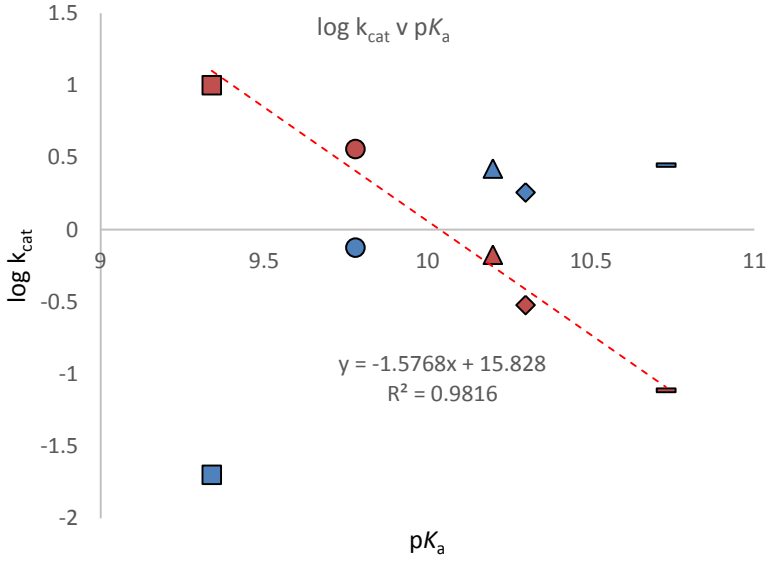

Figure 62. (I) MAO A and B steady-state kcat relationship to substrate pKa. MAO A in blue, MAO B in red (□ = $BnNH_2$, ○= 2-phenethylamine, ▲ = tryptophan, ○ = 5-methoxytryptophan, ▬ = 5-hydroxytryptophan (serotonin)

At physiological pH, these correlations could be related to the protonation state of the amine; with MAO-B oxidising neutrally charged amines and MAO-B preferring protonated ammonium cations.

We propose for the case of MAO-A, given its structural similarity to the B isozyme, the rate-determining step is also H-atom abstraction. However, the redox states of the flavin may be different prior to abstraction. For MAO-A, the required semiquinone species could be accessed by CT from a *reduced* flavin to dioxygen. Cationic species such as the proposed ammonium are rate enhancers of flavin reoxidation, as shown in the case of the protonated histidine for glucose oxidase.[170] Similarly, the protonated substrate should assist CT between reduced flavin and O_2, transiently forming $HOO^{\bullet}$ which would abstract hydrogen from amine in this case. The key role of lysine (K296) + H_2O is again key in charge dispersal after CT by removing the flavin N(5) proton.

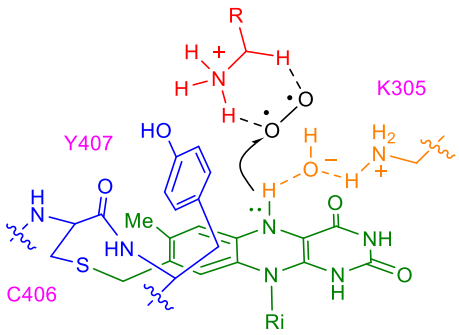

Figure 63. Proposed key mechanistic step in MAO-A mechanism

It is possible that MAO-A evolved in order to process more basic amines at physiological pH, particularly as MAO-A is known for oxidising non-nucleophilic *cationic* iminium substrates e.g. 1-methyl-4-phenyl-dihydropyridine ($MPDP^+$, **27**).

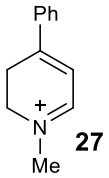

Figure 64. Structure of $MPDP^+$

This proposed mechanism fits with both the differing O_2 V_{max} values for the two isozymes, as well as the substrate's role in assisting charge transfer *and* charge dispersion behaviour being consistent with the substrate-specific rate enhancements observed in both oxidative and reductive half reactions.[19] The semiquinone mediated radical oxidation can thus be viewed as coupled to a two-electron cycle (MAO-B) or a direct O_2 reduction (MAO-A).

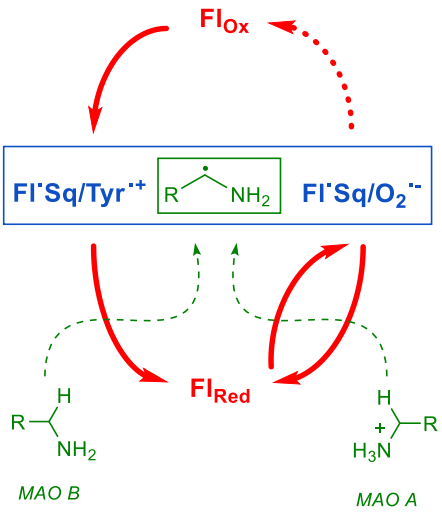

Scheme 111. Simplified depiction of proposed MAO isozyme redox cycling

5 Cu/alloxan-catalysed amine oxidation

5.1 Transition metal chemistry of alloxan

After discovering the activity of alloxan as a co-catalyst in flavin-catalysed amine oxidation, we considered two pertinent observations about this molecule. One was the importance of iron species *in vivo* for the generation of reactive oxygen species in alloxan-induced diabetes. This appears to occur *via* one-electron reoxidation of dialuric acid to the semioxidised form, which generates superoxide.[171] Fenton/Haber-Weiss type chemistry[172,173] may also play a role in these processes.

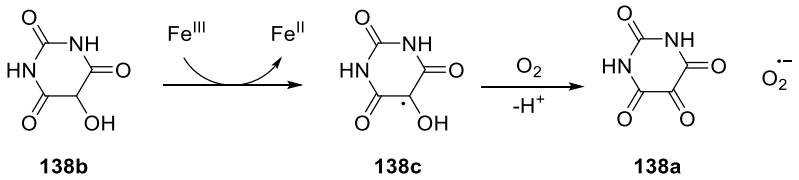

Scheme 112. Possible role of iron in generation of reactive oxygen species in alloxan-induced diabetes

The effect of the presence of iron was demonstrated by the addition of the metal chelator diethylene triamine pentaacetic acid (DTPA) alleviating the effects of alloxan induced diabetes.[174]

Additionally, recent work on amine oxidation with iron catalysis by Xu demonstrates that Fe(III)/TEMPO catalyses the aerobic oxidation of amines to the corresponding imines.[117] The reaction was also successful without TEMPO but yields were lower unless conducted under an atmosphere of oxygen.

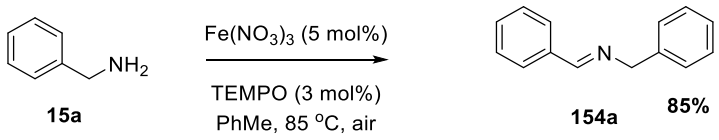

Scheme 113. Ferric nitrate / nitrosyl radical catalysed amine oxidation

We first investigated the activity of Fe salts on our system, replacing the previous flavin/alloxan pair with a Fe(II) or Fe(III) salt. Although various iron salts promoted reaction, it was difficult to force the reaction to completion, as it tended to stall (see entries 3 and 4). The system was also rather insensitive to any alteration of conditions, with only a slight yield increase upon switching from Fe(III) to Fe(II) and addition of disodium EDTA improving the reaction efficiency.

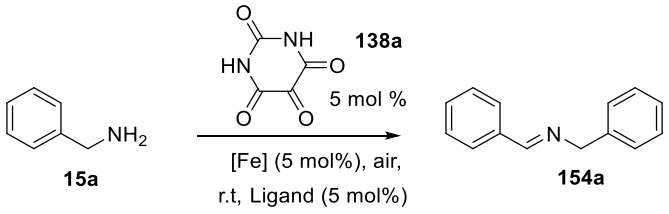

Table 14. Iron/alloxan catalysed amine oxidation

Entry	[Fe]	Solvent	Ligand	Time / h	Conversion / %[a]
1	$Fe(acac)_3$	TFE	-	3	22
2[b]	$Fe(acac)_3$	TFE	-	3	0
3	$FeCl_3.6H_2O$	TFE	-	5	42
4	$FeCl_3.6H_2O$	TFE	-	20	42
5	$FeCl_3.6H_2O$	TFE	1,10-phenanthroline	5	26
6	$FeCl_2.4H_2O$	TFE	$EDTA.2Na.2H_2O$	16	67
7	$FeCl_2.4H_2O$	HFIP	$EDTA.2Na.2H_2O$	3	10
8	$FeCl_2.4H_2O$	H_2O	$EDTA.2Na.2H_2O$	3	0

[b]Without inclusion of alloxan

Additionally, upon a change of solvent to acetonitrile and a higher loading of alloxan we were surprised to find that the 'background' i.e. metal free reaction was relatively efficient, which we suspected might be through a transamination-type mechanism.

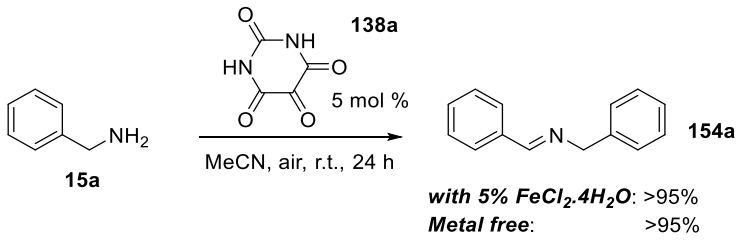

Scheme 114. Metal free amine oxidation by alloxan in MeCN

5.2 Cu containing amine oxidases

In addition to the flavin-dependent family of amine oxidoreductases, there is an additional class of amine oxidases – the copper-containing amine oxidases. These are dependent on enzyme-bound copper but also an organic cofactor.[175]

The first of these to be discovered was pyrroloquinoline quinone (PPQ), present in PPQ amine oxidase; this was described by Hauge in 1964 as the 'third class' of redox active cofactors in bacteria, after flavoenzymes and NAD-dependent enzymes.[176] Furthermore, in 1990 Klinman discovered another biogenic redox active quinone; trihydroxyphenylalanyl quinone (TOPA-quinone). Tryptophan tryptophylquinone (TTQ) is another similar cofactor, also generated by post-translational amino acid modification.[177]

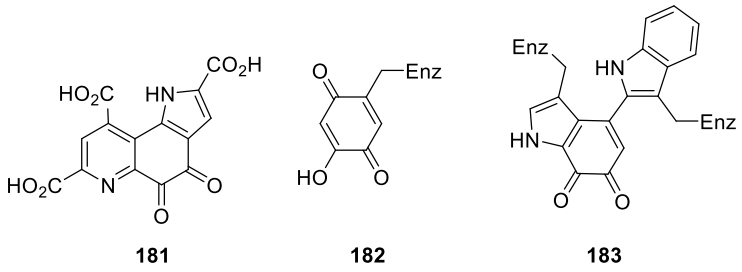

Figure 65. Quinones biologically relevant to amine oxidation, structures of PPQ **181**, TOPA-quinone **182** and TTQ **183**

These enzymes are thought to proceed mechanistically through a covalent, pyridoxal-like transamination mechanism.[178] Initial condensation of amine onto the active carbonyl centre is followed by substitution by a nucleophile (water or another amine) to form the product aldehyde/imine, then the two-electron reduced form is reoxidised by O_2. The role of copper is to facilitate this O_2-mediated reoxidation.[179]

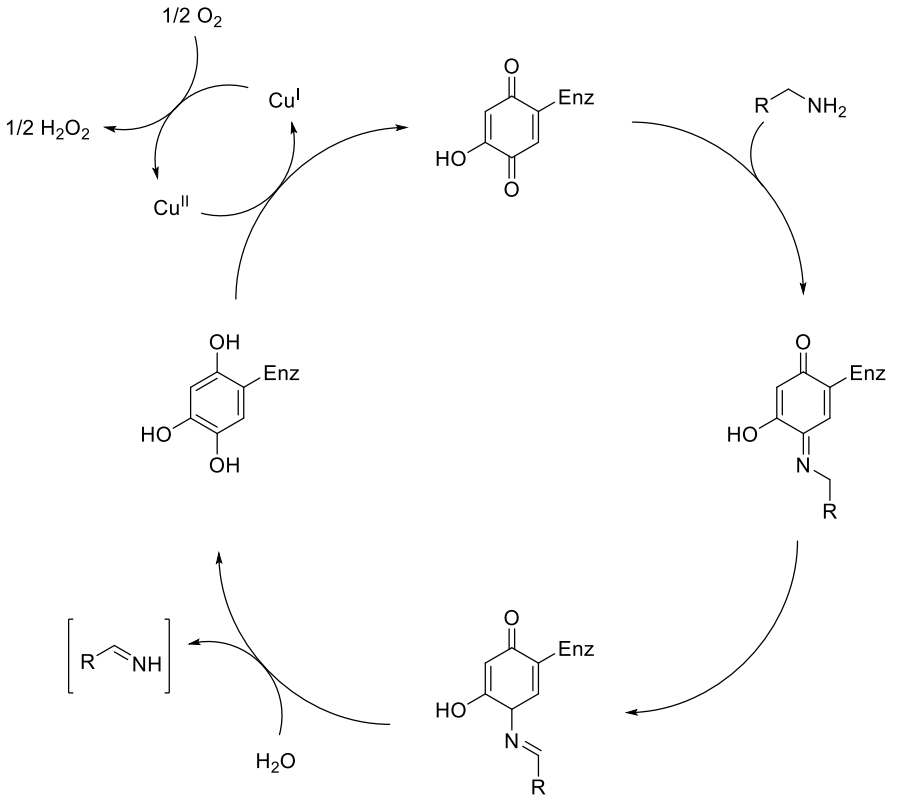

Scheme 115. Quinoidal transamination (TOPA-quinone) amine oxidation mechanism

Work on modelling these enzymes began with Largeron's electrochemistry work, where the combination of a reduced quinone and a Hg electrode generated a quinoidal species which promoted the oxidation of first benzylamine and then was expanded to aliphatic amines.[180]

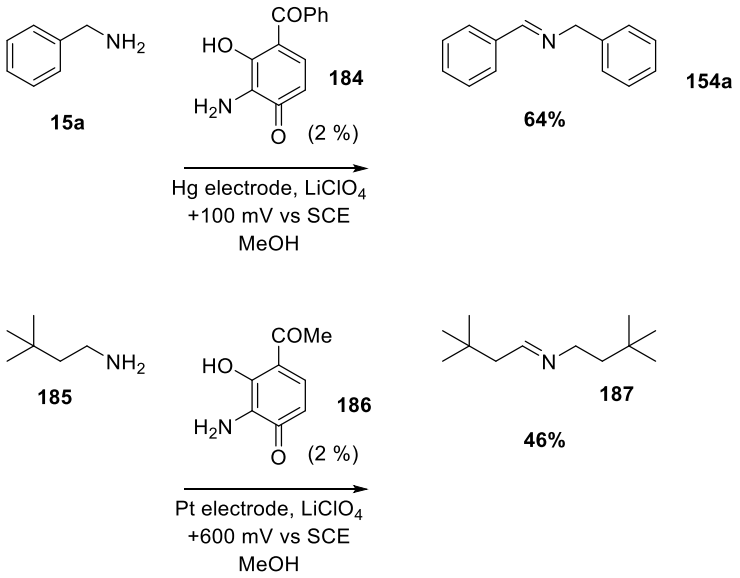

Scheme 116. Electrochemical oxidations of amines by quinones

The same group eventually developed a more biologically relevant example using a Cu(I) salt, copper 2-methylsalicylate, and the same quinone **186**. This oxidised a range of primary amines, including benzylic and aromatic amines.[118]

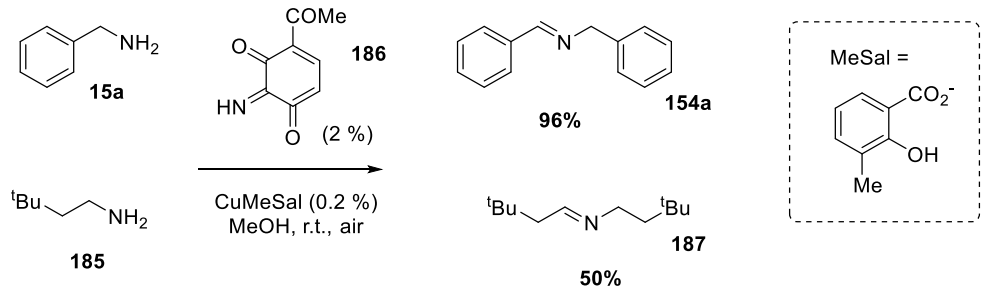

Scheme 117. Oxidative homocoupling of amines using **186** and CuMeSal.

This methodology was also utilised to oxidatively cross-couple two dissimilar amines, with one more easily oxidised than the other, such as a benzylic amine as the oxidised partner and a simple aliphatic amine as the 'alkylating amine'. Some examples, such as the cross-coupling of 4-methylbenzylamine **15c** with secondary amine **188** gave a very high selectivity.

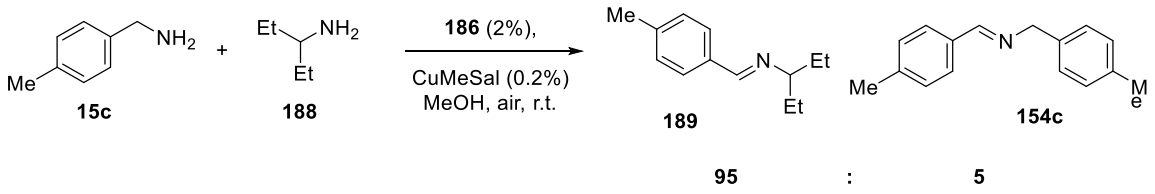

Scheme 118. Example of TOPA-quinone like oxidative cross coupling

Stahl and co-workers developed quinone **166** as a catalyst for selective oxidation of benzylic amines using O_2 as stoichiometric oxidant, in the absence of a copper co-catalyst. They also found it possible to oxidatively cross-couple benzylic with aliphatic or α-branched amines.[116] In this case, aliphatic amines were not oxidised at all under the conditions.

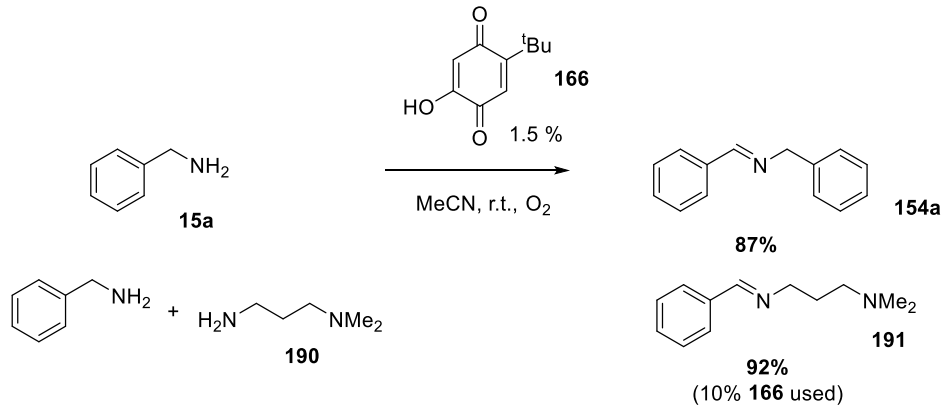

Scheme 119. Oxidative homo- and cross- coupling of amines with quinone **x**

Kobayashi also developed a quinone-based system for amine oxidation, with the unexpected formation of benzylidene benzylamine observed on reaction with catechol, oxygen and platinum/iridium nanoclusters, which was expected to oxidise and cyclise to form a benzoxazole.[181]

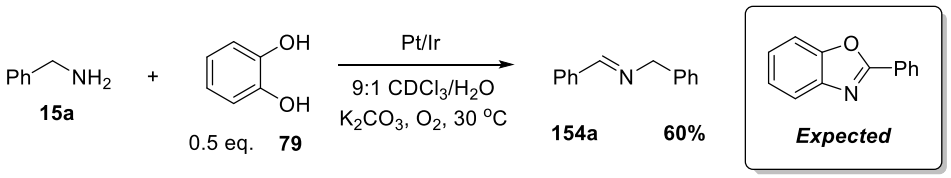

Scheme 120. Tandem Pt/Ir and catechol promoted oxidation of benzylamine

The methodology was expanded to a range of imines, with loading of 2-*tert*-butylcatechol in the range of 15-60 mol%. However, control experiments by the group suggest a hydride transfer or hydrogen atom transfer mechanism, with a transamination mechanism such as that observed for CuAOs explicitly ruled out.

We considered the possible quinoid-like character of alloxan and thus the possibility of access to transamination-type oxidation chemistry, using alloxan but potentially going through a *different* pathway to the proposed mechanism of the flavinium type oxidations. Alloxan should have the ability to tautomerise to a quinone-like structure.

Additionally, there are reports of alloxan stoichiometrically undergoing 'ninhydrin like' reactivity with amines, with concomitant formation of murexide like coloured dyes.[182] This bears some similarity to the work of Srogl, previously referred to in the preceding chapter whereby the combination of copper(I) 3-methylsalicylate and ascorbic acid **192** oxidises amines to aldehydes. However, the use of substoichiometric **192** was contraindicated by the formation of self-condensed imines similar to murexide.[167]

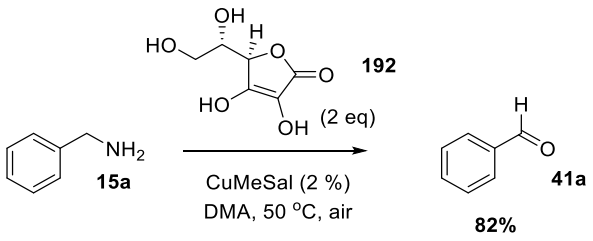

Scheme 121 Ascorbic acid-mediated, copper-catalysed amine oxidation

Considering the well precedented rate acceleration of this type of reaction by copper, it was decided to see if this reaction would increase in efficiency in the presence of a copper source. This might lead to a new method of amine oxidation with the same chemoselectivity as either the flavin or quinone oxidations, using only commercially available reagents and air as terminal oxidant, with alloxan playing the role of the quinone in Scheme 115 as depicted in Scheme 122.

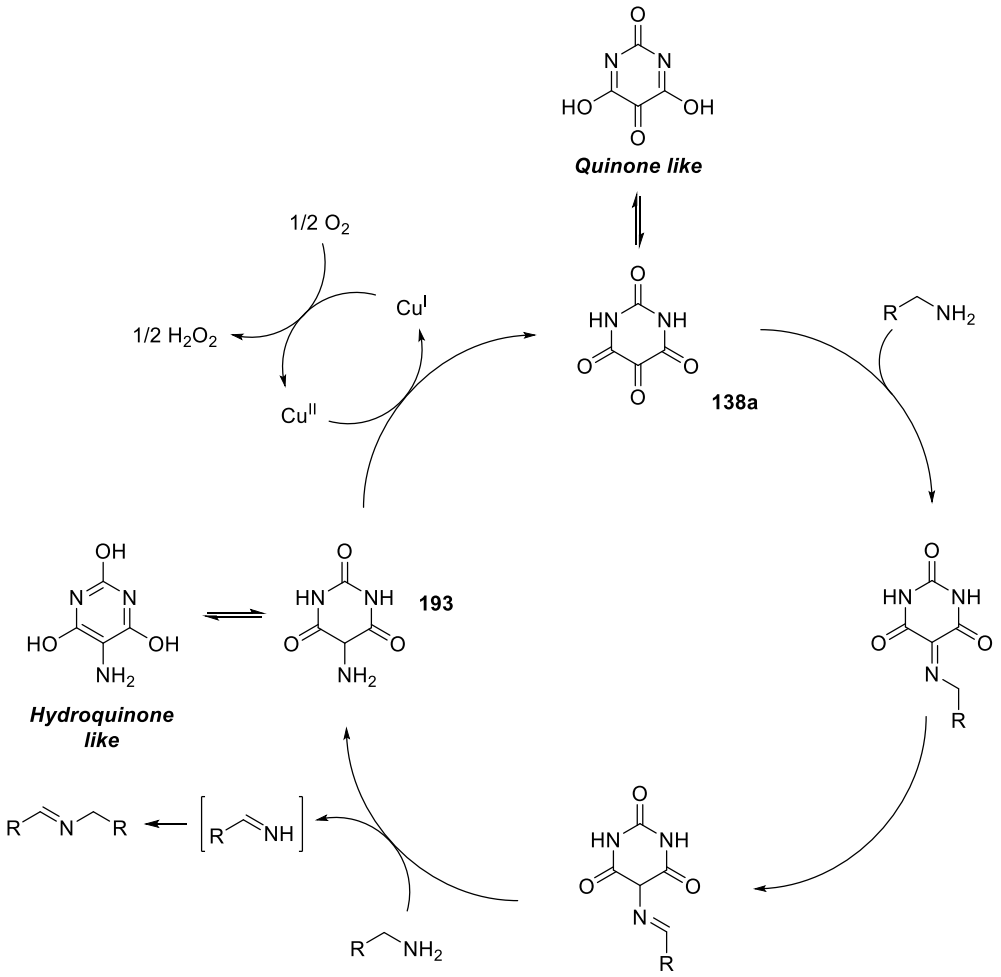

Scheme 122. Proposed mechanism

5.3 Cu/alloxan catalysed amine oxidation

In our initial screen, Cu(I) performed better than Cu(II), and the reaction was complete in much less time than metal free with 5% loading of alloxan. CuCl was superior to CuI as a suitable simple copper salt. Acetonitrile was the best solvent for the reaction, with methanol offering poor reactivity and less polar solvents essentially returning starting material, possibly due to insolubility of either or both of the catalysts.

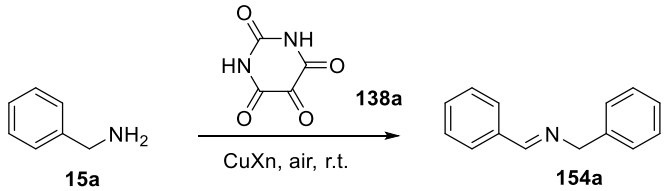

Table 15. Optimisation of Cu / alloxan catalysed amine oxidation

Entry	CuX_n [mol%]	**3** [mol %]	Solvent	t [h]	Conv.[a] [%] (yield) [%][b]
1	CuI (1)	5	MeCN	2	58
2	CuCl (1)	5	MeCN	2.5	100
3	$CuCl_2$ (1)	5	MeCN	2	16
4	CuCl (1)	5	MeOH	2	12
5	CuCl (1)	5	CH_2Cl_2	2	6
6	CuCl (1)	5	THF	2	<5
7	CuCl (1)	2.5	H_2O	0.5	<5
8	CuCl (1)	2.5	MeCN[c]	2	15
9	CuCl (1)	2.5	MeCN[d]	4	21
10	CuCl (1)	2.5	MeCN[e]	3	100 (76)

[a]Assayed against relevant ^{1}H NMR signals [b]Isolated yield [c]Under $CaCl_2$ drying tube, containing 4 Å molecular sieves [d]Containing 1000 ppm water [e]With sonication

Initially upon decreasing the loading of alloxan to 2.5% we found the reaction was complete in a reasonable amount of time (3-4 h). However, the reaction was not completely reproducible, possibly between different bottles of MeCN solvent. It is possible this could be due to water helping to solubilise alloxan, but too high a water concentration forcing the equilibrium between alloxan monohydrate (the form in which it is sold) and the tricarbonyl too far towards the hydrate state.

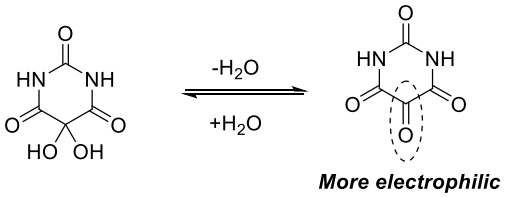

Scheme 123. Interconversion of alloxan tricarbonyl and monohydrate forms

We eventually solved this problem by the use of dry (SPS-grade) MeCN, with sonication of the reaction mixture. This appeared to be more reliable than the use of HPLC or reagent grade solvents despite the presumed uptake of H_2O from ambient air during the reaction. This could be any combination of promoting the break up of aggregates of MeCN-insoluble alloxan, the increased uptake of O_2, as well as coincidentally but importantly mildly heating the reaction; to 30 ˚C. This allowed for a reproducible and efficient reaction using a relatively low loading of organocatalyst.

We then proceeded to investigate a series of benzylic amines (Table 16); similar substrates as those used in the previous flavin/alloxan catalysed system (Chapter 3, Table 10)

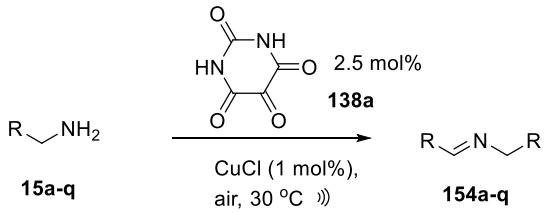

Table 16. Cu / alloxan catalysed amine oxidation – substrate scope

Entry	R	Time / h	Product	Yield/%
1	Ph	3	**154a**	76
2	4-Me-C_6H_4	3	**154c**	91
3	4-OMe-C_6H_4	3	**154b**	98
4	4-^{t}Bu-C_6H_4	3	**154d**	92
5	4-Cl-C_6H_4	16	**154e**	70
6	4-F-C_6H_4	3	**154f**	96
7	4-CF_3-C_6H_4	5	**154g**	82
8	3-Me-C_6H_4	3	**154h**	91
9	3-OMe-C_6H_4	3	**154i**	83
10	2-Me-C_6H_4	3	**154j**	79
11	2-OMe-C_6H_4	16	**154k**	83
12	2-Cl-C_6H_4	3	**154l**	98
13	2-furyl	16	**154m**	20 (47[a])
14	2-thiophenyl	3	**154n**	96
14	2-napthyl	3	**154o**	65
15	piperonyl	8	**154p**	90
16	3,4-$(OMe)_2$-C_6H_3	3	**154q**	72

[a]Copper(I)-3-methylsalicylate used as Cu source

Most amines were oxidised readily by the system. Notably, it appeared that there was less electronic dependence than in the case of the flavin/alloxan catalysed procedure. For example, *p*-CF_3-substituted benzylamine **15g** was a reasonable substrate for the reaction, in contrast to difficulties we had in oxidising this substrate with the flavin-catalysed methodology.

Interestingly, neither 2-methoxybenzylamine **15k** nor 2-furylmethanamine **15m** were easily oxidised, with **15m** in particular requiring extended reaction times and having low yields (Table 16, entry 13). We proposed this was due to the chelation of copper by the starting material, as shown. We increased the yield for this substrate moderately by the use of copper(I) methylsalicylate (CuMeSal) as used by Largeron,[118] as we theorised this might be a moderately more robust form of the active copper species, however, yields were still only moderate.

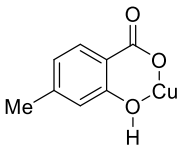

Figure 66. Structure of CuMeSal

These issues with the oxidation of heterocyclic benzylic amines have been reported as problematic in transition metal catalysed amine oxidations,[116,117] however, 2-thiophenylmethylamine **15n** surprisingly was oxidised in high yield, despite copper not being such a 'hard' metal that it would be expected to be highly selective for binding to oxygen over sulfur.

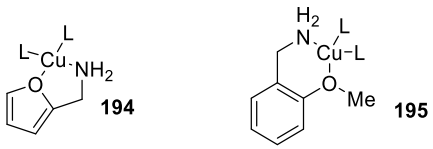

Figure 67. Proposed structures of chelates **194** and **195**

The α-branched substrate 1-phenethylamine **169** yielded the imine product in reasonable yield, despite this not being a good substrate for flavin-catalysed amine oxidation. No major changes to the conditions were required, whereas under Stahl's high catalyst loadings and the presence of NaHCHO, a base, were required in order to see any reaction.

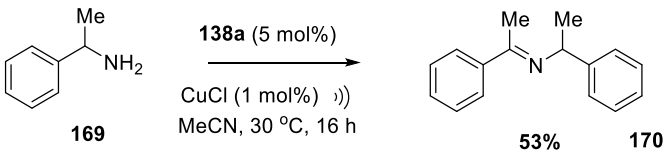

Scheme 124. Oxidation of 1-phenyethylamine **169**

Upon the use of the *R* enantiomer in order to see if racemisation occurred, we observed ee (by $[\alpha]_D$) between 50% - 100% depending on the run. However, this is not a particularly accurate technique to probe whether racemisation occurs, and attempts to determine retention of stereochemistry by chiral HPLC were thwarted by apparent instability of the imine on a chiral column.

We attempted to further probe this reaction by synthesising the enantiopure product by condensation from acetophenone **196** and amine *(R)*-**169**, measuring the $[\alpha]_D$ and testing if resubjection of product to reaction conditions decreased enantioselectivity. However, we were surprised to find that the stereocentre was racemised upon heating in toluene in the presence of $MgSO_4$.

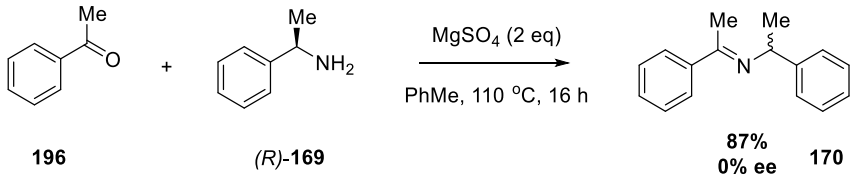

196 *(R)*-**169** **87%** **0% ee** **170**

Scheme 125. Racemisation during formation of **170**

In another approach to probe hydrogen scrambling, we performed the reaction in CD_3CN to look for C-D exchange with the solvent, from a benzylic radical or similar. We saw no evidence of exchange with solvent, isolating the same product **170** upon reaction in CD_3CN. However, this does not rule out scrambling of hydrogen atoms if the exchange was with another species e.g. alloxan **138a**.

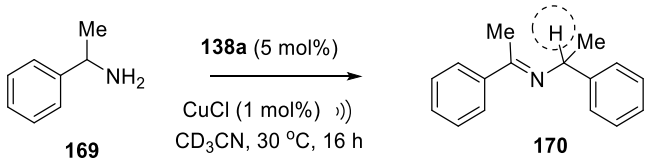

169 **170**

Scheme 126. Retention of benzylic proton upon reaction in CD_3CN

5.4 Cu/alloxan catalysed amine oxidative cross coupling

We proceeded to investigate a series of oxidative cross-coupling reactions of benzylic amines with less 'oxidisable' amines, similar to that shown in Table 10 for the flavin system. In this case aliphatic amines were found not to act as inhibitors. Therefore, we were able to use them as substrates in this reaction. However, surprisingly and in contrast to the results obtained by Stahl, we observed better selectivity and reactivity of anilines than aliphatic amines in this reaction. This could be due to aliphatic amines having a somewhat inhibitory effect, or for a slower rate of equilibration and 'self sorting' in this case.

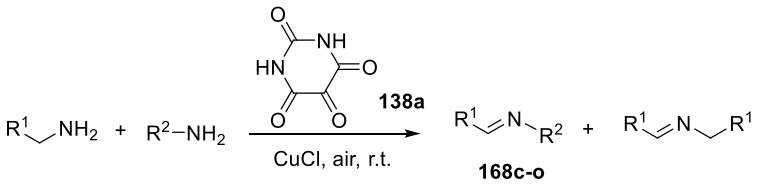

Table 17. Oxidative coupling of benzylic amines with other amines

Entry	R^1	$R^{2]}$	Product	Yield [%][a]	Selectivity[b]
1	4-Me-C_6H_4	4-Me-C_6H_4	**168c**	96	25:1
2	4-Me-C_6H_4	4-OMe-C_6H_4	**168d**	90	>25:1
3	Ph	4-OMe-C_6H_4	**168i**	64	>25:1
4	4-Me-C_6H_4	4-F-C_6H_4	**164f**	84	16:1
5	4-F-C_6H_4	4-OMe-C_6H_4	**168j**	72	>25:1
6	4-Cl-C_6H_4	4-OMe-C_6H_4	**168k**	55	>25:1
7	2-thiophenyl	Ph	**168l**	55	1:1.6
8	2-OMe-C_6H_4	Ph	**168m**	87	11.5:1
9	Ph	^{n}Oct	**168n**	11 (24)[d]	2.2:1
10	Ph	$(CH_2)_2$Ph	**168o**	19 (29)[d]	2:1
11	Ph	4-pyridyl	-	68[c]	<1:25

[a]Isolated yield, assuming 100% cross-coupled product. [b]Assessed by ^{1}H NMR spectroscopy. [c]Yield of homocoupled product [d]Assessed by comparison to an internal standard of 1,3,5-trimethoxybenzene; yield of cross coupled product only (total imines in parentheses)

We were surprised to find that 2-thiophenyl methylamine **15n** did not cross-couple with high selectivity to aniline; perhaps in this case we did see some Cu chelation despite it being a reasonable homocoupling substrate. 4-amineopyridine (Table 17, entry 11) did not condense with the oxidation product, yielding only homocoupled **154c**. Most other couplings of benzylic amines and anilines were very selective. Selectivity appeared to be more dictated by aniline nucleophilicity than benzylic amine electronics, with electron withdrawing amines and *p*-anisidine (Entries 5,6) yielding a single product).

We proceeded to synthesise those imines which were not formed as a single product by condensation, as in the previous work on this type of chemistry.

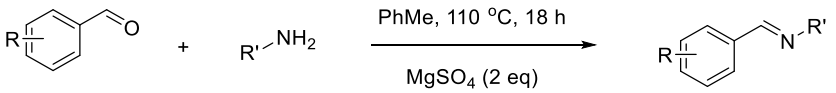

Table 18. Condensation of imines to cross-check data

Entry	R	R'	Yield/%
1	2-OMe	Ph	93
2	2-thiophenyl	Ph	58
3	H	^{n}Oct	97
4	H	CH_2CH_2Ph	64

5.5 Mechanistic studies

Having extensively studied the mechanism of our flavin-catalysed system, we decided to investigate the mechanism of the Cu(I)/alloxan catalysed amine oxidation in order to probe the similarities and differences of these two reactions.

Firstly, the order of reaction in [amine] was probed by similar means to those previously used in the flavin catalysed reaction, of varying concentration and measuring the formation of imine against an internal standard of naphthalene by normal phase HPLC.

We found the reaction to appear zero order 'by slope' – that is we could plot a linear relationship between time and [amine].

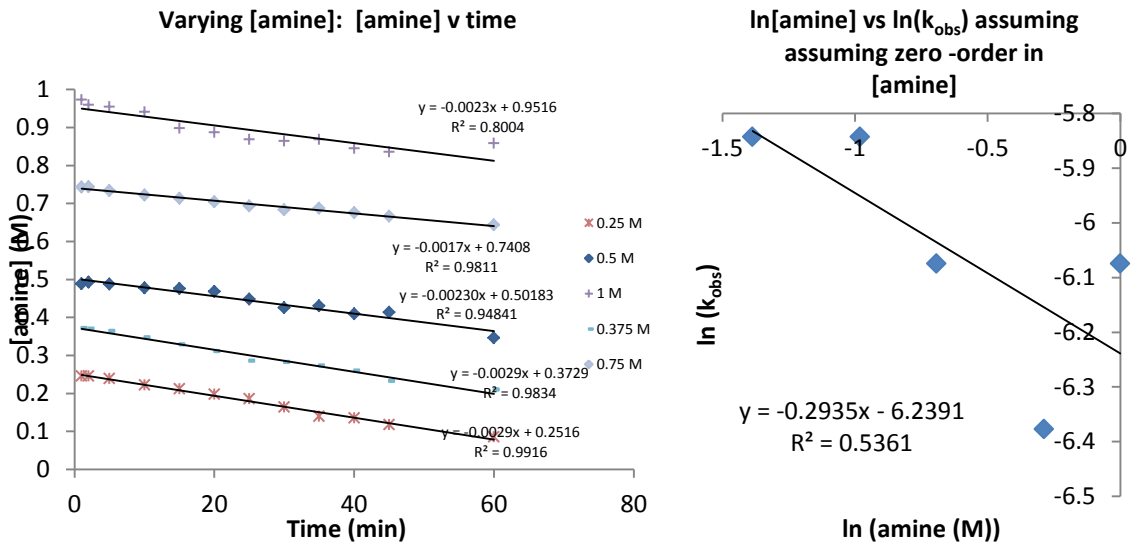

Figure 68. Plot of [amine] vs. time and log/log plot

However, when we plotted the log/log plot we obtained a non-linear but non-zero relationship of rate to concentration, suggesting more complex mechanistic behaviour and perhaps a change in order of reaction, or a mechanism not involving a simple rate-determining step.

We also found we could also obtain a reasonable fit using a logarithmic (first order) treatment of [amine], however the resultant log/log plot still did not give a clear rate law.

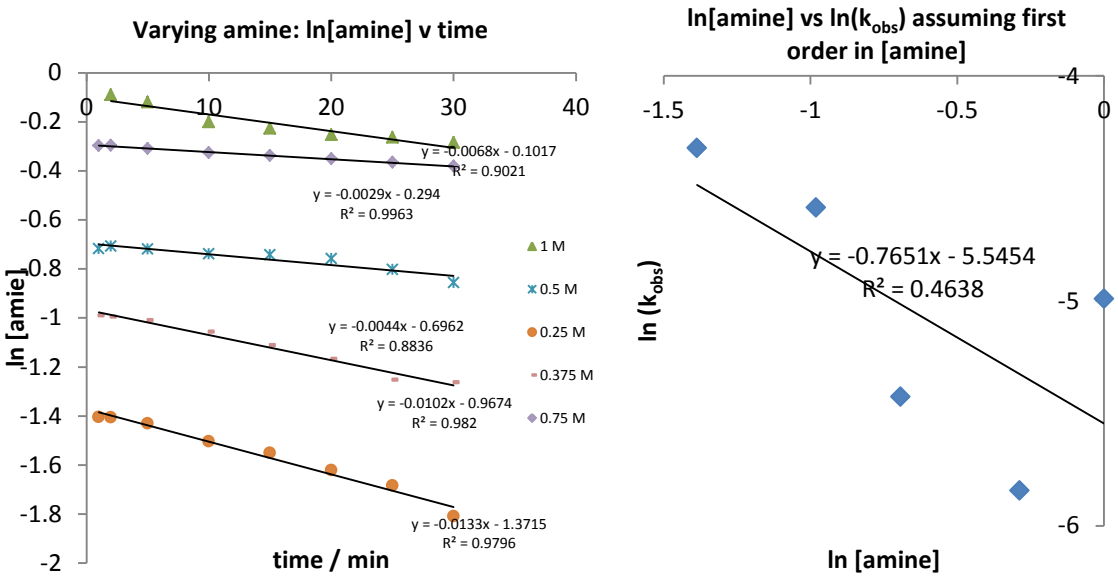

Figure 69. Plot of ln[amine] vs. time and log/log plot

From this we suspected the reaction was essentially zero order in amine; however there was deviation or a change in rate over the range of concentrations studied. If anything, the reaction appeared to display a downward (inverse) order trend, but this seems implausible without more convincing evidence for this type of effect.

We then varied the concentration of [alloxan] in a similar manner. With the zero order treatment, it appeared likely that the reaction was first order in alloxan, based on our log-log plot.

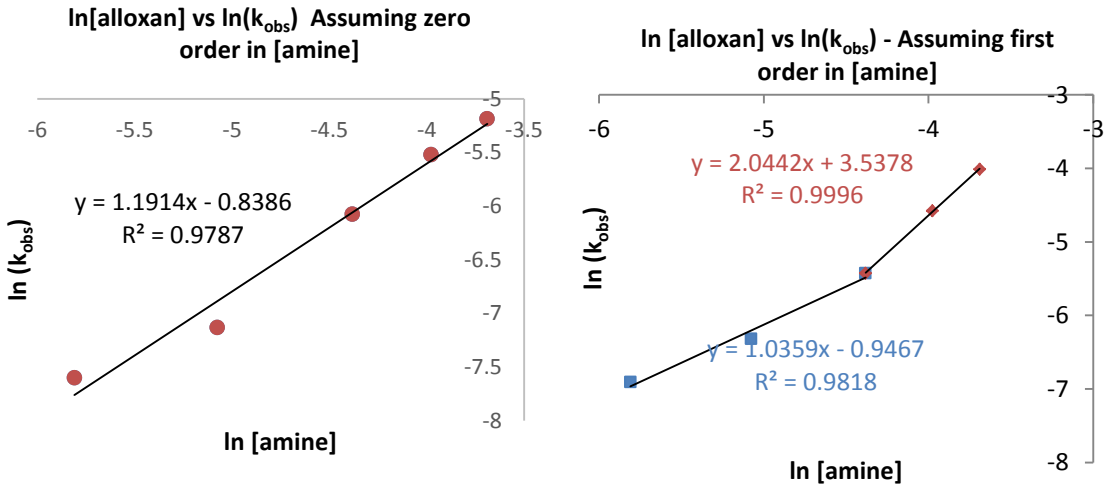

Figure 70. log/log plots of rate vs. [alloxan]

Interestingly, using the assumption that reaction is first order in [amine] gave a *change in order* from first to second order in [alloxan] above 0.0125 M. Although we do not consider this a first order reaction, this has parallels with Bruice's observation when studying the reactions of phenanthrolinequinones and amines that these follow *pseudo*-first order kinetics but deviate at low [amine] (i.e. high [quinone]) due to increased radical character.[183] It is therefore a possibility that the reaction is entirely quinone-like at low concentrations of amine but at higher concentrations reaction is more radical in character and perhaps has some similarities to the flavin-containing system.

Finally, we varied the concentration of [Cu], and this also appeared to be essentially first order, both using the zero order and first order approximations.

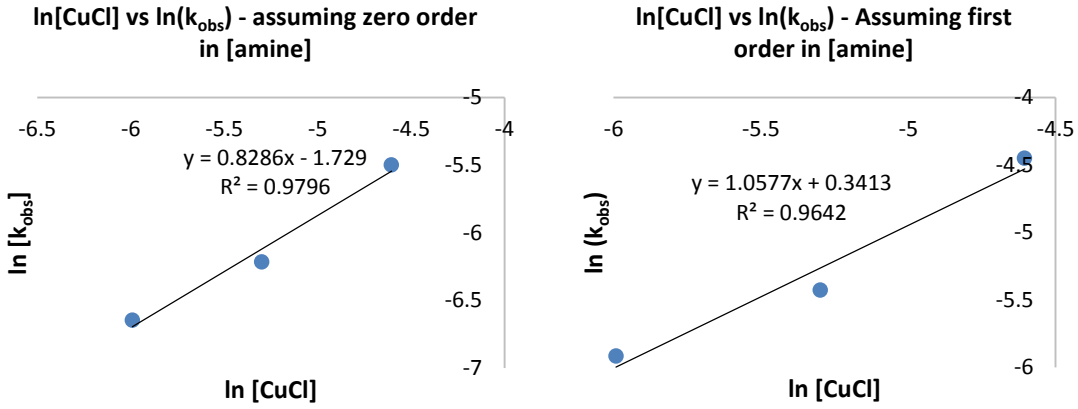

Figure 71. log/log plots of rate vs. [CuCl]

It therefore appears that the rate-determining step is either a Cu(II) mediated reoxidation of reduced alloxan or alternatively a one –electron reduction of alloxan by Cu(I).

We also decided to look at the effect of enrichment in O_2 on the reaction. We were surprised to find that the imine was initially formed more rapidly in the presence of 1 atm O_2, but proceeded to stall completely. This suggests that O_2 accelearates the reaction, but that excess O_2 concentration leads to catalyst deactivation.

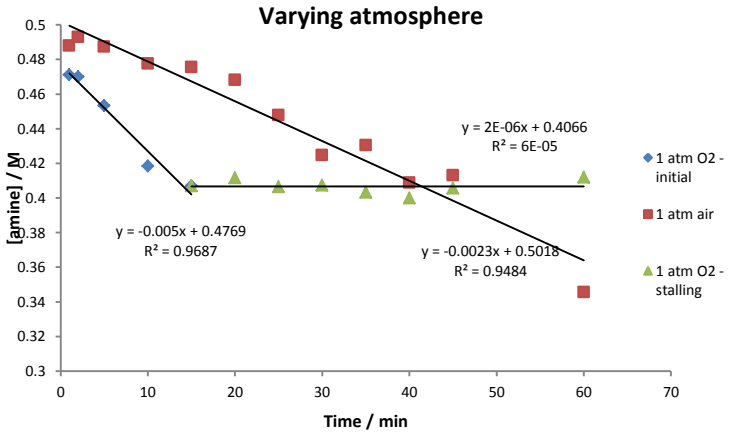

Figure 72. Effect of O_2 compared with air atmosphere on amine oxidation

5.5.1 EPR Spectroscopy

We decided to probe the various stages of the reaction by EPR spectroscopy, for two reasons: firstly, we wanted to see if there was a noticeable Cu(II) signal upon mixture of alloxan and CuCl, prior to amine addition, or if the amine was additionally required, and secondly to see if any organic radicals were observable in this case.

Before addition of amine, there is no visible EPR spectrum, either of organic radicals or of any Cu(II) species, showing the system is almost entirely diamagnetic d^{10} Cu(I) at this stage.

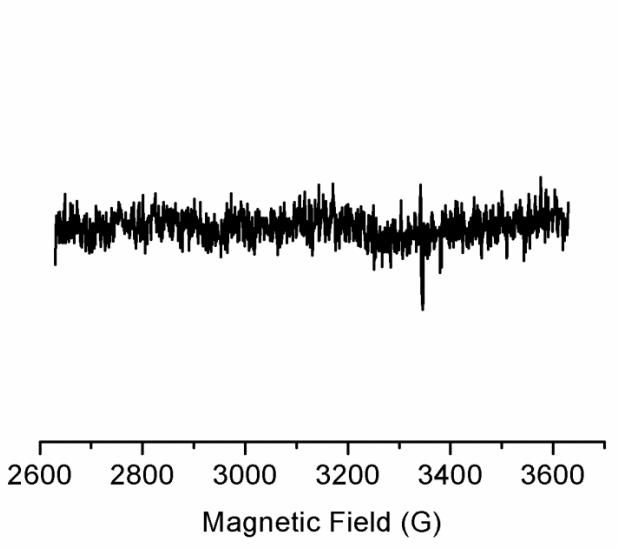

Figure 73. EPR Spectrum of alloxan + CuCl in MeCN under air

Upon addition of amine **15a**, we see an EPR spectru highly characteristic of Cu(II), in a d^9 configuration, with the nuclear spin of copper (I=3/2 for both isotopes; natural abundance 69.1% of ^{63}Cu and 30.9% of ^{65}Cu).

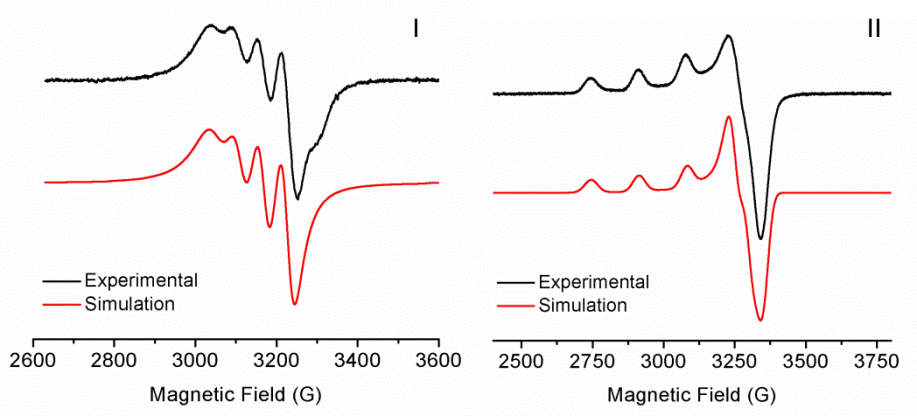

Figure 74. I Room-temperature solution X-band (9.6 GHz) EPR Spectrum directly after amine addition: Simulation parameters: g_{iso} = 2.134; A_{iso} = -55 G; Tumbling effect modeled with : - a = 41, b = 7.5 c =3, d = 0.5 **II** Frozen solution (120K) X-band EPR Spectrum of same system, **Simulation:** g_1 = 2.04, g_2 = 2.075, g_3 = 2.242; A_1 = 10 G, A_2 = 10 G, A_3 = 165 G; Linewidth (W) : Gaussian (W_1= 20 G, W_2 = 20 G, W_3 = 25 G)

At 120 K, (**II**) molecules are frozen in specific, non-averaged orientations with respect to the magnetic field and it is possible to determine the g tensors along various axes. Simulation of the frozen solution EPR spectrum gives a g_{zz} value much larger than g_{xx}, and g_{yy}, suggesting axial symmetry square planar or axially –elongated), with the unpaired electron placed in the d_{x2-y2} orbital.

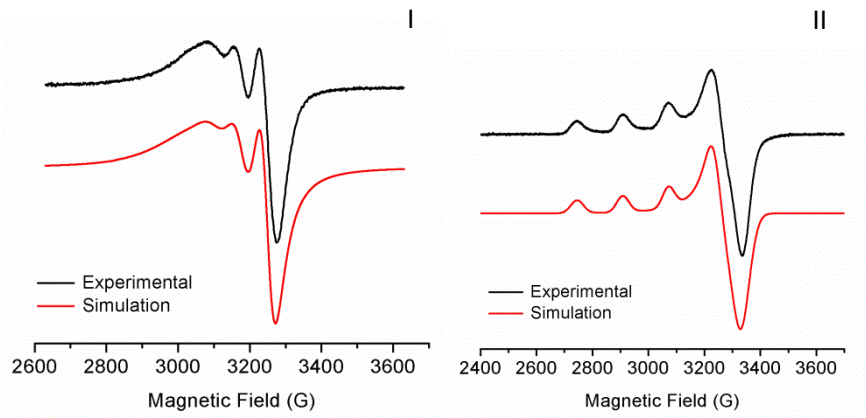

Figure 75. **I** Room-temperature solution EPR Spectrum of reaction x after 2 h**:** g(iso) = 2.129; A(iso) = -65 G; Tumbling - a = 70, b = 26, c = 8, d = 2. **II** Frozen Solution (120 K) X-band EPR Spectrum of same system g_1 = 2.055, g_2 = 2.055, g_3 = 2.242; A_1 = 10 G, A_2 = 10 G, A_3 = 160 G; Linewidth = Gaussian, 1 = 20 G, 2 = 20 G, 3 = 25 G

After 2 h reaction time, we see a very similar Cu(II) spectrum. Some aspects of the spectrum, particularly at r.t. (**I**) however, have changed, indicating a potential ligand change around Cu that would fit with benzylamine **15a** being a ligand for Cu which is itself consumed in the reaction. Of note in this hypothesis is that the methylene amine signal is very broad when we attempt *in situ* ^{1}H NMR analysis. Although there is only 2 mol% Cu present, it can presumably 'hop' between amine ligands faster than the NMR timescale.

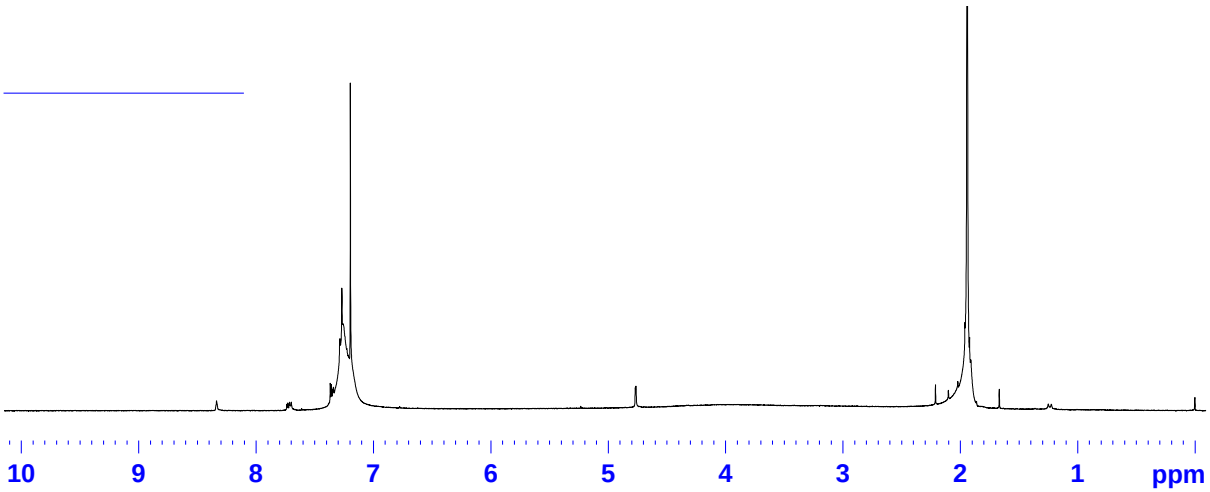

Figure 76. NMR spectrum of benzylamine + 1% CuCl + **138a** after 15 mins

5.5.2 Proposed mechanism

Taking all these factors into consideration, we considered the possibility that the reaction in fact also proceeds through a mechanism with radical character. A Cu-containing species being involved in the rate-determining step but a lack of appreciable build up of Cu(II) before the addition of amine seemed inconsistent with the quinoidal mechanism, where Cu(II) would need to be present before the first turnover in order to mediate O_2 reoxidation of alloxan from dialuric acid. Additionally, we saw no evidence of the formation of murexide in this reaction, which would be expected to form if a dialuric acid intermediate was involved, and also be expected to be a catalyst deactivation pathway.[167]

We propose, based on the previously discussed data, that we see a rapid pre-equilibrium between alloxan and its one electron reduced form, nevertheless far enough towards the starting alloxan/Cu(I) pair that we do not observe formation of the Cu(II) by EPR at this stage. A further reaction of O_2 could add into an alloxan radical and form a peroxy radical.

Upon amine addition, the small amount of formed peroxyl would abstract a hydrogen atom, forming a hydroperoxide, extruding H_2O_2 to regenerate alloxan. As discussed by Scaiano, alloxan accepts an electron from the α-amino radical to form a semireduced alloxan again, which is reoxidised. [159]

A rate determining step involving [Cu] does not fit with the copper single electron transfers being in rapid equilibrium; however, an alternative rationalisation is that CuCl may be de-aggregated and activated by the presence of amine (given we would expect Cu ammine complexes to be formed).

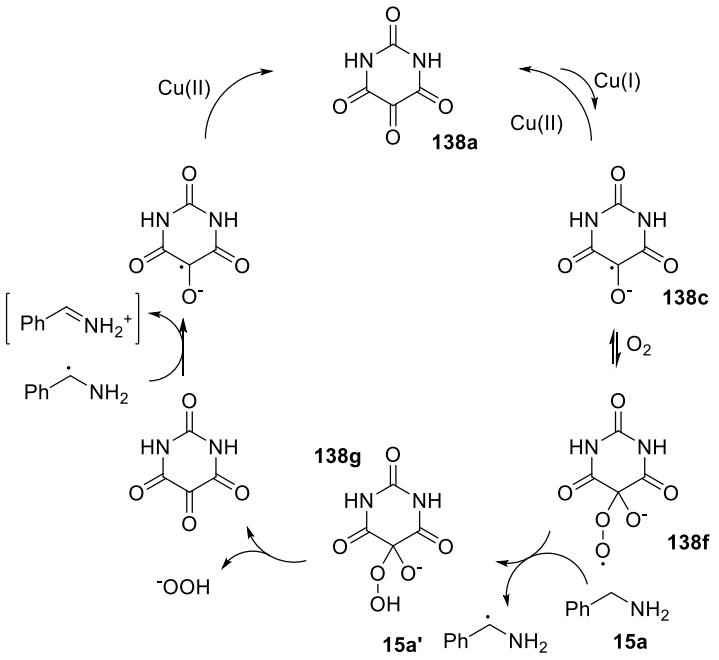

Scheme 127. Alternative plausible mechanism for Cu/alloxan catalysed amine oxidation

Finally, *N,N*-dimethylalloxan **163** did not promote reaction, suggesting tautomers and acidic protons are important in this pathway. This could be evidence for the quinoidal mechanism, however it may be also related to stabilising the negatively charged intermediate **138f**. Additionally, the general oxidisability of alloxan is enhanced relative to the dimethyl analogue.[114,115]

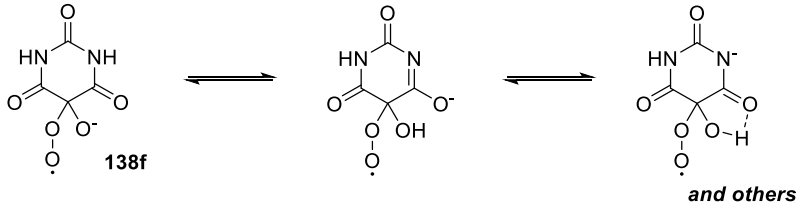

Scheme 128. Involvement of tautomerisation in stabilisation of peroxyl radical anion **138f**

5.6 Diimide-mediated alkene reduction

Diimide, N_2H_2 (also known as diazene) is an unstable oxidation product of hydrazine, which slowly disproportionates to hydrazine and N_2. Diimide can exist in both *cis* and *trans* forms, proceeding *via* reversible protonation

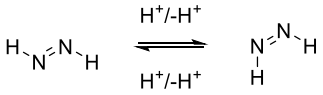

Scheme 129. Diimide and its isomerisation

The major use of diimide, which is always generated *in situ,* is as an alternative reagent to hydrogen gas in the reduction of unsaturated molecules, generally alkenes. One advantage of this is the obviation in many cases of the need for transition metal catalyst. Another is the selectivity for alkenes, with functional groups such as benzyl ethers and thiols which would normally either be cleaved by or interfere with Pd-catalysed hydrogenolysis.

Generally, diimide is generated by the action of an oxidant on hydrazine, or by base-promoted elimination of sulfonylhydrazides.

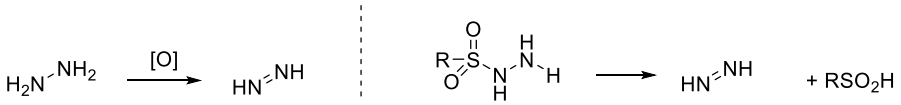

Scheme 130. Diimide formation by either hydrazine oxidation or base-promoted sulfonylhydrazide elimination

The formed *cis*-diazene is then able to transfer H_2 to an alkene, with the formation of nitrogen gas providing a powerful thermodynamic driving force for this reaction.

A more recent development is an organocatalytic method of generating diimide: flavin-catalysed diimide hydrogenations, pioneered by Imada.[93] The flavin first binds to hydrazine to form the adduct, which is probably the active reductant in the process rather than 'free' N_2H_2, due to lower rates of disproportionation and so lower required N_2H_4 loadings than in classical diimide chemistry.[96] The flavin will then eliminate N_2 to form dihydroflavin which spontaneously reoxidises in O_2 with generation of H_2O_2 which is also a potential oxidant for generation of N_2H_2.[93]

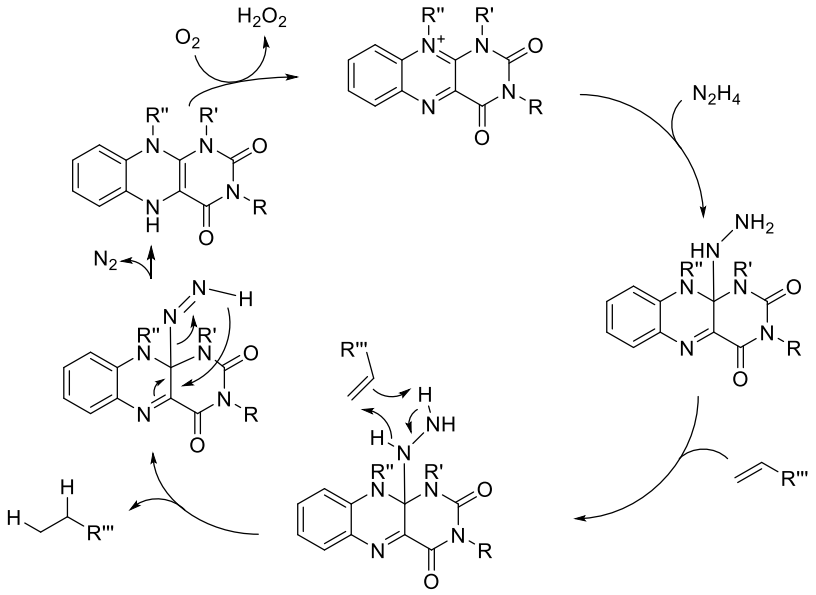

Scheme 131. Possible mechanism for flavin-catalysed diimide hydrogenation

We reasoned that, whether acting as a radical oxidant or a quinoidal dipolar one, alloxan, as a highly electrophilic and redox active molecule could be a candidate for a new reagent to promote hydrazine oxidation and subsequent reduction of alkenes. Postulated advantages of alloxan over existing methods are its commercial availability and lower molecular weight than flavin catalysts.

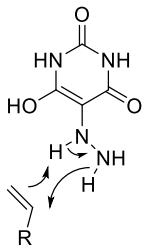

Figure 77. Proposed key step in alloxan-catalysed diimide hydrogenation

We found that indeed alloxan promoted the reaction of allyl benzyl ether with hydrazine and air to form the propyl benzyl ether **198a**. Notably, this compound would be expected to be difficult to synthesise *via* palladium-catalysed hydrogenation due to the competing hydrogenolysis of the benzyl ether.

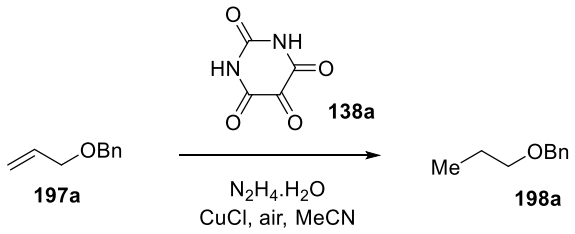

Table 19. Optimisation of **138a**/CuCl catalysed reduction of **197a**

Entry	CuCl [mol%]	**3** [mol %]	$N_2H_4.H_2O$ (eq)	T / ˚C	t [h]	Conv.[a] [%] (yield) [%][b]
1	0	5	1.25	25	20	18
2[a]	0	5	1.25	25	20	14[c]
3	0	5	2.5	25	18	28
4[b]	0	5	2.5	85	24	74
5	1	5	2.5	25	3	55
6	1	5	2.5	85	8	100
7[c]	1	5	2.5	40	18	100 (93)
8	1	0	2.5	25	8	0

[a]Assayed against relevant ^{1}H NMR signals [b]Isolated yield [c]Performed under O_2 atmosphere

Addition of an enriched oxygen atmosphere had minimal effect on reaction efficiency. A slight gain was achieved by increasing hydrazine loading. Heating the reaction increased the conversion to the alkane, as did adding a small amount of Cu(I) salt, as in the amine oxidation from which this process ultimately derives. Although use of $CuSO_4$ and similar chemicals has been reported for diimide reductions,[184] we did not find any background activity with CuCl alone, and notably this process has not been previously reported for Cu(I), nor with such a low loading of N_2H_4. In the end we settled on a balance of mild heating and use of Cu(I) to promote efficient reaction.

We then investigated a range of alkenes and alkynes to probe the scope of our new process. The results are shown in Table 20.

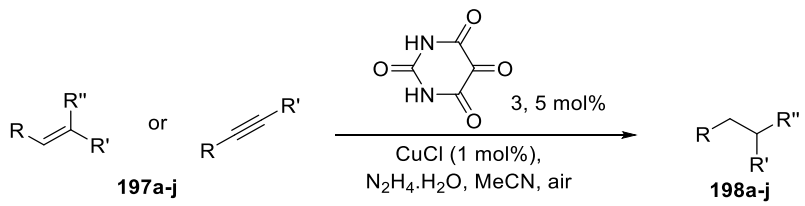

197a-j

198a-j

Table 20. Alloxan / CuCl catalysed reduction of alkenes and alkynes by N_2H_4

Entry	Substrate	Product	$NH_2NH_2.H_2O$ (equiv)	T / °C	time / h	Yield / %[a]
1	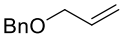	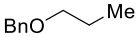	2.5	40	18	93
2	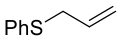	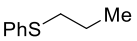	5	40	18	91
3	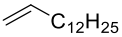	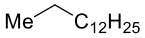	2.5	40	18	93[b]
4	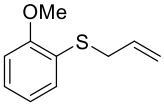	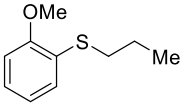	5	40	18	95
5	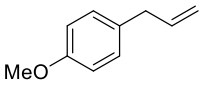	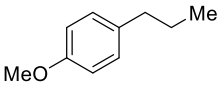	2.5	40	18	98
6	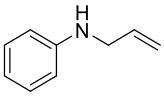	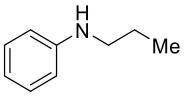	2.5	40	18	90
7	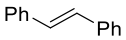	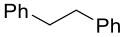	5	85	24	77[b]
8	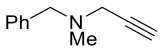	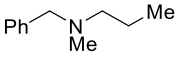	5	40	18	69
9	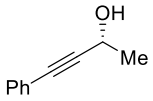	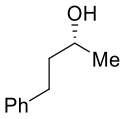	5	40	72	87
10	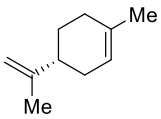	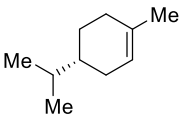	2.5	85	3	71[c]

[a]Isolated Yield [b] ^{1}H NMR conversion [c]GC yield

We found that most allyl substrates were easily reduced to the corresponding propyl group. The reaction tolerated benzyl ethers, basic nitrogen atoms, and sulfides. More substituted alkenes such as stilbene (Table 20, entry 7) were more difficult to reduce, and surprisingly the long-chain alkyl 1-tetradecene was also hard to obtain completely free of alkane. In the latter case we suspected that the starting material might be immiscible with acetonitrile, however addition of toluene to homogenise the reaction mixture yielded the same result. Terminal alkynes were also easily reduced to the corresponding alkane, and even an internal alkyne was fully reducible with an extended reaction time, without perturbation of the stereocenter. Limonene was selectively and rapidly hydrogenated on the terminal alkene, as would be expected due to it being less substituted and more accessible to transfer of H_2. In this case, yield was determined by GC, calibrated against independently synthesised dihydrolimonene produced by PtO_2-catalysed hydrogenation.[185]

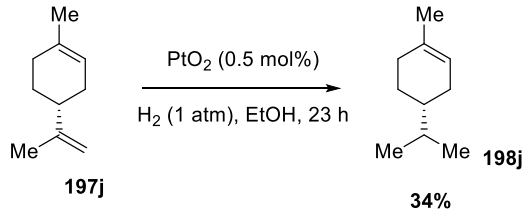

Scheme 132. Synthesis of dihydrolimonene **198j**

5.6.1 Diimide-mediated reduction: mechanistic discussions

Upon attempting the reaction with allyl ether **197a** under an atmosphere of argon, partitioning the reaction between water and dichloromethane prior to allowing oxygen into the reaction mixture, we observed 29% conversion to reduced product **y**. This is significantly less reaction than in the presence of air (55% at 25 ˚C after only 3 h). Although this surprising result could be due to residual air somehow entering the reaction, it could also point to two alternative mechanisms, which would explain some of the complex kinetic behaviour we observe.

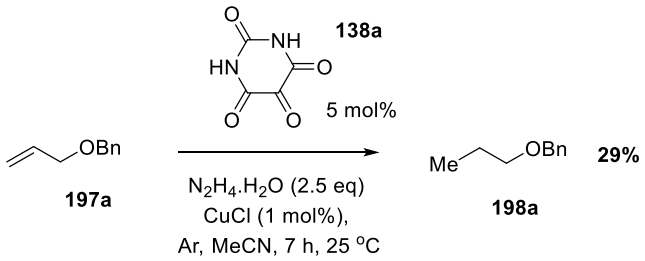

Scheme 133. Possible reactivity in the absence of O_2

The mechanistic step depicted in Figure 77 seems to fit with the previously assumed reactions for sulfonylhydrazide and flavin-catalysed diimide reductions. However, to start from oxidised alloxan, the only plausible way to regenerate the catalyst would be to eliminate a diazonium, which from a position between two carbonyl groups seems an unlikely candidate for either S_N1 or S_N2 displacement. However, reaction could proceed through a carbine-type intermediate in this instance.

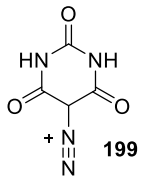

Figure 78. Possible alloxan diazonium intermediate

A mechanism oxidising hydrazine to diimide in a manner analogous to that of the radical possibility for amine oxidation can be invoked (Scheme 134).

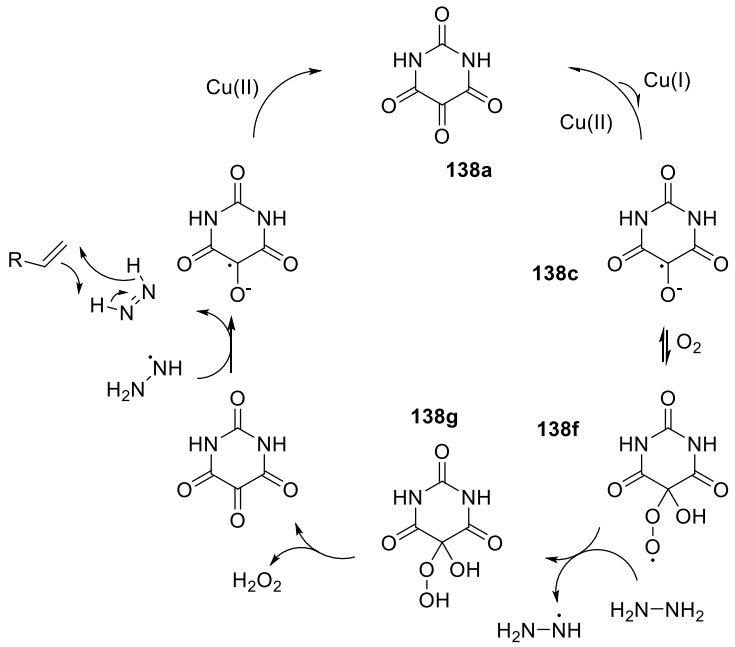

Scheme 134. Possible radical mechanism for alloxan –catalysed diimide generation

The pre-equilibrium between oxidised **138a** and reduced **138c** remains as discussed. A H-atom is then abstracted from hydrazine. H_2O_2 elimination gives regenerated **138a**, which accepts an electron from intermediate **y**. Rapid proton transfer gives a hydrazine which reacts with the substrate, and catalyst reoxidation with generated Cu(II) completes the cycle. Given the energies of H-abstraction from hydrazine and hydrogen peroxide (for a representative peroxyl) are 5.0 kcal mol^{-1} and 90 kcal mol^{1} respectively, the thermodynamics of these H-abstraction processes should be favourable.[186]

Alternatively, two consecutive electron transfer from hydrazine to alloxan, or Cu(II) could initiate the catalytic cycle *via* two proton-coupled electron transfers, with Cu(II) being previously generated by reaction with additional alloxan **138a**.[187]

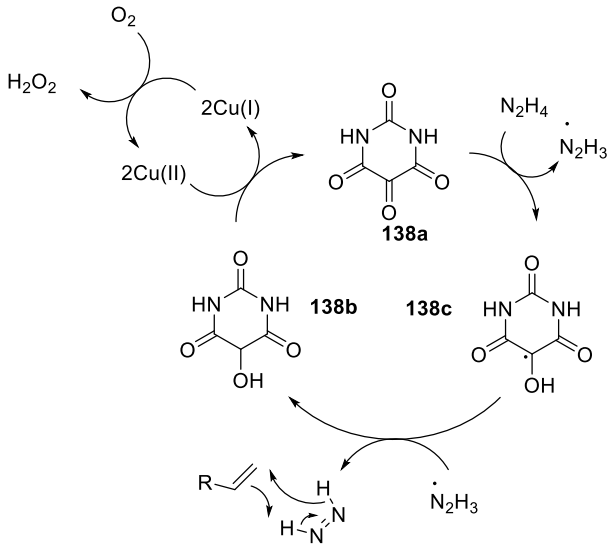

Scheme 135. Alternative radical mechanism. This could additionally involve Cu(II) electron transfer to hydrazine

6. Flavin-catalysed indole deuteration

6.1 Indoles and flavoenzymes

Indoles are bicyclic heterocycles comprised of fused benzene and pyrrole rings. Indoles relevant to biology include the natural (proteogenic) amino acid tryptophan, as well as the neurotransmitters serotonin and melatonin, the latter two of which are substrates for the flavoenzyme MAO (post-deacylation).[7,16,19,188]

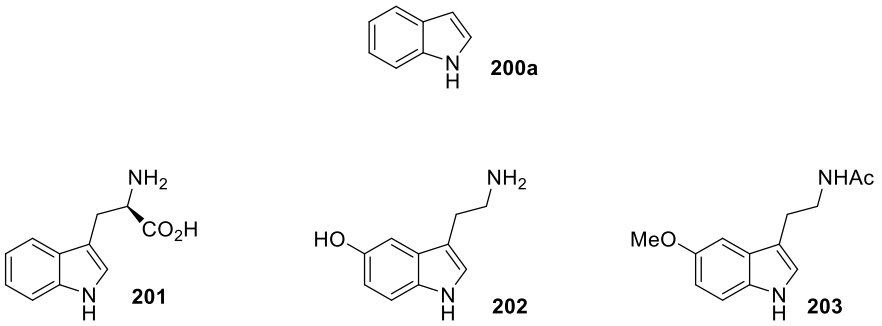

Figure 79. Structures of indole (**200a**) and tryptophan, serotonin and melatonin (**201, 202** and **203** respectively)

A previously discussed indole, relevant to flavin chemistry, is the MAO inhibitor harmine, which like a variety of other carbolines, is a noncovalent competitive inhibitor of this enzyme.[189]

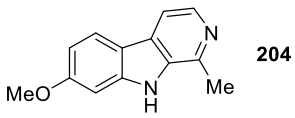

Figure 80. Structure of Harmine

Flavoenzymes also have relevance to the biosynthesis of indole natural products. An example being the first step in the biosynthesis of the antibiotic rebeccamycin **206**; where a flavin *halogenase* transfers an electrophilic chlorine to tryptophan.[190]

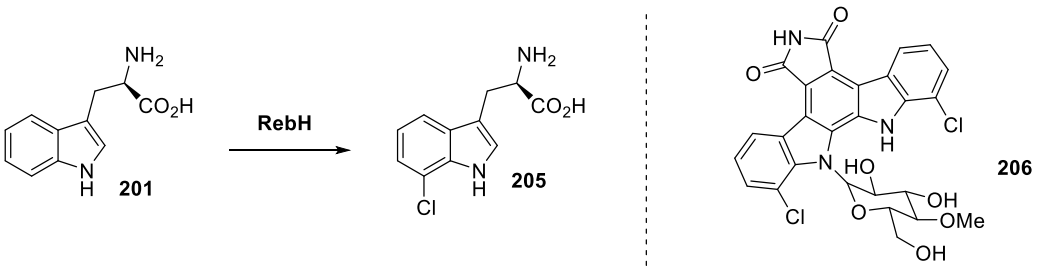

Scheme 136. First biosynthetic step and structure of rebeccamycin

This enzyme, RebH, is an example of a flavin-dependent halogenase. The next step in the rebeccamycin synthesis also involves a flavoenzyme, with the oxidase RebD promoting dimerisation and cyclisation to form a central pyrrole ring; in a rare example of C-C bond formation promoted by a flavoenzyme.[191]

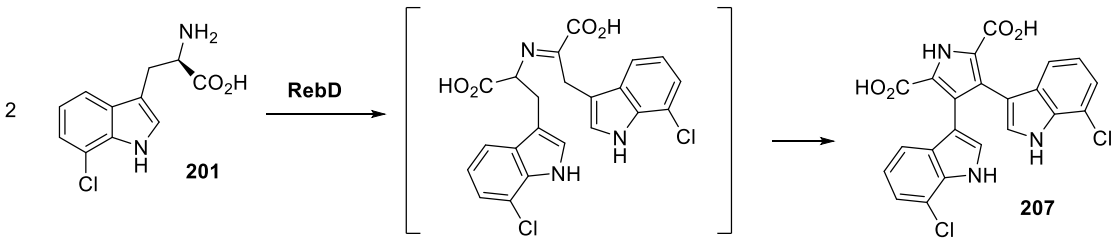

Scheme 137. Pyrrole formation catalysed by RebD

Flavin monooxygenase chemistry is also relevant to the biosynthesis of indoles, with the auxin (plant hormone) indole-3-acetic acid being formed from indole-3-acetamide. This in which itself is generated by the flavoenzyme tryptophan-2-monooxygenase (TMO) from tryptophan.[192]

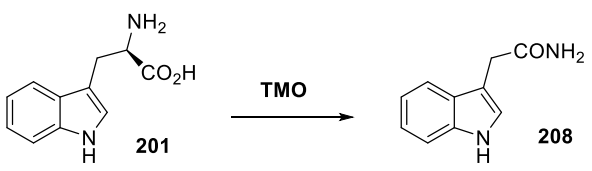

Scheme 138. TMO oxidation of tryptophan

6.2 Flavin-indole charge transfer chemistry

Flavins, as electron deficient molecules, are known to form charge transfer complexes with electron-rich molecules such as an indoles, β-carbolines, purines or pyrimidines.[193]

There is evidence that some of these charge transfer complexes proceed to a one-electron reduction of the flavin by the electron rich donor molecule, as part of the enzyme's activity. One example is the biosynthesis of the nikkomycin antibiotics which progresses through the nikD enzyme. This promotes the oxidation of piperideine-2-carboxylate **208** to picolinic acid **42n**; overall an unusual four-electron oxidation. The enzyme is related to amino acid oxidases.[194]

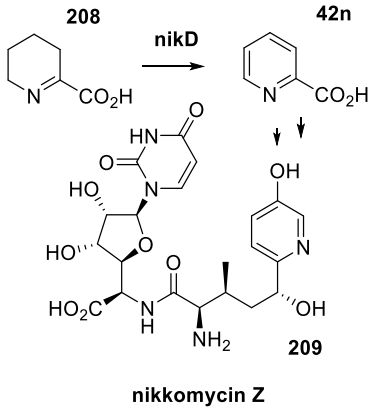

Scheme 139. Biosynthesis of nikkomycin Z **209** – key oxidation step promoted by nikD

This amine oxidation involves the key step of a single electron transfer from tryptophan to flavin as elucidated by mutation studies in conjunction with UV/visible spectroscopy. [195] The crystal structure of nikD shows a CT interaction and a closest contact distance of 3.17 Å, and it is thought that this interaction mediates single electron transfer type processes.[194]

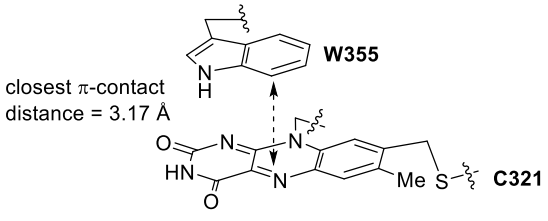

Figure 81. Interaction of indole with flavin in nikD active site

A number of studies have explored model systems in the context of charge transfer from indoles to flavin moieties.[196-198] Furthermore, Rotello has extensively used model flavins in the context of charge transfer chemistry with a wide variety of donors. The use of tethers

such as diaminotriazines has allowed a wide variety of CT donors, initially fairly unpolarised arenes as depicted.[196]

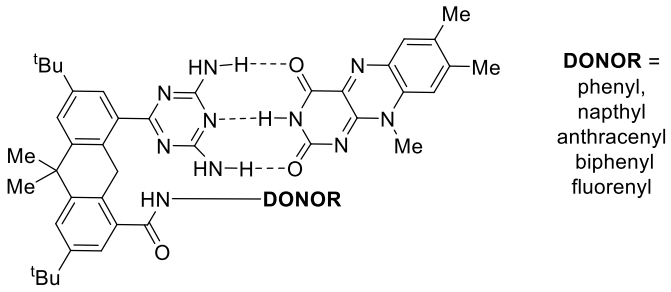

Figure 82. CT interaction of tethered flavin with varying donors.

This methodology was later extended to more unnatural donors such as porphyrins.[199,200]

Direct evidence for flavin-indole single electron transfer was observed by Skibsted, in a reaction of photoexcited triplet state riboflavin and indole, forming the radical cation which was captured with spin traps such as 2-methyl 2-nitrosopropane (MNP) to form nitrosoindole **210**.[201] Hadad and Platz proposed an indole-flavin radical pair would ultimately lead to flavin-indole C-C bond formation yielding adduct **211**, based on DFT methods and time resolved IR spectroscopy.[202]

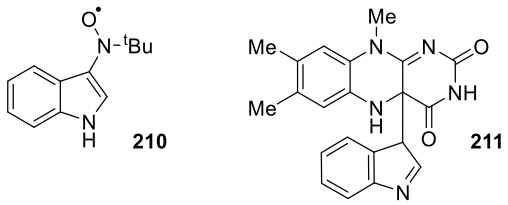

Figure 83. Spin-trapped indolyl radical 2**10** and indole flavin radical pair adduct **211**

Additionally, the cryptochrome enzyme is a blue-light sensitive flavoenzyme common in both plants and animals, centred on a flavin-indole CT interaction. Among its functions are phototrophism (growth in response to light) in plants,[203] regulation of circadian rhythms in animals[204] and for avian signalling and magnetoception.[205,206]

6.3 Flavin indole charge transfer biomimicry

Initially, we intended to mimic flavin-dependent halogenases to transfer 'Cl^+' to an electron rich indole such as that seen in rebeccamycin biosynthesis. We considered the possibility that this type of reactivity could progress through either monooxyganase like chemistry, or oxidase like (one or two electron). The idea was in order either to generate a hypochlorite-like flavin chloroxide, analogous to flavin hydroperoxide **148**, or else react flavin with a chloride source such that the chloride was oxidised to Cl(0) or Cl(I).

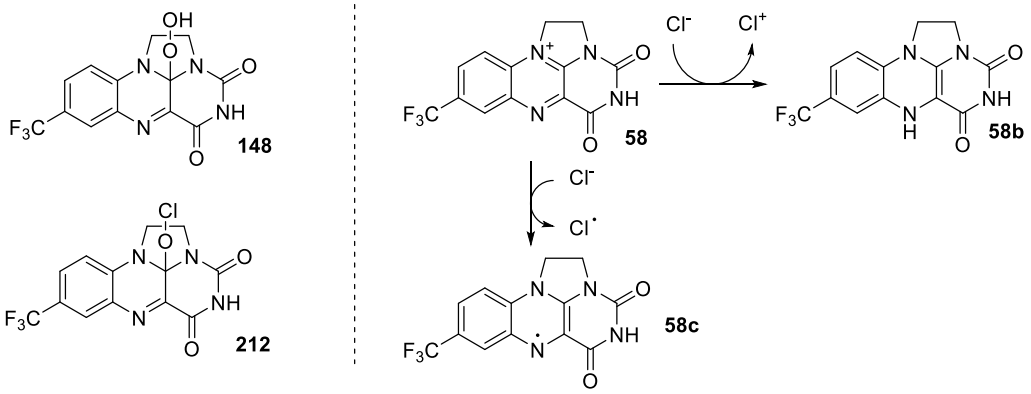

Scheme 140. Proposed flavin halogenase mimicry

Upon mixing of flavin, 2-phenylindole, H_2O_2 and LiCl as a chloride source, we observed complete disappearance of the C3 indole signal, but the same reactivity in the absence of halogen source.

At first we suspected oxidation to an indole dimer, as reported in a recent paper using $FeCl_3$ catalysis and O_2.[207] However, reaction was also possible in the absence of an external oxidant.

It transpired, as we were performing ^{1}H NMR studies in MeOD, that we were in fact performing a facile C3-deuteration of indole **200b**, which was completed in only 1 minute. This was confirmed by ^{2}D NMR spectroscopy and mass spectrometry.

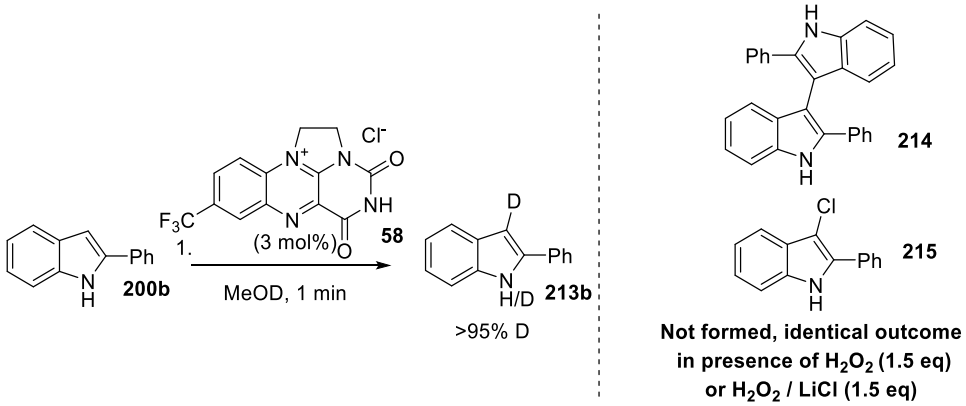

Scheme 141 Initial deuteration of **200b**.

Rapid, mild and selective deuteration of organic compounds is an extremely important process for mechanistic investigations into novel chemical reactions.[138] Additionally, recent investigations into the metabolic stability of drugs and other biologically active molecules has led to the possibility of deuterated drugs having improved pharmacokinetic properties by comparison to their protium counterparts[208,209] with a recent example being CTP-499, a drug candidate for diabetic nephropathy.[210].

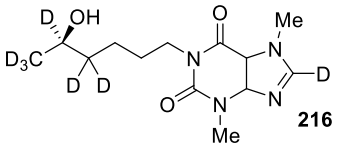

Figure 84. Structure of CTP-499 **216**

For these reasons, in the course of development of novel chemical reactions a variety of methods for deuterating indoles have been developed. Current methods of deuteration of indoles and other nitrogen heterocycles often have the disadvantages of high temperatures, use of strongly acidic or basic conditions, long reaction times, or the use of expensive deuterium sources such as D_2SO_4 or ^tBuOD.[211,212] Additionally, these reactions may be non-selective for specific indole positions or require chromatography to separate by-products produced by the harsh reaction conditions.

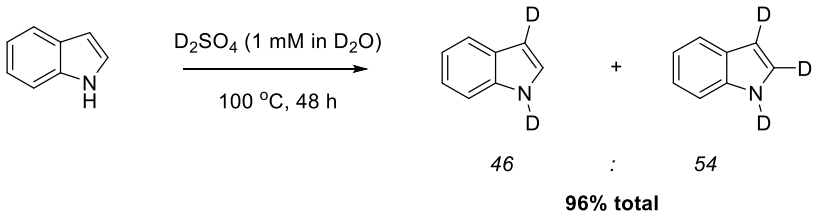

Scheme 142. Deuteration of indole by D_2SO_4, with over-deuteration

The generality of the flavin-catalysed method was probed by attempted deuteration of a series of indoles, using only a 1 minute reaction time at room temperature, then extending to 15 mins if reaction appeared to occur but sluggishly. The results are shown in Table 21. Partial deuteration of N(1) occurred over the reaction time.

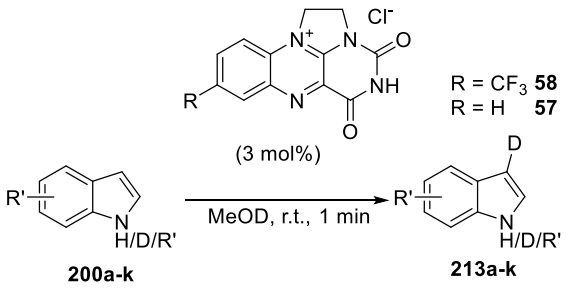

Table 21. Deuteration of indoles with **58**/MeOD

Entry[a]	R	Product	%deut[b]
1	2-Ph	**213b**	>95
2	2-Me	**213c**	15 (94[c])
3	H	**213a**	15 (95[c])
4	5-OH	**213d**	83
5	5-Me	**213e**	46 (83[c])
6	5-I	**213f**	9 (65[c])
7	5-CO_2Me	**213g**	6
8	5-CN	**213h**	0
9	5-Cl	**213i**	0
10	7-OMe	**213j**	11 (33[c])
11	1-Me	**213k**	13 (46[c])
12	2-Ph	**213b**	25[d]

[a]R = CF_3 unless otherwise stated [b]Measured by ^{1}H NMR integration of C3 proton, NMR spectra contained no side products and mass return was >95% in all cases. [c]15 minute reaction [d] Catalyst **57** used

We found striking differences in reactivity between more electron rich indoles, which generally reacted well and rapidly (**213b, 213d**) and those that were essentially unreactive to the conditions (**213g**, **213h**, **213i**) Interestingly, **213b**, which has a similar size of π-system to **58**, was the best substrate, suggesting that the strength of any stacking interaction may contribute to reactivity trends, rather than simple nucleophilicity of indole/reactivity towards D^+. *N*-substituted 1-methylindole **213k** was deuterated, suggesting indolyl proton is not involved in mediating this pathway.

One key experiment was to probe whether the deuteration was proceeding by the generation of an acidic (i.e. D^+) species by the combination of flavin and indole. When we repeated the experiment using 10 mol% 2,6-lutidine as a base, the amount of deuteration dropped from 95% to 35% over the 1 min period, suggesting an acid mediated reaction pathway. However, the colour changes observed also did not occur greatly in the presence of base, suggesting perhaps the presence of pyridine species somehow disrupts the charge transfer pathways suspected to be operating in this reaction. We attempted the deuteration both in the absence of light and under Ar (in the absence of O_2), and in both cases, appreciable differences were not observed (93% deuteration under Ar, 86% deuteration when protected from light).

In cases where the reaction was successful, we observed the most intense colour changes (entries 1, 4), so we considered that it may be the deuteration is initiated by the formation of a flavin-indole charge transfer pair. This is supported by a study showing that the presence of electron donating and withdrawing groups on indoles had a pronounced effect on the stability of the complex formed with flavin, with electron rich groups having the most stable complexes as would be expected from their electrostatic properties.[193] The less oxidising flavin (without the CF_3 group) was also somewhat effective for deuteration.[68] We were able to observe a very broad charge -transfer band in the UV/visible spectrum between 550 and 800 nm upon the addition of flavin **58** to a methanolic 2-phenylindole solution, corresponding to the almost black colour we observe in the reaction itself.

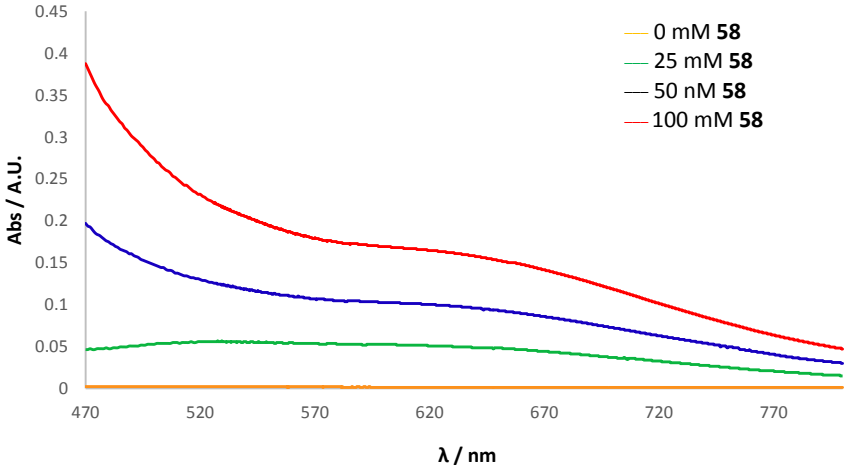

Figure 85. UV/visible spectrum of **58** + **200b**, showing CT region of minimal interference from spectrum of **58** (**58** spectrum subtracted)

Using the des-CF_3 substituted flavin **57**, we observed that while this was still an effective catalyst for deuteration (although less so than the typical **58**), but there was not a strong charge transfer interaction in this case. At the maximum flavin concentration attempted in the preceding experiment (100 mM), a very weak CT interaction was observed. Attempts to increase the concentration further failed owing to the decreased solubility in organic solvents, including methanol, of flavin **57**.

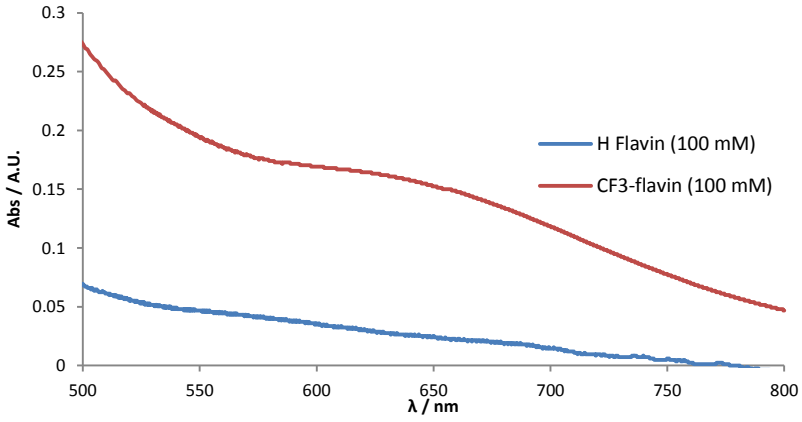

Figure 86. Difference in CT spectra of **58** and **57** upon mixing with 2-phenylindole **200b** (**58** and **57** spectra subtracted respectively).

6.4 Flavin-catalysed indole deuteration: kinetics

We found that monitoring the reactions by *in situ* ^{1}H NMR spectroscopy allowed a comparison of the two methods. The order of reaction with respect to the flavin catalysed reaction shown in Table 21 using unsubstituted indole as substrate initially appeared first order by taking the natural logarithm of the conversion, giving a straight line. However, by varying [indole], we found rate hardly varied with concentration.

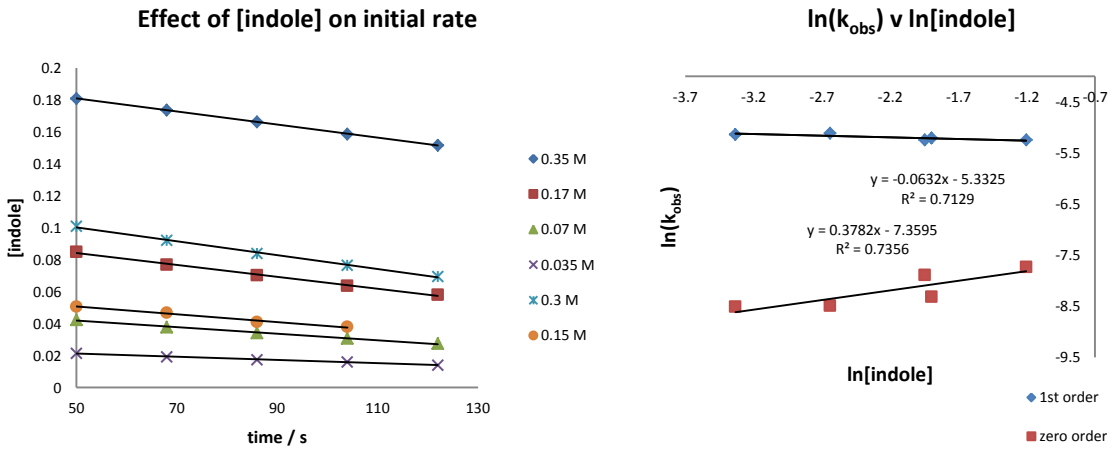

Figure 87. Effect of [indole] on rate

A log-log plot showed that the reaction is in fact zero order in [indole] over this range. Interestingly, the same treatment varying [flavin] gave a second order rate law suggesting two flavins are involved in the rate determining step. The reasons for this are unclear, but could be an aggregation type behaviour whereby two flavins are complexed to the indole during charge transfer (See Chapter 4, Figure 46). This would, however, mean association was rate-limiting *prior* to indole addition.

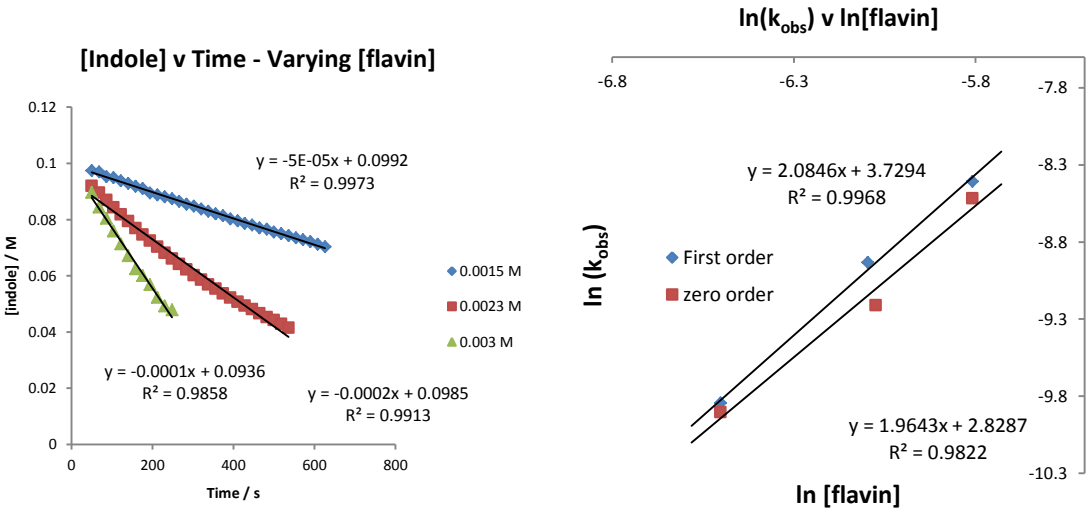

Figure 88. Effect of [flavin] on rate

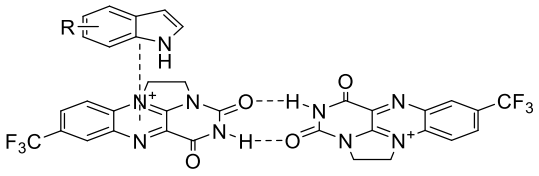

Figure 89. Possible dimeric flavin-indole adduct

6.5 Flavin-indole charge transfer complexes: X-Ray crystallography

A model flavin-indole CT complex suitable for X-ray diffraction studies was developed by Ishida, with the model flavin carboxylate **217** and tryptamine **12**. The intermolecular distances are between 3.221-3.392 Å, with additional electrostatic and H-bonding stabilisation between the ammonium and carboxylate groups.[197]

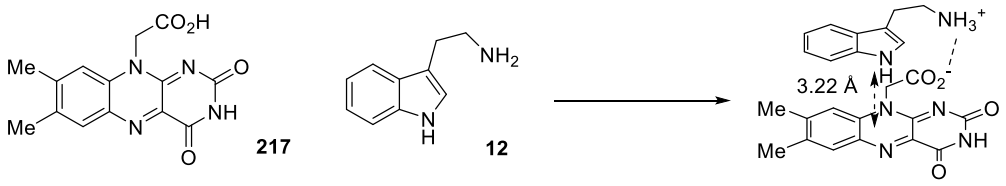

Scheme 143. Formation of indole – flavin CT complex

Additionally, the authors state that the close contact between the indole and the site of reduction to semiquinone, N(5), suggests that flavin-indole CT might be involved in the formation of semiquinoid species in enzymatic processes.

Inspired by this work, we attempted to crystallise our proposed CT complex, both in order to explicitly demonstrate that this was the species responsible for the UV spectral changes depicted in Figure 85, and to compare the indole-flavin intermolecular distance to those previously observed both in the model system and in nikD.

Upon growing crystals from a 1:1 mixture of flavin **58** and 2-phenylindole **200b** in methanol, small, dark coloured crystals suitable for X-ray crystallography were obtained. The unit cell contained one molecule of flavin **58**, one molecule of indole **200b**, one chloride counter-ion and one molecule of methanol solvent. The presence of negatively charged chloride indicates that if a full electron transfer from flavin to indole has occurred, the positive charge would lie on the indole, not flavin, as the flavin would be protonated.

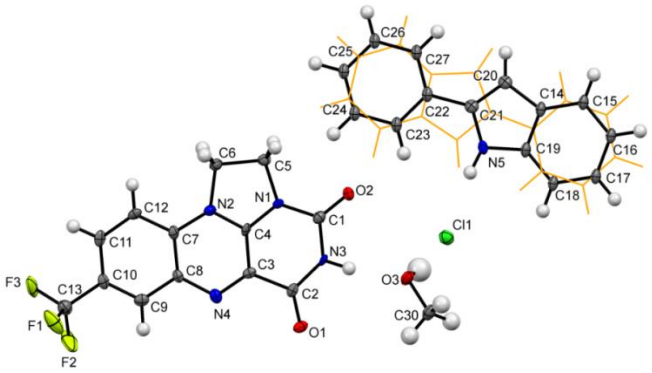

Figure 90. Asymmetric unit of CT complex

As is illustrated by the orange lines, there is disorder in the crystal in that due to its size and electronics, this indole can pack in either direction with the flavin, as the electron rich section will always be facing the electron deficient section of flavin. This may be an additional entropic factor in the favourability of binding for this particular indole.

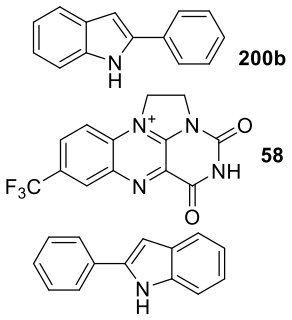

Figure 91. Two possible Flavin-Indole orientations

The nature of the π-stacking interaction is shown in the unit cell below.

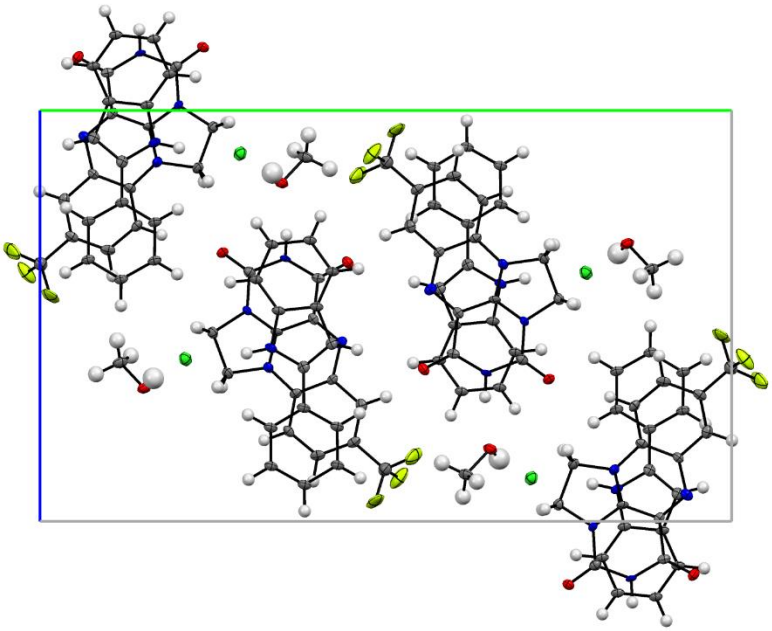

Figure 92. CT complex, viewed down a axis

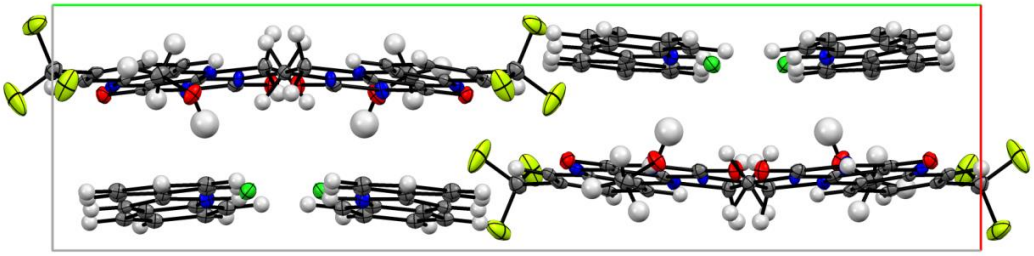

Figure 93. CT complex, viewed down c axis

Finally, a perspective view is shown, giving a flavin-indole closest π-distance of 3.39 Å. This also shows that the interaction is very similar to that proposed in Figure 81. The distance is comparable with that observed for the nikD enzyme, which is 3.17 Å.

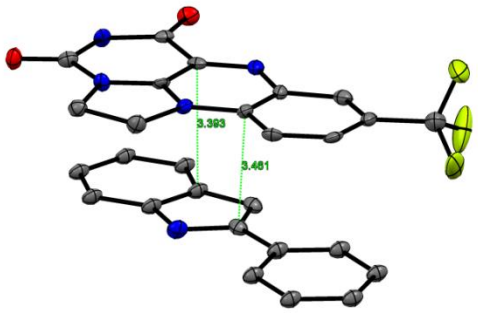

Figure 94. Charge transfer interaction and intermolecular distances of **58** and **200b**

Upon attempting the same crystallisation in 5:1 MeOH/water, yellow crystals were additionally formed. These transpired to contain one molecule of indole **200b**, solvent, and two molecules of the flavin-indole covalent adduct **218**.

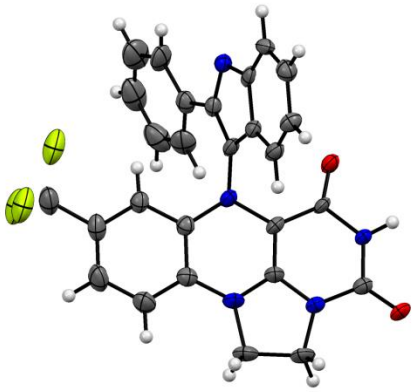

Figure 95. Flavin indole adduct crystal structure **218**

This can be contrasted with the site of attachment of flavin proposed by Hadad and Pfaltz, but does fit a radical recombination of flavin **58** and indole **200b** based on our DFT calculations in Figure 27 (Chapter 4).

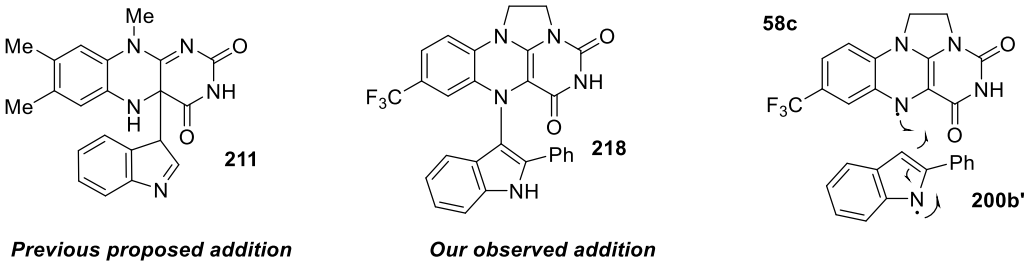

Figure 96. Alternative sites of indole attachment to flavins

This mechanism also involves removal of H_2, presumably post electron transfer. Given the presence of air in the crystallisation vial it is possible that oxygen would be the electron acceptor in this case.

Upon isolation of this molecule, the methylene bridge protons were not readily resolved in the ^{1}H NMR spectrum, despite the structure being confirmed additionally by HRMS, and the two bridge carbons being apparent in the ^{13}C NMR spectrum. This could be due to paramagnetic broadening. Upon switching NMR solvent from d^{6}-acetone to CD_3CN one methylenebridge proton signal was clear, which appeared as a triplet. However, the other signal was still extremely broad, though now visible as a broad peak between 4.05 and 3.65 ppm.

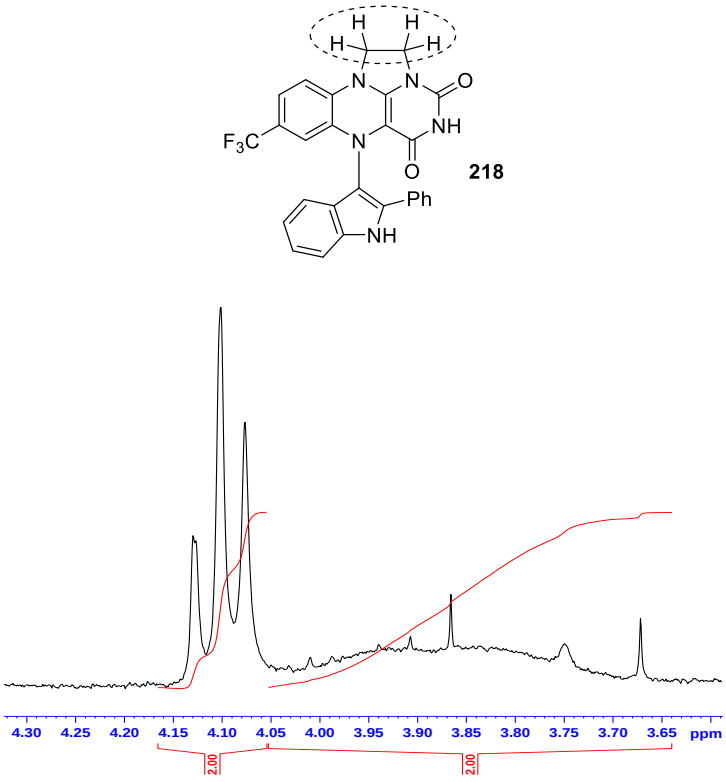

Figure 97. ^{1}H NMR broadening of methylene bridge protons

6.6 Acetyl chloride mediated indole deuteration

Inspired by the possibility of simple acidic conditions being able to rapidly deuterate indoles without extended heating, we designed a simple method for deuteration using inexpensive commercial reagents. Using 10 mol% AcCl to generate deuterated methanolic DCl *in situ* from a MeOD solution, a wide variety of indoles could again be deuterated rapidly and selectively (Table 22).

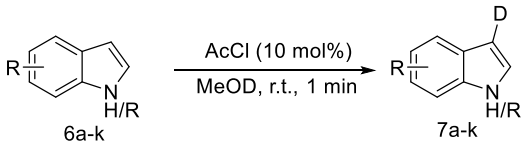

Table 22. Deuteration of indoles with AcCl / MeOD

Entry	R	Product	%deut[a]
1	2-Ph	**213b**	93
2	2-Me	**213c**	83
3	H	**213a**	86 (>95[b])
4	5-OH	**213d**	82
5	5-Me	**213e**	43
6	5-I	**213f**	51 (81[b])
7	5-CO_2Me	**213g**	15 (81[b])
8	5-CN	**213h**	21 (84[b])
9	5-Cl	**213i**	14 (94[b])
10	7-OMe	**213j**	0
11	1-Me	**213k**	62

[a]Measured by ^{1}H NMR integration of C3 proton, NMR spectra contained no side products and mass return was >95% in all cases. [b]15 minute s

The AcCl-mediated reaction was complete generally quicker than with flavin catalysis , although the loading was higher. As a simple method for deuterating indoles for mechanistic studies, it appears to be superior to previously used methods.[211]

Monitoring the acetyl chloride mediated or initiated reaction using *in situ* ^{1}H NMR spectroscopy, this time using the slower reacting 5-chloroindole (as indole reacted too quickly), showed an appreciable difference in rate upon varying concentration, although it was not possible to obtain a clear rate law in this case. Varying the concentration of acetyl chloride did not greatly affect the rate of deuteration. Therefore, although the reaction is acid mediated it appears there may be a difference in mechanistic pathway between this and the flavin-catalysed transformation.

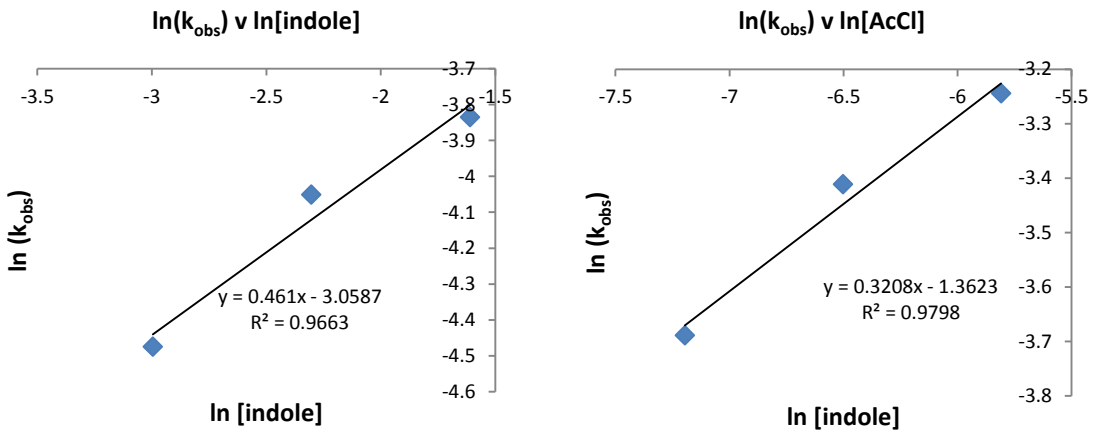

Figure 98. Kinetics for AcCl catalysis

7. Conclusions and future work

7.1 Conclusions

Flavin catalysis has been investigated in the context of an H_2O_2 mediated aldehyde oxidation, an aerobic amine oxidation with alloxan as co-catalyst, and a deuteration of indoles. In the course of these investigations we uncovered further catalytic reactions, including the utility of alloxan (accelerated by a Cu(I) co-catalyst) in amine oxidation and diimide-like reduction. Mechanistic studies have probed the biological relevance of these new catalytic processes.

7.1.1 Flavin-catalysed aldehyde oxidation

A novel flavin-catalysed aldehyde oxidation, forming carboxylic acids, using H_2O_2 as terminal oxidant was developed. This was effective for both aromatic and aliphatic aldehydes. The reaction appeared to proceed *via* a Bayer-Villiger type reaction mechanism, based on the selectivity for electron deficient substrates and the formation of Dakin oxidation products where an electron rich aldehyde is used. This is similar to the mechanism of flavin-containing monooxygenases such as *bacterial luciferase*.

7.1.2 Flavin-catalysed amine oxidation

An aerobic oxidation of primary amines catalysed by flavin **58** has been developed, with Me_2S acting as a reductant. Extensive investigations uncovered *alloxan* **138a** as a required co-catalyst. The reaction was selective for primary benzylic amines, with most reacting well with the exception of electron deficient substrates. ‘Oxidative cross coupling’ was effective between benzylic amines and anilines, with dependence on both oxidisability and aniline nucleophilicity. Other (aliphatic) amines were inhibitors of this reaction. Coupling of electronically dissimilar amines led to a formation of the product of oxidation of the more electron rich amine, **171a** in reasonable selectivity, in an example of an amine oxidation ‘self sorting’ process.

7.1.3 Flavin-catalysed amine oxidation: Mechanistic studies

The mechanism of the flavin/alloxan-catalysed amine oxidation was investigated by a variety of techniques. Firstly, EPR spectroscopy showed flavin radical cation **58d** and benzylamine-derived radical **172** as key intermediates present in the reaction. Secondly, kinetic monitoring showed a variety of features, including fractional order in both catalysts (although differing in behaviour), a ^{2}H kinetic isotope effect, and a negative Hammett correlation. The latter two in particular are similar to the MAO-B enzyme at pH 9. Other investigations used include probing the aggregation state by ^{1}H NMR DOSY spectroscopy, showing a degree of aggregation of **58** between 2 and 3 when measured in TFE, and UV/visible spectroscopy, showing charge transfer interactions between **58** and Me_2S, as well as that rate of formation of murexide **178** appears to be independent of rate of amine oxidation.

Overall, we propose a mechanism for amine oxidation based on amine C-H abstraction mediated by a flavin semiquinone, with alloxan acting as an additional redox mediator. Informed by this, as well as the pH dependence of MAO based on the work of Ramsay, we propose a mechanism for the MAO isozymes containing an identical rate determining step but with two *redox differentiated* flavins.

7.1.4 Cu/Alloxan catalysed amine oxidation

We have developed an aerobic amine oxidation catalysed by alloxan **138a** and CuCl. Selectivity differs from the amine oxidation discussed in Chapters 3 and 4 in that it does not appear to be so dependent on substrate electronic effects. This methodology can also be applied to cross-coupling type reactions, with this being fairly dependent on aniline nucleophilicity. Kinetics showed a complex mechanism but it appeared that a rate determining step was Cu(II) – mediated alloxan reoxidation *or* Cu(I) mediated alloxan reduction. The mechanism may show concentration dependence as discussed by Bruice.[183] EPR showed a Cu(II) species upon amine addition, but no organic radicals could be discerned. We were able to apply this methodology in a manner analogous to flavin chemistry, to Cu/alloxan catalysed oxidation of hydrazine to diimide and subsequent alkene reduction. This reduced a range of alkenes and alkynes, mostly neutrally polarised as is typical for diimide reductions.

7.1.5 Flavin-Indole charge transfer chemistry

As well as a charge transfer interaction, common for flavins and indoles, flavin **58** was found to rapidly and selectively C3-deuterate the indole when conducted in CD_3OD. This was dependent on indole electronics, as would be expected for a CT interaction. The kinetics showed an unusual second-order dependence on flavin, perhaps due to an aggregation behaviour. The CT interaction was measured and found to be very broad. Crystal structures were obtained both of the indole-flavin adduct, showing the π stacking interaction, and a covalent adduct when crystallisation was performed in the presence of water. We have additionally developed a simple indole deuteration based on *in situ* DCl generation by way of the action of AcCl on CD_3OD. This is significantly faster than current acid-mediated indole deuteration processes.

7.2 Future work

7.2.1 Tandem metal/organic cofactor oxidative catalysis

Cooperative metal-organic catalysis is common in nature; two examples are that of the Cu/quinone amine oxidase family of enzymes and p450 enzymes using Fe and flavin/NADH, the latter of which demonstrate a wide variety of redox activities and are particularly important in C-H oxidation biochemistry.[213] A new approach to oxidation catalysis building on this work would be to harness the reactivity of flavins, quinones and Hantzch esters (NADH mimics) with modern metal-catalysed oxidation chemistry in order to access new reactivity under aerobic conditions. In principle, any reaction using stoichiometric H_2O_2 and a metal catalyst could be replaced by an appropriate flavin and reducing agent such as hydrazine, Zn^0, Hantzch's ester, $Na_2S_2O_4$ or other hydride-transfer agents. Advantages include avoiding the necessity of handling potentially explosive H_2O_2,[214] and the thousandfold increased reactivity of flavin hydroperoxides (Scheme 144) over H_2O_2 itself.[52]

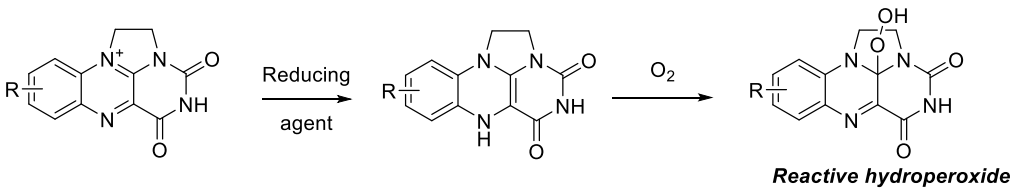

Scheme 144. Generation of flavin hydroperoxides as H_2O_2 equivalents for metal redox catalysis

Scheme 145 depicts candidate aerobic non-heme iron selective oxidations[215] and rhenium-catalysed oxidations e.g. epoxidations. The former may be viewed as mimetic of flavin-dependent cytochrome p450s (flavocytochromes),[216] whilst the latter is especially well precedented as there is a report of flavin hydroperoxides performing oxygen-transfer chemistry to rhenium.[217]

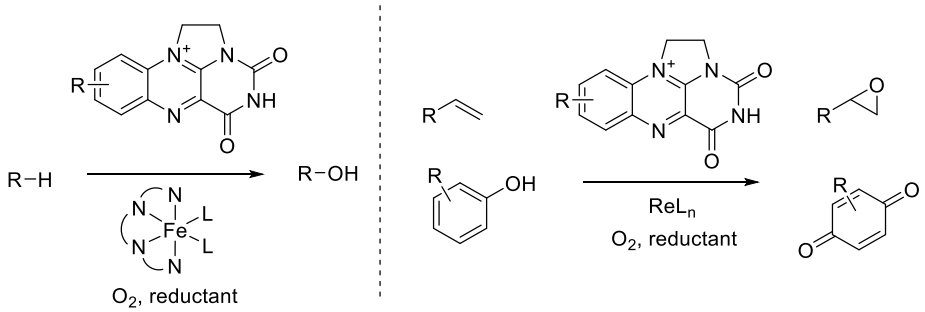

Scheme 145. Examples of flavin-mediated aerobic TM oxidation chemistry

Additionally, there is scope for the replacement further terminal oxidants with biomimetic aerobic equivalents, increasing atom economy and making these processes more efficient, particularly on scale. Examples of terminal oxidants in metal catalysis which could be replaced include hypervalent iodine reagents ($PhI(OAc)_2$/IBX), persulfates (peroxysulfate/Oxone®), peracids (peracetic acid/*m*CPBA) and quinones (DDQ/benzoquinone).

7.2.2 Tandem metal/organic cofactor reductive catalysis

Recent advances in Fe catalysis have involved the reductive coupling of *via* hydrogen-atom transfer (Scheme 146).[218,219] A key proposed mechanistic step is hydride transfer from a silane to an olefin such that a carbon-centred radical is formed. An alternative hydride transfer could also occur from reduced cofactor-type species such as the dihydroflavin or Hantzch ester. This methodology could additionally be expanded to replace the highly toxic and even less atom economical tin hydrides used in other reductive couplings.

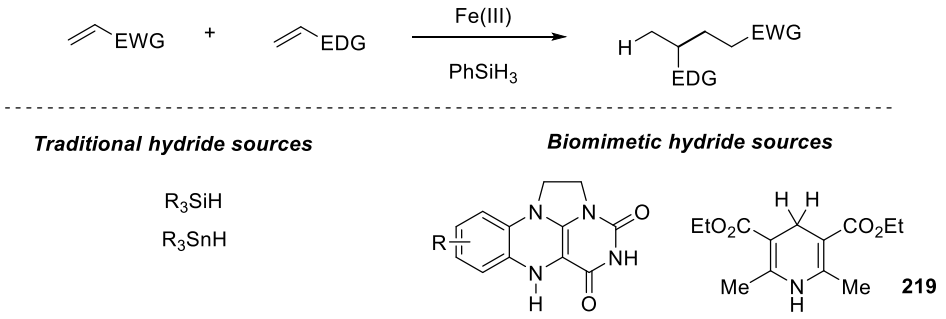

Scheme 146. Biomimetic hydride sources as green, user-friendly reagents for reductive iron-catalysed C-H bond formation

In the case of this aspect, although Baran's olefin cross-coupling is highlighted as a key challenge to apply biomimetic hydride transfer to, there is a more open-ended aspect to it. Indeed, many 'classic' radical C-C bond forming reactions use the explosive and highly toxic AIBN as initiator and the toxic and high molecular weight Bu_3SnH as hydride transfer agent. In principle, *both* these reagents could be replaced by a flavin-type catalyst in selected reactions; the first *via* the flavin semiquinone and the second a dihydroflavin.

8. Experimental

8.1 General Information

All reagents were purchased from commercial suppliers: Acros Organics, Alfa Aesar, Sigma Aldrich or Fluorochem and used without further purification. Flash chromatography was performed on chromatography grade, silica, 60 Å particle size 35-70 micron from Sigma Aldrich using the solvent system as stated. ^{1}H and ^{13}C NMR was performed on Brüker Avance 250 (^{1}H 250 MHz) Brüker Avance 300 (^{1}H 300 MHz and ^{13}C 75 MHz), Brüker Avance 400 (^{1}H 400 MHz and ^{13}C 100 MHz) and Brüker Avance 500 (^{1}H 500 MHz and ^{13}C 125 MHz) as stated. Chemical shifts are reported in parts per million (ppm) relative to tetramethylsilane (TMS) (δ = 0.00). Coupling constants are reported in Hertz (Hz) and signal multiplicity is denoted as singlet (s), doublet (d), triplet (t), quartet (q), quintet (quin.), sextet (sex.), septet (sept.), multiplet (m), and broad (br). High resolution mass spectrometry electrospray (ESI) was performed on a Brüker µTOF using electrospray ionisation (ESI) in either positive or negative ionisation. HPLC data was recorded on an Agilent 1260 Infinity system using an Agilent Eclipse XDB-CN 5 µm, 4.6 x 150 mm cyano column.

Diffusion ordered NMR spectra (DOSY) were acquired on a Bruker AV500 operating at 500.13 MHz for 1H, using a stimulated echo pulse sequence with a longitudinal eddy current delay (LED). Experiments were run at room temperature (293 K) with the probe heater turned off to reduce convection effects within the NMR tube. Values for Δ / δ were set to 50 and 4 ms respectively, with 16 scans acquired at each gradient strength g, which was incremented in 16 linear steps from 2.41 to 47.74 Gcm-1. Data were processed using Bruker Dynamics Center v2.2.

X-Ray experiments conducted on Beamline 11.3.1 at the Advanced Light Source, Berkeley, were conducted using a Bruker AXS D8 diffractometer equipped with an Apex II CCD area detector.The sample temperature was controlled using an Oxford Cryosystems Cryostream Plus and data collection, indexing and integration procedures completed using Bruker software Apex II.

Single-crystal X-ray experiments at the University of Bath were conducted using an Agilent Technologies Dual-Source Supernova diffractometer, equipped with an Eos Series 2 detector. Data were collected using Mo Kα radiation (λ = 0.71073 Å) to a resolution of 0.8 Å. The sample temperature was controlled using an Oxford Cryosystems Cryostream Plus, with experiments conducted at 100 K. The diffraction data were collected, indexed and integrated using the Agilent Technologies software CrysAlis Pro and the structures were solved using the program SHELXT. Crystal[220] structure refinement was completed using the program SHELXL[221] and the results visualised using the CCDC software Mercury.[222]

UV/vis spectra were collected on either a Shimadzu UV-1800 or Agilent Cary 60 instrument, and stopped flow kinetics on a Hi-Tech Scientific Stopped Flow instrument.

Compounds **57** and **59** were previously synthesised by Dr. Barrie Marsh, according to the published procedure.[57] Characterisation was performed in order to check purity, and synthesis is reported.

8.2 Experimental section

General Procedure for flavinium-catalysed oxidation of aldehydes to carboxylic acids (General Procedure A)

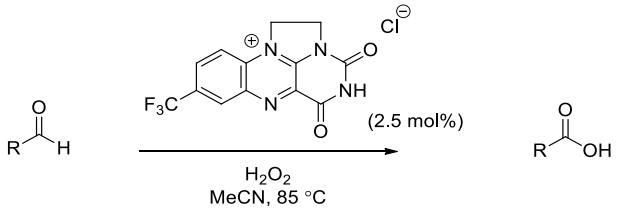

Hydrogen peroxide solution (35% w/w) was added to a mixture of aldehyde (0.75 mmol) and catalyst **58** (6 mg, 0.019 mmol, 2.5 mol %) in acetonitrile (1 mL). The mixture was stirred for 18 h in a sealed tube at 85 ^{o}C. Upon cooling, saturated aqueous $NaHCO_3$ (5 mL) was added followed by CH_2Cl_2 (5 mL). The mixture was separated and the aqueous layer acidified (pH ≈ 5) with conc. HCl. The organics were then extracted three times with CH_2Cl_2 or EtOAc (3 x 5 mL). The combined organic extracts were dried over $MgSO_4$ and solvent removed *in vacuo*. No further purification was required unless otherwise stated.

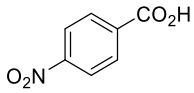

4-Nitrobenzoic acid (42b)

Following general procedure A using 4-nitrobenzaldehyde **42c** (115 mg) with 35% aqueous H_2O_2 (82.5 µL, 1.125 mmol) gave 4-nitrobenzoic acid **43c** (112 mg, 89%) as a yellow solid. Final extraction with EtOAc.

^{1}H NMR (400 MHz, d_6-DMSO) δ_H 8.29 (d, J = 8.0 Hz, 2H), 8.14 (d, J = 8.0 Hz, 2H); ^{13}C NMR (100 MHz, $CDCl_3$) δ_C 165.8, 150.0, 136.4, 130.7, 123.7. Data in accordance with the literature.[223]

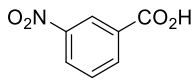

3-Nitrobenzoic acid (42d)

Following general procedure A using: 3-nitrobenzaldehyde **42d** (115 mg) with 35% aqueous H_2O_2 (82.5 µL, 1.125 mmol) gave 3-Nitrobenzoic acid **43d** (102 mg, 80%) as a yellow solid. Final extraction with EtOAc.

^{1}H NMR (400 MHz, $CDCl_3$) δ_H 10.63 (br s, 1H), 8.95 (app. td, *J* = 1.3, 0.5 Hz, 1H), 8.49 (ddd, 7.8, 1.3, 0.5 Hz, 1H), 8.45 (app. dt, *J* = 7.8, 1.3 Hz, 1H) 7.73 (app. t, *J* = 7.8 Hz, 1H); ^{13}C NMR (100 MHz, $CDCl_3$) δ_C 170.2, 148.6, 135.9, 131.0, 130.1, 128.5, 125.4. Data in accordance with the literature.[223]

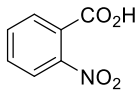

2-Nitrobenzoic acid (42e)

Following general procedure A using: 2-nitrobenzaldehyde **42e** (115 mg) with 35% aqueous H_2O_2 (82.5 µL, 1.125 mmol) gave 2-nitrobenzoic acid **43e** (113 mg, 90%) as a yellow solid. Final extraction with EtOAc.

^{1}H NMR (500 MHz, d_6-DMSO) δ_H 14.00 (br s, 1H), 7.95 (d, *J* = 8.8 Hz, 1H), 7.85 (d, *J* = 8.8 Hz, 1H), 7.75 (app. quin., *J* = 8.8 Hz, 2H); ^{13}C NMR (125 MHz, d_6 – DMSO) δ_C 166.1, 148.5, 133.2, 132.5, 130.0, 127.4, 123.8. Data in accordance with the literature.[223]

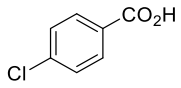

4-Chlorobenzoic acid (42f)

Following general procedure A using: 4-chlorobenzaldehyde **42f** (105 mg) with 35% aqueous H_2O_2 (270 µL, 3.75 mmol) gave 4-chlorobenzoic acid **43f** (110 mg, 94%) as a white solid. Final extraction with EtOAc.

^{1}H NMR (500 MHz, d_6-DMSO) δ_H 13.45 (br s, 1H), 7.93 (d, *J* = 8.5 Hz, 2H), 7.52 (d, *J* = 8.5 Hz, 2H); ^{13}C NMR (125 MHz, d_6-DMSO) δ=166.5, 137.8, 131.2, 129.7, 128.7. Data in accordance with the literature.[224]

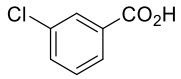

3-Chlorobenzoic acid (42g)

Following general procedure A using: 3-chlorobenzaldehyde **42g** (85 µL) with 35% aqueous H_2O_2 (270 µL, 3.75 mmol) gave 3-chlorobenzoic acid **43g** (110 mg, 94%) as a white solid. Final extraction with EtOAc.

^{1}H NMR (500 MHz, $CDCl_3$) δ_H 8.10 (app. t, *J* =1.8 Hz, 1H), 8.01 (app. dt, *J* = 7.9, 1.2 Hz, 1H), 7.60 (ddd, *J* = 7.9, 1.8, 1.2 Hz, 1H), 7.43 (t, *J* = 7.9 Hz, 1H); ^{13}C NMR (125 MHz, $CDCl_3$) δ_C 171.0, 134.9, 134.1, 131.1, 130.4, 130.0, 128.5. Data in accordance with the literature.[225]

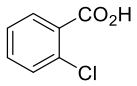

2-Chlorobenzoic acid (42h)

Following general procedure A using: 2-chlorobenzaldehyde **42hf** (84 µL) with 35% aqueous H_2O_2 (270 µL, 3.75 mmol) gave 2-chlorobenzoic acid **43h** (109 mg, 91%) as a white solid. Final extraction with EtOAc.

^{1}H NMR (500 MHz, $CDCl_3$) δ_H 8.05 – 8.02 (m, 1H), 7.49 (m, 2H), 7.38 – 7.34 (m, 1H); ^{13}C NMR (125 MHz, $CDCl_3$) δ_C 171,0, 134.9, 133.8, 132.7, 131.7, 128.6, 126.9. Data in accordance with the literature.[226]

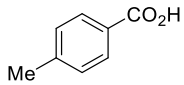

4-Methylbenzoic acid (42i)

Following general procedure A using: 4-tolualdehyde **42i** (89 µL) with 35% aqueous H_2O_2 (270 µL, 3.75 mmol) gave 4-methylbenzoic acid **43i** (78 mg, 77%) as a white solid. Final extraction with CH_2Cl_2.

^{1}H NMR (400 MHz, $CDCl_3$) δ_H 8.01 (d, *J* = 8.1 Hz, 2H), 7.28 (d, *J* = 8.1 Hz, 2H), 2.44 (s, 3H); ^{13}C NMR (100 MHz, $CDCl_3$) δ_C 172.4, 144.8, 130.4, 129.3, 126.7, 21.9. Data in accordance with the literature.[224]

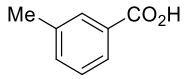

3-Methylbenzoic acid (42j)

Following general procedure A using: 3-tolualdehyde **42j** (88 µL) with 35% aqueous H_2O_2 (270 µL, 3.75 mmol) gave 3-methylbenzoic acid **43j** (92 mg, 90%) as a white solid. Final extraction with CH_2Cl_2.

^{1}H NMR (500 MHz, $CDCl_3$) δ_H 7.96 – 7.91 (m, 2H), 7.60 (d, *J* = 7.6 Hz, 1H), 7.37 (app. t, *J* = 7.6 Hz, 1H), 2.43 (s, 3H); ^{13}C NMR (125 MHz, $CDCl_3$) δ_C 172.5, 138.5, 134.8, 130.9, 129.4, 128.5, 127.5, 21.4. Data in accordance with the literature.[227]

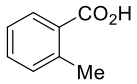

2-Methylbenzoic acid (42k)

Following general procedure A using: 2-tolualdehyde **42k** (88 µL) with 35% aqueous H_2O_2 (270 µL, 3.75 mmol) gave 2-methylbenzoic acid **43k** (65 mg, 64%) as a white solid. Final extraction with CH_2Cl_2.

^{1}H NMR (400 MHz, $CDCl_3$) δ_H 8.09 (dd, *J* = 7.7, 1.4 Hz, 1H), 7.46 (app. td, *J* = 7.7, 1.4 Hz, 1H), 7.3 (app. t, *J* = 7.7 Hz, 2H), 2.68 (s, 3H); ^{13}C NMR (100 MHz, $CDCl_3$) δ_C 173.5, 141.5, 133.1, 132.1, 131.7, 128.5, 126.0, 22.3. Data in accordance with the literature.[224]

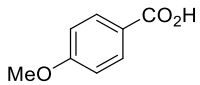

4-Methoxybenzoic acid (42b)

Following general procedure A using: 4-methoxybenzaldehyde **42b** (90 µL) with 35% aqueous H_2O_2 (270 µL, 3.75 mmol) gave 4-methoxybenzoic acid **43b** (26 mg, 23%) as a white solid. Final extraction with CH_2Cl_2.

^{1}H NMR (500 MHz, $CDCl_3$) δ_H 8.07 (d, *J* = 8.9 Hz, 2H), 6.95 (d, *J* = 8.9 Hz, 2H), 3.88 (s, 2H); ^{13}C NMR (125 MHz, $CDCl_3$) δ_C 171.7, 164.2, 132.5, 121.8, 113.9, 55.6. Data in accordance with the literature.[225]

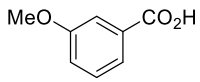

3-Methoxybenzoic acid (42l)

Following general procedure A using: 3-methoxybenzaldehyde **42l** (80 µL) with 35% aqueous H_2O_2 (270 µL, 3.75 mmol) gave 3-methoxybenzoic acid **43l** (42 mg, 37%) as a white solid. Final extraction with CH_2Cl_2.

^{1}H NMR (500 MHz, $CDCl_3$) δ_H 7.73 (app. dt, *J* = 7.6, 1.2 Hz, 1H) 7.63 (dd, *J* = 2.6, 1.2 Hz, 1H), 7.39 (app. t, *J* = 8.0 Hz, 1H), 7.17 (ddd, *J* = 8.3, 2.6, 1.2 Hz, 1H), 3.87 (s, 3H); ^{13}C NMR (125 MHz, $CDCl_3$) δ_C 172.1, 159.8, 130.7, 130.0, 122.9, 120.7, 114.6, 55.6. Data in accordance with the literature.[223]

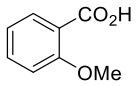

2-Methoxybenzoic acid (42m)

Following general procedure A using: 2-methoxybenzaldehyde **42m** (90 µL) with 35% aqueous H_2O_2 (270 µL, 3.75 mmol) gave 2-methoxybenzoic acid **43m** (61 mg, 53%) as a white solid. Final extraction with CH_2Cl_2.

^{1}H NMR (500 MHz, $CDCl_3$) δ_H 8.17 (dd, *J* = 7.7, 1.8 Hz, 1H), 7.58 (ddd, *J* = 8.4, 7.7, 1.8 Hz, 1H), 7.14 (app. td, *J* = 7.7, 0.9 Hz, 1H), 7.06 (d, *J* = 8.4 Hz, 1H), 4.08 (s, 3H); ^{13}C NMR (125 MHz, $CDCl_3$) δ_C 165.7, 158.2, 135.2, 133.9, 122.3, 117.7, 111.8, 56.8. Data in accordance with the literature.[223]

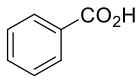

Benzoic acid (42a)

Following general procedure A using: benzaldehyde **42a** (75 µL) with 35% aqueous H_2O_2 (270 µL, 3.75 mmol) gave benzoic acid **43a** (65 mg, 73%) as a white solid. Final extraction with CH_2Cl_2.

^{1}H NMR (500 MHz, $CDCl_3$) δ_H 8.12 (dd, *J* = 8.0, 1.4 Hz, 2H), 7.62 (tt, *J* = 7.6, 1.4 Hz, 1H), 7.48 (app. t, *J* = 7.8 Hz, 2H); ^{13}C NMR (125 MHz, $CDCl_3$) δ_C 172.0, 134.0, 130.4, 129.4, 128.7. Data in accordance with the literature.[224]

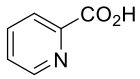

Picolinic acid (42n)

Following general procedure A using: pyridine-2-carboxaldehyde **42n** (80 mg) with 35% aqueous H_2O_2 (82.5 µL, 1.125 mmol) followed by concentration of residue *in vacuo*, suspension in diethyl ether (2 mL) and vacuum filtration gave picolinic acid **43n** (83 mg, 90%) as a light brown solid.

^{1}H NMR (500 MHz, d_6-DMSO) δ_H 8.70 (ddd, J = 4.7, 1.6, 1.0 Hz, 1H), 8.04 (app. dt, J = 7.7, 1.0 Hz, 1H), 7.97 (app. dt, J = 4.2, 1.3 Hz, 1H), 7.62 (ddd, J = 7.7, 4.2, 1.3 Hz, 1H); ^{13}C NMR (125 MHz, d_6-DMSO) δ_C 166.6, 149.9, 138.0, 148.8, 127.6, 125.1. Data in accordance with the literature.[225]

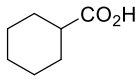

Cyclohexane carboxylic acid (146a)

Following general procedure A using: cyclohexane-carboxaldehyde **145a** (90 µL) with 35% aqueous H_2O_2 (82.5 µL, 1.125 mmol) gave cyclohexane-carboxylic acid **146a** (103 mg, 99%) as an oil. Final extraction with CH_2Cl_2.

^{1}H NMR (400 MHz, $CDCl_3$, rotamers) δ_H 11.30 (br s, 1H), 2.37 – 2.28 (m, 1H), 1.98 – 1.89 (m, 2H), 1.80 – 1.72 (m, 2H), 1.67 – 1.60 (m, 2H), 1.50 – 1.39 (m, 2H), 1.35 – 1.16 (m, 3H); ^{13}C NMR (100 MHz, $CDCl_3$, rotamers) δ_C 182.9, 43.1, 28.9, 25.8, 25.4. Data in accordance with the literature.[228]

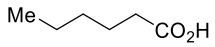

Hexanoic acid (146b)

Following general procedure A using: hexanal **145b** (92 µL) with 35% aqueous H_2O_2 (82.5 µL, 1.125 mmol) gave hexanoic acid **146b** (75 mg, 86%) as an oil. Final extraction with CH_2Cl_2.

^{1}H NMR (400 MHz, $CDCl_3$) δ_H 2.35 (t, J = 7.6 Hz, 2H), 1.64 (app. quin., J = 7.6 Hz, 2H), 1.36 – 1.29 (m, 4H), 0.90 (m, 3H); ^{13}C NMR (100 MHz, $CDCl_3$) δ_C 180.2, 34.2, 31.4, 24.5, 22.4, 14.0. Data in accordance with the literature.[229]

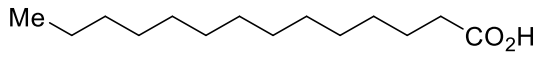

1-Tetradecanoic acid (146c)

Following general procedure A using: 1-tetradecanal **145c** (159 mg) with 35% aqueous H_2O_2 (82.5 µL, 1.125 mmol) followed by concentration of the residue *in vacuo*, then column chromatography (silica gel, 9:1 40/60 petroleum ether:EtOAc, R_f = 0.4) gave 1-tetradecanoic acid **146c** (120 mg, 70%) as a white solid.

^{1}H NMR (500 MHz, $CDCl_3$) δ_H 2.34 (t, *J* = 7.6 Hz, 2H), 1.63 (app. quin., *J* = 7.6 Hz, 2H), 1.39-1.20 (m, 20H), 0.88 (m, 3H); ^{13}C NMR (125 MHz, $CDCl_3$), δ_C 180.5, 34.2, 32.1, 29.8, 29.8, 29.8, 29.7, 29.6, 29.5, 29.4, 29.2, 24.8, 22.8, 14.2. Data in accordance with the literature.[230]

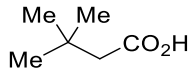

3,3-Dimethylbutanoic acid (146d)

Following general procedure A using: 3,3-dimethylbutyraldehyde **145d** (94 µL) with 35% aqueous H_2O_2 (82.5 µL, 1.125 mmol) gave 3,3-dimethylbutanoic acid **146d** (85 mg, 98%) as an oil. Final extraction with CH_2Cl_2.

^{1}H NMR (400 MHz, $CDCl_3$) δ_H 2.23 (s, 2H), 1.06 (s, 9H); ^{13}C NMR (100 MHz, $CDCl_3$) δ_C 179.3, 47.9, 30.7, 29.7. Data in accordance with the literature.[231]

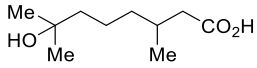

7-Hydroxycitronellic acid (146e)

Following general procedure A using: 7-hydroxycitronellal **145e** (92 µL) with 35% aqueous H_2O_2 (82.5 µL, 1.125 mmol) gave 7-hydroxycitronellic acid **146e** (111 mg, 85%) as an oil. Final extraction with CH_2Cl_2.

^{1}H NMR (500 MHz, $CDCl_3$) δ_H 2.35 (dd, *J* = 15.0, 6.7 Hz, 1H), 2.17 (dd, *J* = 15.0, 6.7 Hz, 1H), 1.99 (app. sex., *J* = 6.7 Hz, 1H), 1.51 – 1.29 (m, 6H), 1.22 (s, 6H), 0.98 (d, *J* = 6.7 Hz, 3H); ^{13}C NMR (125 MHz, $CDCl_3$) δ_C 177.7, 71.2, 44.0, 41.4, 37.2, 30.3, 29.5, 29.3, 21.8, 19.9.[232]

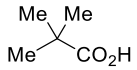

Pivalic acid (146f)

Following general procedure A using: pivaldehyde **145f** (80 µL) with 35% aqueous H_2O_2 (82.5 µL, 1.125 mmol) gave pivalic acid **146f** (46 mg, 60%) as an oil. Final extraction with CH_2Cl_2.

^{1}H NMR (500 MHz, $CDCl_3$) δ_H 1.23 (s, 9H); ^{13}C NMR (125 MHz, $CDCl_3$) δ_C 185.2, 38.7, 27.1. Data in accordance with the literature.[233]

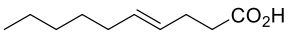

***E*-4-decenoic acid (146g)**

Following general procedure A using: *E*-4-decenal **145g** (140 µL) with 35% aqueous H_2O_2 (82.5 µL, 1.125 mmol) gave *E*-4-decenoic acid **146g** (81 mg, 64%) as an oil. Final extraction with CH_2Cl_2.

^{1}H NMR (400 MHz, $CDCl_3$) δ_H 5.53 – 5.36 (m, 2H), 2.44 – 2.38 (m, 2H), 2.35 – 2.27 (m, 2H), 1.97 (m, 2H), 1.37 – 1.20 (m, 6H), 0.88 (m, 3H); ^{13}C NMR (100 MHz, $CDCl_3$) δ_C 179.3, 132.3, 127.6, 34.2, 32.6, 31.5, 29.2, 27.7, 22.6, 14.2. Data in accordance with the literature.[234]

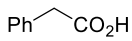

Phenylacetic acid (146h)

Following general procedure A using: phenylacetaldehyde **145h** (88 µL) with 82.5 µL 35% aqueous H_2O_2 (1.125 mmol) gave phenylacetic acid **146h** (56 mg, 55%) as a white solid. Final extraction with CH_2Cl_2.

^{1}H NMR (500 MHz, $CDCl_3$) δ_H 12.17 (br s, 1H), 7.46–7.34 (m, 5H), 3.73 (s, 2H); ^{13}C NMR (125 MHz, $CDCl_3$) δ_C 178.5, 133.3, 129.4, 128.7, 127.4, 41.1. Data in accordance with the literature.[235]

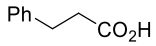

Hydrocinnamic acid (146i)

Following general procedure A using: hydrocinnamaldehyde **145i** (100 µL) with 35% aqueous H_2O_2 (82.5 µL, 1.125 mmol) gave hydrocinnamic acid **146i** (48 mg, 42%) as a semi solid. Final extraction with CH_2Cl_2.

^{1}H NMR (500 MHz, $CDCl_3$) δ_H 7.33 -7.20 (m, 5H), 2.98 (t, *J* = 7.8 Hz, 2H), 2.70 (t, *J* = 7.8 Hz, 2H); ^{13}C NMR (125 MHz, $CDCl_3$) δ_C 179.2, 140.3, 128.7, 128.4, 126.5, 35.7, 30.7. Data in accordance with the literature.[228]

General Procedure for flavinium/alloxan-catalysed oxidative dimerisation of aromatic amines (General Procedure B)

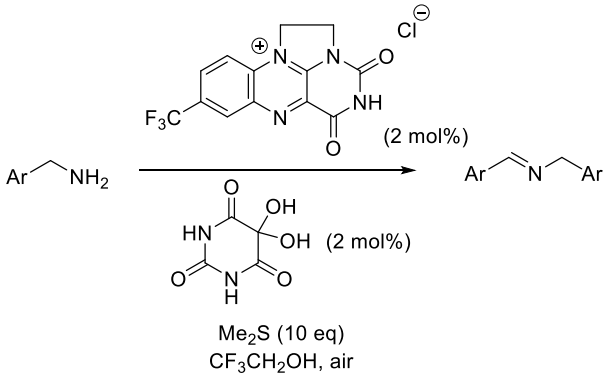

Dimethyl sulfide (0.37 mL, 5 mmol) was added to a mixture of flavin catalyst **58** (1.7 mg, 5 µmol, 1 mol%) and alloxan monohydrate **138a** (0.8 mg, 5 µmol, 1 mol%) in 2,2,2-trifluoroethanol (1 mL). The solution was stirred under air for 10 minutes, then amine (0.5 mmol) was added dropwise by syringe and stirred under air for 2 h, after which time a further 1 mol% **58** and 1 mol% **138a** were added. After reaction was complete, the solvent was removed *in vacuo*, and the crude imine was purified by washing through a small pad of base-washed silica (1:2 petrol:EtOAc + 2% Et_3N).

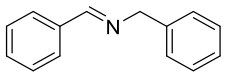

N-benzylidene-1-phenylmethanamine (154a)

Following General Procedure B using benzylamine **15a** (55 µL) for 5 h gave N-benzylidene-1-phenylmethanamine **134a** as an oil (46 mg, 94%).

^{1}H NMR (300 MHz, $CDCl_3$) δ_H 8.41 (s, 1H), 7.84 – 7.76 (m, 2H), 7.49 – 7.21 (m, 8H), 4.84 (s, 2H); ^{13}C NMR (75 MHz, $CDCl_3$) δ_C 162.1, 139.4, 136.3, 130.9, 128.7, 128.6, 128.4, 128.1, 127.1, 65.2. IR ν_{max} (neat) 3365, 3283, 3062, 3029, 1643, 1451 cm^{-1}. HRMS (ESI, +ve) *m/z* calcd. for $C_{14}H_{13}N$ 196.1133, found: 196.1126 $(M+H)^+$. Data in accordance with the literature.[116]

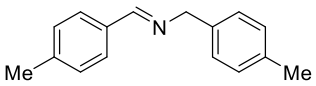

N-(4-methylbenzylidene)-1-(p-tolyl)methanamine (154c)

Following General Procedure B using 4-methylbenzylamine **15c** (64 µL) for 5 h gave N-(4-methylbenzylidene)-1-(p-tolyl)methanamine **154c** as a white solid (55 mg, 99%). ^{1}H NMR (300 MHz, $CDCl_3$) δ_H 8.24 (s, 1H), 7.57 (d, 2H, J=8.1), 7.16-7.01 (m, 6H), 4.67 (s, 2H), 2.28 (s, 3H), 2.24 (s, 3H); ^{13}C NMR (75 MHz, $CDCl_3$) δ_C 161.8, 141.1, 136.6, 136.4, 133.7, 129.4, 129.2, 128.3, 128.0, 64.9, 21.6, 21.2. IR ν_{max} 2918, 2854, 1638, 1513, 795 cm^{-1}. HRMS (ESI, +ve) *m/z* calcd. for $C_{16}H_{17}N$ 224.1439, found: 224.1456 $(M+H)^+$. Data in accordance with the literature.[116]

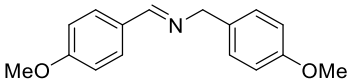

N-(4-methoxybenzylidene)-1-(4-methoxyphenyl)methanamine (154b)

Following General Procedure B using 4-methoxybenzylamine **15b** (65 µL) for 5 h gave N-(4-methoxybenzylidene)-1-(4-methoxyphenyl)methanamine **154b** as an oil (61 mg, 95%). ^{1}H NMR (300 MHz, $CDCl_3$) δ_H 8.20 (s, 1H), 7.62 (d, 2H, J=8.6), 7.16 (d, 2H, J=8.7), 6.86-6.75 (m, 4H), 4.64 (s, 2H), 3.74 (s, 3H), 3.70 (s, 3H); ^{13}C NMR (75 MHz, $CDCl_3$) δ_C 161.7, 161.0, 158.7, 131.7, 129.9, 129.2, 129.2, 114.0, 113.9, 64.5, 55.4, 55.3. IR ν_{max} (neat) 3353, 2952, 1653, 1602, 1557, 1514, 1259 cm^{-1}. HRMS (ESI, +ve) *m/z* calcd. for $C_{16}H_{17}NO_2$ 256.1346, found: 256.1338 $(M+H)^+$. Data in accordance with the literature.[116]

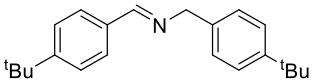

N-(4-(tert-butyl)benzylidene)-1-(4-(tert-butyl)phenyl)methanamine (154d)

Following General Procedure B using (4-(tert-butyl)phenyl)methanamine **15d** (88 µL) for 5 h gave N-(4-(tert-butyl)benzylidene)-1-(4-(tert-butyl)phenyl)methanamine **154d** as an oil (71 mg, 92%). ^{1}H NMR (300 MHz, $CDCl_3$) δ_H 8.29(s, 1H), 7.64 (d, 2H, J=8.7), 7.38 – 7.15 (m, 6H), 4.70 (s, 2H), 1.25 (s, 9H), 1.23 (s, 9H). ^{13}C NMR (75 MHz, $CDCl_3$) δ_C 161.8, 154.2, 149.9, 136.6, 133.7, 128.2, 127.8, 125.7, 125.5, 65.0, 35.0, 34.6, 31.5, 31.4. IR ν_{max} (neat) 2962, 1643, 836 cm^{-1}. HRMS (ESI, +ve) *m/z* calcd. for $C_{22}H_{29}NNa$ 330.2198, found: 330.2198. Data in accordance with the literature.[116]

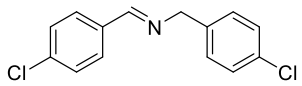

N-(4-chlorobenzylidene)-1-(4-chlorophenyl)methanamine (154e)

Following General Procedure B using 4-chlorobenzylamine **15e** (61 µL) for 18 h gave N-(4-chlorobenzylidene)-1-(4-chlorophenyl)methanamine **154e** as a white powder (51 mg, 77%). ^{1}H NMR (300 MHz, $CDCl_3$) δ_H 8.27 (s, 1H), 7.64 (d, 2H, J=8.6), 7.31 (d, 2H, J=8.5), 7.27 - 7.16 (m, 4H), 4.69 (s, 2H), ^{13}C NMR (75 MHz, $CDCl_3$) δ_C 161.0, 137.7, 137.0, 134.5, 132.9, 129.6, 129.4, 129.1, 128.8, 64.3. IR ν_{max} 2860, 1642, 1593, 1489, 1092 cm^{-1}. HRMS (ESI, +ve) *m/z* calcd. for $C_{14}H_{11}NCl_2$ 264.0340, found: 264.0347 $(M+H)^+$. Data in accordance with the literature.[116]

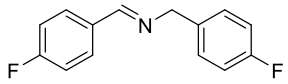

N-(4-fluorobenzylidene)-1-(4-fluorophenyl)methanamine (154f)

Following General Procedure B using 4-fluorobenzylamine **15f** (57 µL) for 18 h gave N-(4-chlorobenzylidene)-1-(4-chlorophenyl)methanamine **154f** as an oil (57 mg, 98%). ^{1}H NMR (300 MHz, $CDCl_3$) δ_H 8.26 (s, 1H), 7.73 - 7.64 (m, 2H), 7.26 - 7.15 (m, 2H), 7.07 - 6.88 (m, 4H), 4.68 (s, 2H), ^{13}C NMR (75 MHz, $CDCl_3$) δ_C 166.2, 163.7, 162.8, 160.7, 160.5, 135.0 (d, $J_{C,F}$ = 3.2 Hz), 132.4 (d, $J_{C,F}$ = 3.2 Hz), 130.3 (d, $J_{C,F}$ = 8.8 Hz), 129.6 (d, $J_{C,F}$ = 8.8 Hz), 115.8 (d, $J_{C,F}$ = 22.2 Hz), 115.4 (d, $J_{C,F}$ = 22.2 Hz), 64.3. ^{19}F NMR (469 MHz, $CDCl_3$) δ_F -109.2 - -109.3 (m), -115.9 - -116.0 (m). IR ν_{max} 3041, 2843, 1647, 1601, 1507, 1219 cm^{-1}. HRMS (ESI, +ve) *m/z* calcd. for $C_{14}H_{12}F_2N$ 232.0938, found: 232.0953 $(M+H^+)$. Data in accordance with the literature.[116]

.

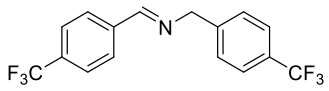

N-(4-(trifluoromethyl)benzylidene)-1-(4-(trifluoromethyl)phenyl)methanamine (154g)

Following General Procedure B using 4-(trifluoromethyl)benzylamine **15g** (71 µL) for 18 h with 4% alloxan and 4% flavin gave N-(4-(trifluoromethyl)benzylidene)-1-(4-(trifluoromethyl)phenyl)methanamine **154g** as an oil (31 mg, 37%). ^{1}H NMR (300 MHz, $CDCl_3$) δ_H 8.47 (s, 1H), 7.91 (d, 2H, J=8.1 Hz), 7.74 – 7.55 (m, 4h), 7.47 (d, 2H, J=8.1 Hz) 4.90 (s, 2H), ^{13}C NMR (75 MHz, $CDCl_3$) δ_C 161.3, 143.0, 139.0, 132.9, 132.5, 128.7, 128.6, 125.8 (q, JC,F = 3.9 Hz), 125.6 (q, JC,F = 3.9 Hz), 122.5, 64.6. ^{19}F NMR (469 MHz, $CDCl_3$) δ_F -62.4 (s), -62.8 (s). IR ν_{max} (neat) 2928, 1651, 1323, 1123, 1065 cm^{-1}. HRMS (ESI, +ve) *m/z* calcd. for $C_{16}H_{11}NF_6$ 332.0895, found: 332.0874 $(M+H)^+$. Data in accordance with the literature.[116]

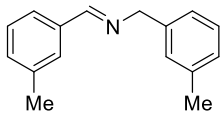

N-(3-methylbenzylidene)-1-(m-tolyl)methanamine (154h)

Following General Procedure B using 3-methylbenzylamine **15h** (63 µL) for 5 h gave N-(3-methylbenzylidene)-1-(m-tolyl)methanamine **154h** as an oil (51 mg, 91%). ^{1}H NMR (300 MHz, $CDCl_3$) δ_H 8.26 (s, 1H), 7.56 (s, 1H), 7.50 – 7.40 (m, 1H), 7.26 – 7.08 (m, 3H), 7.08 – 6.94 (m, 3H), 4.69 (s, 2H), 2.28 (s, 3H), 2.25 (s, 3H), ^{13}C NMR (75 MHz, $CDCl_3$) δ_C 162.2, 139.2, 138.4, 138.2, 136.2, 131.7, 128.8, 128.5, 128.5, 127.8, 126.0, 125.2, 65.2. IR ν_{max} (neat) 3024, 2919, 1644 cm^{-1}. HRMS (ESI, +ve) *m/z* calcd. for $C_{16}H_{17}N$ 224.1439, found: 224.1430 $(M+H)^+$. Data in accordance with the literature.[117]

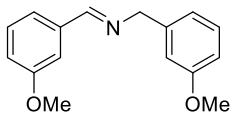

N-(3-methoxybenzylidene)-1-(3-methoxyphenyl)methanamine (154i)

Following General Procedure B using 3-methoxybenzylamine **15i** (64 µL) for 5 h gave N-(3-methoxybenzylidene)-1-(3-methoxyphenyl)methanamine **154i** as an oil (46 mg, 72%). ^{1}H NMR (400 MHz, $CDCl_3$) δ_H 8.4 (s, 1H), 7.49 – 7.43 (m, 1H), 7.42 – 7.28 (m, 3H), 7.10 – 6.83 (m, 4H), 4.86 (s, 2H), 3.90 (s, 3H), 3.87 (s, 3H), ^{13}C NMR (100 MHz, $CDCl_3$) δ_C 162.2, 160.0, 159.9, 140.9, 137.7, 129.7, 129.6, 121.8, 120.4, 117.7, 113.8, 112.6, 111.8, 65.0, 55.5, 55.3. IR ν_{max} (neat) 2936, 2835, 1643, 1599, 1583, 1261, 1038 cm^{-1}. HRMS (ESI, +ve) *m/z* calcd. for $C_{16}H_{17}NO_2Na$ 278.1157, found: 278.1135 ($M+Na^+$). Data in accordance with the literature.[117]

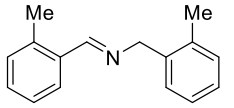

N-(2-methylbenzylidene)-1-(o-tolyl)methanamine (154j)

Following General Procedure B using 2-methylbenzylamine **15j** (62 µL) for 5 h gave N-(3-methoxybenzylidene)-1-(3-methoxyphenyl)methanamine **154j** as an oil (53 mg, 96%). ^{1}H NMR (300 MHz, $CDCl_3$) δ_H 8.58 (s, 1H), 7.88 – 7.81 (m, 1H), 7.26 – 7.06 (m, 7H), 4.74 (s, 2H), 2.42 (s, 3H), 2.31 (s, 3H), ^{13}C NMR (75 MHz, $CDCl_3$) δ_C 160.7, 137.8, 137.7, 136.2, 134.3, 130.9, 130.4, 130.2, 128.4, 127.8, 127.1, 126.3, 126.2, 63.4, 19.5, 19.4. IR ν_{max} (neat) 2962, 1643, 1461, 742 cm^{-1}. HRMS (ESI, +ve) *m/z* calcd. for $C_{16}H_{17}N$ 224.1439, found: 224.1457 $(M+H)^+$. Data in accordance with the literature.[116]

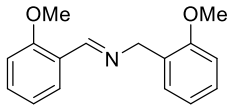

N-(2-methoxybenzylidene)-1-(2-methoxyphenyl)methanamine (154k)

Following General Procedure B using 2-methoxybenzylamine **15k** (65 µL) for 5 h gave N-(2-methoxybenzylidene)-1-(2-methoxyphenyl)methanamine **154k** as an oil (43 mg, 68%). ^{1}H NMR (300 MHz, $CDCl_3$) δ_H 8.76 (s, 1H), 7.95 (dd, *J* = 7.7, 1.8 Hz, 1H), 7.36 – 7.07 (m, 3H), 6.99 – 6.72 (m, 4H), 4.75 (s, 2H), 3.77 (s, 3H), 3.75 (s, 3H), ^{13}C NMR (75 MHz, $CDCl_3$) δ_C 158.9, 158.4, 157.1, 131.9, 129.2, 128.2, 128.0, 127.6, 124.9, 120.8, 120.6, 111.1, 110.2, 59.8, 55.6, 55.4. IR ν_{max} 2938, 1635, 1599, 1487, 1241 cm^{-1}. HRMS (ESI, +ve) *m/z* calcd. for $C_{16}H_{17}NO_2$ 256.1338, found: 256.1358 $(M+H)^+$. Data in accordance with the literature.[116]

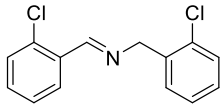

N-(2-chlorobenzylidene)-1-(2-chlorophenyl)methanamine (154l)

Following General Procedure B using 2-chlorobenzylamine **15l** (60 µL) for 18 h gave N-(2-chlorobenzylidene)-1-(2-chlorophenyl)methanamine **154l** as a white powder (44 mg, 66%). ^{1}H NMR (300 MHz, $CDCl_3$) δ_H 8.79 (s, 1H), 8.06-8.00 (m, 2H) 7.37-7.08 (m, 6H), 4.86 (s, 2H), ^{13}C NMR (75 MHz, $CDCl_3$) δ_c 159.9, 136.9, 135.3 133.5, 133.2, 131.8, 129.9, 129.8, 129.4, 128.6, 128.4, 127.1, 127.0, 62.3. IR ν_{max} 3067, 2893, 1638, 1442, 1051, 749 cm^{-1}; . HRMS (ESI, +ve) *m/z* calcd. for $C_{14}H_{12}Cl_2N$ 264.0347, found: 264.0349 $(M+H)^+$. Data in accordance with the literature.[117]

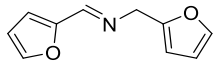

1-(furan-2-yl)-N-(furan-2-ylmethylene)methanamine (154m)

Following General Procedure B using furfurylamine **15m** (44 µL) for 18 h gave N-(2-chlorobenzylidene)-1-(2-chlorophenyl)methanamine **154m** as an oil (31 mg, 70%). ^{1}H NMR (300 MHz, $CDCl_3$) δ_H 8.12 (s, 1H), 7.52 (d, 1H, J = 1.6), 7.38 (q, 1H, J = 1.0), 6.78 (d, 1H, J = 3.4), 6.47 (q, 1H, J = 1.7), 6.34 (q, 1H, J = 1.3), 6.28 (dd, 1H, J_1 = 0.6, J_2 = 3.2), 4.75 (s, 2H); ^{13}C NMR (75 MHz, $CDCl_3$) δ_C 151.8, 151.34, 151.2, 145.0, 142.3, 114.6, 111.7, 110.4, 107.9, 56.9. IR ν_{max} (neat) 1674, 1499, 1246 cm^{-1}; . HRMS (ESI, +ve) *m/z* calcd. for $C_{10}H_9NO_2Na$ 198.0530, found: 198.0533 $(M+Na)^+$. Data in accordance with the literature.[116]

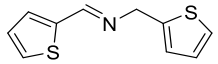

1-(thiophen-2-yl)-N-(thiophen-2-ylmethylene)methanamine (154n)

Following General Procedure B using 2-thiophenemethylamine **15n** (51 µL) for 5 h gave 1-(thiophen-2-yl)-N-(thiophen-2-ylmethylene)methanamine **154n** as an oil (45 mg, 87%). ^{1}H NMR (300 MHz, $CDCl_3$) δ_H 8.42 (s, 1H), 7.42 (dt, *J* = 4.8, 1.0 Hz, 1H), 7.33 (dd, *J* = 3.6, 1.0 Hz, 1H), 4.8, 1.6 Hz, 1H), 7.07 (dd, *J* = 5.0, 3.6 Hz, 1H), 7.03 – 6.95 (m, 2H), 4.95 (s, 1H), ^{13}C NMR (75 Hz, $CDCl_3$) δ_C 155.5, 142.2, 141.6, 131.1, 129.5, 127.5, 127.7, 125.4, 125.0, 58.6. IR ν_{max} 3101, 2869, 1628, 1430, 695 cm^{-1}. HRMS (ESI, +ve) *m/z* calcd. for $C_{10}H_{11}S_2N$ 208.0255, found: 208.0259. Data in accordance with the literature.[118]

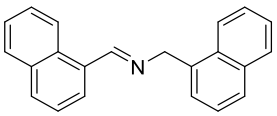

1-(naphthalen-1-yl)-N-(naphthalen-1-ylmethylene)methanamine (154o)

Following General Procedure B using 1-napthylmethylamine **15o** (73 µL) for 5 h gave 1-(naphthalen-1-yl)-N-(naphthalen-1-ylmethylene)methanamine **154o** as an oil (53 mg, 72%). ^{1}H NMR (300 MHz, $CDCl_3$) δ_H 9.09 (s, 1H), 8.96 (d, *J* = 8.1 Hz, 1H), 8.26 (d, *J* = 8.1 Hz, 1H), 8.00 – 7.77 (m, 5H), 7.63 – 7.44 (m, 7H), 5.42 (s, 2H), ^{13}C NMR (75 MHz, $CDCl_3$) δ_C 162.1, 135.6, 134.0, 133.9, 131.8, 1331.7, 131.4, 131.3, 129.3, 128.8, 128.7, 127.9, 127., 126.3, 126.2, 126.0, 125.8, 125.8, 125.4, 124.5, 124.1, 63.4. IR ν_{max} (neat) 3045, 2836, 1631, 1618, 1508 cm^{-1}. HRMS (ESI, +ve) *m/z* calcd. for $C_{22}H_{18}N$ 296.1439, found: 296.1455 $(M+H)^+$. Data in accordance with the literature.[116]

General Procedure for flavinium/alloxan-catalysed oxidative cross-coupling of aromatic amines with anilines (General Procedure C)

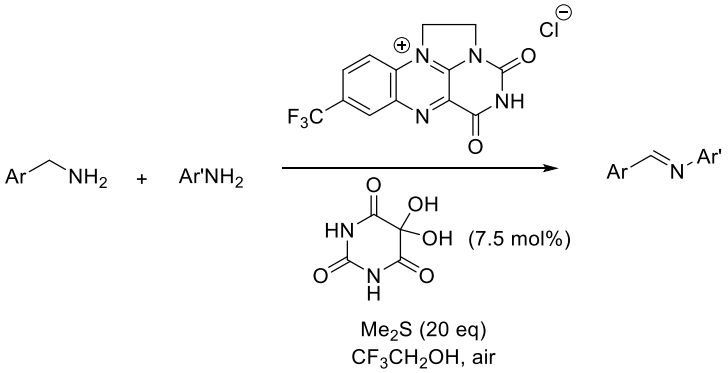

Dimethyl sulfide (0.37 mL, 5 mmol) was added to a mixture of flavin catalyst **58** (2.2 mg, 3.2 µmol, 2.5 mol%) and alloxan monohydrate **138a** (1 mg, 3.2 µmol, 2.5 mol%) in 2,2,2-trifluoroethanol (1 mL). The solution was stirred under air for 10 minutes, then aniline (0.375 mmol) was added by syringe followed by benzylic amine (0.25 mmol) were added dropwise by syringe and stirred under air, with additional 2.5 mol% **58** and 2.5 mol% **138a** added after a period of 3 h and 6 h, then stirred for an additional 18 h. After reaction was complete, the solvent was removed *in vacuo*, and the crude imine was purified by washing through a small pad of base-washed silica (1:2 petrol:EtOAc + 2% Et_3N).

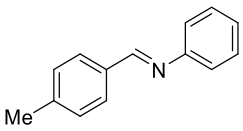

N-(4-methylbenzylidene)aniline (168b)

Following General Procedure B using aniline **164b** (34 µL) and 4-methylbenzylamine **15c** (32 µL) gave N-(4-methylbenzylidene)aniline **168b**. Yield was determined by ^{1}H NMR spectroscopy with an internal standard of 5 mol% 1,3,5-trimethoxybenzene. NMR data in square brackets is from the minor homo-coupled product **154c** at a ratio of 17:1 towards the cross-coupled product. ^{1}H NMR (300 MHz, $CDCl_3$) δ_H 8.34 (s, 1H), [8.26 (s, 0.1H)], 7.72 (d, 2H, J = 8.1), [7.59 (d, 2H, J = 8.1)], 7.36 – 7.02 (m, 7H), [6.71 – 6.88 (m, 7H)], [4.69 (s, 2H)], 2.34 (s, 3H), [2.30 (s, 3H)], [2.26 (s, 3H)]; ^{13}C NMR (75 MHz, $CDCl_3$) δ_C 161.8, 141.1, 136.6, 136.4, 133.7, [129.4], [129.2], 128.3, 128.0, 64.9, 21.6, 21.2.

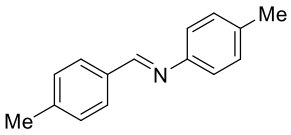

4-methyl-N-(4-methylbenzylidene)aniline (168c)

Following General Procedure B using *p*-toluidine **164c** (40 mg) and 4-methylbenzylamine **15c** (32 µL) gave 4-methyl-N-(4-methylbenzylidene)aniline **168c** as a white solid (52 mg, 99%). ^{1}H NMR (300 MHz, $CDCl_3$) δ_H 8.43 (s, 1H), 7.78 (d, 2H, J= 8.2 Hz), 7.31 – 7.08 (m, 8H), 2.42 (s, 3H), 2.37 (s, 3H). ^{13}C NMR (75 MHz, $CDCl_3$) δ_C 159.6, 149.7, 135.6, 133.8, 133.4, 132.7, 129.8, 129.5, 128.7, 120.8, 21.6, 21.0. IR ν_{max} (neat/cm^{-1}) 2879, 1624, 1512, 1168. HRMS (ESI, +ve) *m/z* calcd. for $C_{15}H_{16}N$ 210.1283, found: 210.1278 $(M+H)^+$

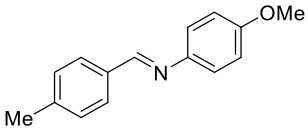

4-methoxy-N-(4-methylbenzylidene)aniline (168d)

Following General Procedure B using *p*-anisidine **164d** (46 mg) and 4-methylbenzylamine **15c** (32 µL) gave 4-methoxy-N-(4-methylbenzylidene)aniline **168d** as a brown solid (56 mg, 99%). NMR data in square brackets is from the minor homo-coupled product **154c** at a ratio of 9:1 towards the cross-coupled product. ^{1}H NMR (300 MHz, $CDCl_3$) δ_H 8.46 (s, 1H) [8.24 (s, 1H)], 7.80 (d, 2H, J = 8.1) [7.57 (d, 2H, J=8.1)], 7.31 – 7.14 (m, 6H) [7.13-7.01 (m, 6H)], [4.67 (s, 2H)], 3.83 (s, 3H), 2.43 (s, 3H) [2.28 (s, 3H)], [2.24 (s, 3H)]; ^{13}C NMR (75 MHz, $CDCl_3$) δ_C [161.8], 158.5, 158.1, 145.1, [141.1], [136.6,] [136.4],133.9, [133.7], 129.5, [129.4], [129.2], 128.6, [128.3], [128.0], 122.2, 116.4, 114.8, 114.3, 64.9, 55.7, 55.5, 21.6, [21.4], [21.2].

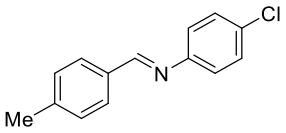

4-Chloro-N-(4-methylbenzylidene)aniline (168e)

Following General Procedure B using 4-chloroaniline **164e** (48 mg) and 4-methylbenzylamine **15c** (32 µL) gave 4-chloro-N-(4-methylbenzylidene)aniline **164e** as a white solid (47 mg, 82%). NMR data in square brackets is from the minor homo-coupled product **154c** at a ratio of 1.6:1 towards the cross-coupled product. ^{1}H NMR (300 MHz, $CDCl_3$) δ_H 8.42 (s, 1H) [8.24 (s, 1H)], 7.79 (d, 2H, J = 8.1), [7.57 (d, 2H, J=8.1)], 7.32 – 7.04 (m, 6H), [7.16-7.01 (m, 6H)], [4.67 (s, 2H)], 2.43 (s, 3H), [2.28 (s, 3H), 2.24 (s, 3H)]; ^{13}C NMR (75 MHz, $CDCl_3$) δ_C 162.8, [161.8], 160.2, 159.5, 148.2, 142.0, [141.1], [136.6], [136.4], [133.7], 133.5, 129.6, [129.4], [129.2], 128.8, [128.3], [128.0], 122.3, 116.0, 115.7, [64.9], 21.7, [21.6], [21.2].

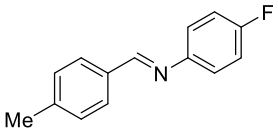

4-fluoro-N-(4-methylbenzylidene)aniline (168f)

Following General Procedure B using 4-fluoroaniline **164f** (42 mg) and 4-methylbenzylamine **15c** (32 µL) gave 4-fluoro-N-(4-methylbenzylidene)aniline **164f** as a white solid (52 mg, 98%). NMR data in square brackets is from the minor homo-coupled product **154c** at a ratio of 4:1 towards the cross-coupled product. ^{1}H NMR (300 MHz, $CDCl_3$) δ_H 8.30 (s, 1H), [8.24 (s, 1H)], 7.70 (d, 2H, J = 8.2), [7.57 (d, 2H, J=8.1)], 7.30 – 6.96 (m, 6H), [7.16-7.01 (m, 6H)], [4.67 (s, 2H)], 2.33 (s, 3H), [2.28 (s, 3H)], [2.24 (s, 3H)]; ^{13}C NMR (75 MHz, $CDCl_3$) δ_C [161.8], 160.7, 150.7, 142.1, [141.1], [136.6], [136.4], [133.7], 133.4, 130.2 (d, $J_{C,F}$ = 160.2 Hz), 129.6, [129.4], 129.3 (d, $J_{C,F}$ = 10.8 Hz), 129.2, 128.9, [128.3], 128.1 (d, $J_{C,F}$ = 22.2 Hz), 128.0, 122.2, 116.2, [64.9], 21.7, [21.6], [21.2].

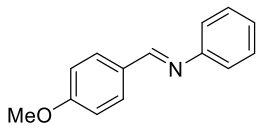

N-(4-methoxybenzylidene)-4-methylaniline (168g)

Following General Procedure B using aniline **164b** (34 µL) and 4-methoxybenzylamine **15b** (31 µL) gave 4-fluoro-N-(4-methylbenzylidene)aniline **168g** as an oil (54 mg, 96%). NMR data in square brackets is from the minor homo-coupled product **154b** at a ratio of 7:1 towards the cross-coupled product. ^{1}H NMR (300 MHz, $CDCl_3$) δ_H 8.30 (s, 1H), [8.20 (s, 1H)], 7.77 (d, 2H, J=8.9), [7.62 (d, 2H, J=8.6)], 7.30 (t, 2H, J=8.1), [7.16 (d, 2H, J=8.7)], 7.19-7.08 (m, 5H), 6.90 (d, 2H, J=8.8), [6.86-6.75 (m, 4H)], [4.64 (s, 2H)], 3.78, (s, 3H), [3.74 (s, 3H), 3.70 (s, 3H)] ^{13}C NMR (75 MHz, $CDCl_3$) δ_C 162.2, [161.0], 159.8, 152.4, 130.6, [129.8], 129.3, 129.1, 125.6, 120.9, [114.2], [113.9], 55.5, [55.3].

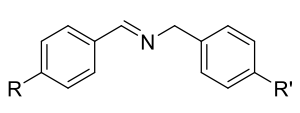

R = R' = CF_3
R = CF_3, R' = Me
R = Me, R' = CF_3
R = R' = Me

1-p-tolyl-N-(4-(trifluoromethyl)benzylidene)methanamine (171a)

N-(4-methylbenzylidene)-1-(4-(trifluoromethyl)phenyl)methanamine (171b)

Dimethyl sulfide (0.37 mL, 5 mmol) was added to a mixture of flavin catalyst **58** (3.4 mg, 5 µmol, 4 mol%) and alloxan monohydrate **138a** (1.5 mg, 5 µmol, 4 mol%) in 2,2,2-trifluoroethanol (1 mL). The solution was stirred under air for 10 minutes, then 4-methylbenzyamine **15c** (33 µL, 0.25 mmol) was added dropwise by syringe and stirred under air. After 1 h, 4-(trifluoromethyl)benzylamine **15g** was added, and after a further 1 h additional 4 mol% **58** and 4 mol% **138a** were added. The reaction was stirred for an additional 16 h. After reaction was complete, the solvent was removed *in vacuo*, and the ratio of products was determined by ^{1}H NMR spectroscopy, comparing peaks to known synthesised imines.

General Procedure for copper/alloxan-catalysed oxidative dimerisation of aromatic amines (General Procedure D)

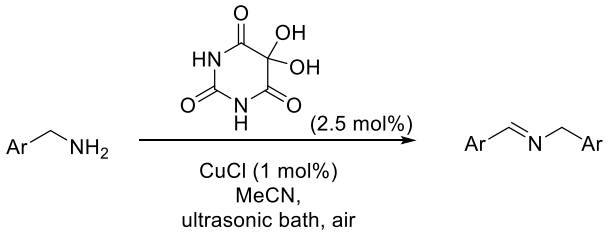

Copper (I) chloride (0.5 mg, 5 µmol, 1 mol%) and alloxan monohydrate **138a** (2 mg, 12.5 µmol, 2.5 mol%) were added to a test tube containing MeCN in an ultrasonic bath. After 5 minutes, amine (0.5 mmol) was added by syringe and the mixture was sonicated under air for 3 h. After reaction was complete, the solvent was removed *in vacuo*, and the crude imine was purified by washing through a small pad of base-washed silica (1:2 petrol:EtOAc + 2% Et_3N).

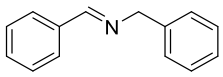

N-benzylidene-1-phenylmethanamine (154a)

Following General Procedure D using benzylamine **15a** (55 µL) gave N-benzylidene-1-phenylmethanamine **154a** as an oil (37 mg, 76%).

^{1}H NMR (300 MHz, $CDCl_3$) δ_H 8.41 (s, 1H), 7.84 – 7.76 (m, 2H), 7.49 – 7.21 (m, 8H), 4.84 (s, 2H); ^{13}C NMR (75 MHz, $CDCl_3$) δ_C 162.1, 139.4, 136.3, 130.9, 128.7, 128.6, 128.4, 128.1, 127.1, 65.2. Data in accordance with results for flavin catalysis.

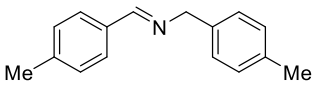

N-(4-methylbenzylidene)-1-(p-tolyl)methanamine (154c)

Following General Procedure D using 4-methylbenzylamine **15c** (64 µL) gave N-(4-methylbenzylidene)-1-(p-tolyl)methanamine **154c** as a white solid (51 mg, 91%). ^{1}H NMR (300 MHz, $CDCl_3$) δ_H 8.24 (s, 1H), 7.57 (d, 2H, J=8.1), 7.16-7.01 (m, 6H), 4.67 (s, 2H), 2.28 (s, 3H), 2.24 (s, 3H); ^{13}C NMR (75 MHz, $CDCl_3$) δ_C 161.8, 141.1, 136.6, 136.4, 133.7, 129.4, 129.2, 128.3, 128.0, 64.9, 21.6, 21.2. Data in accordance with results for flavin catalysis.

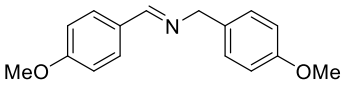

N-(4-methoxybenzylidene)-1-(4-methoxyphenyl)methanamine (15b)

Following General Procedure D using 4-methoxybenzylamine **15b** (65 µL) gave N-(4-methoxybenzylidene)-1-(4-methoxyphenyl)methanamine **154b** as an oil (63 mg, 98%). ^{1}H NMR (300 MHz, $CDCl_3$) δ_H 8.20 (s, 1H), 7.62 (d, 2H, J=8.6), 7.16 (d, 2H, J=8.7), 6.86 - 6.75 (m, 4H), 4.64 (s, 2H), 3.74 (s, 3H), 3.70 (s, 3H); ^{13}C NMR (75 MHz, $CDCl_3$) δ_C 161.7, 161.0, 158.7, 131.7, 129.9, 129.2, 129.2, 114.0, 113.9, 64.5, 55.4, 55.3. Data in accordance with results for flavin catalysis.

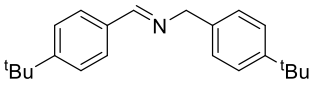

N-(4-(tert-butyl)benzylidene)-1-(4-(tert-butyl)phenyl)methanamine (154d)

Following General Procedure D using (4-(tert-butyl)phenyl)methanamine **15d** (88 µL) gave N-(4-(tert-butyl)benzylidene)-1-(4-(tert-butyl)phenyl)methanamine **154d** as an oil (71 mg, 92%). ^{1}H NMR (300 MHz, $CDCl_3$) δ_H 8.29(s, 1H), 7.64 (d, 2H, J=8.7), 7.38 – 7.15 (m, 6H), 4.70 (s, 2H), 1.25 (s, 9H), 1.23 (s, 9H). ^{13}C NMR (75 MHz, $CDCl_3$) δ_C 161.8, 154.2, 149.9, 136.6, 133.7, 128.2, 127.8, 125.7, 125.5, 65.0, 35.0, 34.6, 31.5, 31.4. Data in accordance with results for flavin catalysis.

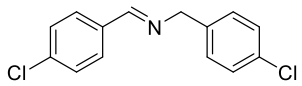

N-(4-chlorobenzylidene)-1-(4-chlorophenyl)methanamine (154e)

Following General Procedure D using 4-chlorobenzylamine **15e** (61 µL) with reaction performed over 16 h gave N-(4-chlorobenzylidene)-1-(4-chlorophenyl)methanamine **154e** as a white powder (46 mg, 70%). ^{1}H NMR (300 MHz, $CDCl_3$) δ_H 8.27 (s, 1H), 7.64 (d, 2H, J=8.6), 7.31 (d, 2H, J=8.5), 7.27 - 7.16 (m, 4H), 4.69 (s, 2H), ^{13}C NMR (75 MHz, $CDCl_3$) δ_C 161.0, 137.7, 137.0, 134.5, 132.9, 129.6, 129.4, 129.1, 128.8, 64.3. Data in accordance with results for flavin catalysis.

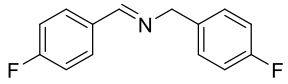

N-(4-fluorobenzylidene)-1-(4-fluorophenyl)methanamine (154f)

Following General Procedure D using 4-fluorobenzylamine **15f** (57 µL) gave N-(4-chlorobenzylidene)-1-(4-chlorophenyl)methanamine **154f** as an oil (56 mg, 96%). ^{1}H NMR (400 MHz, $CDCl_3$) δ_H 8.26 (s, 1H), 7.73 - 7.64 (m, 2H), 7.26 - 7.15 (m, 2H), 7.07 - 6.88 (m, 4H), 4.68 (s, 2H), ^{13}C NMR (100 MHz, $CDCl_3$) δ_C 166.2, 163.7, 162.8, 160.7, 160.5, 135.0 (d, $J_{C,F}$ = 3.2 Hz), 132.4 (d, $J_{C,F}$ = 3.2 Hz), 130.3 (d, $J_{C,F}$ = 8.8 Hz), 129.6 (d, $J_{C,F}$ = 8.8 Hz), 115.8 (d, $J_{C,F}$ = 22.2 Hz), 115.4 (d, $J_{C,F}$ = 22.2 Hz), 64.3. Data in accordance with results for flavin catalysis.

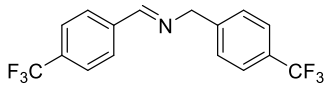

N-(4-(trifluoromethyl)benzylidene)-1-(4-(trifluoromethyl)phenyl)methanamine (154g)

Following General Procedure D using 4-(trifluoromethyl)benzylamine **15g** (71 µL) with 4% alloxan and 4% flavin gave N-(4-(trifluoromethyl)benzylidene)-1-(4-(trifluoromethyl)phenyl)methanamine **154g** as an oil (53 mg, 63%). ^{1}H NMR (300 MHz, $CDCl_3$) δ_H 8.47 (s, 1H), 7.91 (d, 2H, J=8.1 Hz), 7.74 – 7.55 (m, 4h), 7.47 (d, 2H, J=8.1 Hz) 4.90 (s, 2H), ^{13}C NMR (75 MHz, $CDCl_3$) δ_C 161.3, 143.0, 139.0, 132.9, 132.5, 128.7, 128.6, 125.8 (q, JC,F = 3.9 Hz), 125.6 (q, JC,F = 3.9 Hz), 122.5, 64.6. Data in accordance with results for flavin catalysis.

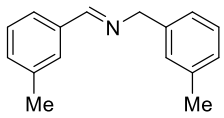

N-(3-methylbenzylidene)-1-(m-tolyl)methanamine (154h)

Following General Procedure D using 3-methylbenzylamine **15h** (63 µL) gave N-(3-methylbenzylidene)-1-(m-tolyl)methanamine **154h** as an oil (44 mg, 79%). ^{1}H NMR (400 MHz, $CDCl_3$) δ_H 8.26 (s, 1H), 7.56 (s, 1H), 7.50 – 7.40 (m, 1H), 7.26 – 7.08 (m, 3H), 7.08 – 6.94 (m, 3H), 4.69 (s, 2H), 2.28 (s, 3H), 2.25 (s, 3H), ^{13}C NMR (100 MHz, $CDCl_3$) δ_C 162.2, 139.2, 138.4, 138.2, 136.2, 131.7, 128.8, 128.5, 128.5, 127.8, 126.0, 125.2, 65.2. Data in accordance with results for flavin catalysis.

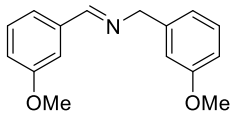

N-(3-methoxybenzylidene)-1-(3-methoxyphenyl)methanamine (154i)

Following General Procedure D using 3-methoxybenzylamine **15i** (64 µL) gave N-(3-methoxybenzylidene)-1-(3-methoxyphenyl)methanamine **154i** as an oil (53 mg, 83%). ^{1}H NMR (500 MHz, $CDCl_3$) δ_H 8.36 (s, 1H), 7.40 (s, 1H), 7.36 – 7.24 (m, 3H), 7.02 – 6.97 (m, 1H), 6.95 – 6.88 (m, 2H), 6.85 – 6.78 (m, 1H), 4.81 (s, 2H), 3.85 (s, 3H), 3.82 (s, 3H), ^{13}C NMR (125 MHz, $CDCl_3$) δ_C 162.1, 160.0, 159.9, 141.0, 137.7, 129.7, 129.6, 121.8, 120.5, 117.7, 113.8, 112.6, 111.8, 65.0, 55.5, 55.3. Data in accordance with results for flavin catalysis.

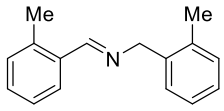

N-(2-methylbenzylidene)-1-(o-tolyl)methanamine (154j)

Following General Procedure D using 2-methylbenzylamine **15j** (62 µL) gave N-(3-methoxybenzylidene)-1-(3-methoxyphenyl)methanamine **154j** as an oil (53 mg, 96%). ^{1}H NMR (300 MHz, $CDCl_3$) δ_H 8.58 (s, 1H), 7.88 – 7.81 (m, 1H), 7.26 – 7.06 (m, 7H), 4.74 (s, 2H), 2.42 (s, 3H), 2.31 (s, 3H), ^{13}C NMR (75 MHz, $CDCl_3$) δ_C 160.7, 137.8, 137.7, 136.2, 134.3, 130.9, 130.4, 130.2, 128.4, 127.8, 127.1, 126.3, 126.2, 63.4, 19.5, 19.4. Data in accordance with results for flavin catalysis.

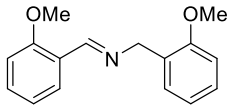

N-(2-methoxybenzylidene)-1-(2-methoxyphenyl)methanamine (154k)

Following General Procedure D using 2-methoxybenzylamine **15k** (65 µL) with reaction performed over 16 h gave N-(2-methoxybenzylidene)-1-(2-methoxyphenyl)methanamine **154k** as an oil (53 mg, 83%). ^{1}H NMR (400 MHz, $CDCl_3$) δ_H 8.76 (s, 1H), 7.95 (dd, *J* = 7.7, 1.8 Hz, 1H), 7.36 – 7.07 (m, 3H), 6.99 – 6.72 (m, 4H), 4.75 (s, 2H), 3.77 (s, 3H), 3.75 (s, 3H), ^{13}C NMR (100 MHz, $CDCl_3$) δ_C 158.9, 158.4, 157.1, 131.9, 129.2, 128.2, 128.0, 127.6, 124.9, 120.8, 120.6, 111.1, 110.2, 59.8, 55.6, 55.4. Data in accordance with results for flavin catalysis.

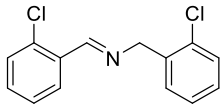

N-(2-chlorobenzylidene)-1-(2-chlorophenyl)methanamine (154l)

Following General Procedure D using 2-chlorobenzylamine **15l** (60 µL) gave N-(2-chlorobenzylidene)-1-(2-chlorophenyl)methanamine **154l** as a white powder (65 mg, 98%). ^{1}H NMR (500 MHz, $CDCl_3$) δ_H 8.88 (s, 1H), 8.15 – 8.10 (m, 2H) 7.50 – 7.13 (m, 7H), 4.96 (s, 2H); ^{13}C NMR (125 MHz, $CDCl_3$) δ_c 159.9, 137.0, 135.5, 133.6, 133.3, 131.9, 130.0, 129.8, 129.5, 128.6, 128.5, 127.2, 127.1. Data in accordance with results for flavin catalysis.

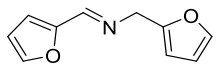

1-(furan-2-yl)-N-(furan-2-ylmethylene)methanamine (154m)

Following General Procedure D using furfurylamine **15m** (44 µL) and copper (I) methylsalicylate (2.1 mg, 5 µmol, 1%) as Cu source gave N-(2-chlorobenzylidene)-1-(2-chlorophenyl)methanamine **154m** as an oil (18 mg, 44%). ^{1}H NMR (300 MHz, $CDCl_3$) δ_H 8.12 (s, 1H), 7.52 (d, 1H, J = 1.6), 7.38 (q, 1H, J = 1.0), 6.78 (d, 1H, J = 3.4), 6.47 (q, 1H, J = 1.7), 6.34 (q, 1H, J = 1.3), 6.28 (dd, 1H, J_1 = 0.6, J_2 = 3.2), 4.75 (s, 2H); ^{13}C NMR (75 MHz, $CDCl_3$) δ_C 151.8, 151.34, 151.2, 145.0, 142.3, 114.6, 111.7, 110.4, 107.9, 56.9. Data in accordance with results for flavin catalysis.

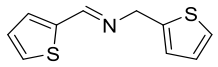

1-(thiophen-2-yl)-N-(thiophen-2-ylmethylene)methanamine (154n)

Following General Procedure D using 2-thiophenemethylamine **15n** (51 µL) for 5 h gave 1-(thiophen-2-yl)-N-(thiophen-2-ylmethylene)methanamine **154n** as an oil (50 mg, 96%). ^{1}H NMR (400 MHz, $CDCl_3$) δ_H 8.42 (s, 1H), 7.42 (dt, *J* = 4.8, 1.0 Hz, 1H), 7.33 (dd, *J* = 3.6, 1.0 Hz, 1H), 4.8, 1.6 Hz, 1H), 7.07 (dd, *J* = 5.0, 3.6 Hz, 1H), 7.03 – 6.95 (m, 2H), 4.95 (s, 1H), ^{13}C NMR (100 MHz, $CDCl_3$) δ_C 155.5, 142.2, 141.6, 131.1, 129.5, 127.5, 127.7, 125.4, 125.0, 58.6. Data in accordance with results for flavin catalysis.

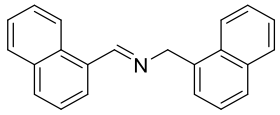

1-(naphthalen-1-yl)-N-(naphthalen-1-ylmethylene)methanamine (154o)

Following General Procedure D using 1-napthylmethylamine **15o** (73 µL) gave 1-(naphthalen-1-yl)-N-(naphthalen-1-ylmethylene)methanamine **154o** as an oil (48 mg, 65%). ^{1}H NMR (400 MHz, $CDCl_3$) δ_H 9.09 (s, 1H), 8.96 (d, *J* = 8.1 Hz, 1H), 8.26 (d, *J* = 8.1 Hz, 1H), 8.00 – 7.77 (m, 5H), 7.63 – 7.44 (m, 7H), 5.42 (s, 2H), ^{13}C NMR (100 MHz, $CDCl_3$) δ_C 162.1, 135.6, 134.0, 133.9, 131.8, 1331.7, 131.4, 131.3, 129.3, 128.8, 128.7, 127.9, 127., 126.3, 126.2, 126.0, 125.8, 125.8, 125.4, 124.5, 124.1, 63.4. Data in accordance with results for flavin catalysis.

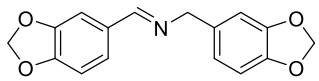

[(2H-1,3-benzodioxol-5-yl)methyl][(2H-1,3-benzodioxol-5-yl)methylidene]amine (154p)

Following General Procedure D using piperonylamine **15p** (62 µL) with reaction performed over 8 h gave **154p** as a white powder (63 mg, 90%). ^{1}H NMR (300 MHz, $CDCl_3$) 8.23 (s, 1H), 7.39 (d, *J* = 1.5 Hz, 1H), 7.14 (dd, *J* = 8.0, 1.5 Hz, 1H), 6.87 – 6.68 (m, 4H), 5.99 (s, 2H), 5.93 (s, 2H), 4.68 (s, 2H); ^{13}C NMR (75 MHz, $CDCl_3$) δ_C 161.0, 150.1, 128.4, 127.9, 146.7, 133.5, 131.1, 124.7, 121.2, 108.7, 108.3, 108.2, 106.9, 101.6, 101.0, 64.6. IR ν_{max} (neat) 2877, 1645, 1441, 1244 cm^{-1}. HRMS (ESI, +ve) *m/z* calcd. for $C_{16}H_{13}NO_4$ 284.0936, found: 284.0923 $(M+H)^+$. Data in accordance with the literature.[116]

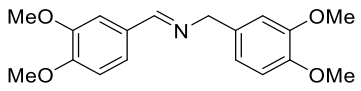

[(3,4-dimethoxyphenyl)methyl][(3,4-dimethoxyphenyl)methylidene]amine (154q)

Following General Procedure D using 3,4-dimethoxybenzylamine **15q** (75 µL) gave **154q** as a white powder (57 mg, 72%). ^{1}H NMR (300 MHz, $CDCl_3$) δ_H 8.28 (s, 1H), 7.47 (s, 1H), 7.24 – 7.14 (m, 1H), 6.94 – 6.77 (m, 4H), 4.74 (s, 2H), 4.02 – 3.81 (m, 12H); ^{13}C NMR (75 MHz, $CDCl_3$) δ_C 161.4, 151.6, 149.5, 149.1, 148.2, 132.1, 128.5, 123.4, 120.3, 222.6, 111.3, 110.5, 109.0, 64.8, 56.1, 56.1, 56.1, 56.0. IR ν_{max} 3010, 2927, 2840, 1645, 1584, 1509, 1260, 1020 cm^{-1}. HRMS (ESI, +ve) *m/z* calcd. for $C_{18}H_{21}NO_4$ 316.1570, found: 316.1549 $(M+H)^+$. Data in accordance with the literature.[236]

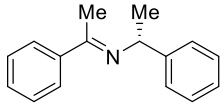

[(1R)-1-phenethyl](1-phenethylidene)amine (predominantly *E*) (170)

Following General Procedure D using *(R)*-α-methylbenzylamine **169** (61 µL) for 16 h gave **170** as an oil (28 mg, 50%), in a 9.5:1 mixture of geometrical isomers ^{1}H NMR (400 MHz, $CDCl_3$) δ_{Hmajor} 7.97 – 7.90 (m, 2H), 7.63 – 7.24 (m, 10H), 4.92 (q, *J* = 6.6 Hz, 1H), 4.92 (s, 3H), 1.63 (d, *J* = 6.6 Hz, 3H); $\delta_{Hminor,visible}$ 4.51 (q, *J* = 6.6 Hz), 2.40 (s, 3H), 1.49 (d, *J* = 6.6 Hz, 3H); ^{13}C NMR (100 MHz, $CDCl_3$) δ_{Cmajor} 136.6, 146.3, 141.6, 129.5, 128.5, 128.3, 126.9, 126.8, 126.6, 59.9, 25.2, 15.7; $\delta_{Cminor,visible}$ 167.5, 145.8, 139.5, 128.6, 125.9, 60.9, 29.5, 24.7. IR ν_{max} (neat) 2969, 1633, 1446, 1266 cm^{-1}; HRMS (ESI, +ve) *m/z* calcd. for $C_{16}H_{18}N$ 224.1438 found: 224.1448; $[\alpha]^{20}_D$ -70˚ (c 0.1, $CHCl_3$) (lit = -73.3˚, c 2.14, $CHCl_3$[237]). Major isomer data in accordance with literature (minor isomer may be visible on literature spectra but is not explicitly reported).[238]

General Procedure for copper/alloxan-catalysed oxidative cross-couping of aromatic amines (General Procedure E)

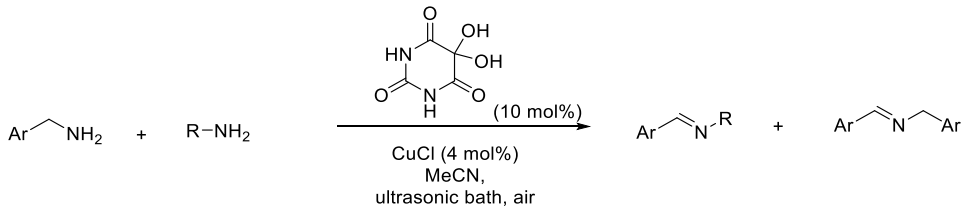

Copper (I) chloride (0.5 mg, 5 µmol, 2 mol%) and alloxan monohydrate **138a** (2 mg, 12.5 µmol, 5 mol%) were added to a test tube containing MeCN in an ultrasonic bath. After 5 minutes, 'alkylating' amine (0.375 mmol) followed by benzylic amine (0.25 mmol) were added by syringe and the mixture was sonicated under air. After 2 h a further 2 mol% CuCl and 5 mol% **138a** were added, and the mixture was sonicated for a further 22 h. Solvent was removed *in vacuo*, and the crude imine(s) were purified by washing through a small pad of base-washed silica.

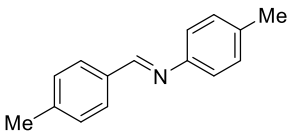

4-methyl-N-(4-methylbenzylidene)aniline (168c)

Following General Procedure B using 4-methylbenzylamine **15c** (32 µL) and *p*-toluidine **164c** (40 mg) gave 4-methyl-N-(4-methylbenzylidene)aniline **168c** as a white solid (50 mg, 96%). ^{1}H NMR (300 MHz, $CDCl_3$) δ_H 8.35 (s, 1H), 7.70 (d, 2H, J = 8.2 Hz), 7.23 – 7.00 (m, 8H), 2.33 (s, 3H), 2.29 (s, 3H) ^{13}C NMR (75 MHz, $CDCl_3$) δ_C 159.7, 149.7, 141.8, 135.7, 133.9, 129.8, 129.6, 128.8, 120.9, 21.7, 21.1. Data in accordance with condensed product.

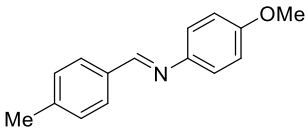

4-methoxy-N-(4-methylbenzylidene)aniline (168d)

Following General Procedure E using 4-methylbenzylamine **15b** (32 µL) and *p*-anisidine **164d** (46 mg) gave 4-methoxy-N-(4-methylbenzylidene) **168d** as a white solid (51 mg, 90%). ^{1}H NMR (300 MHz, $CDCl_3$) δ_H 8.35 (s, 1H), 7.69 (d, 2H, J = 7.3 Hz), 7.28 – 7.03 (m, 4H), 6.84 (d, 2H, J = 8.8 Hz), 3.73 (s, 3H), 2.32 (s, 3H) ^{13}C NMR (75 MHz, $CDCl_3$) δ_C 158.6, 158.2, 145.2, 141.6, 134.0, 129.6, 128.7, 122.3, 114.4, 55.6, 21.7. Data in accordance with the literature.[239]

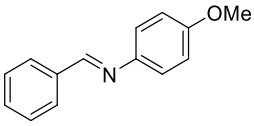

4-methoxy-N-(benzylidene)aniline (168i)

Following General Procedure E using benzylamine **15a** (28 µL) and *p*-anisidine **164d** (46 mg) gave 4-methoxy-N-(benzylidene)aniline **168i** as a white solid (34 mg, 64%). ^{1}H NMR (300 MHz, $CDCl_3$) δ_H 8.40 (s, 1H), 7.88 – 7.77 (m, 2H), 7.45 – 7.33 (m, 3H), 7.17 (d, J = 8.9 Hz, 2H), 6.86 (d, J = 8.9 Hz, 2H), 3.75 (s, 2H) ^{13}C NMR (75 MHz, $CDCl_3$) δ_C 158.6, 158.4, 145.0, 136.5, 131.2, 128.9, 128.7, 122.3, 114.4, 55.6. IR ν_{max} 2916, 1622, 1245 cm^{-1} HRMS (ESI, +ve) *m/z* calcd. for $C_{14}H_{13}NONa$ 234.0895, found: 234.0893 $(M+Na)^+$. Data in accordance with the literature.[239]

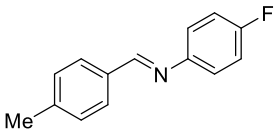

4-fluoro-N-(4-methylbenzylidene)aniline (168f)

Following general procedure E using 4-methylbenzylamine **15c** (32 µL) and 4-fluoroaniline **164f** (36 µL) gave 4-fluoro-N-(4-methylbenzylidene)aniline **168f** as a white solid (45 mg, 84%) ^{1}H NMR (300 MHz, $CDCl_3$) δ_H 8.33 (s, 1H), 7.71 (d, 7.74 – 7.66 (m, 2H), 7.28 – 6.94 (m, 6H), 2.35 (s, 3H) ^{13}C NMR (125 MHz, $CDCl_3$) δ_C 162.2, 160.3, 160.2 (d, $J_{C,F}$ = 2 Hz), 148.4 (d, $J_{C,F}$ = 3 Hz), 142.1, 133.7, 129.3 (d, $J_{C,F}$ = 97 Hz), 122.4 (d, $J_{C,F}$ = 8 Hz), 116.0 (d, $J_{C,F}$ = 22 Hz), 21.8. Data in accordance with condensed product.

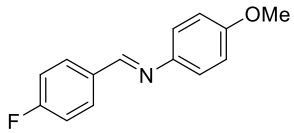

4-methoxy-N-(4-fluorobenzylidene)aniline (168j)

Following general procedure E using 4-fluorobenzylamine **15f** (29 µL) and *p*-anisidine **164d** (46 mg) gave 4-methoxy-N-(4-fluorobenzylidene)aniline **168j** as a white solid (41 mg, 72%). ^{1}H NMR (300 MHz, $CDCl_3$) δ_H 8.36 (s, 1H), 7.84 – 7.76 (m, 2H), 7.20 – 7.00 (m, 4H), 6.90 – 6.79 (m, 2H), 3.75 (s, 3H) ^{13}C NMR (75 MHz, $CDCl_3$) δ_C 164.6 (d $J_{C,F}$ = 252 Hz), 158.4, 157.0, 144.7, 132.9 (d, $J_{C,F}$ = 3 Hz), 130.6 (d, $J_{C,F}$ = 9 Hz), 122.3, 116.0 (d, $J_{C,F}$ = 22 Hz), 114.5, 55.6. IR ν_{max} (neat) 2843, 1621, 1596, 1502 cm^{-1}; HRMS (ESI, +ve) *m/z* calcd. for $C_{14}H_{13}NOF$ 229.0981, found: 246.1013 $(M+H)^+$. Data in accordance with the literature.[239]

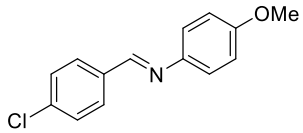

4-methoxy-N-(4-chlorobenzylidene)aniline (168k)

Following general procedure E using 4-chlorobenzylamine **15e** (30 µL) and *p*-anisidine **164d** (46 mg) gave 4-methoxy-N-(4-chlorobenzylidene)aniline **168k** as a white solid (34 mg, 55%). ^{1}H NMR (300 MHz, $CDCl_3$) δ_H 8.37 (s, 1H), 8.49 (d, *J* = 8.5 Hz, 2H), 7.36 (d, *J* = 8.5 Hz, 2H), 7,17 (d, *J* = 8.8 Hz, 2H), 6.86 (d, *J* = 8.8 Hz, 2H), 3.77 (s, 3H), ^{13}C NMR (75 MHz, $CDCl_3$) δ_C 158.6, 156.9, 144.6, 139.1, 135.1, 129.9, 129.2, 122.4, 114.6, 55.7. IR ν_{max} 3013, 1620, 1595 cm^{-1} HRMS (ESI, +ve) *m/z* calcd. for $C_{14}H_{13}NOCl$ 246.0680, found: 246.0706 $(M+H)^+$. Data in accordance with the literature.[239]

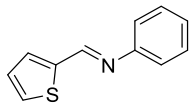

N-phenyl-1-(thiophen-2-yl)methanamine (168l)

Following general procedure E using 2-thiophenemethylamine **15n** (26 µL) and aniline **164b** (36 µL) gave a 1:1.6 mixture (26 mg) of cross-coupled product **168l** and **154n**. Data for **168l** overlays in ^{1}H and ^{13}C NMR with that obtained from an authentic sample of **168l** synthesised by condensation.

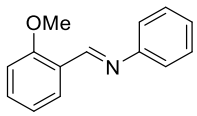

N-(2-methoxybenzylidene)aniline (168m)

Following general procedure E using 2-methoxybenzylamine **15k** (33 µL) and aniline **164b** (36 µL) gave N-(2-methoxybenzylidene)aniline **168m** as an oil (41 mg, 87%) ^{1}H NMR (500 MHz, $CDCl_3$) δ_H 8.93 (s, 1H), 8.17 – 8.14 (m, 2H), 7.48 – 7.38 (m, 3H), 7.27 – 7.20 (m, 3h), 7.08 – 7.03 (m, 1H), 6.99 – 6.95 (m, 1H), 3.91 (s, 3H), ^{13}C NMR (125 MHz, $CDCl_3$) δ_C 159.6, 156.6, 152.9, 132.8, 129.1, 137.6, 125.7, 121.2, 121.0, 111.2, 55.7. IR ν_{max} 3062, 2838, 1619, 1588, 1249 cm^{-1} (ESI, +ve) *m/z* calcd. for $C_{14}H_{14}NO$ 212.1075, found: 212.1079 $(M+H)^+$, Data in accordance with the literature.[239]

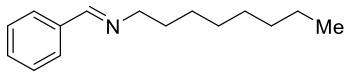

(N-benzlidene)octylamine (168n)

Following general procedure E using benzylamine **15a** (28 µL) and octylamine **164a** (62 µL) gave a mixture of products. Amounts of imines were gauged by addition of an internal standard of 1,3,5-trimethoxybenzene after SiO_2 filtration, and analysis by ^{1}H NMR spectroscopy. Imines were compared with authentic samples prepared by condensation.

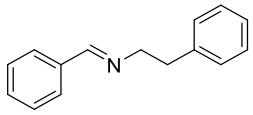

(N-benzlidene)2-phenethylamine (168o)

Following general procedure E using benzylamine **15a** (28 µL) and 2-phenethylamine **16** (47 µL) gave a mixture of products. Amounts of imines were gauged by addition of an internal standard of 1,3,5-trimethoxybenzene after SiO_2 filtration, and analysis by ^{1}H NMR spectroscopy. Imines were compared with authentic samples prepared by condensation.

General procedure for the reduction of alkenes or alkynes (General Procedure F)

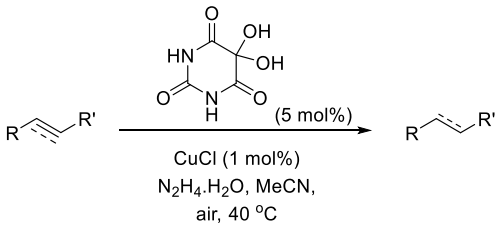

To a stirring solution of alloxan monohydrate **138a** (8 mg, 0.05 mmol) and copper(I) chloride (1 mg, 0.01 mg) in acetonitrile (2 mL) was added alkene or alkyne (1 mmol) followed by hydrazine monohydrate, the latter of which caused the mixture to become instantaneously cloudy. The reaction was heated to 40 °C. The crude reaction mixture was diluted with Et_2O and passed through a plug of silica, then analysed.

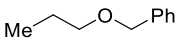

Propyl benzyl ether (198a)

Following general procedure F using allyl benzyl ether **197a** (154 µL) and hydrazine monohydrate (120 µL, 2.5 eq) gave propyl benzyl ether **198a** as an oil (139 mg, 93%) ^{1}H NMR (500 MHz, $CDCl_3$) δ_H 7.43 – 7.27 (m, 5H), 4.55 (s, 2H), 3.48 (2H, t, *J* = 6.7 Hz), 1.69 (2H, apparent sex., *J* = 7.1 Hz), 1.00 (3H, t, *J* = 7.4 Hz) ^{13}C NMR 138.8, 128.4, 127.7, 127.5, 72.9, 72.2, 23.0, 10.7. IR ν_{max} (neat) 2962, 2855, 1454, 1097 cm^{-1} HRMS (ESI, +ve) *m/z* calcd. for $C_{14}H_{10}O$ 150.0995, found: 150.1032 $(M+H)^+$. Data in accordance with the literature.[92]

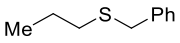

Propyl phenyl sulfide (198b)

Following general procedure F using allyl phenyl sulfide **197b** (148 µL) and hydrazine monohydrate (240 µL, 5 eq) gave propyl phenyl sulfide **198b** as an oil (138 mg, 91%) ^{1}H NMR (300 MHz, $CDCl_3$) δ_H 7.42 – 7.12 (m, 5H), 2.93 (t, 2H, *J* = 7.4 Hz), 1.71 (apparent p, 2H, *J* = 7.4 Hz) 1.06 (t, 3H, *J* = 7.4 Hz), ^{13}C NMR (75 MHz, $CDCl_3$) δ_C 137.0, 128.9, 128.9, 125.7, 35.6, 22.6, 13.5. IR ν_{max} 2962, 1584, 1480, 1438 cm^{-1} HRMS (ESI, -ve) *m/z* calcd. for C_8H_9S 137.0430, found: 137.0422 $(M-CH_3)^-$. Data in accordance with the literature.[92]

$C_{14}H_{30}$

Tetradecane (198c)

Following general procedure F using 1-tetradecene **197c** (253 µL) and hydrazine monohydrate (120 µL, 2.5 eq) gave a mixture of tetradecane **198c** and a small amount of starting material, analysed by ^{1}H NMR spectroscopy.

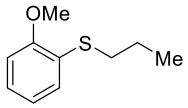

(2-methoxyphenyl)propyl sulfide (198d)

Following general procedure F using (2-methoxyphenyl)allyl sulfide **197d** (90 mg, 0.5 mmol), alloxan **138a** (4 mg, 5 mol%), CuCl (0.5 mg, 1 mol%), hydrazine monohydrate (120 µL, 6 mmol) and acetonitrile (1 mL) gave (2-methoxyphenyl)propyl sulfide **198d** as an oil (86 mg, 95%). ^{1}H NMR (500 Mhz, $CDCl_3$) δ_H 7.26 (d, *J* = 7.9 Hz, 1H), 7.16 (td, *J* = 11.5, 1.4 Hz, 1H), 6.92 (td, *J* = 11.5, 1.4 Hz, 1H), 6.85 (d, *J* = 7.9 Hz, 1H), 3.89 (s, 3H), 2.87 (t, *J* = 7.3 Hz, 2H) 1.69 (apparent p., *J* = 7.3 Hz, 2H), 1.04 (t, *J* = 7.3 Hz, 3H); ^{13}C NMR (125 MHz, $CDCl_3$) δ_C 157.3, 129.0, 126.8, 125.3, 121.1, 110.5, 55.9, 34.1, 22.5, 13.7 IR ν_{max} 2960, 1577, 1474, 1240 cm^{-1} HRMS (ESI, +ve) *m/z* calcd. for $C_{10}H_{15}SO$ 183.0838, found: 183.0840 $(M+H)^+$

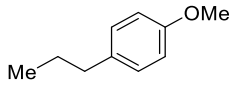

4-propylanisole (198e)

Following general procedure F using 4-allylanisole **197e** (154 µL) and hydrazine monohydrate (120 µL, 2.5 eq) gave 4-propylanisole **198e** as an oil (147 mg, 98%) ^{1}H NMR (500 MHz, $CDCl_3$) 7.10 (d, *J* = 8.6 Hz, 2H), 6.84 (d, *J* = 8.6 Hz, 2H), 3.80 (s, 3H), 2.54 (t, *J* = 7.6 Hz, 2H), 1.62 (apparent sex., *J* = 7.5 Hz, 2H), 0.94 (t, *J* = 7.3 Hz, 3H), ^{13}C NMR (125 MHz, $CDCl_3$) δ_C 157.8, 135.0, 129.5, 113.8, 55.4, 37.3, 24.9, 13.9; IR ν_{max} (neat) 3331, 3288, 3167, 2876, 1471, 1080 cm^{-1}; HRMS (ESI, +ve) *m/z* calcd. for $C_{10}H_{15}O$ 151.1123, found: 151.1147 $(M+H)^+$. Data in accordance with the literature.[240]

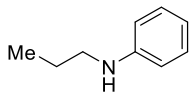

N-propylaniline (198f)

Following general procedure F using N-allylaniline **197f** (136 µL) and hydrazine monohydrate (120 µL, 2.5 eq) gave N-propylaniline **198f** as an oil (121 mg, 90%) ^{1}H NMR (500 MHz, $CDCl_3$) δ_H 7.18 (apparent t, *J* = 7.9 Hz, 2H), 6.70 (t, *J* = 7.9 Hz, 1H), 6.62 (apparent t, *J* = 7.9 Hz, 2H), 3.09 (t, *J* = 7.1 Hz, 2H), 1.65 (apparent sex., *J* = 7.3 Hz, 2H), 1.00 (t, *J* = 7.5 Hz, 3H), ^{13}C NMR (125 MHz, $CDCl_3$) δ_C 148.6, 129.3, 117.2, 112.8, 45.9, 22.8, 11.8. IR ν_{max} (neat) 3406, 2960, 2873, 1602, 1505 cm^{-1}. HRMS (ESI, +ve) *m/z* calcd. for $C_9H_{14}N$ 136.1126, found: 136.1137 $(M+H)^+$ Data in accordance with the literature.[241]

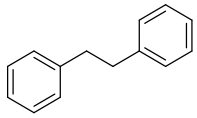

Bibenzyl (198g)

Following general procedure F using stilbene **197g** (180 mg) and and hydrazine monohydrate (240µL, 2.5 eq) gave a mixture of stilbene and bibenzyl **198g** which was analysed by ^{1}H NMR spectroscopy.

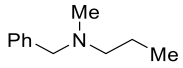

(*N*,*N*,*N*)-Benzyl methyl propyl amine (198h)

Following general procedure F using pargyline **19** (169 µL) and hydrazine monohydrate (240 µL, 5 eq) gave (*N*,*N*,*N*)-Benzyl methyl propyl amine **198h** as an oil (112 mg, 69%). ^{1}H NMR (300 MHz, $CDCl_3$) 7.26 – 7.04 (m, 5H), 3.36 (s, 2H), 2.22 (t, 2H, *J* = 7.5 Hz), 2.07 (s, 3H), 1.42 (apparent sex., 2H, *J* = 7.4 Hz), 0.79 (t, 3H, *J* = 7.3 Hz) ^{13}C NMR (75 MHz, $CDCl_3$) δ_C 139.2, 129.1, 128.2, 126.9, 62.3, 59.5, 42.2, 20.5, 11.9. IR ν_{max} (neat) 3337, 3203, 1656, 1603 cm^{-1} HRMS (ESI, +ve) *m/z* calcd. for $C_{18}H_{21}NO_4$ 164.1434, found: 164.1471 $(M+H)^+$. Data in accordance with the literature.[242]

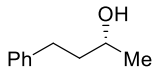

(2R)-4-phenylbutan-2-ol (198i)

Following general procedure F using (2R)-4-phenylbut-3-yn-2-ol **197i** (73 mg, 0.5 mmol), alloxan **138a** (4 mg, 5 mol%), CuCl (0.5 mg, 1 mol%), hydrazine monohydrate (120 µL, 2.5 mmol) and acetonitrile (1 mL) for 72 h gave (2R)-4-phenylbutan-2-ol **198i** as an oil (65 mg, 87%). ^{1}H NMR (300 MHz, $CDCl_3$) δ_H 7.34 – 7.15 (m, 5H), 3.83 (apparent sex, 1H, *J* = 6.2 Hz), 2.83 – 2.60 (m, 2H), 1.83 – 1.72 (m, 2H), 1.56 (bs, 1H), 3.83 (d, 3H, *J* = 6.2 Hz) ^{13}C NMR (75 MHz, $CDCl_3$) δ_C 142.2, 128.5, 128.5, 126.0, 67.7, 41.0, 32.2, 23.8. IR ν_{max} (neat) 3351, 2966, 1453 cm^{-1} HRMS (ESI, +ve) *m/z* calcd. for $C_{10}H_{14}ONa$ 164.1434, found: 164.1471 $(M+Na)^+$ $[\alpha]^{20}_D$ -11.8˚ (c 0.925, $CHCl_3$) (lit = -12.9˚, c 0.55, $CHCl_3$). Data in accordance with the literature.[243]

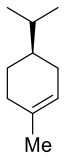

Dihydrolimonene (198j)

Following general procedure F using *(S)*-limonene **197j** (80 µL, 0.5 mmol), alloxan **138a** (4 mg, 5 mol%), CuCl (0.5 mg, 1 mol%), hydrazine monohydrate (60 µL, 2.5 mmol), naphthalene (3.2 mg, 5 mol%) as an internal standard and acetonitrile (1 mL) for 3 h gave dihydrolimonene **198j** as an oil. Yield was quantified by GC, comparing to an authentic sample of dihydrolimonene produced by PtO_2 – catalysed hydrogenation.

General procedure for the synthesis of imines by condensation (General Procedure G)

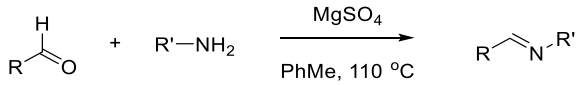

Amine (1 mmol) and aldehyde (1 mmol) were added to a suspension of $MgSO_4$ (240 mg, 2 mmol) in toluene (2 mL) and heated to 110 ˚C for 18 h. The mixture was cooled to room temperature and filtered under gravity. The solvent was removed *in vacuo* and were isolated as pure compounds.

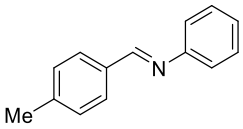

N-(4-methylbenzylidene)aniline (168b)

Following general procedure G using 4-methylbenzaldehyde **42i** (117 µL) and aniline **164b** (91 µL) gave N-(4-methylbenzylidene)aniline **168b** as an oil (191 mg, 98%). ^{1}H NMR (300 MHz, $CDCl_3$) δ_H 8.47 (s, 1H), 7.93 – 7.85 (m, 2H), 7.52 – 7.24 (m, 7H), 2.47 (s, 3H)); ^{13}C NMR (75 MHz, $CDCl_3$) δ_C 160.2, 152.2, 141.8, 133.7, 129.4, 129.1, 128.8, 125.8, 120.9, 21.6; FTIR (neat/cm^{-1}) ν_{max}:2886, 1621, 1609, 1586 cm^{-1}; HRMS (ESI, +ve) *m/z* calcd. for $C_{14}H_{14}N$ 196.1126, found: 196.1141 $(M+H)^+$.

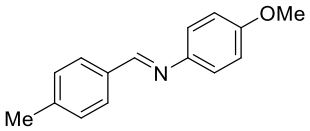

N-(4-methylbenzylidene)-4-methoxyaniline (168d)

Following general procedure G using 4-methylbenzaldehyde **42i** (117 µL) and 4-anisidine **164d** (123 mg) gave **168d** as a solid (165 mg, 73%) ^{1}H NMR (300 MHz, $CDCl_3$) δ_H 8.29 (s, 1H) 7.72 – 7.59 (m, 2H), 7.19 – 7.05 (m, 4H), 6.85 – 6.73 (m, 2h), 3.67 (s, 3H), 2.27 (s, 3H); ^{13}C NMR (75 MHz, $CDCl_3$) δ_C 158.4, 145.0, 141.4, 133.9, 129.5, 128.6, 122.2, 114.4, 55.4, 21.6; 2913, FTIR (neat/cm^{-1}) ν_{max} IR ν_{max} 2913, 1622, 1501, 1245, 1023 cm^{-1}.[1]; HRMS (ESI, +ve) *m/z* calcd. for $C_{15}H_{16}NO$ 226.1232, found: 226.1244 $(M+H)^+$. Data in accordance with the literature.[244]

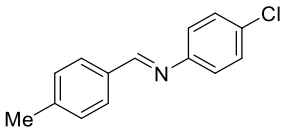

N-(4-methylbenzylidene)-4-chloroaniline (168e)

Following general procedure G using 4-methylbenzaldehyde **42i** (117 µL) and 4-chloroaniline **164e** (127 mg) gave N-(4-methylbenzylidene)-4-chloroaniline **168e** as a solid (224 mg, 97%) ^{1}H NMR (300 MHz, $CDCl_3$) δ_H 8.26 (s, 1H), 7.71 – 7.62 (m, 2H), 7.34 – 6.93 (m, 6H), 2.30 (s, 3H); ^{13}C NMR (75 MHz, $CDCl_3$) δ_C 160.8, 150.7, 142.3, 133.5, 131.4, 129.7, 129.3, 129.0, 122.3, 21.7; FTIR (neat/cm^{-1}) ν_{max} 2915, 1622, 1476 cm^{-1}; HRMS (ESI, +ve) *m/z* calcd. for $C_{14}H_{13}NCl$ 230.0737, found: 230.0727 $(M+H)^+$.

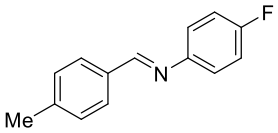

N-(4-methylbenzylidene)-4-fluoroaniline (168f)

Following general procedure G using 4-methylbenzyaldehyde **42i** (117 µL) and 4-fluoroaniline **164f** (94 µL) gave N-(4-methylbenzylidene)-4-fluoroaniline **168f** as an oil (202 mg, 95%) ^{1}H NMR (300 MHz, $CDCl_3$) δ_H 8.23 (s, 1H), 7.73 – 7.62 (m, 2H), 7.20 – 6.84 (m, 6H), 2.26 (s, 3H); ^{13}C NMR (75 MHz, $CDCl_3$) δ_C 161.2 (d, $J_{C,F}$ = 244 Hz), 160.1 (d, $J_{C,F}$ = 2 Hz), 148.2 (d, $J_{C,F}$ = 3 Hz) 142.0, 133.6, 129.2 (d, $J_{C,F}$ = 55 Hz), 122.4 (d, $J_{C,F}$ = 5 Hz), 115.9 (d, $J_{C,F}$ = 12 Hz), 21.6; ^{19}F NMR (469 MHz, $CDCl_3$) δ_F -117.68 (apparent hep, $J_{F,H}$ = 4.4 Hz) IR ν_{max} (neat/cm^{-1}) 1683, 1623, 1607, 1498 cm^{-1}; MP : 64 – 66 ˚C, HRMS (ESI, +ve) *m/z* calcd. for $C_{14}H_{13}NF$ 214.1032, found: 214.1036 $(M+H)^+$

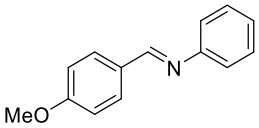

N-(4-methoxybenzylidene)aniline (168g)

Following general procedure G using 4-methoxylbenzaldehyde **42b** (122 µL) and aniline **164b**(91 µL) gave N-(4-methoxybenzylidene)aniline **168g** as a solid (200 mg, 95%) ^{1}H NMR (300 MHz, $CDCl_3$) δ_H 8.40, 7.88 (d, J = 8.8 Hz, 2H), 7.47 – 7.35 (m, 2H), 7.31 – 7.20 (m, 3H), 7.00 (d, J = 8.8 Hz, 2H), 3.85 (s, 3H); ^{13}C NMR (75 MHz, $CDCl_3$) δ_C 162.2, 159.6, 152.3, 130.5, 129.3, 129.1, 125.6, 120.9, 114.2, 55.4; IR ν_{max} (neat/cm^{-1}) 3002, 2909, 1622, 1603, 2674, 1507, 1355 cm^{-1}; HRMS (ESI, +ve) *m/z* calcd. for $C_{14}H_{14}NO$ 212.1075, found: 212.1067 $(M+H)^+$

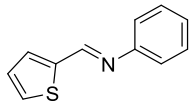

N-phenyl-1-(thiophen-2-yl)methanamine (168l)

Following general procedure G using 2-thiophene carboxaldehyde **42o** (93 µL) and aniline (93 µL) gave N-phenyl-1-(thiophen-2-yl)methanamine **168l** as a solid (108 mg, 58%) ^{1}H NMR (500 MHz, $CDCl_3$) δ_H 8.58 (s, 1H), 7.54 – 7.46 (m, 2H), 7.44 – 7.34 (m, 2H), 7.29 – 7.18 (m, 3H), 7.17 – 7.10 (m, 1H); ^{13}C NMR (125 MHz, $CDCl_3$) δ_C 153.2, 151.6, 143.0, 132.3, 130.5, 129.3, 127.9, 126.2, 121.1. ; IR ν_{max} (neat) 3076, 2874, 1613, 1585, 1192 cm^{-1}; HRMS (ESI, +ve) *m/z* calcd. for $C_{11}H_9NS$ 188.0534, found: 288.0559 $(M+H)^+$. Data in accordance with the literature.[117]

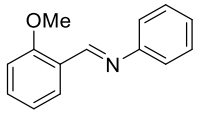

2 N-(2-methylbenzylidene)aniline (168m)

Following general procedure G using 2-methoxybenzaldehyde **42k** (136 mg) and aniline **164b** (91 µL) gave 2 N-(2-methylbenzylidene)aniline **168m** as a solid (195 mg, 93%) ^{1}H NMR (500 MHz, $CDCl_3$) δ_H 8.93 (s, 1H), 8.16 (d, *J* = 7.8 Hz, 1H), 7.45 (d, *J* = 7.8 Hz, 1H), 7.39 (t, *J* = 8.2 Hz, 2H), 7.23 (apparent d, *J* = 7.2 Hz, 3H), 7.06 (t, *J* = 7.8 Hz, 1H), 6.96 (d, *J* = 8.2 Hz, 1H), 3.90 (s, 3H). ^{13}C NMR (125 MHz, $CDCl_3$) 159.6, 156.6, 152.9, 132.8, 129.2, 127.7, 125.8, 124.9, 121.2, 121.0, 111.2, 55.7. IR ν_{max} (neat/cm^{-1}) 2838, 1619, 1588, 1249. HRMS (ESI, +ve) *m/z* calcd. for $C_{14}H_{14}NO$ 212.1075, found: 212.1095 $(M+H)^+$. Data in accordance with the literature.[239]

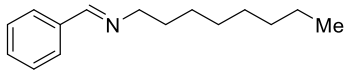

N-(benzylidene)octylamine (168n)

Following general procedure G using benzaldehyde **42a** (102 µL) and octylamine **164a** (165 µL) gave N-(benzylidene)octylamine **168n** as a solid (210 mg, 97%) ^{1}H NMR (500 MHz, $CDCl_3$) δ_H 8.28 (s, 1H), 7.77 – 7.70 (m, 2H), 7.46 – 7.35 (m, 3H), 3.61 (t, *J* = 7.1 Hz, 2H), 1.70 (apparent p, *J* = 7.1 Hz, 2H), 1.52 – 1.14 (m, 10H), 1.00 – 1.80 (m, 3H); ^{13}C NMR (125 MHz, $CDCl_3$) δ_C 160.8, 136.5, 130.6, 128.7, 128.2, 62.0, 32.0, 31.1, 29.6, 29.4, 27.5, 22.8, 14.2; FTIR (neat/cm^{-1}) 2924, 2853, 1647 cm^{-1}; ; IR ν_{max} (neat) 2925, 2853, 1647, 1452 cm^{-1}; HRMS (ESI, +ve) *m/z* calcd. for $C_{15}H_{24}N$ 218.1909, found: 218.1923 $(M+H)^+$

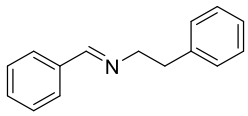

N-(benzylidene)-2-phenethylamine (168o)

Following general procedure G benzaldehyde **42a** (102 µL) and 2-phenethlamine **16** (126 µL) gave N-(benzylidene)-2-phenethylamine **168o** (133 mg, 64%) as a semi-solid. ^{1}H NMR (500 MHz, $CDCl_3$) δ_H 8.18 (s, 1H), 7.82 – 7.66 (m, 2H), 7.51 – 7.12 (m, 8H), 3.93 – 3.81 (m, 2H), 3.11 – 2.97 (m, 2H); ^{13}C NMR (125 MHz, $CDCl_3$) δ_C 140.1, 136.4, 130.7, 129.2, 128.7, 128.5, 128.2, 126.2, 126.2, 63.3, 37.7; ; IR ν_{max} (neat) 3022, 2833, 1648, 1493, 1450 cm^{-1}. MP 30-32 ˚C HRMS (ESI, +ve) *m/z* calcd. for $C_{15}H_{16}N$ 210.1283, found: 210.1316 $(M+H)^+$.

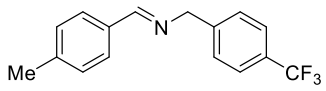

N-(4-methylbenzylidene)-1-(4-(trifluoromethyl)phenyl)methanamine (171a)

Following General Procedure G using 4-methylbenzaldehyde **42i** (118 µL) and 4-(trifluoromethyl)benzylamine **15g** (144 µL) gave N-(4-methylbenzylidene)-1-(4-(trifluoromethyl)phenyl)methanamine **171a** (260 mg, 94%) as a white solid. ^{1}H NMR (400 MHz, $CDCl_3$) δ_H 8.45 (s 1H), 7.78 (d, *J* = 8.0 Hz, 2H), 7.67 (d, *J* = 8.0 Hz, 2H), 7.54 (d, *J* = 8.0 Hz, 2H), 7.31 (d, *J* = 8.0 Hz, 2H), 4.91 (s, 2H), 2.46 (s, 3H) ; ^{13}C NMR (100 MHz, $CDCl_3$) δ_C 162.8, 143.8, 141.5, 133.4, 129.5, 129.3 (q, $J_{C,F}$ = 34 Hz), 128.4, 128.2, 125.8, 125.5 (q, $J_{C,F}$ = 4 Hz), 123.1, 64.4, 21.6; ^{19}F NMR (375 MHz, $CDCl_3$) δ_F -180 (s); FTIR (neat/cm^{-1}) ν_{max}: 2845, 2806, 1650.; MP: 71 – 73 ºC; HRMS (ESI, -ve) *m/z* calcd. for $C_{16}H_{14}NF_3$ 276.1000, found: 276.0995 $(M-H)^-$

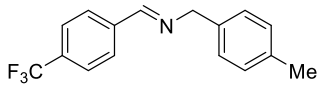

1-p-tolyl-N-(4-(trifluoromethyl)benzylidene)methanamine (171b)

Following General Procedure G using 4-(trifluoromethyl)benzaldehyde **42p** and 4-methylbenzylamine **15c** gave 1-p-tolyl-N-(4-(trifluoromethyl)benzylidene) **171b** (100 mg, 37%) as a white solid. ^{1}H NMR (400 MHz, $CDCl_3$)) δ_H 8.48 (s, 1H), 7.97 (d, *J* = 8.2 Hz, 2H), 7.52 (d, *J* = 8.2 Hz, 2H), 7.34 (d, *J* = 8.1 Hz, 2H), 7.27 (d, *J* = 8.1 Hz, 2H), 4.91 (s, 2H), 2.45 (s, 3H); ^{13}C NMR (400 MHz, $CDCl_3$) δ_C 160.2, 139.5, 136.9, 135.8, 132.3 (q, $J_{C,F}$ = 33 Hz), 129.3, 128.6, 128.1, 125.6 (q, $J_{C,F}$ = 4 Hz), 125.4, 122.7; ^{19}F NMR (375 MHz, $CDCl_3$) δ_F -63 (s); FTIR (neat/cm^{-1}) ν_{max}: 2926, 2860, 1647.; MP: 85 – 86 ºC ; HRMS (ESI, +ve) *m/z* cal cd. for $C_{16}H_{16}NF_3$ 278.1156, found: 278.1128 $(M+H)^+$

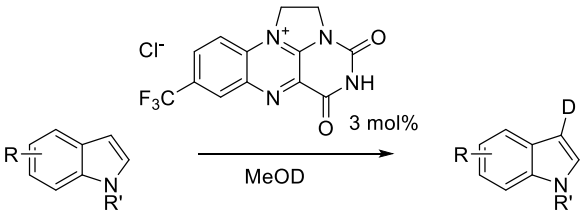

General Procedure for flavin-catalysed deuteration of indole (General procedure H)

To a small vial (5 mL) of 0.5 mL CD3OD was added 0.1 mmol of indole, followed by 3 mol % (1 mg) **58** The vial was shaken and left to stand at room temperature for one minute or alternatively capped and left to stand at room temperature for 15 minutes. The reaction was then quenched with diethyl ether before being run through a pipette column with silica gel washed with a 1:2 mixture of petroleum ether/ethyl acetate (2% triethylamine). Solvent was removed by rotary evaporation.

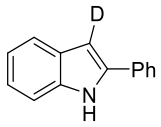

3-deutero-2- phenylindole (213b)

General procedure G (1 minute) using 2-phenylindole **200b** (19 mg). Full characterisation was performed on this compound and is shown below.

^{1}H NMR (500 MHz, $CDCl_3$) δ_H 7.70 (d, *J* = 7.5 Hz, 2H), 7.66 (d, *J* = 7.6 Hz, 1H), 7.47 Hz (apparent t, *J* = 7.5 Hz, 2H), 7.35 (t, *J* = 7.5 Hz, 1H), 7.22 (apparent t, *J* = 7.6 Hz, 1H), 7.15 (apparent t, *J* = 7.6 Hz, 1H).^{13}C NMR (125 MHz, $CDCl_3$) δ_C 138.0, 137.0, 132.5, 129.3, 127.9, 125.3, 122.5, 120.8, 120.4, 111.0, 100.2 (d, $J_{C,D}$ = 75 Hz). ^{2}D NMR (75 MHz, CD_3OD) δ_D 6.81 (s) .IR ν_{max} (neat) 3443, 3048, 2564, 1668, 1456, 1445, 1349 cm^{-1}. HRMS (ESI, -ve) Calcd. for $C_{14}H_9ND$, 193.0876. Found: 193.0887 $(M-H)^-$

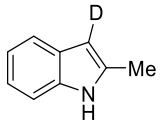

3-deutero-2-methylindole (213c)

General procedure G (15 minutes) using 2-methylindole **200c** (13 mg).

^{1}H NMR (250 MHz, $CDCl_3$) δ_H 7.87 (br s, 1H), 7.56 – 7.48 (m, 1H), 7.33 – 7.25 (m, 1H), 7.17 – 7.02 (m, 2H), 6.22 (s, 0.06 H), 2.44 (s, 3H).

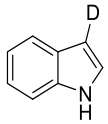

3-deuteroindole (213a)

General procedure G (15 minutes) using indole **200a** (12 mg).

^{1}H NMR (300 MHz, $CDCl_3$) δH 7.69 (d, J = 7.9 Hz, 1 H), 7.44 (d, J = 8.0, 1 H), 7.22-7.10 (m, 4 H), 6.58 (s, 0.16 H).

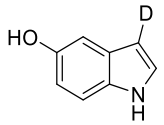

3-deutero-5-hydroxyindole (213d)

General procedure G (1 minute) using 5-hydroxyindole **200d** (13 mg).

^{1}H NMR (250 MHz, $CDCl_3$) δ_H 7.25 (t, *J* = 4.3 Hz, 3 H), 7.19 (s, 1 H), 7.00 (d, *J* = 2.4 Hz, 1 H), 6.78 (dd, *J* = 8.7, 2.5 Hz, 1 H), 6.43 (d, *J* = 2.4 Hz, 0.17 H).

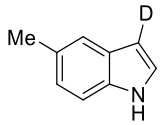

3-deutero-5-methylindole (213e)

General procedure G (15 minutes) using 5-methylindole **200e** (13 mg)

1H NMR (250 MHz, CDCl3) δ_H 8.05 (br s, 1 H), 7.44 (s, 1 H), 7.28 (m, 1 H), 7.17 (s, 1 H), 7.03 (d, *J* = 8.26 Hz, 1 H), 6.48 (d, *J* = 2.5 Hz, 0.17 H), 2.46 (s, 3 H).

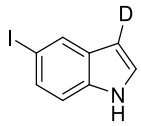

3-deutero-5-iodoindole (213f)

General procedure G (15 minutes) using 5-iodoindole **200f** (24 mg).

^{1}H NMR (300 MHz, $CDCl_3$) δ_H 8.19 (br s, 1 H), 7.99 (s, 1 H), 7.44 (dd, *J* = 8.5, 1.9 Hz, 1 H), 7.18 (d, *J* = 8.5 Hz, 2 H), 6.48 (d, *J* = 1.9 Hz, 0.35 H).

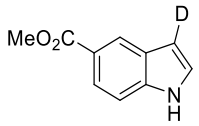

3-deutero-methylindole-5-carboxylate (213g)

General procedure G (1 minute) using methyl indole-5-carboxylate **200g** (18 mg).

^{1}H NMR (250 MHz, $CDCl_3$) δ_H 8.42 (s, 1 H), 7.91 (d, 8.7 Hz, 1H), 7.41 (d, *J* = 8.7 Hz, 1 H), 7.27 (m, 2 H), 6.65 (m, 0.94 H), 3.93 (s, 3 H)

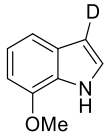

3-deutero-7-methoxyindole (213j)

General procedure G (15 minutes) using 7-methoxyindole **200j** (15 mg)

^{1}H NMR (250 MHz, $CDCl_3$) δ_H 8.18 (br s, 1 H), 7.16-7.01 (m, 3 H), 6.67 (s, 0.67 H), 6.53 (m, 1 H), 3.97 (s, 3 H)

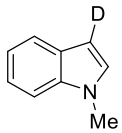

1-methylindole (213k)

General procedure G (15 minutes) using 1-methylindole **200k** (12 μL).

^{1}H NMR (250 MHz, $CDCl_3$) δ_H 7.64 (d, J = 8.04 Hz, 1 H), 7.35-7.05 (m, 4 H), 6.49 (d, *J* = 2.5 Hz, 0.54 H), 3.80 (s, 3 H).

General Procedure for acetyl chloride-catalysed deuteration of indole (General Procedure H)

To a small vial (5 mL) of 0.5 mL CD3OD was added 0.1 mmol of indole, followed by 10 μL of acetyl chloride solution (30 μL acetyl chloride in 1 mL CD3OD). The vial was shaken and left to stand at room temperature for one minute or alternatively capped and left to stand at room temperature for 15 minutes. The reaction was then quenched with diethyl ether before being run through a pipette column with silica gel washed with a 1:2 mixture of petroleum ether/ethyl acetate (2% triethylamine). Solvent was removed by rotary evaporation.

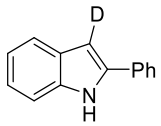

3-deutero-2-phenylindole (213b)

General procedure H (1 minute) using 2-phenylindole **200b** (19 mg).

^{1}H NMR (250 MHz, $CDCl_3$) δ_H 8.37 (br s, 1 H), 7.66 (m, 3 H), 7.48-7.10 (m, 6 H), 6.84 (s, 0.07 H).

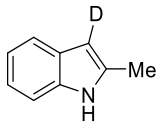

3-deutero-2-methylindole (213c)

General procedure H (15 minutes) using 2-methylindole **200c** (13 mg).

^{1}H NMR (250 MHz, $CDCl_3$) δ_H 7.56 – 7.48 (m, 1H), 7.33 – 7.25 (m, 1H), 7.17 – 7.02 (m, 2H), 6.15 (br s, 0.17 H), 2.44 (s, 3H).

NB. In this case it is possible, due to the broad signal the NH has been deuterated and shifted, and we do not observe residual C3. We assumed the 'worst' case that the broad peak is C3 proton.

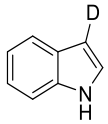

3-deuteroindole (213a)

General procedure H (15 minute) using indole **200a** (12 mg). Full characterisation was performed on this compound and is shown below.

^{1}H NMR (500 MHz, $CDCl_3$) δ_H 7.67 (d, *J* = 8.0 Hz, 1H), 7.41 (d, *J* = 8.0 Hz, 1H), 7.24 – 7.19 (m, 2H), 7.16 – 7.12 (m, 1H).^{13}C NMR (125 MHz, $CDCl_3$) δ_C 135.7, 127.9, 124.0, 122.1, 120.8, 119.9, 111.1, 102.5 (t, $J_{C,D}$ = 26 Hz).^{2}D NMR (75 MHz, CD_3OD) δ_D 6.48 (apparent s). IR ν_{max} (neat) 3413, 2922, 2852, 1455, 1324 cm^{-1}. HRMS (ESI, -ve) Calcd. for C_8H_5ND 117.0563. Found: 117.0572 $(M-H)^-$

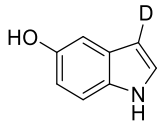

3-deutero-5-hydroxyindole (213d)

General procedure H (1 minute) using 5-hydroxyindole **200d** (13 mg).

^{1}H NMR (250 MHz, $CDCl_3$) δ_H 7.27-7.24 (apparent d, *J* = 8.5 Hz, 2 H), 7.19 (s, 1 H), 7.04 (apparent d, *J* = 7.0 Hz, 1 H), 6.78 (dd, *J* = 8.5, 2.4 Hz, 1 H), 6.43 (d, *J* = 2.4 Hz, 0.18 H).

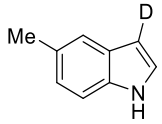

3-deutero-5-methylindole (213e)

General procedure H (1 minute) using 5-methylindole **200e** (13 mg)

^{1}H NMR (250 MHz, $CDCl_3$) (br s, 1 H), 7.44 (s, 1 H), 7.28 (m, 1 H), 7.17 (s, 1 H), 7.03 (d, *J* = 8.26 Hz, 1 H), 6.48 (m, 0.57 H), 2.46 (s, 3 H).

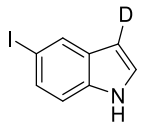

5-iodoindole (213f)

General procedure H (15 minutes) using 5-iodoindole **213f** (24 mg).

^{1}H NMR (250 MHz, $CDCl_3$) δ_H 7.99 (s, 1 H), 7.44 (dd, *J* = 8.5, 2.0 Hz, 1 H), 7.18 (d, *J* = 8.5 Hz, 2 H), 6.48 (d, *J* = 2.0 Hz, 0.19 H).

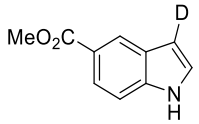

3-deutero-methylindole-5-carboxylate (213g)

General procedure H (15 minutes) using methyl indole-5-carboxylate **200g** (18 mg).

^{1}H NMR (250 MHz, $CDCl_3$) δ_H 8.42 (s, 1 H), 7.91 (d, *J* = 8.7 Hz, 1H), 7.41 (d, *J* = 8.7 Hz, 1 H), 7.27 (m, 2 H), 6.65 (m, 0.19 H), 3.93 (s, 3 H)

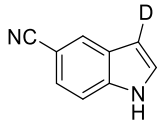

3-deutero-5-cyanoindole (213h)

General procedure H (15 minutes) using 5-cyanoindole **200h** (14 mg)

^{1}H NMR (250 MHz, $CDCl_3$) δ_H 8.01 (s, 1 H), 7.48-7.35 (m, 3 H), 6.65 (s, 0.16 H).

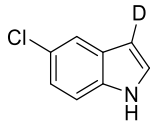

3-deutero-5-chloroindole (213i)

General procedure H (15 minutes) using 5-chloroindole **200i** (15 mg).

^{1}H NMR (250 MHz, $CDCl_3$) δ_H 7.54 (d, *J* = 2.2 Hz, 1H), 7.28 – 7.02 (m, 3H), 6.42 (d, *J* = 2.2 Hz, 0.06 H).

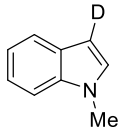

3-deutero-1-methylindole (213k)

General procedure H (1 minute) using 1-methylindole **200k** (13 μL) with 3 mol % acetyl chloride.

1H NMR (250 MHz, CDCl3) δ_H 7.64 (d, *J* = 8.1 Hz, 1 H), 7.35 (d, *J* = 8.1 Hz, 1 H), 7.22 (apparent d, *J* = 8.1 Hz, 1 H), 7.15-7.06 (m, 2 H), 6.50 (m, 0.27 H), 3.81 (s, 3 H).

2,2-dideuterobenzylamine (175)

According to the published procedure,[245] 1M THF solution of lithium aluminium deuteride (9.4 mL, 9.4 mmol) was diluted with dry THF (5 mL) and cooled to 0 ˚C . Benzonitrile **174** (0.88 mL, 8.5 mmol) was added dropwise as a solution in dry THF (5 mL). The solution was warmed to r.t. then refluxed for 16 h. The reaction was cooled in ice, and quenched sequentially with Et_2O (5 mL), H_2O (0.5 mL) and 10% NaOH (0.7 mL). The mixture was filtered through celite and water (5 mL) was added and the mixture was extracted with ether (3 x 10 mL). The solution was dried with $MgSO_4$ and solvent was removed *in vacuo*. The oil was purified by Kugelrohr distillation (2 mmHg, 37 ˚C) to give 2,2-dideuterobenzylamine **175** as a clear oil (480 mg, 52%). ^{1}H NMR (300 MHz, $CDCl_3$) δ_H 7.45 – 7.2 (m, 5H), 1.88 – 1.56 (bs, 2H); ^{13}C NMR (75 MHz, $CDCl_3$) δ_c 143.3, 128.6, 127.2, 126.9, 45.9; IR (neat) ν_{max} 2924, 2854, 2796, 1643, 1467, 1117 cm^{-1}; HRMS (ESI, +ve) *m/z* calcd. for $C_7H_5D_2$ 93.0668, found: 93.0677 $(M\text{-}NH_3)^+$. Data in accordance with that previously published

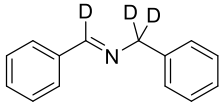

Benzenemethan-*d*$_2$-amine, N-(phenylmethylene-*d*) (176)

Following General Procedure B using 2,2-dideuterobenzylamine 1**75** (56 µL) for 5 h gave Benzenemethan-*d*$_2$-amine, N-(phenylmethylene-*d*) **176** as an oil (25 mg, 50%). ^{1}H NMR (500 MHz, $CDCl_3$) δ_H 7.86 – 7.77 (m, 2H), 7.49 – 7.24 (m, 8H); ^{13}C NMR (125 MHz, $CDCl_3$) δ_C 161.6 (t, $J_{C,D}$ = 23 Hz), 139.3, 126.3, 130.8, 128.7, 128.6, 128.3, 128.1, 127.1, 64.4 (p, $J_{C,D}$ = 20 Hz); IR ν_{max} (neat) 3059, 3026, 2137, 1627, 1448 cm^{-1}; HRMS (ESI, +ve) *m/z* calcd. for $C_{14}H_{10}D_3N$ 199.1315, found: 199.1341 $(M+H)^+$.

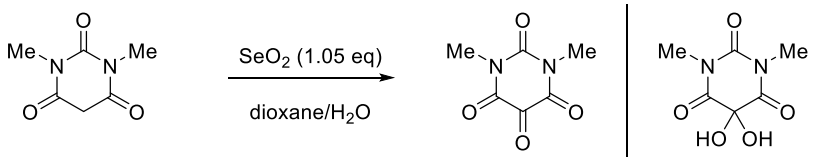

***N,N*-dimethylalloxan (163)**

In a modification of the published procedure,[113] to a solution of selenium dioxide (0.75 g, 6.8 mmol) in dioxane (3 mL) and water (180 µL) was added *N,N*-dimethylbarbituric acid **162** (1.06 g, 6.4 mmol) as a suspension in dioxane (5 mL) using an addition funnel. The mixture was refluxed for 72 h, then cooled and filtered through celite, solvent was removed *in vacuo*, and the crude product was recrystallized from benzene/hexane to give *N,N*-dimethylalloxan **162** as a white powder (226 mg, 21%), and was observed in DMSO as a 2:1 ratio of its monohydrate to the free carbonyl; ^{1}H NMR (300 MHz, d_6-DMSO) δ_H hydrate: 7.76 (s, 2H), 3.13 (s, 6H), carbonyl: 3.21 (s, 3H); ^{13}C NMR (75 MHz, d_6-DMSO) δ_C 168.1, 164.5, 156.3, 150.8, 150.6, 85.5, 28.4; IR ν_{max} (neat) 3364, 1679, 1445, 1368, 1106 cm^{-1}; HRMS (ESI, +ve) *m/z* calcd. for $C_6H_8N_2O_5Na$ 211.0314, found: 211.0331 $(M+Na)^+$; M.P. = 250-255 °C (lit = 254-5 °C). Data in accordance with that previously published.[246]

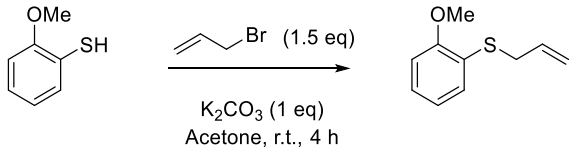

(2-methoxyphenyl)allyl sulfide (197d)

To a refluxing mixture of 2-methoxythiophenol (243 µL, 2 mmol) and K_2CO_3 (260 mg, 2 mmol) in acetone (5 mL), under an atmosphere of N_2, was added allyl bromide (173 µL, 2 mmol) dropwise. After 90 minutes, a further portion of allyl bromide (85 µL, 1 mmol) was added. After a total reaction time of 4 h the reaction was cooled and filtered. Acetone was removed *in vacuo* and the mixture was partitioned between Et_2O (20 mL) and water (5 mL). The aqueous layer was washed with Et_2O (2 x 10 mL), the combined organic layers were dried with $MgSO_4$ and solvent was removed *in vacuo*. The product was purified by column chromatography (0 – 2% EtOAc / pet. ether) to give (2-methoxyphenyl)allyl sulfide **197d** as an oil (204 mg, 56%). ^{1}H NMR (500 MHz, $CDCl_3$) δ_H 7.30 (d, *J* = 7.6 Hz, 1H), 7.20 (t, *J* = 7.9 Hz, 1H), 6.91 (d, *J* = 7.6 Hz, 1H), 6.86 (t, *J* = 7.9 Hz, 1H), 5.89 (apparent sex., *J* = 8.1 Hz, 1H), 5.14 (d, *J* = 17.0 Hz, 1H), 5.10 (d, *J* = 10.0 Hz, 1H), 3.90 (s, 3H), 3.55 (d, *J* = 6.9 Hz, 2H); ^{13}C NMR (125 MHz, $CDCl_3$) δ_C 158.0, 133.8, 130.7, 127.7, 121.5, 117.7, 110.6, 55.9, 35.6.; IR ν_{max} 2835, 1578, 1475, 1241 cm^{-1} HRMS (ESI, +ve) *m/z* calcd. for $C_{10}H_{12}SONa$ 203.0507, found: 203.0516 $(M+Na)^+$

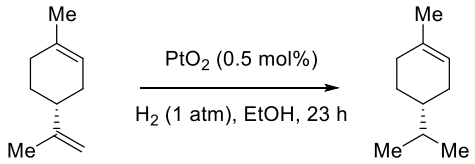

_S_-Dihydrolimonene (198j)

To a solution of *S*-limonene **197j** (0.6 mL, 3.7 mmol) in EtOH (5 mL) was added PtO_2 (1 mg, 20 μmol) and hydrogenated under 1 atm H_2 for 23 h. The reaction mixture was stirred at RT for 23 hr after which the reaction mixture was filtered through Celite washing with DCM (5 mL). The filtrate was concentrated *in vacuo* to give **198j** as a yellow liquid (172 mg, 34%) ^{1}H NMR (500 MHz, $CDCl_3$) δ_H 5.38 (s, 1H), 2.05 – 1.86 (m, 3H), 1.80 – 1.65 (m, 2H), 1.64 (s, 3H), 1.46 (apparent hex., J = 6.7 Hz, 1H), 1.29 – 1.14 (m, 2H), 0.88 (apparent t, J = 6.7 Hz, 6H), ^{13}C NMR (125 MHz, $CDCl_3$) δ_C 134.1, 121.2, 40.2, 32.4, 31.0, 29.1, 26.6, 23.6, 20.1, 19.8. IR ν_{max} (neat) 2957, 2916, 2872, 1448, 1367 cm^{-1}, LRMS (EI) 138 (M^+) GC-MS (EI) *m/z* calcd. for $C_{10}H_{18}$: 138.14, found: 138.2. Retention time = 5.017 min. Data in accordance with literature.[185]

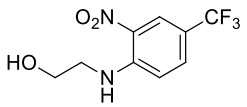

4-(trifluoromethyl)-2-nitro-N-(2-hydroxyethyl)aniline (135)

To a solution of 4-chloro-3-nitrobenzotrifluoride **132** (3.82 mL, 26 mmol) in EtOH (70 mL) was added ethanolamine (4.71 mL, 78 mmol) followed by K_2CO_3 (3.96 g, 28.6 mmol), and the mixture was stirred at 90 °C for 18 h. The reaction was cooled to r.t. and the orange solution was poured into 50 mL ice water. The organics were extracted with CH_2Cl_2 (3 x 50 mL) and the combined organic layers were washed with brine (30 mL). The organic layer was dried with $MgSO_4$ and solvent was removed *in vacuo*. 4-(trifluoromethyl)-2-nitro-N-(2-hydroxyethyl)aniline **135** (6.50 g, 99%) was obtained as a yellow solid. ^{1}H NMR (300 MHz, $CDCl_3$) δ_H 8.49 (br s, 1H), 8.44 (s, 1H), 7.61 (d, J = 9.1 Hz, 1H), 6.99 (d, J = 9.1 Hz, 1H), 4.00 – 3.93 (m, 2H), 3.59 – 3.50 (m, 2H); ^{13}C NMR (75 MHz, $CDCl_3$) δ_C 147.2, 132.3 131.2, 125.5, 125.1, 122.0 (q, $J_{C,F}$ = 275 Hz), 114.7, 60.8, 45.1; ^{19}F NMR (469 MHz, $CDCl_3$) δ_F -62.0; IR ν_{max} (neat) 3373, 3297, 2953, 2635, 1574, 1285, 1255, 1134, 1056 cm^{-1}; MP 43 – 46 ˚C; HRMS (ESI, +ve) *m/z* calcd. for $C_9H_9N_2O_3F_3Na$ 273.0463, found: 273.0436 $(M+Na)^+$ Data in accordance with literature.[68]

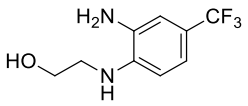

2-((2-hydroxyethyl)amino)-5-(trifluoromethyl)aniline (137)

To a solution of 4-(trifluoromethyl)-2-nitro-N-(2-hydroxyethyl)aniline **135** (2.5 g, 10 mmol) in MeOH (20 mL) at 0 °C was added ammonium formate (3.15 g, 50 mmol) followed by 10 wt% palladium on carbon (0.50 g). The mixture was allowed to warm to r.t. and stirred for 4 h. The black suspension was then filtered through celite and washed with CH_2Cl_2 (60 mL). The organic layer was washed with saturated $NaHCO_3$ solution (30 mL) followed by brine (30 mL). The organic layer was dried with $MgSO_4$ and solvent was removed *in vacuo*. 2-((2-hydroxyethyl)amino)-5-(trifluoromethyl)aniline **137** (1.24 g, 56%) was obtained as a light pink solid. ^{1}H NMR (500 MHz, d^6-DMSO) δ_H 6.86 – 6.80 (m, 2H), 6.56 – 6.50 (m, 1H), 5.06 (t, J = 5.5 Hz, 1H), 5.06 (br s, 2H), 4.78 (t, J = 5.5 Hz, 1H), 3.64 (apparent q, J = 5.8 Hz, 2H), 5.77 (apparent q, J = 5.8 Hz, 2H). ^{13}C NMR (125 MHz, d^6-DMSO) δ_C 159.5, 135.6, 126.0 (q, $J_{C,F}$ = 270 Hz), 116.8 (q, $J_{C,F}$ = 31 Hz), 115.0 (q, $J_{C,F}$ = 4 Hz), 109.9 (q, $J_{C,F}$ = 3 Hz), 108.5, 59.7, 46.1. ^{19}F NMR (469 MHz, d^6-DMSO) -59.0 (s). IR ν_{max} (neat/cm^{-1}) 3461, 3344, 3310, 3236, 1950, 1653, 1612, 1440, 1328, 1099 cm^{-1}. MP 92 – 94 ˚C. HRMS (ESI, -ve) Calcd. for $C_9H_{10}F_3N_2O$, 219.0740. Found: 219.0736 (M-H)$^-$. Data in accordance with literature.[68]

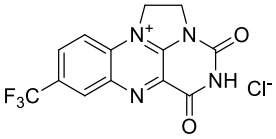

7-(Trifluoromethyl)-1,10-ethylenealloxazinium chloride (58)

2-((2-hydroxyethyl)amino)-5-(trifluoromethyl)aniline **137** (1.24 g, 5.6 mmol) was dissolved in 15 mL glacial acetic acid and stirred under an atmosphere of N_2. Alloxan monohydrate **138a** (0.89 g, 5.6 mmol) was added followed by boric acid (0.35 g, 5.6 mmol) and the mixture was stirred at 50 °C under N_2 in the dark for 18 h. The suspension was then cooled in ice and rapidly filtered, and the filtrate dried under vacuum. The yellow solid obtained was placed under N_2 in the dark and $SOCl_2$ (20 mL) was added slowly. The mixture was then stirred at 50 °C for 24 h. $SOCl_2$ was removed by filtration, washing with CH_2Cl_2, and the yellow solid was recrystallised by initial hot filtration with 2,2,2-trifluoroethanol, followed by removal of solvent and dissolution in formic acid followed by re-precipitation with Et_2O to give 7-(Trifluoromethyl)-1,10-ethyleneisoalloxazinium chloride **58** (1.80 g, 93%) as a bright yellow solid. ^{1}H NMR (500 MHz, CD_3CO_2D) δ_H 8.92 (s, 1H), 8.58 (d, *J* = 7.4 Hz, 1H), 8.45 (d, *J* = 7.4 Hz, 1H), 8.14 (s, 1H), 5.66 (t, *J* = 7.5 Hz, 2H), 4.95 (t, *J* = 7.5 Hz, 2H); ^{13}C NMR (125 MHz, CD_3CO_2D) δ_C 164.9, 157.2, 145.6, 145.2, 139.8, 135.5, 135.1, 134.4, 131.5, 130.4, 119.6, 51.8, 45.7 (19F,^{13}C couplings were visible but not easily resolvable); ^{19}F NMR (469 MHz, CD_3CO_2D) δ_F -63.4; IR ν_{max} (neat) 3387, 2930, 2752, 1760, 1717, 1610, 1374, 1138 cm^{-1}; MP 192 – 194 ˚C; HRMS (ESI, +ve) Calcd. for $C_{13}H_8F_3N_4O_2$, 309.0599. Found: 309.0579 $(M)^+$. Data in accordance with the literature. [68]

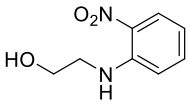

2-nitro-N-(2-hydroxyethyl)aniline (134)

To a solution of 1-fluoro-2-nitrobenzene **131** (1.96 mL, 18.5 mmol) in EtOH (40 mL) was added ethanolamine (3.31 mL, 55.5 mmol) followed by K_2CO_3 (2.8 g, 20 mmol), and the mixture was stirred at 90 °C for 18 h. The reaction was cooled to r.t. and the red solution was poured into 50 mL ice water. The organics were extracted with CH_2Cl_2 (3 x 50 mL) and the combined organic layers were washed with brine (30 mL). The organic layer was dried with $MgSO_4$ and solvent was removed *in vacuo*. 4-(trifluoromethyl)-2-nitro-N-(2-hydroxyethyl)aniline **134** (2.67 g, 81%) was obtained as a red solid. $^1\delta_H$ 8.23 (br s, 1H), 8.17 (apparent dd, *J* = 8.6, 1.7 Hz, 1H), 7.48 – 7.40 (m, 1H), 6.89 (d, *J* = 8.6 Hz, 1H), 6.69 – 6.63 (m, 1H), 3.94 (t, *J* = 5.4 Hz, 2H), 3.51 (apparent q, *J* = 5.4 Hz, 2H), 1.94 (br s, 1H). ^{13}C NMR (125 MHz, $CDCl_3$) δ_C 145.6, 136.4, 132.4, 127.1, 115.7, 113.9, 61.1, 45.1. IR ν_{max} (neat) 3463, 3336, 2964, 2877, 1622, 1567, 1508, 1418 cm^{-1}, MP 73 – 74 °C (lit: 74 – 75 °C[247]) HRMS (ESI, +ve) *m/z* calcd. for $C_8H_{11}N_2O_3$ 183.0770, found: 183.0734 $(M+H)^+$. Data in accordance with literature.[68]

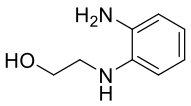

2-((2-hydroxyethyl)amino)-aniline (136)

To a solution of 2-nitro-N-(2-hydroxyethyl)aniline **134** (728 mg, 4 mmol) in MeOH (15 mL) at 0 ºC was added ammonium formate (1.26 g, 20 mmol) followed by 10 wt% palladium on carbon (104 mg). The mixture was allowed to warm to r.t. and stirred for 4 h. The black suspension was then filtered through celite and washed with CH_2Cl_2 (60 mL). The organic layer was washed with saturated $NaHCO_3$ solution (30 mL) followed by brine (30 mL). The organic layer was dried with $MgSO_4$ and solvent was removed *in vacuo* Purification by flash chromatography (EtOAC) gave 2-((2-hydroxyethyl)amino)-aniline **136** (584 mg, 96%) as a white solid. ^{1}H NMR (500 MHz, d^6-DMSO) δ_H 6.60 – 6.37 (m, 4H), 4.66 (t, *J* = 5.5 Hz, 2H), 4.41 (br s, 2H), 4.31 (br s, 1H), 3.60 (apparent q, *J* = 5.5 Hz, 2H), 3.10 – 3.04 (m, 1H); ^{13}C NMR (125 MHz, d^6-DMSO) δ_C 136.7, 135.8, 118.2, 117.4, 114.7, 110.3, 60.1, 46.5; IR ν_{max} (neat) 3403,3342, 3217, 2938, 1604, 1049 cm^{-1}, MP 104 - 105 ˚C (lit: 108 ˚C[248]), HRMS (ESI, +ve) *m/z* calcd. for $C_8H_{13}N_2O$ 153.1028, found: 153.1005 $(M+H)^+$. Data in accordance with literature.[68]

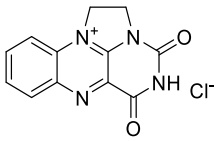

1,10-ethylenealloxazinium chloride (57)

Aniline **136** (200 mg, 1.3 mmol) was dissolved in 5 mL glacial acetic acid and stirred under an atmosphere of N_2. Alloxan monohydrate **138a** (210 mg, 1.3mmol) was added followed by boric acid (82 mg, 1.37 mmol) and the mixture was stirred at 50 °C under N_2 in the dark for 1 h. The suspension was then cooled in ice and rapidly filtered, and the filtrate dried under vacuum. The orange solid obtained was placed under N_2 in the dark and $SOCl_2$ (7 mL) was added slowly. The mixture was then stirred at 50 °C for 18 h. $SOCl_2$ was removed by filtration, washing with CH_2Cl_2, and the yellow was purified by dissolution in formic acid followed by re-precipitation with Et_2O to give 1,10-ethylenealloxazinium chloride **57** (101 mg, 30%) as an orange-brown solid. ^{1}H NMR (500 MHz, 5:1 CF_3CO_2D/CD_3CO_2D) δ_H 8.49 (d, *J* = 8.4 Hz, 1H), 8.31 (t, *J* = 7.7 Hz, 1H), 8.08 (t, *J* = 7.7 Hz, 1H), 8.00 (d, *J* = 8.4 Hz, 1H), 5.49 (t, *J* = 7.6 Hz, 2H), 4.88 (t, *J* = 7.6 Hz, 2H). ^{13}C NMR (125 MHz, 5:1 CF_3CO_2D/CD_3CO_2D) δ_C 158.7, 146.0, 143.2, 141.3, 141.2, 133.2, 132.3, 131.0, 129.5, 116.5, 51.1, 45.1. IR ν_{max} (neat) 3385, 3080, 2937, 2759, 1728, 1633, 1379 cm^{-1} MP 218-220 ˚C (lit = 216 – 219 ˚C) HRMS (ESI, +ve) *m/z* calcd. for $C_{13}H_9N_4O_2$ 241.0720, found: 241.0725 $(M)^+$. Data in accordance with literature.[68]

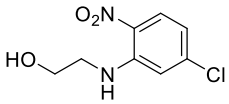

2-(5-chloro-2-nitrophenylamino)ethanol (140)

To a solution of 2,4-dichloro-1-nitrobenzene **139** (5.63 g, 26.1 mmol) in EtOH (100 mL) was added ethanolamine (5.52 mL, 78.3 mmol) followed by K_2CO_3 (3.96 g, 28.7 mmol and the mixture was stirred at 90 °C for 18 h. The reaction was cooled to r.t. and the red solution was poured into 50 mL ice water. The organics were extracted with CH_2Cl_2 (3 x 50 mL) and the combined organic layers were washed with brine (30 mL). The organic layer was dried with $MgSO_4$ and solvent was removed *in vacuo*. The product was purified by column chromatograph (DCM → 9:1 DCM/EtOAC) to give 2-(5-chloro-2-nitrophenylamino)ethanol **140** (1.79 g, 31%) as an orange solid. ^{1}H NMR (500 MHz, $CDCl_3$) δ_H 8.29 (br s, 1H), 8.13 (d, *J* = 9.1 Hz, 1H), 6.89 (d, *J* = 2.2 Hz, 1H), 6.63 (dd, *J* = 9.1, 2.2 Hz, 1H), 3.96 (t, *J* = 5.3 Hz, 2H), 3.48 (apparent q, *J* = 5.3 Hz, 2H), 1.69 (br s, 1H). ^{13}C NMR (125 MHz, $CDCl_3$) δ_C 146.0, 143.0, 128.8, 128.5, 116.3, 113.4, 60.9, 45.1. IR ν_{max} (neat) 3470, 3324, 2964, 2884, 1615, 1562, 1188 cm^{-1}. MP 114 – 117 ˚C (lit = 116 ˚C[248]) HRMS (ESI, +ve) *m/z* calcd. for $C_8H_{10}N_2O_3Cl$ 217.0374, found: 217.0363 $(M+H)^+$. Data in accordance with literature.[68]

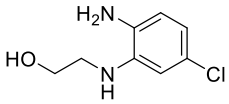

2-((2-hydroxyethyl)amino)-4-chloroaniline (141)

To a suspension of **140** (491 mg, 2.27 mmol) and mossy tin (808 mg, 6.81 mmol) in water (11 mL) at 100 ˚C was added HCl (conc., 4 mL) dropwise. The reaction was then allowed to cool and further cooled in ice for 30 min. The mixture was made basic with 50% NaOH, then extracted with EtOAc (3 x 15 mL), dried with $MgSO_4$ and solvent removed *in vacuo*. **141** (323 mg, 76 %) was obtained as a white solid. ^{1}H NMR (300 MHz, $CDCl_3$) δ_H 7.25 (s, 1H), 6.73 – 6.54 (m, 2H), 3.97 – 3.80 (m, 2H), 3.34 – 3.18 (m, 2H), 2.93 (apparent br s, 3H); ^{13}C NMR (75 MHz, $CDCl_3$) δ_C 138.8, 132.9, 125.8, 118.4, 117.4, 112.1, 61.2, 46.2; IR ν_{max} (neat) 3348, 3324, 2818, 1599, 1418, 1054 cm^{-1}; MP 98 – 100 ˚C (lit = 104 ˚C[248]); HRMS (ESI, +ve) Calcd. for $C_8H_{12}N_2OCl$, 187.0638. Found: 187.0611 $(M+H)^+$. Data in accordance with literature.[68]

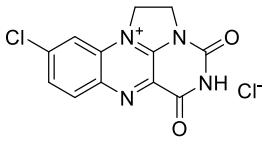

8-chloro-1,10-ethylenealloxazinium chloride (59)

Aniline **141** (300 mg, 1.6 mmol) was dissolved in 5 mL glacial acetic acid and stirred under an atmosphere of N_2. Alloxan monohydrate **138a** (256 mg, 1.6 mmol) was added followed by boric acid (100 mg, 1.65 mmol) and the mixture was stirred at 50 °C under N_2 in the dark for 18 h. The suspension was then cooled in ice and rapidly filtered, and the filtrate dried under vacuum. The orange solid obtained was placed under N_2 in the dark and $SOCl_2$ (5 mL) was added slowly. The mixture was then stirred at 50 °C for 18 h. $SOCl_2$ was removed by filtration, washing with CH_2Cl_2, and the yellow was purified by dissolution in formic acid followed by re-precipitation with Et_2O to give 8-chloro-1,10-ethylenealloxazinium chloride **59** (322 mg, 65%) as a yellow solid. ^{1}H NMR (500 MHz, 5:1 CF_3CO_2D/CD_3CO_2D) δ_H 8.45 – 8.36 (m, 1H), 8.06 – 7.98 (m, 2H), 5.44 (t, *J* = 8.6 Hz, 2H), 4.87 (t, *J* = 8.6 Hz, 2H). ^{13}C NMR (125 MHz, 5:1 CF_3CO_2D/CD_3CO_2D) δ_C 149.8, 145.7, 143.7, 139.8, 134.2, 133.5, 130.5, 116.3, 115.7, 51.1, 45.1. IR ν_{max} (neat) 3444, 3217, 1738, 1375 cm^{-1}. MP >300 ˚ C (lit > 350 ˚C) HRMS (ESI, +ve) *m/z* calcd. for $C_{13}H_8N_4O_2Cl$ 275.0330, found: 241.0321 $(M)^+$

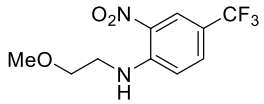

4-(trifluoromethyl)-2-nitro-N-(methoxyethyl)aniline (157)

To a solution of 4-chloro-3-nitrobenzotrifluoride **132** (1.47 mL, 10 mmol) in EtOH (30 mL) was added 2-methoxyethylamine (2.61 mL, 30 mmol) followed by K_2CO_3 (1.38 g, 11 mmol), and the mixture was stirred at 90 °C for 18 h. The reaction was cooled to r.t. and the orange solution was poured into 50 mL ice water. The organics were extracted with CH_2Cl_2 (3 x 50 mL) and the combined organic layers were washed with brine (30 mL). The organic layer was dried with $MgSO_4$ and solvent was removed *in vacuo*. 4-(trifluoromethyl)-2-nitro-N-(2-methoxyethyl)aniline **157** (2.54 g, 96%) was obtained as an orange solid. ^{1}H NMR (300 MHz, $CDCl_3$) δ_H 8.47 (d, J = 1.6 Hz, 1H), 8.44 (br s, 1H), 7.61 (dd, J = 9.1, 1.6 Hz, 1H), 6.96 (d, J = 1.6 Hz, 1H), 3.69 (t, J = 5.3 Hz, 2H), 3.53 (apparent q, J = 5.3 Hz, 2H), 3.44 (s, 3H); ^{13}C NMR (75 MHz, $CDCl_3$) δ_C 147.0, 132.2 (q, $J_{C,F}$ = 3 Hz), 131.3, 125.1 (q, $J_{C,F}$ = 4 Hz), 122.4, 117.6 (q, $J_{C,F}$ = 34 Hz), 114.6, 70.3, 59.3, 43.1; ^{19}F NMR (469 MHz, $CDCl_3$) δ_F -61.9; IR ν_{max} (neat) 3379, 2939, 2902, 1638, 1099 cm^{-1}; MP 101 – 104 ˚C; HRMS (ESI, +ve) Calcd. for $C_{10}H_{12}F_3N_2O_3$, 265.0800. Found: 265.0779 $(M+H)^+$.

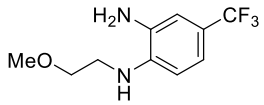

2-((2-hydroxyethyl)amino)-5-(trifluoromethyl)aniline (158)

To a solution of 4-(trifluoromethyl)-2-nitro-N-(methoxyethyl)aniline **157** (802 mg, 3.03 mmol) in EtOH (20 mL) was added palladium on carbon (220 mg), and the flask was filled with an atmosphere of hydrogen. After 2 h the mixture was filtered through celite and washed with CH_2Cl_2. Solvent was removed *in vacuo* and 2-((2-hydroxyethyl)amino)-5-(trifluoromethyl)aniline **158** (710 mg, >99%) was obtained as a white solid. ^{1}H NMR (500 MHz, d^6-DMSO) δ_H 6.88 – 6.80 (m, 2H), 6.57 – 6.49 (m, 1H), 5.03 (br s, 1H), 4.97 (br s, 2H), 3.60 – 3.54 (m, 2H), 3.31 (s, 3H), 3.33 – 3.27 (m, 2H); ^{13}C NMR (125 MHz, d^6-DMSO) δ_C 139.3, 135.6, 156.0 (q, $J_{C,F}$ = 270 Hz), 117.0 (q, $J_{C,F}$ = 32 Hz), 115.0 (q, $J_{C,F}$ = 4 Hz), 110.0 (q, $J_{C,F}$ = 3 Hz), 108.5, 70.7, 58.4, 43.0; ^{19}F NMR (469 MHz, $CDCl_3$) δ_F -59.1; IR ν_{max} (neat)3370, 3317, 3199, 1905, 1329, 1093 cm^{-1}; MP 38 – 41 ˚C; HRMS (ESI, +ve) Calcd. for $C_{10}H_{14}F_3N_2O$, 235.1058. Found: 235.1060 $(M+H^+)$.

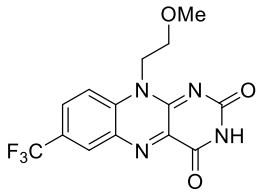

7-(trifluoromethyl)-10-(methoxyethyl)isoalloxazine (159)

2-((2-hydroxyethyl)amino)-5-(trifluoromethyl)aniline **158** (700 mg, 3 mmol) was dissolved in 7 mL glacial acetic acid and stirred under an atmosphere of N_2. Alloxan monohydrate (480 mg, 3 mmol) was added followed by boric acid (200 mg, 3.3 mmol) and the mixture was stirred at 50 °C under N_2 for 1 h. The suspension was then cooled in ice and rapidly filtered, and the filtrate dried under vacuum, washing with CH_2Cl_2. The product was purified by column chromatography (9:1 $CHCl_3$:MeOH), giving **159** as a yellow solid (590 mg, 58%). ^{1}H NMR (500 MHz, d^6-DMSO) δ_H 11.54 (br s, 1H), 8.46 – 8.43 (s, 1H), 8.22 – 8.15 (m, 2H), 4.79 (t, J = 5.3 Hz, 2H), 3.76 (t, J = 5.3 Hz, 2H), 3.24 (s, 3H); ^{13}C NMR (125 MHz, d^6-DMSO) δ_C 159.8, 155.9, 151.5, 141.0, 136.2, 134.2, 130.2 (q, $J_{C,F}$ = 3 Hz), 129.0 (q, $J_{C,F}$ = 4 Hz), 126.1 (q, $J_{C,F}$ = 91 Hz), 122.9, 119.368.9, 59.0, 45.0; ^{19}F NMR (469 MHz, d^6-DMSO) δ_F -60.8; IR ν_{max} (neat) 3042, 2820, 1710, 1660, 1552, 1520, 1132 cm^{-1}; MP 271 – 273 ˚C; HRMS (ESI, +ve) Calcd. for $C_{14}H_{12}F_3N_4O_3$ 341.0862. Found: 341.0846 $(M+H)^+$.

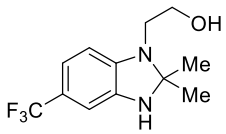

2-[2,2-dimethyl-5-(trifluoromethyl)-2,3-dihydro-1H-1,3-benzodiazol-1-yl]ethan-1-ol (156)

Aniline **137** (1.84 g, 8.4 mmol)was stirred in acetone for 90 minutes at room temperature. Solvent was removed *in vacuo* to give **156** as a solid (1.7 g, 77%) ^{1}H NMR (300 MHz, d^{6}-DMSO) δ_H 6.74 – 6.67 (m, 1H), 6.33 – 6.26 (m, 1H), 6.25 – 6.11 (m, 2H), 4.78 (br s, 1H), 3.50 (t, J = 6.5 Hz, 2H), 3.35 (br s, 1H), 3.15 (t, J = 6.5 Hz, 2H), 1.33 (s, 3H); ^{13}C NMR (75 MHz, d^{6}-DMSO) δ_C 143.7, 139.8, 116.1, 115.8 (q, $J_{C,F}$ = 4 Hz), 100.9, 100.3 (q, $J_{C,F}$ = 3 Hz), 83.0, 76.9, 59.4, 44.7, 26.8 (Some CF couplings may be obscured by other peaks). ^{19}F NMR (469 MHz, $CDCl_3$) δ_F -61.0. IR ν_{max} (neat/cm^{-1}) 3227, 2971, 1458, 1303, 1105 cm^{-1}. HRMS (ESI, +ve) MP 55 – 56 ˚C. *m/z* calcd. for $C_{12}H_{16}F_3N_2O$ 261.1215, found: 261.1217 $(M+H)^+$

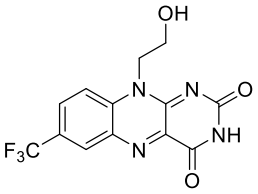

7-(trifluoromethyl)-10-(hydroxyethyl)isoalloxazine (155)

2-((2-hydroxyethyl)amino)-5-(trifluoromethyl)aniline **133**7(700 mg, 3.18 mmol) was dissolved in 6 mL glacial acetic acid and stirred under an atmosphere of N_2. Alloxan monohydrate (430 mg, 3.18 mmol) was added followed by boric acid (173 mg, 3.4 mmol) and the mixture was stirred at 50 °C under N_2 in the dark for 1 h. The suspension was then cooled in ice and rapidly filtered, and the filtrate dried under vacuum. Product was purified by recrystallization from Et_2O/MeOH to give 7-(trifluoromethyl)-10-(hydroxyethyl)isoalloxazine **155** as a yellow solid (701 mg, 68%). ^{1}H NMR (500 MHz, d^{6}-DMSO) δ_H 11.60 (s, 1H) , 8.51 (s, 1H), 8.29 – 8.20 (m, 2H), 4.73 (t, J = 5.8 Hz, 2H), 3.85 (t, J = 5.8 Hz, 2H). ^{13}C NMR (125 MHz, d^{6}-DMSO) δ_C 159.8, 156.0, 140.8, 136.5, 134.3, 130.2 (q, $J_{C,F}$ = 3 Hz), 129.1 (q, $J_{C,F}$ = 3 Hz), 126.2 (q, $J_{C,F}$ = 34 Hz),125.1, 119.4, 57.9, 47.3. ^{19}F NMR (469 MHz, d^{6}-DMSO) δ_F -60.7 (s). IR ν_{max} (neat) 3241, 3011, 2824, 1718, 1594, 1557, 2228. MP 240 – 244 ˚C (decomposition) HRMS (ESI, +ve) *m/z* calcd. for $C_{13}H_{19}F_3N_4O_2Na$ 349.0524, found: 349.0508 $(M+Na)^+$

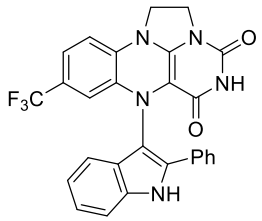

8-(2-phenyl-1H-indol-3-yl)-5-(trifluoromethyl)-1,8,11,13-tetraazatetracyclo[7.6.1.0^{2},^{7}.0^{13},^{16}]hexadeca-2,4,6,9(16)-tetraene-10,12-dione (218)

Flavin **58** (17 mg, 50 µmol) was dissolved in methanol (0.5 mL) and 2-phenylindole **200b** (10 mg, 50 µmol) was added, followed by water (100 µL). After six days, the yellow crystals were washed and decanted with 5:1 MeOH/water (5 x 1 mL), the the product was isolated by column chromatography (100% CH_2Cl_2 → 100% EtOAc + 2% AcOH). **218** was isolated as a yellow solid (1 mg, 4%). ^{1}H NMR (300 MHz, CD_3CN) δ_H 9.67 (s, 9.67, 1H), 8.09 (d, *J* = 7.1 Hz, 2H), 7.95 (d, *J* = 8.0 Hz, 1H), 7.58 – 7.36 (m, 4H), 7.19 (t, *J* = 7.8 Hz, 1H), 7.09 (t, *J* = 7.8 Hz, 1H), 6.96 – 6.89 (m, 1H), 6.50 (d, *J* = 8.0 Hz, 1H), 6.26- 6.22 (m, 1H), 4.15 – 4.04 (m, 2H), 4.02 – 3.70 (br, 2H). ^{13}C NMR (125 MHz, d^{6}-Acetone) δ_C 147.5, 139.0, 138.2, 136.1, 135.0, 132.2, 128.9, 128.5, 128.1, 127.7, 125.5, 125.2 (m), 122.9, 122.2, 120.3, 119.7 (q, $J_{C,F}$ = 4 Hz), 119.6, 117.9, 113.8 (q, $J_{C,F}$ = 4 Hz), 112.7, 111.7, 111.6, 98.3, 45.9, 43.0 (not all C,F coupling resolvable). ^{19}F NMR (471 Hz, d^{6}-Acetone) δ_C -63.4. IR ν_{max} (neat) 3221, 3060, 1718, 1654, 1499, 1331, 1304, 1118. MP 199 – 204 ˚C. HRMS (ESI, -ve) *m/z* calcd. for $C_{27}H_{14}F_3N_5O_2$ 500.1329, found: 500.1331 $(M-H)^-$

General Procedure for kinetic monitoring of imine production using flavin catalysis

Dimethyl sulfide was added to a mixture of flavin catalyst **58**, alloxan monohydrate **138a** and naphthalene (5.1 mg, 40 μmol) in 2,2,2-trifluoroethanol (1 mL). The solution was stirred under air for 10 minutes, then amine was added dropwise by syringe and stirred under air with aliquot samples of ca. 5 μL taken at specified intervals, diluted into ca. 20 μL MeOH in an HPLC vial which was then filled to 1.5 mL with MeCN and analysed by HPLC (UV detection) with naphthalene acting as an internal standard. Standard conditions unless stated to be deviated from were 0.5 M amine, 0.01 M **58** and **138a**, and 5 M Me_2S.

General Procedure for kinetic monitoring of imine production using Cu catalysis

A mixture of alloxan monohydrate **138a**, copper (I) chloride and naphthalene (5.1 mg, 40 μmol) in MeCN (1 mL) was sonicated for 5 mins and amine was added. The reaction was sonicated further under air, with ice added if necessary to maintain the temperature at 30 ˚C, with aliquot samples of ca. 5 μL taken at specified intervals, diluted into ca. 20 μL MeOH in an HPLC vial which was then filled to 1.5 mL with MeCN and analysed by HPLC (UV detection) with naphthalene acting as an internal standard. Standard conditions unless stated to be deviated from were 0.5 M amine, 0.0125 M **138a** and 0.005M CuCl.

General Procedure for kinetic monitoring of indole deuteration

General procedure for kinetic experiments was as those for isolation of deuteroindoles except the contents were placed in an NMR tube and multiple ^1H NMR spectra were automatically gathered without delay using an automation procedure, and ratios of deuteration were measured by integration of the C3 proton relative to another peak. Indole was used for flavin experiments, and 5-chloroindole for those using AcCl.

Unless deviated from, standard conditions were 0.1 mmol indole, 0.5 mL MeOD, 3 mol% flavin and 1.5 mol% AcCl.

DOSY experimental details

Flavin 58**x** was added to 0.5 mL TFE + 50 μL $CDCl_3$ (to lock) and this solution was used for DOSY experiments. Density of TFE was taken as 1.35 mPa.[249]

UV kinetics – Murexide Job Plot experimental details

In a quartz cuvette was placed 2 mL TFE, and flavin and alloxan were added such that the total mole fraction was equal to 10 μmol (equimolar = 1.7 mg flavin **58**, 0.8 mg alloxan **138a**). 180 μL of dimethyl sulfide was added, followed by 27 μL of benzylamine. The solution was rapidly mixed and UV absorbances at 520 nm were collected automatically every second.

Measurement of murexide

Standard conditions were performed for amine oxidation (General procedure B). 30 μL of reaction mixture was dissolved in 2 mL of water and the UV/vis spectrum was taken.

Preparation of aerobic flavin radical 58d

To a solution of flavinium chloride **58** (20 mg, 50 μmol) in 2,2,2-trifluoroethanol (1 mL) was added dimethyl sulfide (370 μL, 5 mmol), and the solution was swirled under air for 1 minute. The solution was then used for EPR analysis. Alternatively, for analysis in deuterated solvent, d_3-2,2,2-trifluoroethanol was instead used.

Preparation of anaerobic flavin radical 58d

To a solution of flavinium chloride **58** (20 mg, 50 μmol) in 2,2,2-trifluoroethanol (1 mL) was added dimethyl sulfide (370 μL, 5 mmol). The solution was purged with nitrogen for 10 minutes, then taken up into a 4 mm X-band EPR tube and opened inside a double-ended Schlenk tube. The solution was frozen and then subjected to four freeze-pump-thaw cycles, then sealed under vacuum and used for EPR analysis. Alternatively, for analysis in deuterated solvent, d_3-2,2,2-trifluoroethanol was instead used.

Preparation of aerobic aminyl radical 172

To a solution of flavinium chloride **58** (20 mg, 50 μmol) and alloxan monohydrate **138a** (4 mg, 25 μmol) in 2,2,2-trifluoroethanol (1 mL) was added dimethyl sulfide (370 μL, 5 mmol), and the solution was swirled under air for 1 minute then left under air for a further 4 minutes. Benzylamine **15a** (55 μL, 0.5 mmol) was added, and the solution was then used for EPR analysis. Alternatively, for analysis in deuterated solvent, d_3-2,2,2-trifluoroethanol was instead used. For experiments with deuterated substrate, $PhCD_2NH_2$ **7** was used in place of benzylamine.

Preparation of anaerobic aminyl radical 172

To a solution of flavinium chloride **58** (20 mg, 50 μmol) and alloxan monohydrate **138a** (4 mg, 25 μmol) in 2,2,2-trifluoroethanol (1 mL) was added dimethyl sulfide (370 μL, 5 mmol), and the solution was purged with nitrogen for 10 minutes. Benzylamine **15a** (55 μL, 0.5 mmol) was added, and the solution was then taken up into a 4 mm X-band EPR tube and opened inside a double-ended Schlenk tube. The solution was frozen and then subjected to four freeze-pump-thaw cycles, then sealed under vacuum and used for EPR analysis. Alternatively, for analysis in deuterated solvent, d_3-2,2,2-trifluoroethanol was instead used. For experiments with deuterated substrate, $PhCD_2NH_2$ **7** was used in place of benzylamine.

EPR samples for investigation of Cu catalysis were prepared according to general procedure D. using **15a**.

8.3 Crystallography Details

Crystal Data for Flavin 58

Basic Structure Description

A single crystal was mounted in paratone oil and flash frozen to 100 K before data collection. The compound crystallises as a formic acid solvate in the monoclinic space group $P2_1/n$ (# 14). The asymmetric unit consists of one flavin cation, one chloride anion and one formic acid solvent molecule. The fused ring system of the flavin adopts a strained planar arrangement, leading to a slightly curved conformation for the cation. A RMS deviation of 0.072 from the mean plane is calculated for the 16 atoms that comprise the phenyl ring system and this curvature appears to be centred above the neighbouring chloride anion. The cation – anion separation in the crystal may be approximated by the distance between the formally charged atoms N(3) and Cl(1), and a N(3) – Cl(1) distance of 3.281 Å is determined between the nearest neighbouring moieties (Figure 2.2).

Single-crystal X-ray data for the compound are displayed in the table below.

Basic Structural Information	
Crystal system	Monoclinic
Space group	$P2_1/n$
Unit cell dimensions	a = 8.1024(3) Å , b = 21.1368(9) Å, c = 9.1023(4) Å , $\alpha = 90^\circ$, β = 99.410(2)° , $\gamma = 90^\circ$
Volume	1537.87(11) Å^3
Z	4
F(000)	792
Completeness (to theta = 27.706°)	99.9%
R(int)	0.038
Largest difference peak and hole	0.632 and -0.327 e Å^{-3}
Final R indices [I>2sigma(I)]	R1 = 0.0368, *w*R2 = 0.0913
Final R indices [all data]	R1 = 0.0477, *w*R2 = 0.0969
Goodness of fit on F^2	1.021
Temperature	100 K
Wavelength	0.7749 Å
Calculated density	1.687 M g m^{-3}
Absorption correction type	Semi-empirical (multi-scan)
Min. and max. transmission	1.0000 and 0.9368
No. of reflections (independent)	26450 (4687)
Data / restraints / parameters	4687 / 0 / 275

Crystal data for flavin indole CT complex

Table 1. Crystal data and structure refinement for s15prr45_twin1_hklf4.

Identification code	chargetransfer	
Empirical formula	C28 H23 Cl F3 N5 O3	
Formula weight	569.96	
Temperature	100(2) K	
Wavelength	0.71073 Å	
Crystal system	Monoclinic	
Space group	P 21/c	
Unit cell dimensions	a = 6.6629(7) Å	α= 90°.
	b = 25.004(3) Å	β= 97.810(12)°.
	c = 14.956(2) Å	γ = 90°.
Volume	2468.6(5) $Å^3$	
Z	4	
Density (calculated)	1.534 Mg/m^3	
Absorption coefficient	0.221 mm^{-1}	
F(000)	1176	
Crystal size	0.300 x 0.030 x 0.020 mm^3	
Theta range for data collection	3.305 to 25.361°.	
Index ranges	-8<=h<=8, -28<=k<=30, -17<=l<=18	
Reflections collected	16521	
Independent reflections	4402 [R(int) = 0.2129]	
Completeness to theta = 25.000°	98.5 %	
Absorption correction	Semi-empirical from equivalents	
Max. and min. transmission	1.00000 and 0.59274	
Refinement method	Full-matrix least-squares on F^2	
Data / restraints / parameters	4402 / 2 / 297	
Goodness-of-fit on F^2	0.947	
Final R indices [I>2sigma(I)]	R1 = 0.0947, wR2 = 0.1995	
R indices (all data)	R1 = 0.2040, wR2 = 0.2517	
Extinction coefficient	n/a	
Largest diff. peak and hole	0.516 and -0.525 $e.Å^{-3}$	

Crystal data for flavin indole covalently bonded adduct 218

Table 1. Crystal data and structure refinement for new.

Identification code	adduct	
Empirical formula	C69 H48 F6 N11 O5	
Formula weight	1225.18	
Temperature	100(2) K	
Wavelength	0.71073 Å	
Crystal system	Triclinic	
Space group	P -1	
Unit cell dimensions	a = 11.4992(8) Å	α= 80.075(4)°.
	b = 13.2277(6) Å	β= 80.054(5)°.
	c = 20.0327(10) Å	γ = 76.358(5)°.
Volume	2889.0(3) $Å^3$	
Z	2	
Density (calculated)	1.408 Mg/m^3	
Absorption coefficient	0.105 mm^{-1}	
F(000)	1266	
Crystal size	0.2 x 0.13 x 0.11 mm^3	
Theta range for data collection	3.336 to 28.591°.	
Index ranges	-15<=h<=14, -16<=k<=17, -22<=l<=26	
Reflections collected	16101	
Independent reflections	11557 [R(int) = 0.0593]	
Completeness to theta = 25.000°	99.1 %	
Absorption correction	Semi-empirical from equivalents	
Max. and min. transmission	1.00000 and 0.73001	
Refinement method	Full-matrix least-squares on F^2	
Data / restraints / parameters	11557 / 49 / 711	
Goodness-of-fit on F^2	0.978	
Final R indices [I>2sigma(I)]	R1 = 0.0916, wR2 = 0.2204	
R indices (all data)	R1 = 0.1753, wR2 = 0.3127	
Extinction coefficient	0.0049(13)	
Largest diff. peak and hole	0.622 and -0.472 $e.Å^{-3}$	

9. Bibliography

(1) Mattevi, A. *Trends Biochem. Sci.* **2006**, *31*, 276.
(2) Macheroux, P.; Kappes, B.; Ealick, S. E. *FEBS J.* **2011**, *278*, 2625.
(3) Serrell, W. H.; Butler, R. E. *Public Health Reports* **1939**, *54*, 2121.
(4) Johansson, L. B. A.; Davidsson, A.; Lindblom, G.; Naqvi, K. R. *Biochemistry* **1979**, *18*, 4249.
(5) Kis, K.; Volk, R.; Bacher, A. *Biochemistry* **1995**, *34*, 2883.
(6) Zheng, Y.-J.; Jordan, D. B.; Liao, D.-I. *Bioorg. Chem.* **2003**, *31*, 278.
(7) Alberts, B., et al. *Essential Cell Biology*; Garland Publishing: New York, 1997.
(8) McMurry, J.; Begley, T. *The Organic Chemistry of Biological Pathways*; Roberts and Company: Englewood, Colorado, 2005.
(9) Fisher, A. J.; Thompson, T. B.; Thoden, J. B.; Baldwin, T. O.; Rayment, I. *J. Biol. Chem.* **1996**, *271*, 21956.
(10) Binda, C.; Newton-Vinson, P.; Hubalek, F.; Edmondson, D. E.; Mattevi, A. *Nat. Struct. Mol. Biol.* **2002**, *9*, 22.
(11) Hajjar, N.; Hodgson, E. *Science* **1980**, *209*, 1134.
(12) Smith, J. R. L.; Jerina, D. M.; Kaufman, S.; Milstein, S. *J. Chem. Soc., Chem. Commun.* **1975**, 881.
(13) Jones, K. C.; Ballou, D. P. *J. Biol. Chem.* **1986**, *261*, 2553.
(14) Massey, V. *J. Biol. Chem.* **1994**, *269*, 22459.
(15) Baldwin, T. O.; Christopher, J. A.; Raushel, F. M.; Sinclair, J. F.; Ziegler, M. M.; Fisher, A. J.; Rayment, I. *Curr. Opin. Struct. Biol.* **1995**, *5*, 798.
(16) Tipton, K. F.; Boyce, S.; O'Sullivan, J.; Davey, G. P.; Healy, J. *Curr. Med. Chem.* **2004**, *11*, 1965.
(17) McEwen, C. M. *J. Biol. Chem.* **1965**, *240*, 2003.
(18) Edmondson, D. E.; Binda, C.; Wang, J.; Upadhyay, A. K.; Mattevi, A. *Biochemistry* **2009**, *48*, 4220.
(19) Tan, A. K.; Ramsay, R. R. *Biochemistry* **1993**, *32*, 2137.
(20) McDermott, R.; Tingley, D.; Cowden, J.; Frazzetto, G.; Johnson, D. D. P. *Proc. Natl. Acad. Sci. U. S. A.* **2009**, *106*, 2118.
(21) Barber, N. In *The Human Beast*; Psychology Today: 2010; Vol. 2014.
(22) Quitkin, F.; Rifkin, A.; Klein, D. F. *Archives of General Psychiatry* **1979**, *36*, 749.
(23) Livingston, M.; Livingston, H. *Drug-Safety* **1996**, *14*, 219.
(24) Youdim, M.; Riederer, P. *Monoamine Oxidases and their Inhibitors*; Elsevier Science, 2011.
(25) Stahl, S. M. a. F., Angela *CNS Spectrums* **2009**, *13*, 855.
(26) Kennedy, S. H. *Journal of Psychiatry and Neuroscience* **1997**, *22*, 127.
(27) Fernandez, H. H.; Chen, J. J. *Pharmacotherapy: The Journal of Human Pharmacology and Drug Therapy* **2007**, *27*, 174S.
(28) Youdim, M. B. H.; Edmondson, D.; Tipton, K. F. *Nat. Rev. Neurosci.* **2006**, *7*, 295.
(29) Riederer, P.; Lachenmayer, L.; Laux, G. *Curr. Med. Chem.* **2004**, *11*, 2033.
(30) Liang, Y.; Quenelle, D.; Vogel, J. L.; Mascaro, C.; Ortega, A.; Kristie, T. M. *mBio* **2013**, *4*.
(31) Bird, A. *Nature* **2007**, *447*, 396.
(32) Edmondson, D. E.; Binda, C.; Mattevi, A. *Arch. Biochem. Biophys.* **2007**, *464*, 269.
(33) Silverman, R. B. *Acc. Chem. Res.* **1995**, *28*, 335.
(34) Davis, G. C.; Williams, A. C.; Markey, S. P.; Ebert, M. H.; Caine, E. D.; Reichert, C. M.; Kopin, I. J. *Psychiatry Research* **1979**, *1*, 249.
(35) Sian, J., Youdim, M. B. H., Riederer, P., Gerlach, M. In *Basic Neurochemistry: Molecular, Cellular and Medical Aspects*; 6 ed.; Lipincott-Raven: Philadelphia, 1999.
(36) Silverman, R. B.; Zieske, P. A. *Biochem. Biophys. Res. Commun.* **1986**, *135*, 154.

(37) Silverman, R. B.; Zieske, P. A. *Biochemistry* **1986**, *25*, 341.
(38) Silverman, R. B.; Zhou, J. P.; Eaton, P. E. *J. Am. Chem. Soc.* **1993**, *115*, 8841.
(39) Tan, A.; Glantz, M. D.; Piette, L. H.; Yasunobu, K. T. *Biochem. Biophys. Res. Commun.* **1983**, *117*, 517.
(40) Husain, M.; Edmondson, D. E.; Singer, T. P. *Biochemistry* **1982**, *21*, 595.
(41) Simpson, J. T.; Krantz, A.; Lewis, F. D.; Kokel, B. *J. Am. Chem. Soc.* **1982**, *104*, 7155.
(42) MacMillar, S.; Edmondson, D. E.; Matsson, O. *J. Am. Chem. Soc.* **2011**, *133*, 12319.
(43) Cottrell, T. L. *The Strength of Chemical Bonds*; 2nd ed.; Butterworth and co.: London, 1958.
(44) Pearce, L. B.; Roth, J. A. *Biochemistry* **1985**, *24*, 1821.
(45) Wang, J.; Edmondson, D. E. *Biochemistry* **2011**, *50*, 7710.
(46) Orru, R.; Aldeco, M.; Edmondson, D. E. *J Neural Transm* **2013**, *120*, 847.
(47) Geha, R. M.; Chen, K.; Wouters, J.; Ooms, F.; Shih, J. C. *J. Biol. Chem.* **2002**, *277*, 17209.
(48) De Colibus, L.; Li, M.; Binda, C.; Lustig, A.; Edmondson, D. E.; Mattevi, A. *Proc. Natl. Acad. Sci. U. S. A.* **2005**, *102*, 12684.
(49) Li, M.; Binda, C.; Mattevi, A.; Edmondson, D. E. *Biochemistry* **2006**, *45*, 4775.
(50) Røhr, Å. K.; Hersleth, H.-P.; Andersson, K. K. *Angew. Chem. Int. Ed.* **2010**, *49*, 2324.
(51) Kemal, C.; Bruice, T. C. *Proc. Natl. Acad. Sci. U. S. A.* **1976**, *73*, 995.
(52) Bruice, T. C.; Noar, J. B.; Ball, S. S.; Venkataram, U. V. *J. Am. Chem. Soc.* **1983**, *105*, 2452.
(53) Oae, S.; Asada, K. O.; Yoshimura, T.; Fujimori, K. *Heterocycles* **1992**, *33*, 189.
(54) Murahashi, S.; Oda, T.; Masui, Y. *J. Am. Chem. Soc.* **1989**, *111*, 5002.
(55) Imada, Y.; Iida, H.; Ono, S.; Murahashi, S.-I. *J. Am. Chem. Soc.* **2003**, *125*, 2868.
(56) Sánchez, M. A.; Mainar, A. M.; Pardo, J. I.; López, M. C.; Urieta, J. S. *Can. J. Chem.* **2001**, *79*, 1460.
(57) Marsh, B. J.; Carbery, D. R. *Tetrahedron Lett.* **2010**, *51*, 2362.
(58) Žurek, J.; Cibulka, R.; Dvořáková, H.; Svoboda, J. *Tetrahedron Lett.* **2010**, *51*, 1083.
(59) Imada, Y.; Kitagawa, T.; Wang, H.-K.; Komiya, N.; Naota, T. *Tetrahedron Lett.* **2013**, *54*, 621.
(60) Murahashi, S.-I.; Zhang, D.; Iida, H.; Miyawaki, T.; Uenaka, M.; Murano, K.; Meguro, K. *Chem. Commun.* **2014**, *50*, 10295.
(61) Laird, T. *Org. Process Res. Dev.* **2010**, *14*, 1479.
(62) Kotoucova, H.; Strnadova, I.; Kovandova, M.; Chudoba, J.; Dvorakova, H.; Cibulka, R. *Org. Biomol. Chem.* **2014**, *12*, 2137.
(63) Mazzini, C.; Lebreton, J.; Furstoss, R. *J. Org. Chem.* **1996**, *61*, 8.
(64) Imada, Y.; Iida, H.; Murahashi, S.-I.; Naota, T. *Angew. Chem. Int. Ed.* **2005**, *44*, 1704.
(65) Chen, S.; Hossain, M. S.; Foss, F. W. *Org. Lett.* **2012**, *14*, 2806.
(66) Chen, S.; Foss, F. W. *Org. Lett.* **2012**, *14*, 5150.
(67) Eswaramoorthy, S.; Bonanno, J. B.; Burley, S. K.; Swaminathan, S. *Proc. Natl. Acad. Sci. U. S. A.* **2006**, *103*, 9832.
(68) Li, W.-S.; Zhang, N.; Sayre, L. M. *Tetrahedron* **2001**, *57*, 4507.
(69) Lindén, A. A.; Hermanns, N.; Ott, S.; Krüger, L.; Bäckvall, J.-E. *Chem. Eur. J.* **2005**, *11*, 112.
(70) Kim, J. M.; Bogdan, M. A.; Mariano, P. S. *J. Am. Chem. Soc.* **1993**, *115*, 10591.
(71) Kim, J. M.; Cho, I. S.; Mariano, P. S. *J. Org. Chem.* **1991**, *56*, 4943.
(72) Li, W.-S.; Sayre, L. M. *Tetrahedron* **2001**, *57*, 4523.
(73) Chen, S.; Hossain, M. S.; Foss, F. W. *ACS Sustainable Chemistry & Engineering* **2013**, *1*, 1045.
(74) Heelis, P. F. *Chem. Soc. Rev.* **1982**, *11*, 15.

(75) Lechner, R.; König, B. *Synthesis* **2010**, *2010*, 1712.
(76) VanRheenen, V.; Kelly, R. C.; Cha, D. Y. *Tetrahedron Lett.* **1976**, *17*, 1973.
(77) Jacobsen, E. N.; Marko, I.; Mungall, W. S.; Schroeder, G.; Sharpless, K. B. *J. Am. Chem. Soc.* **1988**, *110*, 1968.
(78) Jonsson, S. Y.; Färnegårdh, K.; Bäckvall, J.-E. *J. Am. Chem. Soc.* **2001**, *123*, 1365.
(79) Yano, Y.; Tamura, Y.; Hoshino, Y.; Tagaki, W. *Bull. Chem. Soc. Jpn.* **1980**, *53*, 2340.
(80) Yano, Y.; Hoshino, Y.; Tagaki, W. *Chem. Lett.* **1980**, *9*, 749.
(81) Miyashita, A.; Suzuki, Y.; Nagasaki, I.; Ishiguro, C.; Iwamoto, K.-i.; Higashino, T. *Chem. Pharm. Bull.* **1997**, *45*, 1254.
(82) Tam, S. W.; Jimenez, L.; Diederich, F. *J. Am. Chem. Soc.* **1992**, *114*, 1503.
(83) Iwahana, S.; Iida, H.; Yashima, E. *Chem. Eur. J.* **2011**, *17*, 8009.
(84) Shinkai, S.; Yamaguchi, T.; Manabe, O.; Toda, F. *J. Chem. Soc., Chem. Commun.* **1988**, 1399.
(85) Jurok, R.; Cibulka, R.; Dvořáková, H.; Hampl, F.; Hodačová, J. *Eur. J. Org. Chem.* **2010**, *2010*, 5217.
(86) Iida, H.; Iwahana, S.; Mizoguchi, T.; Yashima, E. *J. Am. Chem. Soc.* **2012**, *134*, 15103.
(87) Murahashi, S.-I.; Ono, S.; Imada, Y. *Angew. Chem. Int. Ed.* **2002**, *41*, 2366.
(88) Shuklov, I. A.; Dubrovina, N. V.; Börner, A. *Synthesis* **2007**, *2007*, 2925.
(89) Carbery, D. R. In *Comprehensive Organic Synthesis II (Second Edition)*; Knochel, P., Ed.; Elsevier: Amsterdam, 2014, p 632.
(90) Pasto, D. J.; Taylor, R. T. In *Organic Reactions*; John Wiley & Sons, Inc.: 2004.
(91) Cusack, N. J.; Reese, C. B.; Risius, A. C.; Roozepeikar, B. *Tetrahedron* **1976**, *32*, 2157.
(92) Marsh, B. J.; Carbery, D. R. *J. Org. Chem.* **2009**, *74*, 3186.
(93) Imada, Y.; Iida, H.; Naota, T. *J. Am. Chem. Soc.* **2005**, *127*, 14544.
(94) Imada, Y.; Kitagawa, T.; Ohno, T.; Iida, H.; Naota, T. *Org. Lett.* **2009**, *12*, 32.
(95) Smit, C.; Fraaije, M. W.; Minnaard, A. J. *J. Org. Chem.* **2008**, *73*, 9482.
(96) Marsh, B. J.; Heath, E. L.; Carbery, D. R. *Chem. Commun.* **2011**, *47*.
(97) Richardson, R. D.; Wirth, T. *Angew. Chem. Int. Ed.* **2006**, *45*, 4402.
(98) Dohi, T.; Maruyama, A.; Yoshimura, M.; Morimoto, K.; Tohma, H.; Kita, Y. *Angew. Chem. Int. Ed.* **2005**, *44*, 6193.
(99) Thottumkara, A. P.; Bowsher, M. S.; Vinod, T. K. *Org. Lett.* **2005**, *7*, 2933.
(100) More, J. D.; Finney, N. S. *Org. Lett.* **2002**, *4*, 3001.
(101) Kemal, C.; Bruice, T. C. *J. Am. Chem. Soc.* **1977**, *99*, 7064.
(102) Gelalcha, F. G. *Chem. Rev.* **2007**, *107*, 3338.
(103) Murray, A. T.; Matton, P.; Fairhurst, N. W. G.; John, M. P.; Carbery, D. R. *Org. Lett.* **2012**, *14*, 3656.
(104) Daďová, J.; Kümmel, S.; Feldmeier, C.; Cibulková, J.; Pažout, R.; Maixner, J.; Gschwind, R. M.; König, B.; Cibulka, R. *Chem. Eur. J.* **2013**, *19*, 1066.
(105) Payne, G. B.; Deming, P. H.; Williams, P. H. *J. Org. Chem.* **1961**, *26*, 659.
(106) Sato, K.; Hyodo, M.; Takagi, J.; Aoki, M.; Noyori, R. *Tetrahedron Lett.* **2000**, *41*, 1439.
(107) Fan; Germann, M. W.; Gadda, G. *Biochemistry* **2006**, *45*, 1979.
(108) Fan; Gadda, G. *J. Am. Chem. Soc.* **2005**, *127*, 2067.
(109) Humbert, J.; Hammond, K.; Hathaway, W.; Marcoux, J.; O'Brien, D. *The Lancet* **1970**, *296*, 770.
(110) *Justus Liebigs Annalen der Chemie* **1841**, *38*, 357.
(111) Shaw Dunn, J.; Sheehan, H. L.; McLetchie, N. G. B. *The Lancet* **1943**, *241*, 484.
(112) Lenzen, S. *Diabetologia* **2008**, *51*, 216.
(113) Otsuji, Y.; Wake, S.; Imoto, E. *Tetrahedron* **1970**, *26*, 4139.
(114) Schmittel, M.; Lal, M.; Lal, R.; Röck, M.; Langels, A.; Rappoport, Z.; Basheer, A.; Schlirf, J.; Deiseroth, H.-J.; Flörke, U.; Gescheidt, G. *Tetrahedron* **2009**, *65*, 10842.

(115) Czerwińska, M.; Sikora, A.; Szajerski, P.; Adamus, J.; Marcinek, A.; Gębicki, J.; Bednarek, P. *J. Phys. Chem. A* **2006**, *110*, 7272.
(116) Wendlandt, A. E.; Stahl, S. S. *Org. Lett.* **2012**, *14*, 2850.
(117) Zhang, E.; Tian, H.; Xu, S.; Yu, X.; Xu, Q. *Org. Lett.* **2013**, *15*, 2704.
(118) Largeron, M.; Fleury, M.-B. *Angew. Chem. Int. Ed.* **2012**, *51*, 5409.
(119) Osowska, K.; Miljanić, O. Š. *J. Am. Chem. Soc.* **2010**, *133*, 724.
(120) Belowich, M. E.; Stoddart, J. F. *Chem. Soc. Rev.* **2012**, *41*, 2003.
(121) Carrington, A.; MacLachlan, A. D. *Introduction to Magnetic Resonance*; Chapman and Hall: London, 1979.
(122) Odom, B.; Hanneke, D.; D'Urso, B.; Gabrielse, G. *Phys. Rev. Lett.* **2006**, *97*, 030801.
(123) Gerson, F.; Huber, W. *Electron Spin Resonance Spectroscopy of Organic Radicals*; Wiley-VCH, 2003.
(124) Kevan, L.; Bowman, M. K. *Modern Pulsed and Continuous-Wave Electron Spin Resonance*; Wiley-Interscience: New York, 1990.
(125) Schweiger, A.; Jeschke, G. *Principles of Pulse Electron Paramagnetic Resonance Spectroscopy*; Oxford University Press, 2001.
(126) Höfer, P.; Grupp, A.; Nebenführ, H.; Mehring, M. *Chem. Phys. Lett.* **1986**, *132*, 279.
(127) Dikanov, S. A.; R., C. A. In *Handbook of Applied Solid State Spectroscopy*; R., V. D., Ed.; Springer Science + Business Media: LLC, NY, USA, 2006, p 97.
(128) Dikanov, S. A.; Tsevtkov, Y. D. *Electron Spin Echo Envelope Modulation (ESEEM) Spectroscopy*; CRC Press: Boca Raton, 1992.
(129) Dikanov, S. A.; Tsvetkov, Y. D.; Bowman, M. K.; Astashkin, A. V. *Chem. Phys. Lett.* **1982**, *90*, 149.
(130) Flanagan, H. L.; Singel, D. J. *J. Chem. Phys.* **1987**, *87*, 5606.
(131) Brunelle, P.; Rauk, A. *J. Phys. Chem. A* **2004**, *108*, 11032.
(132) Hennig, M.; Munzarová, M. L.; Bermel, W.; Scott, L. G.; Sklenář, V.; Williamson, J. R. *J. Am. Chem. Soc.* **2006**, *128*, 5851.
(133) Landler, K. J. *Chemical Kinetics*; 3 ed.; HarperCollins: New York, 1987.
(134) Logan, S. R. *Fundamentals of Chemical Kinetics*; Longman Group: Harlow, 1996.
(135) Connors, K. A. *Chemical Kinetics: The study of reaction rates in solution*; VCH: New York, 1990.
(136) Liu, L.; Wang, Z.; Fu, X.; Yan, C.-H. *Org. Lett.* **2012**, *14*, 5692.
(137) Heuts, D. P. H. M.; Scrutton, N. S.; McIntire, W. S.; Fraaije, M. W. *FEBS J.* **2009**, *276*, 3405.
(138) Anslyn, E. V.; Dougherty, D. A. *Modern Physical Organic Chemistry*; University Science Books: Sausalito, 2006.
(139) Anderson, R. S.; Huang, L.; Iannone, R.; Rudolph, J. *J. Phys. Chem. A* **2007**, *111*, 495.
(140) Kurtz, K. A.; Rishavy, M. A.; Cleland, W. W.; Fitzpatrick, P. F. *J. Am. Chem. Soc.* **2000**, *122*, 12896.
(141) Hammett, L. P. *J. Am. Chem. Soc.* **1937**, *59*, 96.
(142) Huang, C. Y. In *Methods Enzymol.*; Daniel, L. P., Ed.; Academic Press: 1982; Vol. Volume 87, p 509.
(143) Morris, G. A. In *eMagRes*; John Wiley & Sons, Ltd: 2007.
(144) Evans, R.; Deng, Z.; Rogerson, A. K.; McLachlan, A. S.; Richards, J. J.; Nilsson, M.; Morris, G. A. *Angew. Chem. Int. Ed.* **2013**, *52*, 3199.
(145) http://nmr.chemistry.manchester.ac.uk/?q=node/290 - Accessed 24/03/15
(146) Einstein, A. *Annalen der Physik* **1905**, *322*, 549.
(147) Wang, X.; Mallory, F. B.; Mallory, C. W.; Beckmann, P. A.; Rheingold, A. L.; Francl, M. M. *J. Phys. Chem. A* **2006**, *110*, 3954.
(148) Macheroux, P. In *Flavoprotein Protocols*; Chapman, S., Reid, G., Eds.; Humana Press: 1999; Vol. 131, p 1.

(149) Miller, J. R.; Edmondson, D. E.; Grissom, C. B. *J. Am. Chem. Soc.* **1995**, *117*, 7830.
(150) Gutierrez, A.; Lian, L.-Y.; Wolf, C. R.; Scrutton, N. S.; Roberts, G. C. K. *Biochemistry* **2001**, *40*, 1964.
(151) Gibson, Q. H.; Swoboda, B. E. P.; Massey, V. *J. Biol. Chem.* **1964**, *239*, 3927.
(152) NAKAMURA, S.; NAKAMURA, T.; OGURA, Y. *J. Biochem. (Tokyo, Jpn.)* **1963**, *53*, 143.
(153) Miller, L. L.; Nordblom, G. D.; Mayeda, E. A. *J. Org. Chem.* **1972**, *37*, 916.
(154) Wöhler, F.; Liebig, J. *Annalen der Pharmacie* **1838**, *26*, 241.
(155) Hartley, W. N. *Journal of the Chemical Society, Transactions* **1905**, *87*, 1791.
(156) Barrabass, S.; Stickdorn, K.; Knoche, W. *J. Chem. Soc., Faraday Trans.* **1995**, *91*, 637.
(157) Hansch, C.; Gao, H. *Chem. Rev.* **1997**, *97*, 2995.
(158) Minisci, F.; Recupero, F.; Cecchetto, A.; Gambarotti, C.; Punta, C.; Faletti, R.; Paganelli, R.; Pedulli, Gian F. *Eur. J. Org. Chem.* **2004**, *2004*, 109.
(159) Scaiano, J. C. *J. Phys. Chem.* **1981**, *85*, 2851.
(160) Ingold, K. U. *Acc. Chem. Res.* **1969**, *2*, 1.
(161) Wohlfarth, C. In *Supplement to IV/6*; Lechner, M. D., Ed.; Springer Berlin Heidelberg: 2008; Vol. 17, p 116.
(162) Baskin, S.; Salem, H. *Oxidants, Antioxidants And Free Radicals*; CRC Press, 1997.
(163) Winterbourn, C. C. *Biochem. J.* **1979**, *182*, 625.
(164) Hector, L. G.; Schultz, H. L. *J. Appl. Phys.* **1936**, *7*, 133.
(165) Nadezhdin, A.; Dunford, H. B. *J. Phys. Chem.* **1979**, *83*, 1957.
(166) Grankvist, K.; Marklund, S.; Sehlin, J.; Taljedal, I. B. *Biochem. J.* **1979**, *182*, 17.
(167) Srogl, J.; Voltrova, S. *Org. Lett.* **2009**, *11*, 843.
(168) Moser, C. C.; Keske, J. M.; Warncke, K.; Farid, R. S.; Dutton, P. L. *Nature* **1992**, *355*, 796.
(169) Rigby, S. E. J.; Hynson, R. M. G.; Ramsay, R. R.; Munro, A. W.; Scrutton, N. S. *J. Biol. Chem.* **2004**, *280*, 4627.
(170) Roth, J. P.; Klinman, J. P. *Proc. Natl. Acad. Sci. U.S.A.* **2003**, *100*, 62.
(171) Winterbourn, C. C.; Munday, R. *Biochem. Pharmacol.* **1989**, *38*, 271.
(172) Fenton, H. J. H. *Journal of the Chemical Society, Transactions* **1894**, *65*, 899.
(173) Haber, F.; Weiss, J. *Naturwissenschaften* **1932**, *20*, 948.
(174) Fischer, L. J.; Hamburger, S. A. *Diabetes* **1980**, *29*, 213.
(175) Buffoni, F.; Blaschko, H. *Benzylamine Oxidase and Histaminase: Purification and Crystallization of an Enzyme from Pig Plasma*, 1964; Vol. 161.
(176) Hauge, J. G. *J. Biol. Chem.* **1964**, *239*, 3630.
(177) Zhu, Z.; Davidson, V. L. *J. Biol. Chem.* **1998**, *273*, 14254.
(178) Klinman, J. P. *Biochimica et Biophysica Acta (BBA) - Proteins and Proteomics* **2003**, *1647*, 131.
(179) Mure, M.; Mills, S. A.; Klinman, J. P. *Biochemistry* **2002**, *41*, 9269.
(180) Largeron, M.; Fleury, M.-B. *J. Org. Chem.* **2000**, *65*, 8874.
(181) Yuan, H.; Yoo, W.-J.; Miyamura, H.; Kobayashi, S. *J. Am. Chem. Soc.* **2012**, *134*, 13970.
(182) Saifer, A.; Oreskes, I. *Anal. Chem.* **1956**, *28*, 501.
(183) Eckert, T. S.; Bruice, T. C. *J. Am. Chem. Soc.* **1983**, *105*, 4431.
(184) Corey, E. J.; Mock, W. L.; Pasto, D. J. *Tetrahedron Lett.* **1961**, *2*, 347.
(185) Hansch, M.; Illa, O.; McGarrigle, E. M.; Aggarwal, V. K. *Chem. Asian. J.* **2008**, *3*, 1657.
(186) Gray, P.; Thynne, J. C. J. *Transactions of the Faraday Society* **1964**, *60*, 1047.
(187) Hayon, E.; Simic, M. *J. Am. Chem. Soc.* **1972**, *94*, 42.
(188) Sharma, V.; Kumar, P.; Pathak, D. *J. Heterocycl. Chem.* **2010**, *47*, 491.
(189) Fuentes, J. A.; Longo, V. G. *Neuropharmacology* **1971**, *10*, 15.
(190) Yeh, E.; Cole, L. J.; Barr, E. W.; Bollinger, J. M.; Ballou, D. P.; Walsh, C. T. *Biochemistry* **2006**, *45*, 7904.

(191) Nishizawa, T.; Grüschow, S.; Jayamaha, D.-H. E.; Nishizawa-Harada, C.; Sherman, D. H. *J. Am. Chem. Soc.* **2006**, *128*, 724.
(192) Zhao, Y.; Christensen, S. K.; Fankhauser, C.; Cashman, J. R.; Cohen, J. D.; Weigel, D.; Chory, J. *Science* **2001**, *291*, 306.
(193) Wilson, J. E. *Biochemistry* **1966**, *5*, 1351.
(194) Kommoju, P.-R.; Bruckner, R. C.; Ferreira, P.; Jorns, M. S. *Biochemistry* **2009**, *48*, 6951.
(195) Bruckner, R. C.; Zhao, G.; Ferreira, P.; Jorns, M. S. *Biochemistry* **2006**, *46*, 819.
(196) Breinlinger, E. C.; Rotello, V. M. *J. Am. Chem. Soc.* **1997**, *119*, 1165.
(197) Inoue, M.; Shibata, M.; Kondo, Y.; Ishida, T. *Biochemistry* **1981**, *20*, 2936.
(198) Zanetti-Polzi, L.; Marracino, P.; Aschi, M.; Daidone, I.; Fontana, A.; Apollonio, F.; Liberti, M.; D'Inzeo, G.; Amadei, A. *Theor. Chem. Acc.* **2013**, *132*, 1.
(199) Boyd, A. S. F.; Carroll, J. B.; Cooke, G.; Garety, J. F.; Jordan, B. J.; Mabruk, S.; Rosair, G.; Rotello, V. M. *Chem. Commun.* **2005**, 2468.
(200) McDonald, N. A.; Subramani, C.; Caldwell, S. T.; Zainalabdeen, N. Y.; Cooke, G.; Rotello, V. M. *Tetrahedron Lett.* **2011**, *52*, 2107.
(201) Huvaere, K.; Skibsted, L. H. *J. Am. Chem. Soc.* **2009**, *131*, 8049.
(202) Martin, C. B.; Tsao, M.-L.; Hadad, C. M.; Platz, M. S. *J. Am. Chem. Soc.* **2002**, *124*, 7226.
(203) Ahmad, M.; Jarillo, J. A.; Smirnova, O.; Cashmore, A. R. *Nature* **1998**, *392*, 720.
(204) Horst, G. T. J. v. d.; Muijtjens, M.; Kobayashi, K.; Takano, R.; Kanno, S.-i.; Takao, M.; Wit, J. d.; Verkerk, A.; Eker, A. P. M.; Leenen, D. v.; Buijs, R.; Bootsma, D.; Hoeijmakers, J. H. J.; Yasui, A. *Nature* **1999**, *398*, 627.
(205) Liedvogel, M.; Maeda, K.; Henbest, K.; Schleicher, E.; Simon, T.; Timmel, C. R.; Hore, P. J.; Mouritsen, H. *PLoS One* **2007**, *2*, e1106.
(206) Liedvogel, M.; Mouritsen, H. *J. R. Soc. Interface* **2010**, *7*, S147.
(207) Niu, T.; Zhang, Y. *Tetrahedron Lett.* **2010**, *51*, 6847.
(208) Katsnelson, A. *Nat Med* **2013**, *19*, 656.
(209) Belleau, B.; Burba, J.; Pindell, M.; Reiffenstein, J. *Science* **1961**, *133*, 102.
(210) Braman, V.; Graham, P.; Cheng, C.; Turnquist, D.; Harnett, M.; Sabounjian, L.; Shipley, J. *Clinical Pharmacology in Drug Development* **2013**, *2*, 53.
(211) Lin, S.; Jacobsen, E. N. *Nat Chem* **2012**, *4*, 817.
(212) Gröll, B.; Schnürch, M.; Mihovilovic, M. D. *J. Org. Chem.* **2012**, *77*, 4432.
(213) Rittle, J.; Green, M. T. *Science* **2010**, *330*, 933.
(214) Shilcrat, S. *Org. Process Res. Dev.* **2011**, *15*, 1464.
(215) Chen, M. S.; White, M. C. *Science* **2007**, *318*, 783.
(216) Xia, Z. X.; Shamala, N.; Bethge, P. H.; Lim, L. W.; Bellamy, H. D.; Xuong, N. H.; Lederer, F.; Mathews, F. S. *Proc. Natl. Acad. Sci. U. S. A.* **1987**, *84*, 2629.
(217) Pouy, M. J.; Milczek, E. M.; Figg, T. M.; Otten, B. M.; Prince, B. M.; Gunnoe, T. B.; Cundari, T. R.; Groves, J. T. *J. Am. Chem. Soc.* **2012**, *134*, 12920.
(218) Lo, J. C.; Yabe, Y.; Baran, P. S. *J. Am. Chem. Soc.* **2014**, *136*, 1304.
(219) Lo, J. C.; Gui, J.; Yabe, Y.; Pan, C.-M.; Baran, P. S. *Nature* **2014**, *516*, 343.
(220) Sheldrick, G. *Acta Crystallographica Section A* **2015**, *71*, 3.
(221) Sheldrick, G. *Acta Crystallographica Section A* **2008**, *64*, 112.
(222) Macrae, C. F.; Bruno, I. J.; Chisholm, J. A.; Edgington, P. R.; McCabe, P.; Pidcock, E.; Rodriguez-Monge, L.; Taylor, R.; van de Streek, J.; Wood, P. A. *J. Appl. Crystallogr.* **2008**, *41*, 466.
(223) Malik, P.; Chakraborty, D. *Synthesis* **2010**, *2010*, 3736.
(224) Nemoto, K.; Yoshida, H.; Egusa, N.; Morohashi, N.; Hattori, T. *J. Org. Chem.* **2010**, *75*, 7855.
(225) Jiang, N.; Ragauskas, A. J. *J. Org. Chem.* **2007**, *72*, 7030.
(226) Van Baelen, G.; Maes, B. U. W. *Tetrahedron* **2008**, *64*, 5604.
(227) Yang, D.; Yang, H.; Fu, H. *Chem. Commun.* **2011**, *47*, 2348.
(228) Schmidt, A.-K. C.; Stark, C. B. W. *Org. Lett.* **2011**, *13*, 4164.
(229) Dintzner, M. R.; Mondjinou, Y. A.; Pileggi, D. J. *Tetrahedron Lett.* **2010**, *51*, 826.

(230) Basit, H.; Pal, A.; Sen, S.; Bhattacharya, S. *Chem. Eur. J.* **2008**, *14*, 6534.
(231) Vasil'ev, A.; Engman, L. *J. Org. Chem.* **2000**, *65*, 2151.
(232) Fkyerat, A.; Burki, N.; Tabacchi, R. *Tetrahedron: Asymmetry* **1996**, *7*, 2023.
(233) Grill, J. M.; Ogle, J. W.; Miller, S. A. *J. Org. Chem.* **2006**, *71*, 9291.
(234) Levin, D.; Warren, S. *J. Chem. Soc., Perkin Trans. 1* **1988**, 1799.
(235) Leggio, A.; De Marco, R.; Perri, F.; Spinella, M.; Liguori, A. *Eur. J. Org. Chem.* **2012**, *2012*, 114.
(236) Curtin, N. J.; Barlow, H. C.; Bowman, K. J.; Calvert, A. H.; Davison, R.; Golding, B. T.; Huang, B.; Loughlin, P. J.; Newell, D. R.; Smith, P. G.; Griffin, R. J. *J. Med. Chem.* **2004**, *47*, 4905.
(237) Marshall, J. A.; Lebreton, J. *J. Am. Chem. Soc.* **1988**, *110*, 2925.
(238) Park, J. H.; Ko, K. C.; Kim, E.; Park, N.; Ko, J. H.; Ryu, D. H.; Ahn, T. K.; Lee, J. Y.; Son, S. U. *Org. Lett.* **2012**, *14*, 5502.
(239) Jiang, Q.; Wang, J.-Y.; Guo, C. *J. Org. Chem.* **2014**, *79*, 8768.
(240) Broggi, J.; Jurčík, V.; Songis, O.; Poater, A.; Cavallo, L.; Slawin, A. M. Z.; Cazin, C. S. J. *J. Am. Chem. Soc.* **2013**, *135*, 4588.
(241) Sreedhar, B.; Reddy, P. S.; Devi, D. K. *J. Org. Chem.* **2009**, *74*, 8806.
(242) Saidi, O.; Blacker, A. J.; Farah, M. M.; Marsden, S. P.; Williams, J. M. J. *Chem. Commun.* **2010**, *46*, 1541.
(243) Zhang, Z.; Jain, P.; Antilla, J. C. *Angew. Chem. Int. Ed.* **2011**, *50*, 10961.
(244) Bolognese, A.; Diurno, M. V.; Mazzoni, O.; Giordano, F. *Tetrahedron* **1991**, *47*, 7417.
(245) Lang, X.; Ji, H.; Chen, C.; Ma, W.; Zhao, J. *Angew. Chem. Int. Ed.* **2011**, *50*, 3934.
(246) Bryon Gill, G.; Idris, M. S. H. *Tetrahedron* **1993**, *49*, 219.
(247) Kommi, D. N.; Jadhavar, P. S.; Kumar, D.; Chakraborti, A. K. *Green Chem.* **2013**, *15*, 798.
(248) Kremer, C. B. *J. Am. Chem. Soc.* **1939**, *61*, 1321.
(249) Filippov, A.; Sulejmanova, A.; Antzutkin, O.; Gröbner, G. *Appl. Magn. Reson.* **2005**, *29*, 439.